

**CHARACTERIZATION AND IDENTIFICATION OF ZN-CD
RESISTANT BACTERIA CONTAINING PLANT GROWTH
PROMOTING PROPERTIES: STUDY BY FT-IR
MICROSPECTROSCOPY AND MOLECULAR
TECHNIQUES**

PAYUNGSAK TABOONMA

A thesis submitted in partial fulfillment of the requirements for
the degree of Master of Science in Biology
at Maharakham University

July 2014

All rights reserved by Maharakham University



**CHARACTERIZATION AND IDENTIFICATION OF ZN-CD
RESISTANT BACTERIA CONTAINING PLANT GROWTH
PROMOTING PROPERTIES: STUDY BY FT-IR
MICROSPECTROSCOPY AND MOLECULAR
TECHNIQUES**

PAYUNGSAK TABOONMA

A thesis submitted in partial fulfillment of the requirements for
the degree of Master of Science in Biology
at Maharakham University

July 2014

All rights reserved by Maharakham University





The examining committee has unanimously approved this thesis, submitted by Mr. Payungsak Taboonma, as a partial fulfillment of the requirements for the Master of Science Program in Biology at Maharakham University.

Examining Committee

P. Chantiratikul

(Asst. Prof. Piyanete Chantiratikul, Ph.D.)

Chairman

(Faculty graduate committee)

W. Nakh

(Asst. Prof. Woranan Nakbanpote, D.Sc.)

Committee

(Advisor)

Aphidech Sangdee

(Asst. Prof. Aphidech Sangdee, Ph.D.)

Committee

(Co-advisor)

Khanitta Somtrakoon

(Asst. Prof. Khanitta Somtrakoon, Ph.D.)

Committee

(Faculty graduate committee)

Nichada Jearanaikoon

(Nichada Jearanaikoon, Ph.D.)

Committee

(External expert)

Maharakham University has granted approval to accept this thesis as a partial fulfillment of the requirements for the Master of Science Program in Biology

Wichian Magtoon

(Prof. Wichian Magtoon, Ph.D.)
Dean of the Faculty of Science

Pradit

(Prof. Pradit Terdtoon, Ph.D.)
Dean of Graduate School

July 22, 2014



ACKNOWLEDGEMENTS

This thesis was granted by the Human Resource Development in Science Project (Science Achievement Scholarship of Thailand, SAST), and I express thanks to Mahasarakham University for financial support.

The thesis would not have been accomplished if without the help from several people. I deeply appreciate Assist. Prof. Dr. Woranan Nakbanpote, my major advisor, Assist. Prof. Dr. Aphidech Sangdee my co-advisor, Department of Biology, Faculty of Science, for their support on bacterial identification, guidance, encouraging, invaluable comment and suggestions throughout this study. I wish to grateful thanks Assist. Prof. Dr. Khanitta Somtrakoon, Department of Biology, Faculty of Science, Assist. Prof. Dr. Piyanete Chantiratikul, Department of Chemistry, Faculty of Science, and Dr. Nichada Jearanaikoon, Synchrotron Light Research Institute (Public Organization) (SLRI) for their kindness advice.

I would like to thanks Dr. Kanjana Thumanu, for consultations and facilities on Fourier transform infrared spectroscopy (FTIR) analysis at SLRI, and recognize Ms. Orapan Meesungnoen for six bacteria isolates used in this research, and are grateful to Dr. Jolyon Dodgson for English proofreading. I am deeply indebted to all members of Sustainable Development Laboratory (SDL) for their being very supportive, and thanks Department of Biology, Faculty of Science, Mahasarakham University for research facilities.

Finally, I grateful thanks my parents, close relatives, and Miss Pantong Panpoka for supporting me throughout all my studies at Mahasarakham University.

Mr. Payungsak Taboonma



TITLE Characterization and identification of Zn-Cd resistant bacteria containing plant growth promoting properties: Study by FT-IR, microspectroscopy and molecular techniques

CANDIDATE Mr. Payungsak Taboonma

DEGREE Master of Science (Biology)

ADVISORS Asst. Prof. Woranan Nakbanpote, D.Sc.
Asst. Prof. Aphidech Sangdee, Ph.D.

UNIVERSITY Mahasarakham University **DATE** 2014

ABSTRACT

Our survey in a zinc mine, Mae Sot, Tak province, Thailand found *Gynura pseudochina* (L.) DC., a Zn/Cd hyperaccumulative plant. Six bacteria, PDMZn2008, PDMCd0501, PDMCd2007, PDMCd2008, PDMZnCd1502 and PDMZnCd2003, were isolated from the rhizosphere of *G. pseudochina* (L.) DC). Preliminary study indicated that the six isolates tolerated Zn and Cd, and contained plant growth promoting properties. However, bacterial identification and plant growth promoting properties, especially quantitatively under heavy metal treatment, should be investigated before their application in phytoremediation processes. Therefore, this research aims to study the bacterial identification by 16S rDNA gene sequencing, and compare this with the separation at the molecular level by Sodium Dodecyl Sulfate-Polyacrylamide Gel Electrophoresis (SDS-PAGE) and Fourier transform (FT-IR) microspectroscopy. Plant growth promoting properties under heavy metal stress were studied both in quantity and bacterial growth. The FT-IR spectra showed that the bacterial cells in the late log phase were suitable for the study of the bacterial identification at the gene and molecular levels. The genotype level of the 16S rDNA sequences identified that PDMZn2008, PDMCd0501, PDMCd2007, PDMCd2008, PDMZnCd1502 and PDMZnCd2003 were the closest related strains to *Brevibacterium epidermidis*, *Serratia marcescens*, *Serratia marcescens*, *Providencia vermicola*, *Providencia vermicola* and *Pseudomonas aeruginosa*, respectively. The dendrograms obtained from the protein patterns and FT-IR spectra were able to separate the six bacterial isolates; however, the dendrograms did not correspond with the phylogenetic tree obtained from the 16S rDNA sequencing.



However, the FT-IR technique could be used for bacterial monitoring in a bioaugmentation process. The heavy metals tolerance was tested by the Minimal Inhibitory Concentration (MIC), which indicated that PDMZnCd2003 could tolerate the nutrient broth (NB) containing Zn and Cd concentrations of 150 mg/l and 70 mg/l, respectively. The isolate also tolerated the NB with Zn plus Cd of 60+60 and 20+150 mg/l. In addition, the Minimum Bactericidal Concentration (MBC) tests indicated that the NB containing 300 mg/l of Cd killed the PDMZnCd2003 cells. The study of plant growth promoting properties under the Zn plus Cd of 20+20 mg/l showed that the heavy metals' stress badly affected the six bacteria's growth and production of Indole-3-Acetic Acid (IAA), nitrogen fixation and phosphate solubilization. Consequently, PDMZnCd2003 was the best isolate for maintaining plant growth promoting properties under the heavy metal stresses. Therefore, *P. aeruginosa* PDMZnCd2003 could serve as an efficient biofertilizer candidate for microbe assisted phytoremediation in Zn/Cd contaminated areas.

Keywords: PGPB, SDS-PAGE, 16S rDNA, FT-IR spectroscopy



ชื่อเรื่อง	การจำแนกสายพันธุ์แบคทีเรียที่สามารถต้านทานต่อโลหะสังกะสี และแคดเมียม และมีคุณสมบัติส่งเสริมการเจริญของพืช : ศึกษาด้วยเทคนิค FT-IR Microspectroscopy และเทคนิคทางโมเลกุล
ผู้วิจัย	นายพยุงค์ศักดิ์ ทาบุญมา
ปริญญา	วิทยาศาสตร์มหาบัณฑิต สาขาวิชา ชีววิทยา
กรรมการควบคุม	ผู้ช่วยศาสตราจารย์ ดร. วรณันต์ นาคบรรพต ผู้ช่วยศาสตราจารย์ ดร.อภิเดช แสงดี
มหาวิทยาลัย	มหาวิทยาลัยมหาสารคาม ปีที่พิมพ์ 2557

บทคัดย่อ

การสำรวจเหมืองแร่สังกะสี อำเภอมะนัง จังหวัดตาก ประเทศไทย พบต้นว่านมหากาฬ (*Gynura pseudochina* (L.) DC.) ที่มีคุณสมบัติสะสมโลหะสังกะสีและแคดเมียมได้สูง และคัดแยกแบคทีเรียจากบริเวณรอบรากต้นว่านมหากาฬได้จำนวน 6 ไอโซเลต คือ PDMZn2008, PDMCd0501, PDMCd2007, PDMCd2008, PDMZnCd1502 และ PDMZnCd2003 ซึ่งผลการทดสอบเบื้องต้นพบมีคุณสมบัติทนโลหะสังกะสีและแคดเมียมและมีคุณสมบัติส่งเสริมการเจริญของพืช อย่างไรก็ตามการประยุกต์ใช้แบคทีเรียที่มีคุณสมบัติดังกล่าวเพื่อส่งเสริมการบำบัดโลหะโดยใช้พืชควรมีการจัดจำแนกสายพันธุ์ และศึกษาการเจริญรวมทั้งคุณสมบัติส่งเสริมการเจริญของพืชภายใต้สภาวะที่มีโลหะหนัก ดังนั้นงานวิจัยนี้จึงมีวัตถุประสงค์เพื่อจัดจำแนกแบคทีเรียโดยการวิเคราะห์ลำดับเบสในส่วนของยีน 16S rDNA เปรียบเทียบกับการจัดจำแนกแบคทีเรียโดยการแยกโปรตีนที่สกัดจากเซลล์แบคทีเรียด้วยกระแสไฟฟ้าบนเจลพอลิอะคริลาไมด์ที่มี SDS เป็นส่วนประกอบ หรือ Sodium Dodecyl Sulfate-Polyacrylamide Gel Electrophoresis (SDS-PAGE) และการจัดจำแนกแบคทีเรียโดยใช้สเปกตรัมของเซลล์แบคทีเรียซึ่งวิเคราะห์จาก Fourier transform (FT-IR) microspectroscopy และศึกษาคุณสมบัติส่งเสริมการเจริญของพืชภายใต้สภาวะที่มีโลหะหนักในเชิงปริมาณและการเจริญของแบคทีเรียโดยผล FT-IR แสดงให้เห็นว่าเซลล์แบคทีเรียที่เจริญในช่วง late log phase มีความเหมาะสมต่อการนำมาศึกษาเปรียบเทียบการจัดจำแนกแบคทีเรียในระดับยีนและระดับโมเลกุล ผลการจำแนกสายพันธุ์แบคทีเรียด้วย 16S rDNA ระบุว่าไอโซเลต PDMZn2008, PDMCd0501, PDMCd2007, PDMCd2008, PDMZnCd1502 และ PDMZnCd2003 ใกล้เคียงกับสายพันธุ์ *Brevibacterium epidermidis*, *Serratia marcescens*, *Serratia marcescens*, *Providencia vermicola*, *Providencia vermicola* และ *Pseudomonas aeruginosa* ตามลำดับ แผนภูมิเดนโดแกรม (dendrogram) จากการวิเคราะห์รูปแบบโปรตีนและรูปแบบ FT-IR สเปกตรัมสามารถแยกแบคทีเรียทั้ง 6 ชนิดออกจากกันได้ แต่ไม่สอดคล้องแผนภูมิต้นไม้วงศ์วานวิวัฒนาการ (phylogenetic tree) ที่จัดจำแนกด้วย 16S rDNA ทั้งนี้เทคนิค FT-IR สามารถใช้ในการตรวจติดตามการเติมจุลินทรีย์เพื่อบำบัดสารมลพิษ (bioaugmentation) การทดสอบความทนทานของแบคทีเรียในอาหารเหลวที่เติมสังกะสีและแคดเมียมโดยการหาค่า Minimal Inhibitory Concentration (MIC) พบว่าไอโซเลต PDMZnCd2003 ทนต่อโลหะสังกะสีและแคดเมียมได้เท่ากับ 150 และ 70 มิลลิกรัมต่อลิตร ตามลำดับ



และทนต่ออาหารเหลวที่เติมสังกะสีร่วมกับแคดเมียมได้เท่ากับ 60+60 และ 20+150 มิลลิกรัมต่อลิตร และการทดสอบค่า Minimum Bactericidal Concentration (MBC) พบว่าอาหารที่เติมแคดเมียมสูงถึง 300 มิลลิกรัมต่อลิตร ฆ่าเชื้อ PDMZnCd2003 ได้ การศึกษาคุณสมบัติส่งเสริมการเจริญเติบโตของพืชภายใต้สภาวะที่เติมสังกะสีร่วมกับแคดเมียมที่ความเข้มข้น 20+20 มิลลิกรัมต่อลิตร พบว่าการเติมโลหะสังกะสีร่วมกับแคดเมียมส่งผลต่อการเจริญและลดความสามารถในการผลิต Indole-3-Acetic Acid (IAA) การตรึงไนโตรเจน และ การละลายฟอสเฟต ของเชื้อแบคทีเรียทั้ง 6 ไอโซเลต และพบว่าภายใต้สภาวะเครียดจากการเติมสังกะสีร่วมกับแคดเมียม ไอโซเลต PDMZnCd2003 คงคุณสมบัติการส่งเสริมการเจริญเติบโตของพืชได้ดีที่สุด จากผลการทดลองข้างต้น *P. aeruginosa* PDMZnCd2003 จึงมีแนวโน้มสามารถใช้เป็นจุลินทรีย์ที่เติมในพื้นที่ปนเปื้อนสังกะสีและแคดเมียมเพื่อช่วยส่งเสริมการบำบัดพื้นที่ปนเปื้อนโลหะหนักสังกะสีและแคดเมียมโดยใช้พืช

คำสำคัญ: 16S rDNA, FT-IR microspectroscopy, PGPB, SDS-PAGE



CONTENTS

	Page
Acknowledgement	i
Abstract in English	ii
Abstract in Thai	iv
List of Contents	vi
List of Tables	ix
List of Figures	xv
List of Abbreviations	xxv
Chapter 1 Introduction	1
1.1 Background	1
1.2 Objectives	3
1.3 Scope of research work	3
1.4 Advantages of the study	4
Chapter 2 Theoretical and literature review	5
2.1 Heavy metal	6
2.2 Bioremediation	9
2.3 Phytoremediation of heavy metals	10
2.4 Microbial-assisted phytoremediation	14
2.5 Plant growth promoting bacteria (PGPB)	16
2.6 Fourier transform infrared (FT-IR) spectroscopy	27
2.7 Polymerase chain reaction (PCR) Amplification	33
2.8 Electrophoresis	34
Chapter 3 Methodology	38
3.1 Research diagram	39
3.2 Materials and Method	40
3.2.1 Microorganisms	40
3.2.2 Morphological, physiological and biochemical characteristics	40
3.2.3 Growth curve of six bacteria isolates	41
3.2.4 Study the quantitative of plant growth promoting properties	42



	Page
3.2.5 Fourier transform infrared (FT-IR) microspectroscopy	43
3.2.6 Identification of bacteria based on 16S rDNA gene	44
3.2.7 SDS-PAGE	44
3.2.8 Assessment of metal toxicity	45
Chapter 4 Results and Discussion	47
4.1 Morphological and biochemical characteristics	47
4.2 Growth curve of bacteria isolates	49
4.2.1 Comparative of two techniques in growth curve of bacteria	49
4.2.2 FT-IR characterization of bacterial growth	53
4.3 Identification of the bacterial isolated	83
4.3.1 Identification by 16S rDNA gene sequences	83
4.3.2 SDS-PAGE	86
4.3.3 FT-IR characteristics of bacteria	90
4.3.4 The comparative the differentiation between FT-IR spectroscopy, protein pattern and 16S rDNA gene	98
4.4 Assessment of metal toxicity	99
4.4.1 Evaluation of metal tolerance	99
4.4.2 Evaluation of metal resistance	101
4.5 Plant-growth promoting properties	103
4.5.1 Indole-3-acetic acid (IAA) production	103
4.5.2 Nitrogen fixation	108
4.5.3 Phosphate solubilization	113
Chapter 5 Conclusion and Suggestion	119
5.1 Conclusion	119
5.2 Suggestions	121
References	122
Appendices	148
Appendix A Bacteria medium	149
Appendix B Morphological and biochemical characteristics	153
Appendix C Biochemical identification	156



	Page
Appendix D Growth curve monitoring	171
Appendix E SDS-PAGE	178
Appendix F Assessment of metal toxicity; MIC	184
Appendix G Plant growth promoting properties	190
Biography	229



LIST OF TABLES

	Page
Table 2.1 Advantages and disadvantages of phytoremediation for heavy metal contaminated areas	13
Table 2.2 Examples of plant growth-promoting rhizobacteria	18
Table 2.3 Examples plant growth-promoting rhizobacteria to control fungi that cause plant disease.	23
Table 4.1 Morphological and biochemical characteristics	48
Table 4.2 Growth phase of the bacterial isolates of PDMZn2008, PDMCd0501, PDMCd2007, PDMCd2008, PDMZnCd1502 and PDMZnCd2003 determined by turbidimetric method and Bradford protein assay.	52
Table 4.3 Kimura 2-parameter genetic distances between F_{ST} pairwise 26 populations for 16S rDNA of the taxa examined.	85
Table 4.4 Characteristic functional groups contributing to the formation of absorption band at the wavenumber ranges of 3000–2800 cm^{-1} , 1800-1500 cm^{-1} , 1500-1400 cm^{-1} and 1200–900 cm^{-1}	93
Table 4.5 The bacterial isolates' tolerance to NA (solid medium) contaminated with various concentrations of Zn, Cd and Zn plus Cd.	100
Table 4.6 Minimal inhibitory concentrations (MICs) of zinc and/or cadmium	102
Table 4.7 Minimal bactericidal concentrations (MBCs) of zinc and/or cadmium	102
Table B-1 Average temperature, humidity and light intensity of the bacterial cultured Condition	154
Table D-1 System pHs and growth curves of PDMZn2008 in nutrient broth, monitored by the turbidimetric method and protein assay	172
Table D-2 System pHs and growth curves of PDMCd0501 in nutrient broth, monitored by the turbidimetric method and protein assay	173
Table D-3 System pHs and growth curves of PDMCd2007 in nutrient broth, monitored by the turbidimetric method and protein assay	174



	Page
Table D-4 System pHs and growth curves of PDMCd2008 in nutrient broth, monitored by the turbidimetric method and protein assay	175
Table D-5 System pHs and growth curves of PDMCd1502 in nutrient broth, monitored by the turbidimetric method and protein assay	176
Table D-6 System pHs and growth curves of PDMZnCd2003 in nutrient broth, monitored by the turbidimetric method and protein assay	177
Table F-1 Experimental design for study the minimum inhibitory concentration (MIC) of zinc, cadmium and zinc plus cadmium.	185
Table F-2 Experimental design for study the minimum inhibitory concentration (MIC) of 20 mg/l cadmium plus various concentrations of zinc	185
Table F-3 Plates after 24 hours in the modified resazurin assay. Pink colour indicates growth and blue means inhibition of growth; these are taken as the minimum inhibitory concentration (MIC) values for zinc, cadmium, and zinc plus cadmium treatment.	188
Table F-4 Plates after 24 hours in the modified resazurin assay. Pink colour indicates growth and blue means inhibition of growth; these are taken as the minimum inhibitory concentration (MIC) values for fixed 20 mg/l of cadmium plus various concentrations of zinc treatment	189
Table G-1 Indole-3-acetic acid (IAA) production, system pHs and growth, monitored by the turbidimetric method at 660 nm, of PDMZn2008 in trypticase soy broth (TSB) containing 0.2% w/v tryptophan	193
Table G-2 Indole-3-acetic acid (IAA) production, system pHs and growth, monitored by the turbidimetric method at 660 nm, of PDMZn2008 in trypticase soy broth (TSB) containing 0.2% w/v tryptophan in the presence of Zn plus Cd (20/20 mg/l)	194
Table G-3 Indole-3-acetic acid (IAA) production, system pHs and growth, monitored by the turbidimetric method at 660 nm, of PDMCd0501 in trypticase soy broth (TSB) containing 0.2% w/v tryptophan	195



	Page
Table G-4 Indole-3-acetic acid (IAA) production, system pHs and growth, monitored by the turbidimetric method at 660 nm, of PDMCd0501 in trypticase soy broth (TSB) containing 0.2% w/v tryptophan in the presence of Zn plus Cd (20/20 mg/l)	196
Table G-5 Indole-3-acetic acid (IAA) production, system pHs and growth, monitored by the turbidimetric method at 660 nm, of PDMCd2007 in trypticase soy broth (TSB) containing 0.2% w/v tryptophan	197
Table G-6 Indole-3-acetic acid (IAA) production, system pHs and growth, monitored by the turbidimetric method at 660 nm, of PDMCd2007 in trypticase soy broth (TSB) containing 0.2% w/v tryptophan in the presence of Zn plus Cd (20/20 mg/l)	198
Table G-7 Indole-3-acetic acid (IAA) production, system pHs and growth, monitored by the turbidimetric method at 660 nm, of PDMCd2008 in trypticase soy broth (TSB) containing 0.2% w/v tryptophan	199
Table G-8 Indole-3-acetic acid (IAA) production, system pHs and growth, monitored by the turbidimetric method at 660 nm, of PDMCd2008 in trypticase soy broth (TSB) containing 0.2% w/v tryptophan in the presence of Zn plus Cd (20/20 mg/l)	200
Table G-9 Indole-3-acetic acid (IAA) production, system pHs and growth, monitored by the turbidimetric method at 660 nm, of PDMZnCd1502 in trypticase soy broth (TSB) containing 0.2% w/v tryptophan	201
Table G-10 Indole-3-acetic acid (IAA) production, system pHs and growth, monitored by the turbidimetric method at 660 nm, of PDMZnCd1502 in trypticase soy broth (TSB) containing 0.2% w/v tryptophan in the presence of Zn plus Cd (20/20 mg/l)	202
Table G-11 Indole-3-acetic acid (IAA) production, system pHs and growth, monitored by the turbidimetric method at 660 nm, of PDMZnCd2003 in trypticase soy broth (TSB) containing 0.2% w/v tryptophan	203



	Page
Table G-12 Indole-3-acetic acid (IAA) production, system pHs and growth, monitored by the turbidimetric method at 660 nm, of PDMZnCd2003 in trypticase soy broth (TSB) containing 0.2% w/v tryptophan in the presence of Zn plus Cd (20/20 mg/l)	204
Table G-13 NH ₃ ⁺ -N production, system pHs and growth, monitored by the turbidimetric method at 660 nm, of PDMZn2008 in N-free malate medium	205
Table G-14 NH ₃ ⁺ -N production, system pHs and growth, monitored by the turbidimetric method at 660 nm, of PDMZn2008 in N-free malate medium in the presence of Zn plus Cd (20/20 mg/l)	206
Table G-15 NH ₃ ⁺ -N production, system pHs and growth, monitored by the turbidimetric method at 660 nm, of PDMCd0501 in N-free malate medium	207
Table G-16 NH ₃ ⁺ -N production, system pHs and growth, monitored by the turbidimetric method at 660 nm, of PDMCd0501 in N-free malate medium in the presence of Zn plus Cd (20/20 mg/l)	208
Table G-17 NH ₃ ⁺ -N production, system pHs and growth, monitored by the turbidimetric method at 660 nm, of PDMCd2007 in N-free malate medium	209
Table G-18 NH ₃ ⁺ -N production, system pHs and growth, monitored by the turbidimetric method at 660 nm, of PDMCd2007 in N-free malate medium in the presence of Zn plus Cd (20/20 mg/l)	210
Table G-19 NH ₃ ⁺ -N production, system pHs and growth, monitored by the turbidimetric method at 660 nm, of PDMCd2008 in N-free malate medium	211
Table G-20 NH ₃ ⁺ -N production, system pHs and growth, monitored by the turbidimetric method at 660 nm, of PDMCd2008 in N-free malate medium in the presence of Zn plus Cd (20/20 mg/l)	212
Table G-21 NH ₃ ⁺ -N production, system pHs and growth, monitored by the turbidimetric method at 660 nm, of PDMZnCd1502 in N-free malate medium	213



Table G-22 NH_3^+ -N production, system pHs and growth, monitored by the turbidimetric method at 660 nm, of PDMZnCd1502 in N-free malate medium in the presence of Zn plus Cd (20/20 mg/l)	214
Table G-23 NH_3^+ -N production, system pHs and growth, monitored by the turbidimetric method at 660 nm, of PDMZnCd2003 in N-free malate medium	215
Table G-24 NH_3^+ -N production, system pHs and growth, monitored by the turbidimetric method at 660 nm, of PDMZnCd2003 in N-free malate medium in the presence of Zn plus Cd (20/20 mg/l)	216
Table G-25 Phosphates solubilization, system pHs and growth, monitored by the turbidimetric method at 660 nm, of PDMZn2008 in NBRIP medium containing 0.5% (w/v) tricalcium phosphate	217
Table G-26 Phosphates solubilization, system pHs and growth, monitored by the turbidimetric method at 660 nm, of PDMZn2008 in NBRIP medium containing 0.5% (w/v) tricalcium phosphate in the presence of Zn plus Cd (20/20 mg/l)	218
Table G-27 Phosphates solubilization, system pHs and growth, monitored by the turbidimetric method at 660 nm, of PDMCd0501 in NBRIP medium containing 0.5% (w/v) tricalcium phosphate	219
Table G-28 Phosphates solubilization, system pHs and growth, monitored by the turbidimetric method at 660 nm, of PDMCd0501 in NBRIP medium containing 0.5% (w/v) tricalcium phosphate in the presence of Zn plus Cd (20/20 mg/l)	220
Table G-29 Phosphates solubilization, system pHs and growth, monitored by the turbidimetric method at 660 nm, of PDMCd2007 in NBRIP medium containing 0.5% (w/v) tricalcium phosphate	221
Table G-30 Phosphates solubilization, system pHs and growth, monitored by the turbidimetric method at 660 nm, of PDMCd2007 in NBRIP medium containing 0.5% (w/v) tricalcium phosphate in the presence of Zn plus Cd (20/20 mg/l)	222



Table G-31 Phosphates solubilization, system pHs and growth, monitored by the turbidimetric method at 660 nm, of PDMCd2008 in NBRIP medium containing 0.5% (w/v) tricalcium phosphate	223
Table G-32 Phosphates solubilization, system pHs and growth, monitored by the turbidimetric method at 660 nm, of PDMCd2008 in NBRIP medium containing 0.5% (w/v) tricalcium phosphate in the presence of Zn plus Cd (20/20 mg/l)	224
Table G-33 Phosphates solubilization, system pHs and growth, monitored by the turbidimetric method at 660 nm, of PDMZnCd1502 in NBRIP medium containing 0.5% (w/v) tricalcium phosphate	225
Table G-34 Phosphates solubilization, system pHs and growth, monitored by the turbidimetric method at 660 nm, of PDMZnCd1502 in NBRIP medium containing 0.5% (w/v) tricalcium phosphate in the presence of Zn plus Cd (20/20 mg/l)	226
Table G-35 Phosphates solubilization, system pHs and growth, monitored by the turbidimetric method at 660 nm, of PDMZnCd2003 in NBRIP medium containing 0.5% (w/v) tricalcium phosphate	227
Table G-36 Phosphates solubilization, system pHs and growth, monitored by the turbidimetric method at 660 nm, of PDMZnCd2003 in NBRIP medium containing 0.5% (w/v) tricalcium phosphate in the presence of Zn plus Cd (20/20 mg/l)	228



LIST OF FIGURES

	Page
Figure 2.1 Plant–microbe interactions. Interaction between plants and microbes in the rhizosphere can be classified as either positive or negative interactions	15
Figure 2.2 A possible mechanism of how stress controller bacteria reduce ethylene levels in the plant root using bacterial ACC deaminase. ACC synthesized in plant tissues by ACC synthase is thought be exuded from plant roots and be taken up by neighboring bacteria. Subsequently, the bacteria hydrolyze ACC to ammonia and 2-oxobutanoate. This ACC hydrolysis maintains ACC concentrations low in bacteria and permits continuous ACC transfer from plant roots to bacteria. Otherwise, ethylene can be produced from ACC and then cause stress responses including growth inhibition. S-AdoMet: S-adenosyl-L-methionine; ACC: 1-aminocyclopropane-1-carboxylate	19
Figure 2.3 Examples of siderophore structures. Desferrichrome is produced by <i>Aspergillus</i> or <i>Ustil</i> and is a hydroxamate siderophore like ferrioxamine. Enterobactin is a catechol siderophore produced by <i>E. coli</i> . Pyoverdine is produced by <i>P. aeruginosa</i> PAO1 and is a mixed siderophore, which carries both hydroxamate and catechol groups. Citrate is considered to be a siderophore. Cepabactin is a 1-hydroxy-2-pyridinone bidentate siderophore produced by <i>Burkholderia cepacia</i> . Pyochelin is a 2-(2-o-hydroxyphenyl-2-thiazolin-4-yl)-3-methylthiazolidine-4-carboxylic acid produced by <i>P. aeruginosa</i> and <i>B. cepacia</i> , which chelates iron via oxygen and nitrogen electron donor atoms	21
Figure 2.4 Various organic/inorganic substances produced by PSB responsible for phosphate solubilization in soils	25
Figure 2.5 The electromagnetic spectrum	29



- Figure 2.6 (a) FTIR spectrometer block scheme of the basic components of an FTIR spectrometer. (b) working principle of a Michelson interferometer consisting of a light source, beam splitter, fixed mirror, moving mirror, detector and a sample (upper panel). A single frequency light source (central panel, left) is modulated to a sinusoidal signal observed by the detector (central panel, right). A white-light source (e.g. emitted from a globar) is transformed to the interferogram (lower panel) 31
- Figure 2.7 Spectra of different microorganisms measured by FT-IR microspectrometry 32
- Figure 2.8 Schematic diagram of the PCR process 35
- Figure 2.9 Run speed of molecular weight markers in SDS gels 37
- Figure 4.1 System pHs during the cultivation of PDMZn2008, PDMCd0501, PDMCd2007, PDMCd2008, PDMZnCd1502 and PDMZnCd2003 in nutrient broth. 50
- Figure 4.2 Growth curves of six bacteria in nutrient broth, monitored by the turbidimetric method and protein assay: (a) PDMZn2008, (b) PDMCd0501, (c) PDMCd2007, (d) PDMCd2008, (e) PDMZnCd1502 and (f) PDMZnCd2003. 51
- Figure 4.3 Normalized average FT-IR spectra of PDMZn2008 cells at lag phase, log phase, late-log phase, stationary phase and death phase. The spectral windows are defined according to the classification. Where, W1 is the fatty acid region ($3000-2800\text{ cm}^{-1}$), W2 is the amide region ($1800-1500\text{ cm}^{-1}$), W3 is the mixed region ($1500-1200\text{ cm}^{-1}$) and W4 is the polysaccharide region ($1200-900\text{ cm}^{-1}$). One spectrum was averaged from 100-125 spectra of each growth phase. 55
- Figure 4.4 Second derivative FT-IR spectra of PDMZn2008 cells at lag phase, log phase, late-log, phase, stationary phase and death phase. The spectral windows are defined according to the classification. 56



- Figure 4.5 Principal component analysis (PCA) applied to FT-IR spectra of PDMZn2008 growth phases. (A) shows the score plots of PC1 and PC4; (B) and (C) show loading plots of PC1 and PC4 in the ranges of 3000-2800 cm^{-1} and 1800-800 cm^{-1} , respectively. 57
- Figure 4.6 Normalized average FT-IR spectra of PDMCd0501 cells at lag phase, log phase, late-log phase, stationary phase and death phase. The spectral windows are defined according to the classification. Where, W1 is the fatty acid region (3000-2800 cm^{-1}), W2 is the amide region (1800-1500 cm^{-1}), W3 is the mixed region (1500-1200 cm^{-1}) and W4 is the polysaccharide region (1200-900 cm^{-1}). One spectrum was averaged from 100-125 spectra of each growth phase. 60
- Figure 4.7 Second-derivative FT-IR spectra of PDMCd0501 cells at lag phase, log phase, late-log, phase, stationary phase and death phase. The spectral windows are defined according to the classification. 61
- Figure 4.8 Principal component analysis (PCA) applied to FT-IR spectra of PDMCd0501 growth phases. (A) shows the score plots of PC1 and PC2; (B) and (C) show loading plots of PC1 and PC2 in the ranges of 3000-2800 cm^{-1} and 1800-800 cm^{-1} , respectively. 62
- Figure 4.9 Normalized average FT-IR spectra of PDMCd2007 cells at lag phase, log phase, late-log phase, stationary phase and death phase. The spectral windows are defined according to the classification. Where, W1 is the fatty acid region (3000-2800 cm^{-1}), W2 is the amide region (1800-1500 cm^{-1}), W3 is the mixed region (1500-1200 cm^{-1}) and W4 is the polysaccharide region (1200-900 cm^{-1}). One spectrum was averaged from 100-125 spectra of each growth phase. 65
- Figure 4.10 Second-derivative FT-IR spectra of PDMCd2007 cells at lag phase, log phase, late-log, phase, stationary phase and death phase. The spectral windows are defined according to the classification. 66



- Figure 4.11 Principal component analysis (PCA) applied to FT-IR spectra of PDMCd2007 growth phases. (A) shows the score plots of PC1 and PC2; (B) and (C) show loading plots of PC1 and PC2 in the ranges of $3000\text{-}2800\text{ cm}^{-1}$ and $1800\text{-}800\text{ cm}^{-1}$, respectively 67
- Figure 4.12 Normalized average FT-IR spectra of PDMCd2008 cells at lag phase, log phase, late-log phase, stationary phase and death phase. The spectral windows are defined according to the classification. Where, W1 is the fatty acid region ($3000\text{-}2800\text{ cm}^{-1}$), W2 is the amide region ($1800\text{-}1500\text{ cm}^{-1}$), W3 is the mixed region ($1500\text{-}1200\text{ cm}^{-1}$) and W4 is the polysaccharide region ($1200\text{-}900\text{ cm}^{-1}$). One spectrum was averaged from 100-125 spectra of each growth phase. 70
- Figure 4.13 Second-derivative FT-IR spectra of PDMCd2008 cells at lag phase, log phase, late-log, phase, stationary phase and death phase. The spectral windows are defined according to the classification. 71
- Figure 4.14 Principal component analysis (PCA) applied to FT-IR spectra of PDMCd2008 growth phases. (A) shows the score plots of PC1 and PC2; (B) and (C) show loading plots of PC1 and PC2 in the ranges of $3000\text{-}2800\text{ cm}^{-1}$ and $1800\text{-}800\text{ cm}^{-1}$, respectively. 72
- Figure 4.15 Normalized average FT-IR spectra of PDMZnCd1502 cells at lag phase, log phase, late-log phase, stationary phase and death phase. The spectral windows are defined according to the classification. Where, W1 is the fatty acid region ($3000\text{-}2800\text{ cm}^{-1}$), W2 is the amide region ($1800\text{-}1500\text{ cm}^{-1}$), W3 is the mixed region ($1500\text{-}1200\text{ cm}^{-1}$) and W4 is the polysaccharide region ($1200\text{-}900\text{ cm}^{-1}$). One spectrum was averaged from 100-125 spectra of each growth phase. 75
- Figure 4.16 Second-derivative FT-IR spectra of PDMZnCd1502 cells at lag phase, log phase, late-log phase, stationary phase and death phase. The spectral windows are defined according to the classification. 76



- Figure 4.17 Principal component analysis (PCA) applied to FT-IR spectra of PDMZnCd1502 growth phases. (A) shows the score plots of PC1 and PC2; (B) and (C) show loading plots of PC1 and PC2 in the ranges of 3000-2800 cm^{-1} and 1800-800 cm^{-1} , respectively. 77
- Figure 4.18 Normalized average FT-IR spectra of PDMZnCd2003 cells at lag phase, log phase, late-log phase, stationary phase and death phase. The spectral windows are defined according to the classification. Where, W1 is the fatty acid region (3000-2800 cm^{-1}), W2 is the amide region (1800-1500 cm^{-1}), W3 is the mixed region (1500-1200 cm^{-1}) and W4 is the polysaccharide region (1200-900 cm^{-1}). One spectrum was averaged from 100-125 spectra of each growth phase. 80
- Figure 4.19 Second-derivative FT-IR spectra of PDMZnCd2003 cells at lag phase, log phase, late-log phase, stationary phase and death phase. The spectral windows are defined according to the classification. 81
- Figure 4.20 Principal component analysis (PCA) applied to FT-IR spectra of PDMZnCd2003 growth phases. (A) shows the score plots of PC1 and PC2; (B) and (C) show loading plots of PC1 and PC2 in the ranges of 3000-2800 cm^{-1} and 1800-800 cm^{-1} , respectively. 82
- Figure 4.21 Phylogenetic tree of 16S rDNA phylotypes based on the algorithm of the neighbor-joining method as determined by distance using Kimura's two-parameter correction. Scale bar represents 2% estimated distance. 84
- Figure 4.22 (A) Whole-cell protein profiles of bacterial isolates obtained by SDS-PAGE. Lines: A, PDMZn2008; B, PDMCd0501; C, PDMCd2007; D, PDMCd2008; E, PDMZnCd1502; F, PDMZnCd2003; M, Molecular weight marker (10-225 kDa), (B) electrophoretic protein patterns and dendrogram based on unweighted pair group method with arithmetic averages algorithm (UPGMA) of the protein patterns of whole-cell bacterial isolates. The mean correlation coefficient is expressed as a percentage ($r \times 100$). 89



Figure 4.23 (A) Normalized average FT-IR spectra and (B) second-derivative FT-IR spectra of six bacterial isolates: PDMZn2008, PDMCd0501, PDMCd2007, PDMCd2008, PDMZnCd1502 and PDMZnCd2003, depicted in the most-discriminatory spectral windows.

The spectral windows are defined according to the classification as follows: W1, the 'fatty acid region' (3000-2800 cm^{-1}); W2, the 'amide region' (1800-1500 cm^{-1}); W3, the 'mixed region' (1500-1200 cm^{-1}); and W4, the polysaccharide region (1200-900 cm^{-1}), dominated by the fingerprint-like absorption bands of the carbohydrates present within the cell wall.

(One spectrum was averaged from 100-125 spectra of sample.)

94

Figure 4.24 PCA score plots and loading plots for six bacterial classifications.

(A) shows the PCA score plot for classification of the spectral data of six bacterial isolates: PDMZn2008, PDMCd0501, PDMCd2007, PDMCd2008, PDMZnCd1502 and PDMZnCd2003, (B-D) represent the loading plots of (A) in the PC1 and PC2 space, (E) shows the PCA scores plot for classification of PDMCd2008, PDMZnCd2003 and PDMCd0501, (F-H) represent the loading plots of (E) in the PC1 and PC2 space, (I) shows the PCA score plot for classification of PDMCd2007, PDMZnCd1502 and PDMZn2008 and (J-L) represent the loading plots of (I) in the PC1 and PC6. The classification is as follows: W1, the 'fatty acid region' (3000-2800 cm^{-1}); W2, the 'amide region' (1800-1500 cm^{-1}); W3, the 'mixed region' (1500-1200 cm^{-1}); and W4, the polysaccharide region (1200-900 cm^{-1}). (One spectrum was averaged from 100-125 spectra of each growth phase.)

95



- Figure 4.25 Dendrogram of bacterial classification based on FT-IR data of six isolates: PDMZn2008, PDMCd0501, PDMCd2007, PDMCd2008, PDMZnCd1502 and PDMZnCd2003. Hierarchical cluster analysis (HCA) method was performed by second derivative and vector normalized of the spectra, considering the spectral ranges (weighting factors in parentheses) of (A) 3000-2800 cm^{-1} , (B) 1800-1500 cm^{-1} , (C) 1500-1200 cm^{-1} , (D) 1200-900 cm^{-1} and (E) 3000-2800 cm^{-1} , 1800-1500 cm^{-1} , 1500-1200 cm^{-1} and 1200-900 cm^{-1} . All spectral ranges were equally weighted Ward's algorithm (second derivative + vector normalization) 97
- Figure 4.26 Growth and pH change of PDMZn2008, PDMCd0501, PDMCd2007, PDMCd2008, PDMZnCd1502 and PDMZnCd2003 under cultivation in Trypticase soy broth (TSB), with the absence and presence of Zn plus Cd (20+20 mg/l). (a) bacterial growth in TSB, (b) bacterial growth in the presence of Zn plus Cd, (c) pH change in TSB and (d) pH change in the presence of Zn plus Cd. 105
- Figure 4.27 IAA production of (a) PDMZn2008, (b) PDMCd0501, (c) PDMCd2007, (d) PDMCd2008, (e) PDMZnCd1502 and (f) PDMZnCd2003 under cultivation in Trypticase soy broth (TSB), with the absence and presence of Zn plus Cd (20+20 mg/l). (—●— control, and - -○- - Zn+Cd 20 mg/l) 106
- Figure 4.28 Comparison of IAA production by PDMZn2008, PDMCd0501, PDMCd2007, PDMCd2008, PDMZnCd1502 and PDMZnCd2003 under cultivation in Trypticase soy broth (TSB) under the (a) absence and (b) presence of Zn plus Cd (20+20 mg/l). 108



- Figure 4.29 Growth and pH change of PDMZn2008, PDMCd0501, PDMCd2007, PDMCd2008, PDMZnCd1502 and PDMZnCd2003 under cultivation in N-free malate medium, with the absence and presence of Zn plus Cd (20+20 mg/l). (a) bacterial growth in the N-free medium, (b) bacterial growth in the presence of Zn plus Cd, (c) pH change in the N-free medium and (d) pH change in the presence of Zn plus Cd. 110
- Figure 4.30 NH₃-N production of (a) PDMZn2008, (b) PDMCd0501, (c) PDMCd2007, (d) PDMCd2008, (e) PDMZnCd1502 and (f) PDMZnCd2003 under cultivation in N-free malate medium, with the absence and presence of Zn plus Cd (20+20 mg/l). (—●— control, and - -○- - Zn+Cd 20 mg/l) 111
- Figure 4.31 Comparison of NH₃-N production by PDMZn2008, PDMCd0501, PDMCd2007, PDMCd2008, PDMZnCd1502 and PDMZnCd2003 under cultivation in N-free malate medium, under the (a) absence and (b) presence of Zn plus Cd (20+20 mg/l). 113
- Figure 4.32 Growth and pH change of PDMZn2008, PDMCd0501, PDMCd2007, PDMCd2008, PDMZnCd1502 and PDMZnCd2003 under cultivation in NBRIP medium consisting of 0.5% w/v tricalcium phosphate, with the absence and presence of Zn plus Cd (20+20 mg/l). (a) bacterial growth in the NBRIP medium, (b) bacterial growth in the presence of Zn plus Cd, (c) pH change in the NBRIP medium and (d) pH change in the presence of Zn plus Cd. 115
- Figure 4.33 Phosphate solubilization of (a) PDMZn2008, (b) PDMCd0501, (c) PDMCd2007, (d) PDMCd2008, (e) PDMZnCd1502 and (f) PDMZnCd2003 under cultivation in NBRIP medium consisting of 0.5% w/v tricalcium phosphate, with the absence and presence of Zn plus Cd (20+20 mg/l). (—●— control, and - -○- - Zn+Cd 20 mg/l) 116



	Page
Figure 4.34 Comparison of phosphate solubilization by PDMZn2008, PDMCd0501, PDMCd2007, PDMCd2008, PDMZnCd1502 and PDMZnCd2003 under cultivation in NBRIP medium consisting of 0.5% w/v tricalcium phosphate, under the (a) absence and (b) presence of Zn plus Cd (20+20 mg/l).	118
Figure B-1 Profiles of temperature, humidity and light intensity during bacterial cultivation	154
Figure B-2 Colony morphology characteristics of the six bacterial isolates growing on nutrient agar (NA) plates for 48 hours	155
Figure B-3 Biochemical characteristics of the six bacterial isolates on triple sugar iron (TSI) agar and peptone iron agar (PIA), cultivated for 48 hours.	155
Figure E-1 Intensity (A) and molecular weight (B) of whole-cell protein profile obtained by SDS-PAGE, determined by Quantity One Version 4 (Bio-Rad)	179
Figure E-2 Intensity of whole-cell protein profiles of (A) PDMZn2008, (B) PDMCd 0501, (C) PDMCd2007, (D) PDMCd2008, (E) PDMZnCd1502 and (F) PDMZnCd2003, obtained by SDS-PAGE and determined by quantity One version 4 (Bio-Rad)	180
Figure E-3 Molecular weight of whole-cell protein profiles of (A) PDMZn2008, (B) PDMCd 0501, (C) PDMCd2007, (D) PDMCd2008, (E) PDMZnCd1502 and (F) PDMZnCd2003, obtained by SDS-PAGE and determined by quantity One version 4 (Bio-Rad)	182
Figure F-1 Experimental design for microtiter plate with 96 wells of the minimum inhibitory concentration (MIC) of zinc, cadmium and zinc plus cadmium	186
Figure F-2 Experimental design for microtiter plate with 96 wells of the minimum inhibitory concentration (MIC) of the fixed 20 mg/l of cadmium plus various concentrations of zinc	187



	Page
Figure G-1 Standard curve of bovine serum albumin for Bradford protein assay	191
Figure G-2 Standard curve for indole-3-acetic acid (IAA) quantitative analysis	191
Figure G-3 Standard curve of NH_3^+ -N for quantitative analysis of nitrogen fixation	192
Figure G-4 Standard curve of potassium dihydrogen phosphates for quantitative analysis of soluble phosphate	192



LIST OF ABBREVIATIONS

OD	Optical density
FTIR	Fourier transform infrared (FT-IR) spectroscopy
ATR	Attenuated Total Reflectance
SDS-PAGE	Sodium dodecyl sulfate polyacrylamide gel electrophoresis
kDa	Kilogram Dolton
rpm	round per minutes
g/m ³	Gram per meter cubed
h	Hour (s)
IAA	Indole-3-acetic acid
IU l ⁻¹	International unit per milliliter
µg l ⁻¹	Microgram per milliliter
µl	Microliter (s)
µm	Micrometer (s)
mA	Milliampere
ml	Milliliter (s)
mg l ⁻¹	Milligram per milliliter
nm	Nanometer
mM	Millimolar
min	Minute (s)
MIC	Minimum inhibitory concentration
MBC	Minimal bactericidal concentration
°C	Degree Ceclcius



CHAPTER 1

Introduction

1.1 Background

Heavy metals are enriched in the environment by human activity of different kinds; examples of such activities include mining and ore refinement. Results of these activities end up in outlets and wastes where heavy metals are transported to the environment. They persist and cannot be deleted from the environment. (Alloway, 1995; Greger, 1999). Metal wastes can exist as individual metals or, more often, as metal mixtures. Baker, et al. (1990) reported that cadmium (Cd) never occurs in isolation in the natural environment but, rather, appears mostly as a guest metal in zinc (Zn) mineralization. The soil in the fields of Phatath Phadaeng sub-district, Mae Sot, Tak Province, Thailand, is a source of Zn mineralisation. High levels of Cd and Zn have been reported in sediment samples from the creek sand, paddy field areas and rice grain in the vicinity of mining (Simmons et al., 2005; Khaokaew, et al., 2011). The health impacts of Cd overexposure on the Mae Sot population in 12 villages have been reported since 2007 (Swaddiwudhipong, et al., 2007; Swaddiwudhipon, et al., 2012). Therefore, the problem of Cd and Zn contamination in the Mae Sot area needs to be remedied.

Phytoremediation has been proposed as an alternative method to remove pollutants from contaminated area or to render pollutants harmless. Phytoextraction, is one of the key processes of phytoremediation that involves the use of metal accumulating (hyperaccumulators) plants to remove metals from soil by concentrating them in harvestable parts of the plant. However, when it is not possible to remove the metals from the contaminated sites by phytoextraction, other viable options, such as in situ immobilization (e.g., phytostabilization) should be considered as an integral part of risk management (Bolan et al., 2014). The success of phytoremediation is dependent on the potential of the plants to yield high biomass and withstand the metal stress. In addition, microbial activities in the root/rhizosphere soils enhance the effectiveness of phytoremediation processes (Rajkumar, et al., 2012). Much research has investigated



the microorganisms in the rhizosphere of metal hyperaccumulative plants by isolating the bacteria that were tolerant to heavy metals and contained plant growth-promoting properties, such as production of 1-amino-1-cyclopropane carboxylic acid (ACC) deaminase and indole-3-acetic-acid (IAA), nitrogen fixation, phosphate solubilisation and producing allelochemicals that include metabolites, siderophores, antibiotics, volatile metabolites, enzyme and others (Ma, et al., 2011; Saraf, et al., 2014). However, the tolerance and responses of bacterial isolates to excess heavy metals should be investigated especially in the metabolite aspects (Poirier et al., 2008; Braud et al., 2009a,b; Acuña et al., 2011).

Gynura pseudochina (L.) DC. (Wan-Maha-Kan), a tuber plant in the Genera Asteraceae, is a Zn/Cd hyperaccumulative plant (Panitlertumpai, et al., 2003; Nakbanpote, et al., 2010). Meesungnoen, et al. (2009) isolated six bacteria from the rhizosphere of *G. pseudochina* growing in zinc and cadmium contaminated soil of a zinc mining area in Phatat Phadaeng sub-district. The bacterial isolates were PDMZn2008, PDMCd0501, PDMCd2007, PDMCd2008, PDMZnCd1502 and PDMZnCd2003. They tolerated to zinc and cadmium and had multiple plant growth promoting properties of IAA production, nitrogen fixation, and phosphate solubilisation. Although they contain good properties, the plant growth promoting bacteria (PGPB) should be identified strain before application. The bacterial physiology and morphology are suitable for genus classification. Molecular technique, especially the sequences of the nucleotide 16S rDNA gene and study on proteins pattern, are needed for species classification. In addition, Fourier transform infrared spectroscopy (FT-IR) technique, which is a rapid and economical method, can be applied for microbial identification by combination with data obtained from the molecular techniques (Naumann, et al., 1988; Naumann, et al., 1996; Schuster, et al., 1999; Naumann, 2000; Yu and Irudayaraj, 2005; Barth, 2007; Ojeda, et al., 2008; Duygu, et al., 2009).

Therefore, this research aims to identify the six bacterial isolates and study their characteristic under treatment with zinc, cadmium, and zinc plus cadmium. The bacterial isolates were identified and compared with three techniques of genotype characteristics of partial 16S rRNA sequence, Fourier Transform Infrared spectroscopy (FT-IR) microspectroscopy, and whole cell protein patterns obtained using Sodium



Dodecyl Sulphate Polyacrylamide Gel Electrophoresis (SDS-PAGE). We determined the MICs (minimal inhibitory concentrations) and MBCs (minimum bactericidal concentration) of the heavy metals, and investigated the effect of Zn/Cd stress on growth promotion abilities for IAA production, N₂-fixation and phosphate solubilisation. The data obtained will be the basic data for monitoring of bacterial inoculation and demonstrate efficient biofertilizer candidates for microbe assisted phytoremediation in the Zn/Cd contaminated area.

1.2 Objectives

The aims of this research were:

1.2.1 To identify the six bacterial isolates and compare with three techniques of genotype characteristics of partial 16S rRNA sequence, FT-IR microspectroscopy, and whole cell protein patterns obtained from SDS-PAGE.

1.2.2 To evaluate the Zn and/or Cd resistance properties

1.2.3 To study the characteristic of plant growth promoting properties under treatment with zinc, cadmium, and zinc plus cadmium.

1.3 Scope of research work

1.3.1 Study the six bacterial isolates of PDMZn2008, PDMCd0501, PDMCd2007, PDMCd2008, PDMZnCd1502 and PDMZnCd2003

1.3.2 Study the bacterial identification by 16S rRNA sequence, FT-IR microspectroscopy, and whole cell protein patterns obtained from SDS-PAGE.

1.3.3 Study the plant growth promoting properties of IAA production, N₂-fixation and phosphate solubilisation in quantities, under absence (control) and presence of zinc plus cadmium of 20+20 mg/l

1.3.4 Determine the Zn and/or Cd tolerant properties by study the bacterial growth on nutrient agar plate (NA) containing various concentration of zinc, cadmium and zinc plus cadmium, and also evaluate by MICs and MBC tests.



1.4 Advantages of the study

1.4.1 The data obtained will be the basic data for monitoring of bacterial inoculation and for preliminary identification of an environmental bacterium by comparing to FT-IR spectra.

1.4.2 The results of Zn and/or Cd tolerance and plant growth promoting properties under the Zn/Cd stress will suggest the six bacterial isolates may be applied as biofertilizer candidates for microbe assisted phytoremediation in the Zn/Cd contaminated area.



CHAPTER 2

Theoretical and literature review

Phytoremediation is the process through which contaminated land is ameliorated by growing plants that have the ability to remove the contaminating chemicals. The processes in phytoremediation include phytodegradation, phytostabilization, phytovolatilization, phytoextraction, and rhizofiltration (Salt, et al., 1998). In addition, the association of plant and microorganism in the rhizosphere seems to enhance removal of the contaminants (Ma et al., 2011; Rajkumar, et al., 2012). Although relatively slow, phytoremediation is environmentally friendly, cheap, requires little equipment or labor, easy to perform. It is an *in situ* method which sites can be cleaned without removing the polluted soil. However, the key factor for successful phytoremediation is identification of a plant that is tolerant and suitable for each area, one which can accumulate high concentrations of the required metal. In addition, the microorganisms in the rhizosphere of metal hyperaccumulative plants have been investigated by isolating the bacteria that are tolerant to heavy metals and contain plant growth promoting properties; such as nitrogen fixation, phosphate solubilization, indole-3-acetic acid (IAA) phytohormone and 1-aminocyclopropane-1-carboxylate (ACC) deaminase production, etc (Ma, et al., 2011; Rajkumar, et al., 2012; Ahemad and Kibret, 2014).

Finally, although phytoremediation has been used widely, but the plant design for successful phytoremediation in any contaminated area should be concerned with geology and the effect of growing the plant on biodiversity. Especially, harvesting management and byproduct utilization should be studied and investigated to convince local people and government of the usefulness of phytoremediation (Nakbanpote, et al., 2010).



2.1 Heavy metal

Heavy metal is a member of a loosely-defined subset of elements that exhibit metallic properties. It mainly includes the transition metals, some metalloids, lanthanides and actinides. Many different definitions are based on density, atomic number or atomic weight, and chemical properties or toxicity. Heavy metals occur naturally in the ecosystem with large variations in concentration. In modern times, anthropogenic sources of heavy metals, i.e. pollution, have been introduced to the ecosystem. (Duffus, 2002; Hogan, 2010).

Heavy metals decrease plant growth by strong binding with essential nutrients and resulting to decrease phytoavailable nutrients, and heavy metals may damage or change soil structure (Jing, et al., 2007). Heavy metals have negative impact on microbial community. An amount of heavy metals, ever slightly, affect to population and biodiversity of microbial ecosystem (Oliveira and Pampuha, 2006; Jing ,et al., 2007). This chapter will focus on the effect of zinc and cadmium, which are the metals used in this research.

2.1.1 Zinc

Zinc is a bluish-white metal that dissolves readily in strong acids. In nature, it occurs as a sulfide, oxide, or carbonate. In solution, it is divalent and can form hydrated Zn^{2+} cations in acids, and zincated anions--probably $Zn(OH)_4^{2-}$ -in strong bases (EPA, 1987). Most of the zinc introduced into aquatic environments eventually is partitioned into the sediments. Zinc release from sediments is enhanced under conditions of high dissolved oxygen, low salinity and low pH. Dissolved zinc usually consists of the toxic aquoion ($Zn(H_2O)_6^{2+}$) and various organic and inorganic complexes. A quoions and other toxic species have their greatest effects on aquatic organisms under conditions of comparatively low pH, low alkalinity, low dissolved oxygen, and elevated temperatures (Eisler, 1993).

2.1.1.1 Benefits of zinc

Zinc can be used for industrial of batteries, coated galvanized steel roofing sheets, used in the industry of color drug and animal foods which will be used in zinc oxide (ZnO) form. Zinc alloys are used heavily. Approximately 300 enzymes are known to require Zn for their activities. Zn is required for DNA synthesis, cell division,



and protein synthesis. Zn-finger proteins are involved in genetic expression of various growth factors and steroid receptors, and several hundred Zn-containing nucleoproteins are probably involved in gene expression of various proteins (Prasad, 1995).

2.1.1.2 Toxicity of zinc

Although zinc is an essential requirement for good health, an excess zinc can be harmful. Excessive absorption of zinc suppresses copper and iron absorption. The free zinc ion in solution is highly toxic to invertebrates, and even vertebrate fish. Muysen, et al. (2006) showed only six micromolar of zinc ion killed 93 % of *Daphnia* in water. A large amount of zinc accumulated in human may be signs of fatigue, fever, dizzy, and cancer (Fosmire, 1990; Eisler, 1993). Zinc is an essential micronutrient for normal plant growth at low concentrations, supra-optimal Zn concentrations might inhibit growth and reduce photosynthesis (Chaney, 1993; Broadley, et al., 2007). The effect of Zn on microbial populations and their activities in field studies of sandy loam soil (received sewage sludge 20 years ago) indicate that Zn at 139.2-289 mg/kg in the soil reduced microbial populations to 42–60% (Brookes et al., 1986), and the field studies on oak forest near abandoned zinc smelter containing Zn at 478 mg/kg affected to decrease the populations of bacteria 86%, fungi 60%, actinomycetes 86%, nitrosomonas 94% and nitrobacter 40% (Pancholy et al.(1975). Zinc affected to fungus by the inhibition of respiration and growth, and decrease germination of fungal spores (Nickerson, 1946; Smith et al., 1978; Somers, 1961). In addition, toxicity of zinc depended on the metal concentration, response of microbe and condition of treatment. Winslow and Haywood (1931) showed 0.5 mM of zinc chloride inhibited growth of *E. coli*. A 10 mM concentration of Zn^{2+} decreased the survival of *Escherichia coli*; enhanced the survival of *Bacillus cereus*; did not significantly affect the survival of *Pseudomonas aeruginosa*, *Nocardia corallina*, and T1, T7, P1, and ø80 coliphages; completely inhibited mycelial growth of *Rhizoctonia solani*; and reduced mycelial growth of *Fusarium solani*, *Cunninghamella echinulata*, *Aspergillus niger* and *Trichoderma viride* (Babich and Stotzky, 1978). In addition, the toxicity of zinc to the fungi, bacteria, and coliphages was unaffected, lessened, or increased by the addition of high concentrations of NaCl. The increased toxicity of zinc in a high concentrations of NaCl was not a result of a synergistic interaction between



Zn^{2+} and elevated osmotic pressures but of the formation of complex anionic $ZnCl$ species that exerted greater toxicities than Zn^{2+} (Babich and Stotzky, 1978).

2.1.2 Cadmium

Cadmium. Cadmium is located at the end of the second row of transition elements with atomic number 48, atomic weight 112.4, density 8.65 g cm^{-3} , melting point 320.9°C , and boiling point 765°C . Together with Hg and Pb, Cd is one of the big three heavy metal poisons and is not known for any essential biological function. In its compounds, Cd occurs as the divalent Cd (II) ion. Cadmium is directly below Zn in the periodic table and has a chemical similarity to that of Zn, an essential micronutrient for plants and animals. This may account in part for Cd's toxicity; because Zn being an essential trace element, its substitution by Cd may cause the malfunctioning of metabolic processes (Campbell, 2006). Cadmium is also present as an impurity in several products, including phosphate fertilizers, detergents and refined petroleum products. In addition, acid rain and the resulting acidification of soils and surface waters have increased the geochemical mobility of Cd, and as a result its surface-water concentrations tend to increase as lake water pH decreases (Alloway, 1995; Campbell, 2006; Wuana and Okieimen, 2011).

2.1.2.1 Benefits of cadmium

Cadmium can be used to coat steel to prevent rust, used as a pigment in the industry such as ceramics, fabric, printer ink, plastics, etc. It can be mixed with other metal alloy to alloy ductility and corrosion resistance, and are used in battery production. The most significant use of Cd is in Ni/Cd batteries, as rechargeable or secondary power sources exhibiting high output, long life, low maintenance, and high tolerance to physical and electrical stress. Cadmium coatings provide good corrosion resistance coating to vessels and other vehicles, particularly in high-stress environments such as marine and aerospace. Other uses of cadmium are as pigments, stabilizers for polyvinyl chloride (PVC), in alloys and electronic compounds (Campbell, 2006).

2.1.2.2 Toxicity of cadmium

Toxicity of cadmium can cause both acute and chronic. The first symptoms of cadmium into the body are severe nausea, vomit, diarrhea, cramp, and saliva flooded mouth, or may be due to shock, cause in renal failure and possibly death (ATSDR, 2010). Cadmium is not an essential element for plant growth. The most general



symptoms of Cd toxicity are stunting and chlorosis (Prasad, 1995; Das, et al., 1997; Deckert, 2005). Cadmium can reduce enzyme activity by interacting with the enzyme–substrate complex, denaturing the enzyme protein, interacting with its active sites or by affecting the synthesis of the enzymes within the microbial cells. Metal-induced changes in the community structure can also modify the enzyme activity (Nannipieri, 1994). Cadmium, besides being an enzyme inhibitor, can have deleterious effects on membrane structure and function by binding to the ligands such as phosphate and the cysteinyl and histidyl groups of proteins (Collins and Stotzky, 1989). Dar (1996) reported a decrease in dehydrogenase activity (DHA) and alkaline phosphatase activity at 50 mg Cd kg in a laboratory study with different soil types. In addition, the effect of Cd on microbial populations and their activities in field studies of sandy loam soil (received sewage sludge 20 years ago), red soil and agricultural sandy loam indicate that CdSO₄ and CdCl at 5–1800 mg/kg soil treatment reduced 14–91% of microbial populations (Brookes et al., 1986; Griffiths et al., 1997; Khan et al., 1997). Such adverse effects impacted by Cd can lead to a reduction in biodiversity and resultant functions in the soil. A gradual change in the microbial community structure was noticed in laboratory-incubated soils amended with Cd (Frostegard, et al., 1993; Griffiths, et al., 1997).

2.2 Bioremediation

Environmental biotechnology; composting and wastewater treatments are familiar examples of old environmental biotechnologies. However, recent studies in molecular biology and ecology offer opportunities for more efficient biological processes. Notable accomplishments of these studies include the clean-up of polluted water and land areas. Bioremediation is defined as the process whereby organic wastes are biologically degraded under controlled conditions to an innocuous state, or to levels below concentration limits established by regulatory authorities (Mueller, et al., 1996).

By definition, bioremediation is the use of living organisms, primarily microorganisms, to degrade the environmental contaminants into less toxic forms. It uses naturally occurring bacteria and fungi or plants to degrade or detoxify substances hazardous to human health and/or the environment. The microorganisms may be indigenous to a contaminated area or they may be isolated from elsewhere and brought



to the contaminated site. Contaminant compounds are transformed by living organisms through reactions that take place as a part of their metabolic processes. Biodegradation of a compound is often the actions of multiple organisms. Bioaugmentation techniques involve the addition of microorganisms with the ability to degrade pollutants to a contaminated site to enhance degradation. For bioremediation to be effective, microorganisms must enzymatically attack the pollutants and convert them to harmless products. As bioremediation can be effective only where environmental conditions permit microbial growth and activity, application of biostimulation often involves the manipulation of environmental parameters to allow microbial growth and degradation to proceed at a faster rate (Vidali, 2001). Different bioremediation strategies are employed depending on the degree of saturation and aeration of an area. In addition, bioremediation can process both *In situ* and *Ex situ* techniques depending on level of contaminants, area, expend, budget, environmental impact on local people, etc.

In situ techniques are defined as those that are applied to soil and groundwater at the site with minimal disturbance. These techniques are generally the most desirable options due to lower cost and less disturbance since they provide the treatment in place avoiding excavation and transport of contaminants (Vidali, 2001; Ghosh and Singh, 2005; Peng, et al., 2009).

Ex situ techniques are those that are applied to soil and groundwater at the site which has been removed from the site via excavation (soil) or pumping (water) (Vidali, 2001). Landfarming is a simple technique in which contaminated soil is excavated and spread over a pre-pared bed and periodically tilled until pollutants are degraded. The goal is to stimulate indigenous biodegradative microorganisms and facilitate their aerobic degradation of contaminants. In general, the practice is limited to the treatment of superficial 10–35 cm of soil. Since landfarming has the potential to reduce monitoring and maintenance costs, as well as clean-up liabilities, it has received much attention as a disposal alternative (Vidali, 2001; Ghosh and Singh, 2005; Peng, et al., 2009).



2.3 Phytoremediation of heavy metals

Phytoremediation is a biological treatment process that utilizes natural processes harbored in (or stimulated by) plants to enhance degradation and removal of contaminants in contaminated soil or groundwater (Alvarez and Illman, 2006).

Advantages and disadvantages of using phytoremediation for remediation a heavy metals contaminated area are shown in Table 2.1. Furthermore, the use of phytoremediation as a secondary or polishing *in situ* treatment step minimizes land disturbance. Increasing public and regulatory acceptance are likely to extend the use of phytoremediation beyond current applications (Ensley, 2000; Tucker and Shaw, 2000). Phytoremediation utilizes physical, chemical and biological processes to remove, degrade, transform, or stabilize contaminants within soil and groundwater. The mechanisms for heavy metal remediation are phytoextraction, rhizofiltration, phytovolatilization, and phytostabilization. The processes are briefly described as following (Raskin, et al., 1997; Raskin and Ensley, 2000; Prasad, 2004; Suresh and Ravishankar, 2004; Ghosh and Singh, 2005).

Phytoextraction or Phytoaccumulation is the extraction and translocation of heavy metals, in soluble form, from shallow contaminated soil to plant tissues, especially to be stored in stems and leaves (harvestable regions). Although the heavy metals are not destroyed, this approach results in considerable reduction in heavy metal mobility. Depending on the type and concentration of the heavy metals, extraction from the plant ashes for recycling purposes might be feasible. This technique is generally used for metals such as nickel, zinc, copper, lead, chromium and cadmium. Plant productivity; accumulation in harvestable portion of plant > 3 tons dry matter/area-year; > 1,000 mg/kg metals lightly contaminated soil near to clean-up standard.

Rhizofiltration is mechanism refers to the use of aquatic plants in wetlands or hydroponic reactors. Generally, plants with large root systems are used. The submerged roots of such plants act as filters for the adsorption and absorption of a wide variety of contaminants. This mechanism is commonly used for treatment of industrial discharge, agricultural runoff, metals and radioactive contamination, with the plant densities of 200-1000 g m² and hydraulic retention time of several days.



Phytovolatilization is depended on the natural ability of a plant to volatilize a contaminant that has been taken up through its roots can be exploited as a natural air-stripping pump system. Volatile pollutants diffuse from the plant into the atmosphere through open stomata in leaves where gas exchange occurs.

Phytostabilization has application and objective to prevent the dispersion of contaminated sediments and soil by using plants (mainly grasses) to minimize erosion by wind or rain action. Plants are used to reduce the bioavailability of environmental pollutants. Conditions for optimum likelihood of success are vigorously growing roots; hydrophobic or immobile chemicals.



Table 2.1 Advantages and disadvantages of phytoremediation for heavy metal contaminated areas.

Advantages	Disadvantages/Limitations
Adaptable to a variety of heavy metal compounds.	Restricted to sites with shallow contamination within rooting zone of remediative plants.
<i>In situ</i> or <i>ex situ</i> application possible with effluent/soil substance respectively.	May take up to several years to remediate a contaminated site.
<i>In situ</i> applications decrease the amount soil disturbance and relatively low cost compared to conventional methods.	Restricted to sites with low contaminant concentrations.
Reduces the amount of waste that has to be sent to landfill (up to 95%), can be further utilized as bio-ore of heavy metals.	Harvested plant biomass from Phyto-extraction may be classified as a hazardous waste hence disposal should be carried out properly
<i>In situ</i> applications decrease the spread of contaminant via air and water.	Climatic conditions are a limiting factor.
Does not require expensive equipment or highly specialized personnel, and easily implemented and maintained.	Introduction of nonnative species may affect biodiversity. Effects to food web and ultimate contaminant fates might be unknown.
In large scale applications the potential energy stored can be utilized to generate thermal energy.	Consumption/utilization of contaminated plant biomass is a cause of concern.

Adapted from: Ghosh and Spingh, 2005; Alvarez and Illman, 2006



2.4 Microbial-assisted phytoremediation

The success of phytoremediation is strongly determined by the amount of plant biomass present and the concentration of heavy metals in plant tissues. Some plant species, so-called hyperaccumulators (e.g. *Thlaspi goesingense*, *Alyssum bertolonii* and *Alyssum murale*), which naturally grow in heavy metal contaminated sites, were found to have the ability to accumulate unusually high concentrations of heavy metals without any impact on their growth and development (Glick, et al., 1999). The high uptake and efficient root-to-shoot transport system endowed with enhanced metal tolerance provide hyperaccumulators with a high potential detoxification capacity (Cobbett and Goldsbrough, 2000; McGrath, et al., 2002; Peer, et al., 2005). However, most hyperaccumulators (e.g. *Thlaspi caerulescens* and *Arabidopsis thaliana*) are not suitable for phytoremediation in the field owing to their small biomass and slow growth (Chaney, et al., 2007). The interaction between microbes and plant roots (rhizosphere) is considered to greatly influence the growth and survival of plants (Figure 2.1). Therefore, alternative phytoremediation methods that exploit rhizosphere bacteria to reduce metal toxicity to plants have been investigated.



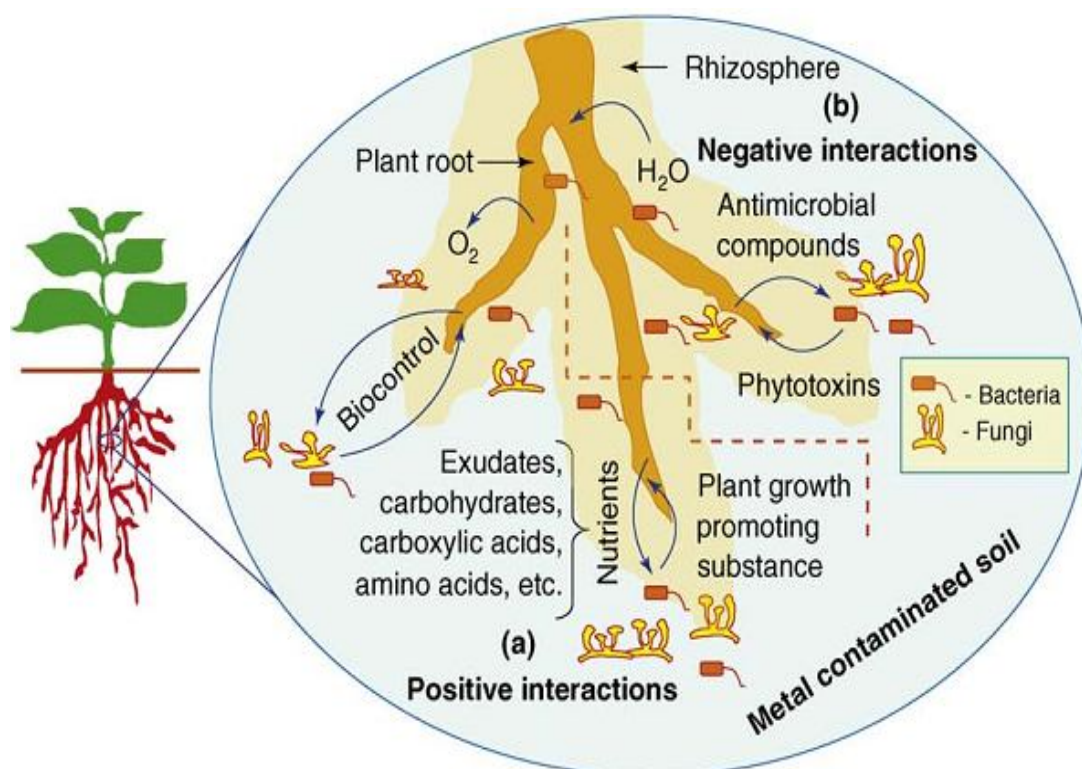


Figure 2.1 Plant–microbe interactions. Interaction between plants and microbes in the rhizosphere can be classified as either positive or negative interactions (Rajkumar, et al., 2010).

Furthermore, the discovery of rhizosphere bacteria that are heavy metal resistant and able to promote plant growth have raised high hopes for ecologically friendly and cost-effective strategies towards reclamation of heavy metal polluted soils (Ma, et al., 2011; Rajkumar, et al., 2012). The exploitation of metal resistant siderophore-producing bacteria (SPB), which are present in the rhizosphere, could be of particular importance as they can provide nutrients, particularly iron, to plants, which could reduce the deleterious effects of metal contamination. In addition, siderophores produced by these rhizosphere bacteria bind heavy metal ions and thus enhance their bioavailability in the rhizosphere of plants. The resulting increase in trace metal uptake by the plants caused by microbial siderophores might enhance the effectiveness of phytoextraction processes of contaminated soil. The following section high-lights the basic biology and chemistry of siderophores produced by bacteria (Rajkumar, et al., 2010).

2.5 Plant growth promoting bacteria (PGPB)

Plant growth-promoting rhizobacteria (PGPR), a group of beneficial plant bacteria, as potentially useful for stimulating plant growth and increasing crop yields has evolved over the past several years to where today researchers are able to repeatedly use them successfully in field experiments (Burr, et al., 1984). PGPR, root-colonizing bacteria are known to influence plant growth by various direct or indirect mechanisms. Several chemical changes in soil are associated with PGPR. Plant growth-promoting bacteria (PGPB) are reported to influence the growth, yield, and nutrient uptake by an array of mechanisms. Some bacterial strains directly regulate plant physiology by mimicking synthesis of plant hormones, whereas others increase mineral and nitrogen availability in the soil as a way to augment growth.

The isolates could exhibit more than two or three PGPR traits, which may promote plant growth directly or indirectly or synergistically (Yasmin, et al., 2007). The plant growth stimulating efficiency of bacterial inoculants is affected to nutrient uptake of maize in two different soils (Egamberdiyeva, 2007). The bacterial inoculation has a much better stimulatory effect on growth, yield and oil content of canola (*Brassica napus*, L.) in nutrient deficient soil (Asghar, et al., 2004). The simultaneous screening of rhizobacteria for growth promotion under biotic conditions and *in vitro* production of auxins is a useful approach for selecting effective PGPR. Some PGPR releases a blend of volatile components like 2, 3-butanediol and acetoin that promote growth of *Arabidopsis thaliana* (Ryu, et al., 2003). The diazotroph bacterial inoculation significantly increases the seed cotton yield, plant height and microbial population in soil (Anjum, et al., 2007). Double and triple combination of indol-3-butyric acid (IBA), bacteria and carbohydrates are more effective in increasing rooting capacity and more quality rooting in case of apple. (Karakurt, et al., 2009). The bacteria isolated from composts which included farm waste compost (FWC), rice straw compost (RSC), *Gliricidia vermin* compost (GVC), and macrofauna associated with FWC when applied with composts show the synergistic effect on the growth of pearl millet (Hameeda, et al., 2006). The use of PGPR with P-enriched compost in an integrated manner improves the growth, yield and nodulation in chickpea (Shahzad, et al., 2008).



2.5.1 Role of Plant growth promoting bacteria (PGPB)

Plant growth-promoting bacteria (PGPB) have the ability to promote a plant's growth (increase biomass) and increase tolerance to toxic heavy metals by nitrogen fixation, phosphate solubilisation, sulfate oxidation and synthesis of phytohormones such as indole-3-acetic acids (IAA), cytokinins, gibberellins and aminocyclo-propane-1-carboxylate (ACC) deaminase and induced systemic resistance (ISR) mechanism in the plant. Other mechanisms are the release of antibiotics, extracellular enzymes, chemical and volatile compounds such as lumichrome that allow respiration in roots and lead to an increase in the size of plants (Malik, et al., 1997; Ramette, et al., 2003; Bano and Fatima, 2009; Yan, et al., 2010). Examples microorganisms to promote plant growth are shown in Table 2.2.

1) *1-ammino-cyclopropane carboxylic acid (ACC) deaminase synthesis*

Ethylene is a plant hormone that is in the form of gases generated by the plant to control growth and developments such as fruitage, fruit ripening, effect of yellow and loss of leaves. If the level of ethylene is very high doses it can inhibit germination and inhibits the elongation of the root. Synthetic pathway of ethylene from the reaction of methionine with ATP and S-adenosylmethionone (SAM) occurs. Then SAM is converted to 1-ammino-cyclopropane carboxylic acid (ACC).



Table 2.2 Examples of plant growth-promoting rhizobacteria

plant growth-promoting rhizobacteria	
<i>Azorhizobium caulinodans</i>	<i>Citrobacter freundii</i>
<i>Azospirillum amazonense</i>	<i>Curtobacterium flaccumfaciens</i>
<i>Azospirillum halopraeferens</i>	<i>Enterobacter agglomerans</i>
<i>Azospirillum irakense</i>	<i>Enterobacter cloacae</i>
<i>Azospirillum lipoferum</i>	<i>Erwinia herbicola</i>
<i>Azospirillum brasilense</i>	<i>Flavomanas oryzihabitans</i>
<i>Bacillus cereus</i>	<i>Klebsiella planticola</i>
<i>Bacillus coagulans</i>	<i>Kluyvra ascorbata</i>
<i>Bacillus laterosporus</i>	<i>Kluyvera cryocrescens</i>
<i>Bacillus licheniformis</i>	<i>Phyllobacterium rubiacearum</i>
<i>Bacillus macerans</i>	<i>Pseudomonas aeruginosa</i>
<i>Bacillus megaterium</i>	<i>Pseudomonas aureofaciens</i>
<i>Bacillus mycoides</i>	<i>Pseudomonas corrugata</i>
<i>Bacillus pasteurii</i>	<i>Pseudomonas fluorescens</i>
<i>Bacillus polymyxa</i>	<i>Pseudomonas marginalis</i>
<i>Bacillus pumilus</i>	<i>Pseudomonas putida</i>
<i>Bacillus sphaericus</i>	<i>Pseudomonas rubrilineans</i>
<i>Bacillus subtilis</i>	<i>Rathyibacter rathayi</i>
<i>Burkholderia cepacia</i>	<i>Serratia marcescens</i>
<i>Burkholderia gladioli</i>	<i>Stenotrophomonas sp.</i>
<i>Burkholderia graminis</i>	<i>Streptomyces griseoviridis</i>

Source: (Glick, et al., 1999)



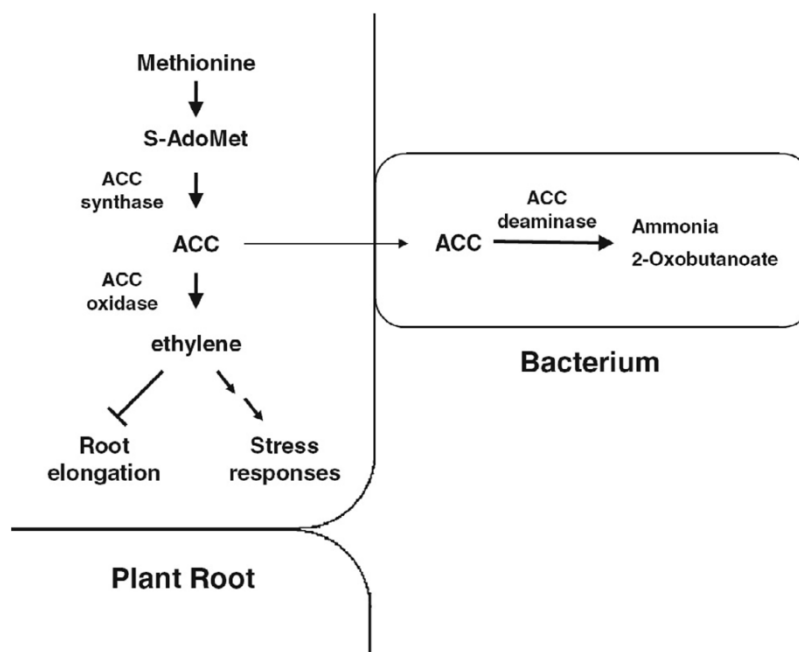


Figure 2.2 A possible mechanism of how stress controller bacteria reduce ethylene levels in the plant root using bacterial ACC deaminase. ACC synthesized in plant tissues by ACC synthase is thought to be exuded from plant roots and taken up by neighboring bacteria. Subsequently, the bacteria hydrolyze ACC to ammonia and 2-oxobutanoate. This ACC hydrolysis maintains ACC concentrations low in bacteria and permits continuous ACC transfer from plant roots to bacteria. Otherwise, ethylene can be produced from ACC and then cause stress responses including growth inhibition. S-AdoMet: S-adenosyl-L-methionine; ACC: 1-aminocyclopropane-1-carboxylate (Adapted from Glick, et al., 1998; Kang, et al., 2010; Ahemad and Kibret, 2014)

The ACC is converted into ethylene by Ethylene-Forming Enzyme activity in the vacuole membrane, ethylene process will be driven by external factors such as wounding water stress etc. and internal factors such as fruit ripening and high oxygen etc. Some PGPR can stimulate plant growth through the mechanism of the enzyme ACC deaminase (Figure 2.2) revealed that PGPR synthesize auxin at high doses ACC synthase enzyme synthesis will be high. The bacteria are digested by ACC 1-amino-cyclopropane carboxylic acid (ACC) deaminase and changed ACC to ammonia and alpha-ketobutyrate (α -KB). The effect of ACC deaminase activity



is reduced level of ACC and cannot inhibit the growth of roots plant (Belimov, et al., 2005; Rajkumar and Freitas, 2008a, b; Saharan and Nehra, 2011).

2) *Siderophore production*

Iron is a nutrient amounts on the surface world, but generally in the form of the compound ferric (Fe^{3+}), while almost all microorganisms require iron for use in the synthesis site in chrome (cytochromes) and several enzymes. Most of the siderophores are water-soluble and can be divided into extracellular siderophores and intracellular siderophores. Generally, rhizobacteria differs regarding the siderophore cross-utilizing ability; some are proficient in using siderophores of the same genus (homologous siderophores) while others could utilize those produced by other rhizobacteria of different genera (heterologous siderophores) (Khan, et al., 2009). Many bacteria species have a siderophore (Figure 2.3). In both Gram-negative and Gram-positive rhizobacteria, iron (Fe^{3+}) in Fe^{3+} -siderophore complex on bacterial membrane is reduced to Fe^{2+} which is further released into the cell from the siderophore via a gating mechanism linking the inner and outer membranes. During this reduction process, the siderophore may be destroyed/recycled (Rajkumar, et al., 2010; Neilands, 1995). Thus, siderophores act as solubilizing agents for iron from minerals or organic compounds under conditions of iron limitation (Indiragandhi, et al., 2008). Not only iron, siderophores also form stable complexes with other heavy metals that are of environmental concern, such as Al, Cd, Cu, Ga, In, Pb and Zn, as well as with radionuclides including U and Np (Neubauer, et al., 2000; Kiss and Farkas, 1998).

3) *Indole-3-acetic-acid (IAA) production*

Indole-3-acetic acid or IAA is the plant hormone auxin is a colorless Microbial synthesis of the phytohormone auxin (indole-3-acetic acid/indole acetic acid/IAA) has been known for a long time. It is reported that 80% of microorganisms isolated from the rhizosphere of various crops possess the ability to synthesize and release auxins as secondary metabolites (Patten and Glick, 1996). Generally, IAA secreted by rhizobacteria interferes with the many plant developmental processes because the endogenous pool of plant IAA may be altered by the acquisition of IAA that has been secreted by soil bacteria (Glick, 2012; Spaepen, et al., 2007). Evidently, IAA also acts as a reciprocal signaling molecule affecting gene expression in



several microorganisms. Consequently, IAA plays a very important role in rhizobacteria-plant interactions (Spaepen and Vanderleyden, 2011).

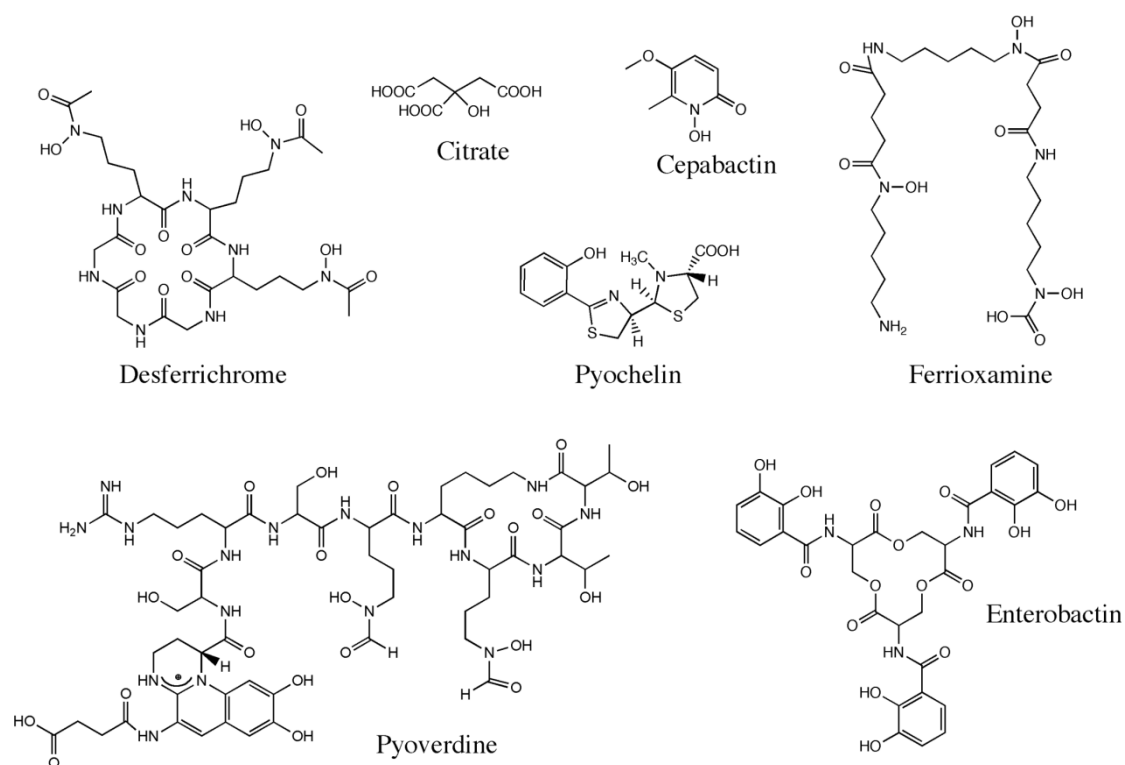


Figure 2.3 Examples of siderophore structures. Desferrichrome is produced by *Aspergillus* or *Ustil* and is a hydroxamate siderophore like ferrioxamine (Leong and Winkelmann, 1998; Braun, 2003). Enterobactin is a catechol siderophore produced by *E. coli* (Raymond, et al., 2003). Pyoverdine is produced by *aeruginosa*, *P. PAO1* and is a mixed siderophore, which carries both hydroxamate and catecholate groups. Citrate is considered to be a siderophore (Yueet, et al., 2003). Cepabactin is a 1-hydroxy-2-pyridinone bidentate siderophore produced by *Burkholderia cepacia* (Klumpp, et al., 2005). Pyochelin is a 2-(2-o-hydroxyphenyl-2-thiazolin-4-yl)-3-methylthiazolidine-4-carboxylic acid produced by *aeruginosa*, *P.* and *cepacia*, *B.* which chelates iron via oxygen and nitrogen electron donor atoms (Cox, et al., 1981; Youard, et al., 2007; Hoegy, et al., 2009).



Moreover, down-regulation of IAA as signaling is associated with the plant defense mechanisms against a number of phyto-pathogenic bacteria as evidenced in enhanced susceptibility of plants to the bacterial pathogen by exogenous application of IAA or IAA produced by the pathogen (Spaepen and Vanderleyden, 2011). IAA has been implicated in virtually every aspect of plant growth and development, as well as defense responses. This diversity of function is reflected by the extraordinary complexity of IAA biosynthetic, transport and signaling pathways (Santner, et al., 2009). Generally, IAA affects plant cell division, extension, and differentiation; stimulates seed and tuber germination; increases the rate of xylem and root development; controls processes of vegetative growth; initiates lateral and adventitious root formation; mediates responses to light, gravity and florescence; affects photosynthesis, pigment formation, biosynthesis of various metabolites, and resistance to stressful conditions. IAA produced by rhizobacteria likely, interfere the above physiological processes of plants by changing the plant auxin pool.

Moreover, bacterial IAA increases root surface area and length, and thereby provides the plant greater access to soil nutrients. Also, rhizobacterial IAA loosens plant cell walls and as a result facilitates an increasing amount of root exudation that provides additional nutrients to support the growth of rhizosphere bacteria (Glick, 2012). Thus, rhizobacterial IAA is identified as an effector molecule in plant–microbe interactions, both in pathogenesis and phytostimulation (Spaepen and Vanderleyden, 2011).

4) *Antibiotics and antifungal Metabolites production*

Many PGPR can be produced Antibiotics (Table 2.3) such as *Pseudomonas fluorescens* as a synthesis of hydrogen cyanide which makes *Pseudomonas* species capable of inhibiting the growth of fungi pathogenic of plants. For example of *Thielabiopsis basicola* can be inhibit the black root rot disease of fungal pathogen in tobacco (Ramette et al., 2003). Some reports found that the variety of microorganisms including *Cladosporium werneckii*, *Pseudomonas cepacia* and *P. solanacearum* can degrade fusaric acid compound to fusaric acid, which causes damage to the plants after the plants were infected by *Fusarium* (Ramamoorthy, et al., 2001).



5) Nitrogen fixation

Nitrogen (N) is the most vital nutrient for plant growth and productivity. Although, there is about 78% N₂ in the atmosphere, it is unavailable to the growing plants. The atmospheric N₂ is converted into plant-utilizable forms by biological N₂ fixation (BNF) which changes nitrogen to ammonia by nitrogen fixing microorganisms using a complex enzyme system known as nitrogenase (Kim and Rees, 1994).

Table 2.3 Examples plant growth-promoting rhizobacteria to control fungi that cause plant disease.

Bacteria	Fungi	Plants
<i>Actinoplanes</i> spp.	<i>Pythium ultimum</i>	Table beet
	<i>Rhizoctonia solani</i>	Table beet
<i>Bacillus</i> spp.	<i>Gaeumannaomyces graminis</i>	Wheat
	var. <i>tritici</i>	
<i>Bacillus subtilis</i> GB03	<i>Fusarium oxysporum</i> sp. <i>ciceris</i>	Mung bean
<i>B. subtilis</i> BACT-D	<i>Pythium aphanidermatum</i>	Tomato
<i>Burkholderia cepacia</i> A3R	<i>Fusarium graminearum</i>	Wheat
	<i>Fusarium</i> spp.	Wheat
<i>Burkholderia cepacia</i> PHQM 100	<i>Phythium</i> spp.	Maize
<i>Comamonas acidovorans</i> HF42	<i>Magnaporthe poae</i>	Kentucky bluegrass
		Kentucky Bluegrass
<i>Enterobacter</i> sp. BF14	<i>Drethlera graminea</i>	Barley
		Oat
<i>Pseudomonas chloroaphis</i> MA342	<i>D. avenea</i>	Oat
	<i>Ustilago avenea</i>	Oat
	<i>Tilletia caries</i>	Wheat
<i>P. chloroaphis</i> PCL 1391	<i>Fusarium oxysporum</i> sp.	Tomato
	<i>radicis-lycopersici</i>	
<i>P. fluorescens</i>	<i>Fusarium oxysporum</i> sp.	Chinese
<i>P. fluorescens</i> Q8r1-96	<i>raphani</i>	Cabbage
	<i>Gaeumannaomyces graminis</i>	Wheat
<i>P. fluorescens</i> VO61	<i>Pythium ultimum</i>	Rice
	<i>Rhizoctonia solani</i>	
<i>P. putida</i>	<i>Fusarium oxysporum</i> sp.	Chinese
	<i>raphani</i>	Cabbage
<i>Stenotrophomonas maltophilia</i> C3	<i>Rhizoctonia solani</i>	Tall fescue

Source: (Glick, et al., 1999)



In fact, BNF accounts for approximately two-thirds of the nitrogen fixed globally, while the rest of the nitrogen is industrially synthesized by the Haber–Bosch process (Rubio and Ludden, 2008). Biological nitrogen fixation occurs, generally at mild temperatures, by nitrogen fixing microorganisms, which are widely distributed in nature (Raymond et al., 2004). Furthermore, BNF represents an economically beneficial and environmentally sound alternative to chemical fertilizers (Ladha, et al., 1997).

6) *Phosphate solubilization and import of nutrients*

Phosphorus (P), the second important plant growth-limiting nutrient after nitrogen, is abundantly available in soils in both organic and inorganic forms (Khan, et al., 2009). Despite of large reservoir of P, the amount of available forms to plants is generally low. This low availability of phosphorous to plants is because the majority of soil P is found in insoluble, while the plants absorb it only in two soluble forms, the monobasic (H_2PO_4^-) and the dibasic (HPO_4^{2-}) ions (Bhattacharyya and Jha, 2012). The insoluble P is present as an inorganic mineral such as apatite or as one of several organic forms including inositol phosphate (soil phytate), phosphomonesters, and phosphotriesters (Glick, 2012). To overcome the P deficiency in soils, there are frequent applications of phosphatic fertilizers in agricultural fields. Plants absorb fewer amounts of applied phosphatic fertilizers and the rest is rapidly converted into insoluble complexes in the soil (Mckenzie and Roberts, 1990). But regular application of phosphate fertilizers is not only costly but is also environmentally undesirable. This has led to search for an ecologically safe and economically reasonable option for improving crop production in low P soils. In this context, organisms coupled with phosphate solubilizing activity, often termed as phosphate solubilizing microorganisms (PSM), may provide the available forms of P to the plants and hence a viable substitute to chemical phosphatic fertilizers (Khan et al., 2006). Of the various PSM(s) inhabiting the rhizosphere, phosphate-solubilizing bacteria (PSB) are considered as promising biofertilizers since they can supply plants with P from sources otherwise poorly available by various mechanisms (Fig. 2.4) (Zaidi, et al., 2009). Bacterial genera like *Azotobacter*, *Bacillus*, *Beijerinckia*, *Burkholderia*, *Enterobacter*, *Erwinia*, *Flavobacterium*, *Microbacterium*, *Pseudomonas*, *Rhizobium* and *Serratia* are reported as the most significant phosphate solubilizing bacteria (Bhattacharyya and Jha, 2012).



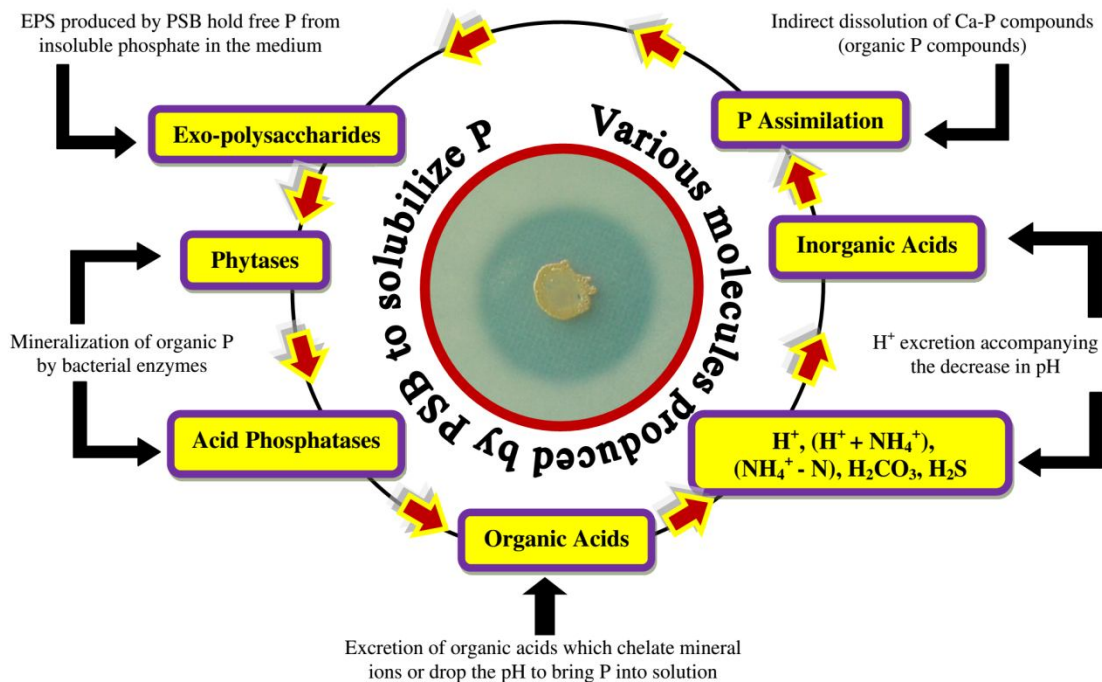


Figure 2.4 Various organic/inorganic substances produced by PSB responsible for phosphate solubilization in soils (Ahemad and Kibret, 2014)

Typically, the solubilization of inorganic phosphorus occurs as a consequence of the action of low molecular weight organic acids which are synthesized by various soil bacteria (Zaidi, et al., 2009). Conversely, the mineralization of organic phosphorus occurs through the synthesis of a variety of different phosphatases, catalyzing the hydrolysis of phosphoric esters (Glick, 2012). Importantly, phosphate solubilization and mineralization can coexist in the same bacterial strain (Tao, et al., 2008).

2.5.2 Utilization of PGPB for remediation of heavy metals

Efficiency in the recovery area is based on the relationship between soil, heavy metals, microorganism and plants. The relationship between plants and microorganism depends on soil properties that affect the movement of heavy metals into the soil to plant roots, secrete compounds, amount of nutrients in the soil, etc., by way of metabolic depression to determine the relationship of species of plants and bacteria in the restoration of contaminated sites (Jing, et al., 2007).



The function of hyperaccumulation depends not only on the plant, but also on the interaction of the plant roots with rhizosphere microbes and the concentrations of bioavailable metals in the soil. The rhizosphere provides a complex and dynamic microenvironment where microorganisms, in association with roots, form unique communities that have considerable potential for the detoxification of hazardous materials. The rhizosphere bacteria play a significant role on plant growth in serpentine soils by various mechanisms. The metal-resistant serpentine isolates increase the efficiency of phytoextraction directly by enhancing the metal accumulation in plant tissues and indirectly by promoting the shoot and root biomass of hyperaccumulators. Hence, isolation of the indigenous and stress-adapted beneficial bacteria serves as a potential biotechnological tool for inoculation of plants for the successful restoration of metal-contaminated ecosystems (Rajkumar, et al., 2009). Plant–microbe interactions in the rhizosphere soils are responsible for various processes that influence plant growth, heavy metal and nutrient mobilization, etc., in metal polluted soils. A wide range of stress tolerant microorganisms (e.g., rhizosphere bacteria and mycorrhizae) associated with plants have the ability to promote the growth of the host plant in polluted soils by various mechanisms (Glick, 2010; Ma, et al., 2009a, 2009b, 2011; Miransari, 2011; Rajkumar, et al., 2009, 2010). Besides, the plant associated microbes residing in the rhizosphere alter pollutant mobility and availability to the plants through release of chelating agents, biosurfactants, acidification, phosphate solubilization and redox changes (Glick, 2010; Ma, et al., 2009b; Rajkumar, et al., 2010, 2012). An example is the production of pyoverdine and pyochelin by rhizosphere bacteria *Pseudomonas aeruginosa*, which increase the concentrations of bioavailable Cr and Pb in the rhizosphere, thus making them available for maize uptake (Braud, et al., 2009b). Dimkpa, et al. (2009) also found that the siderophores produced by *Streptomyces tendae* F4 significantly enhanced uptake of Cd by sunflower plant.



2.6 Fourier transform infrared (FT-IR) spectroscopy

Fourier transform infrared (FT-IR) spectroscopy is a useful technique for microbial identification. The revival of IR-spectroscopy as a means for characterizing microbial samples was initiated after the development of modern interferometric IR-spectroscopy, the availability of low-cost minicomputers and powerful new algorithms for multivariate statistical analysis and pattern recognition methodologies (Naumann, et al., 1988; Maquelin and Kirschner, 2002). In the past four decades, it has been clearly demonstrated by several authors that infrared spectra from bacteria can be used for identification and differentiation (Lipkus, et al., 1990; Curk, et al., 1994; Margarita and Quinteiro, 2000). In addition, FT-IR spectroscopy has been shown to be a powerful technique for the study of biological macromolecules (Siebert, 1995).

2.6.1 Technical properties of FT-IR spectroscopy

FT-IR spectroscopy is a form of vibrational spectroscopy, and the FT-IR spectrum reflects both molecular structure and molecular environment. In this technique, the sample is irradiated with infrared radiation from an infrared source, and the absorption of this radiation stimulates vibrational motions by depositing quanta of energy into vibrational modes (Sacksteder and Barry, 2001; Gomez, et al., 2003). Therefore, a molecule, when exposed to radiation produced by the thermal emission of a hot source (a source of IR energy), absorbs only at frequencies corresponding to its molecular modes of vibration in the region of the electromagnetic spectrum between visible (red) and short waves (microwaves). These changes in vibrational motion give rise to bands in the vibrational spectrum; each spectral band is characterized by its frequency and amplitude (Margarita and Quinteiro, 2000; Sacksteder and Barry, 2001).

The IR region (1 to 100 μM) is subdivided in three zones, far-(100 to 25 μM), mid-(25 to 2.5 μM), and near IR (2.5 to 1 μM) (Figure 2.2). The mid-IR depicts primary molecular vibrations and is the most common and widely employed region for the analysis of substances in chemistry and forensics. All molecules present characteristic absorbance peaks in a section of this region (1350 cm^{-1} to 1000 cm^{-1} ; NB: by convention, the Frequency is usually expressed as wavenumbers using the reciprocal cm as its unit: $1\text{ }\mu\text{M}=10^4\text{ cm}^{-1}$), thus this physical property is considered as a molecular fingerprint. To understand FT-IR spectra of biological samples, some fundamental



knowledge on cell composition and the particular structures of the building blocks in biological samples is essential. It is important to recognize that infrared spectra of complex biological materials do not only describe the composition of cell, but also provide a number of specific bands that are sensitive to structural or conformational changes. It is also matter of fact that the physical state of the sample (hydration or aggregation state etc.) has a severe influence on FT-IR results. This makes it necessary to standardize sampling, preparation, and data acquisition procedures rigorously. IR spectroscopy was greatly improved by the use of a new component: the interferometer and by the application of a mathematical transformation, the fast Fourier transform algorithm which allow for the simultaneous detection of all the transmitted energy (Figure 2.3a, b) (Naumann, 2000).

If cells are regarded as a complex mixture of bimolecular organized within different structures, every microbial cell will have a unique and characteristic spectrum stemming from the vibrational modes of all the molecules within it. The differences of spectral feature was among taxons that are expressed as quantitative differences in the composition and presence of the cell structures of each group could be translated into molecular differences.. For microbiological identification, two basic approaches can be distinguished in the chemometric techniques used at the moment. The first is based upon non-supervised or objective classification methods, analyzing naturally occurring groups in the data set and requiring no a priority knowledge of the sample identity; examples are factor analysis, principal component analysis (PCA) and hierarchical cluster analysis. Based on objective criteria of group membership, unknown samples are assigned to naturally occurring groups in the data set.

Inclusion of well-characterized samples in the analysis scheme allows groups to be identified on the basis of the properties/identities of these reference samples. The second group of chemometric techniques used in microbial identification is supervised techniques, i.e. requiring a priori knowledge of the sample identity.



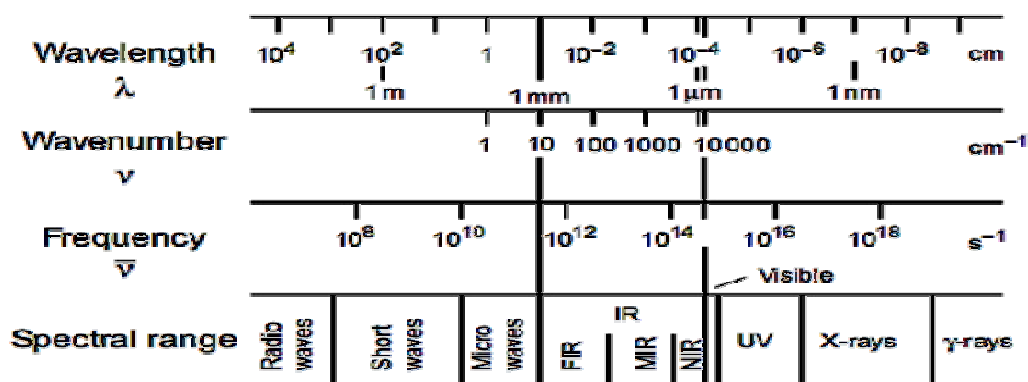


Figure 2.5 The electromagnetic spectrum (Naumann, 2000).

With a set of well-characterized samples, a model can be trained so that it can predict the identity of unknown samples. Examples of supervised methods are linear discriminant analysis (LDA) and artificial neural networks (ANNs) (Naumann, 1998; Margarita and Quinteiro, 2000; Maquelin and Kirschner, 2002).

2.6.2 Applications of FT-IR spectroscopy in microbiology

FT-IR spectra of intact microbial cells are highly specific, fingerprint-like signature which can be used to (i) discriminate between diverse microbial species and strains, (ii) detect *in situ* intracellular components or structures such as inclusion bodies, storage materials or endospores, (iii) detect and quantify metabolically released CO_2 in response to various different substrates, and (iv) characterize growth-dependent phenomena and cell-drug interactions. The characteristic information is extracted from the spectral contours by applying resolution enhancement techniques, difference spectroscopy, and pattern recognition methods such as factor, cluster, linear discriminant analysis, and artificial neural networks. Particularly interesting applications arise by means of a light microscope coupled to the spectrometer. FT-IR spectroscopy of the whole cells is a valuable tool for monitoring the bacterial growth, changes in the spectroscopic features (Figure 2.4) and identification of microorganisms and is used, e.g. in strain collections, medical applications, pharmaceutical industry and drinking water control (Naumann, 1998; Schuster, et al., 1999; Yu and Irudayaraj, 2005; Ueshima, et al., 2008).



Examples of FT-IR application in microbiology, Yu and Irudayaraj (2005) studied the spectral fingerprints of bacteria with technical FT-IR microspectroscopy and analyze the spectral features and check for changes when bacteria undergo metabolism. They showed that FT-IR technique can be used to study the effect of environment on growth and inhibit cell growth. FT-IR spectroscopy technique and a fluorescent staining showed the binding between cadmium and extracellular polymeric substance (EPS) produced by *Pseudomonas putida* cells, and property of cell wall in reducing the cadmium toxicity (Ueshima, et al., 2008). Dziuba, et al (2007) used FT-IR spectroscopy technique to analyze the differences and identify bacterial species in the genus *Lactococcus*, *Leuconostoc* and *Streptococcus pediococcus* and create a FT-IR spectrum database for use in monitoring the species.



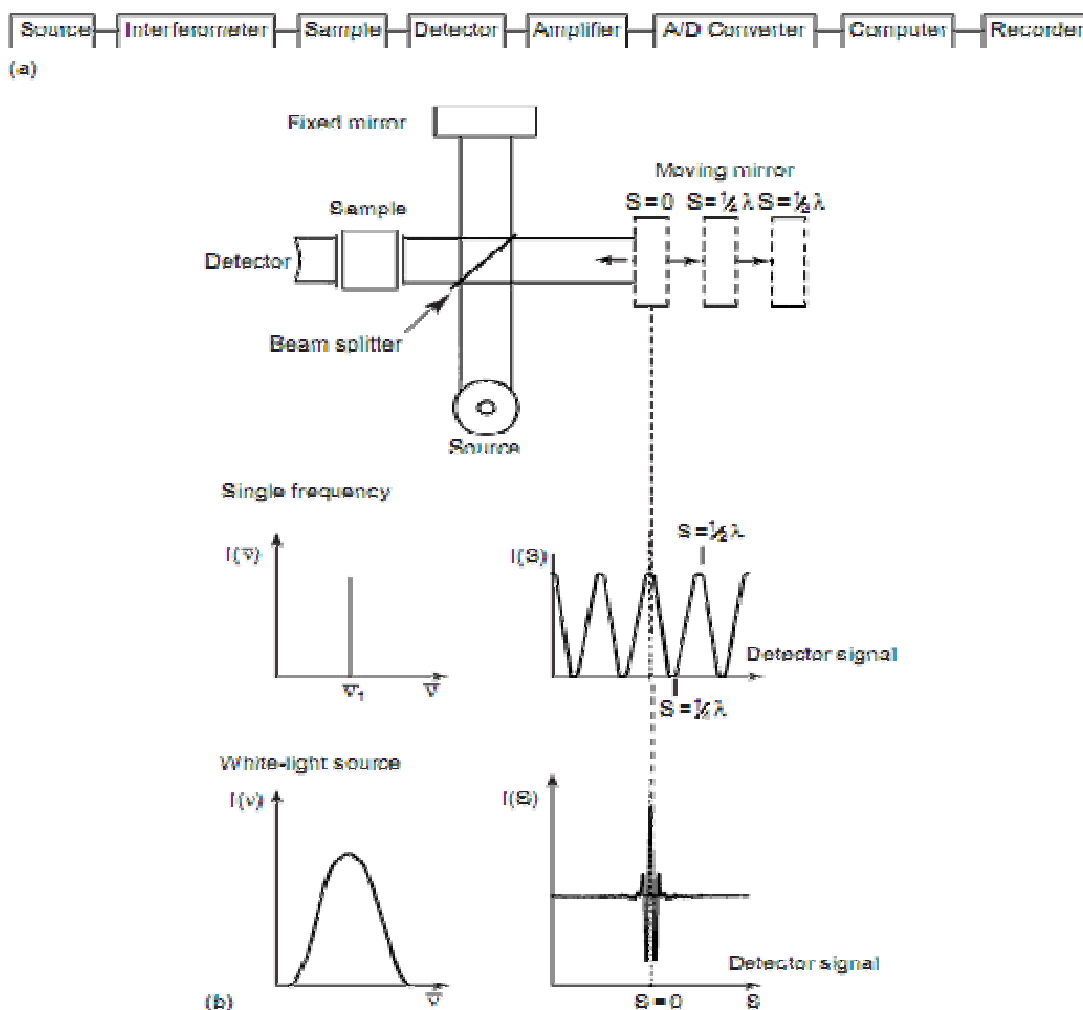


Figure 2.6 (a) FT-IR spectrometer block scheme of the basic components of an FT-IR spectrometer. (b) working principle of a Michelson interferometer consisting of a light source, beam splitter, fixed mirror, moving mirror, detector and a sample (upper panel). A single frequency light source (central panel, left) is modulated to a sinusoidal signal observed by the detector (central panel, right). A white-light source (e.g. emitted from a globar) is transformed to the interferogram (lower panel) (Naumann, et al., 2000).

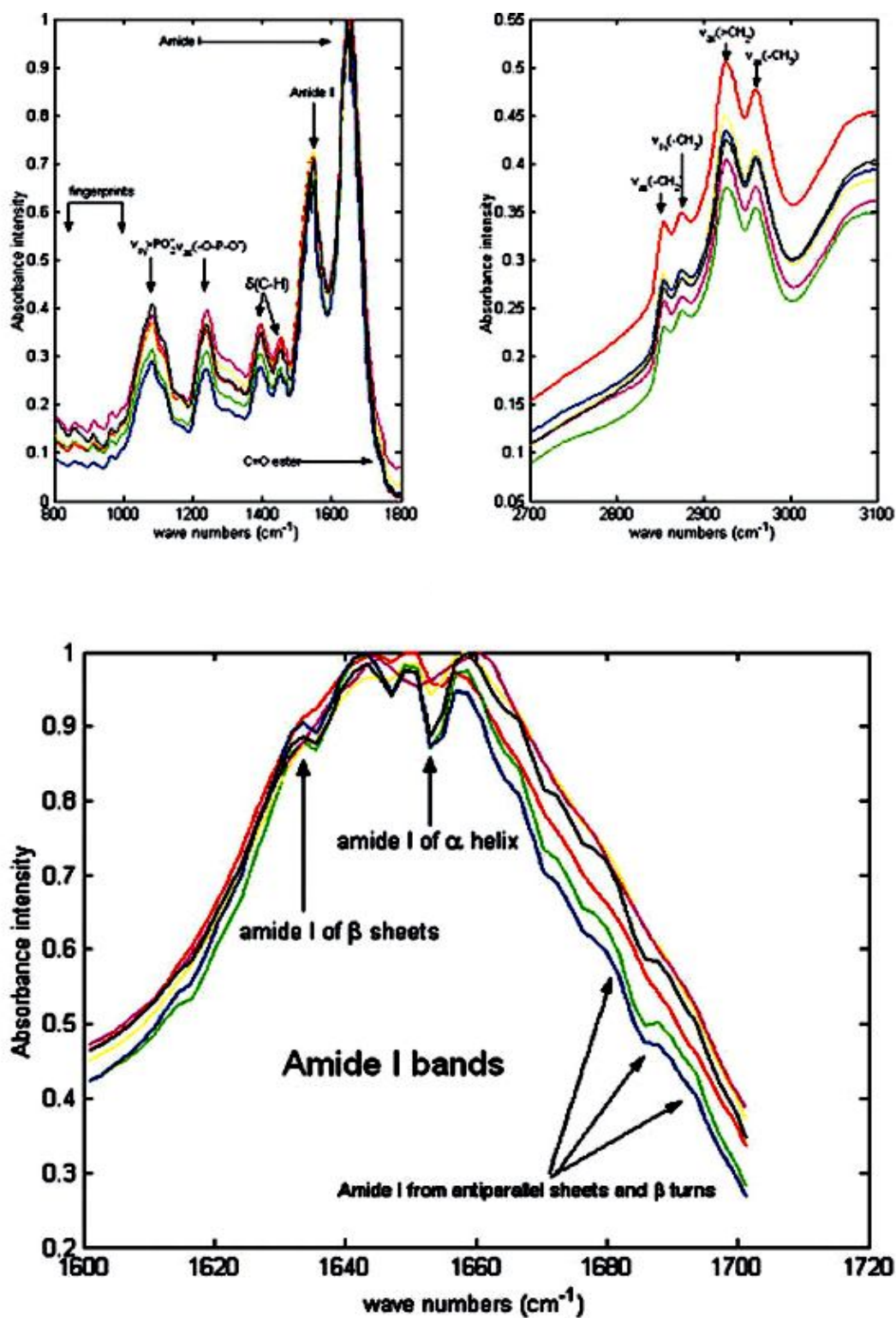


Figure 2.7 Spectra of different microorganisms measured by FT-IR microspectrometry.
(Yu and Irudayaraj, 2005)



2.7 Polymerase chain reaction (PCR) Amplification

The polymerase chain reaction (PCR) is a relatively simple technique that amplifies a DNA template to produce specific DNA fragments *in vitro*. Traditional methods of cloning a DNA sequence into a vector and replicating it in a living cell often require days or weeks of work, but amplification of DNA sequences by PCR requires only hours. While most biochemical analyses, including nucleic acid detection with radioisotopes, require the input of significant amounts of biological material, the PCR process requires very little. Thus, PCR can achieve more sensitive detection and higher levels of amplification of specific sequences in less time than previously used methods. These features make the technique extremely useful, not only in basic research, but also in commercial uses, including genetic identity testing, forensics, industrial quality control and *in vitro* diagnostics. Basic PCR is commonplace in many molecular biology labs where it is used to amplify DNA fragments and detect DNA or RNA sequences within a cell or environment (Saiki, et al., 1985). The PCR process was originally developed to amplify short segments of a longer DNA molecule. A typical amplification reaction includes target DNA, a thermostable DNA polymerase, two oligonucleotide primers, deoxynucleotide triphosphates (dNTPs), reaction buffer and magnesium. Once assembled, the reaction is placed in a thermal cycler, an instrument that subjects the reaction to a series of different temperatures for set amounts of time. This series of temperature and time adjustments is referred to as one cycle of amplification. Each PCR cycle theoretically doubles the amount of targeted sequence (amplicon) in the reaction. Ten cycles theoretically multiply the amplicon by a factor of about one thousand; 20 cycles, by a factor of more than a million in a matter of hours (Saiki, et al., 1985).

Each cycle of PCR includes steps for template denaturation, primer annealing and primer extension (Figure 2.5). The initial step denatures the target DNA by heating higher. In the denaturation process, the two intertwined strands of DNA separate from one another, producing the necessary single-stranded DNA template for replication by the thermostable DNA polymerase. In the next step of a cycle at this temperature (annealing) approximately 40–60°C, the oligonucleotide primers can form stable associations with the denatured target DNA and serve as primers for the DNA polymerase. Finally, the synthesis of new DNA begins as the reaction temperature is



raised to the optimum for the DNA polymerase. For most thermostable DNA polymerases. The extension step lasts. The next cycle begins with a return to 94°C for denaturation. Each step of the cycle should be optimized for each template and primer pair combination. If the temperature during the annealing and extension steps are similar, these two steps can be combined into a single step in which both primer annealing and extension take place. After 20–40 cycles, the amplified product may be analyzed for size, quantity, sequence, etc., or used in further experimental procedures (Bermejo-Alvarez, et al., 2008; Staniszewska, et al., 2007; Promega, 2002).

2.8 Electrophoresis

2.8.1 Principle of electrophoresis

Electrophoresis is the movement of an electrically charged substance under the influence of an electric field. This movement is due to the Lorentz force, which may be related to fundamental electrical properties of the body under study and the ambient electrical condition (Amersham, 1999). Gel electrophoresis is a technique in which charged molecular, such as proteins or DNA, are separated according to physical properties as they are forced through a gel by electrical current. This method is limited to special application; instead gels of polyacrylamide are commonly used. The pore size of these gels can be adjusted by the polyacrylamide concentration (Figure 2.6). If very large pore are required, agarose or starch gels are used instead (Buxbaum, 2007).

2.8.2 Sodium dodecyl sulfate polyacrylamide gel electrophoresis (SDS-PAGE)

Gel electrophoresis is used for the analysis of protein mixtures and allows for quick molecular weight determinations. Hence, SDS gels belong to the protein biochemist like forms to the accountant. It is desirable to establish a gel system that takes only 30 to 45 minutes per gel run. Beautiful bands are desirable, but not necessary. Most proteins bind the detergent SDS to negatively loaded SDS protein complexes with a constant charge to mass ratio (1.4 g SDS/g protein in 1% SDS solutions). SDS denatures the proteins especially after previous reduction with mercaptoethanole or 4, 4'-Dichloro Diphenyl Trichloro ethane (DTT) and prevents protein to protein interactions (quarternary structures).



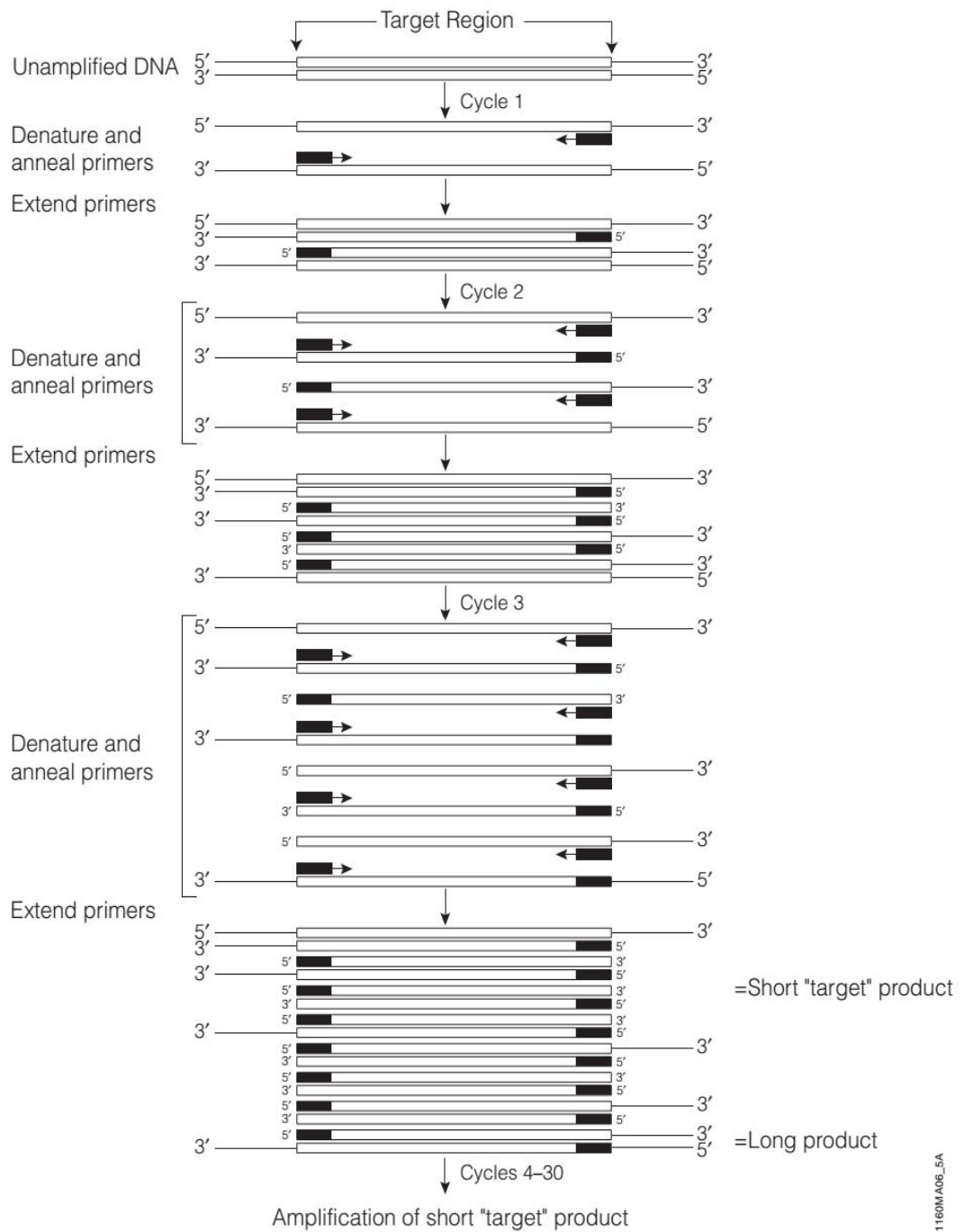


Figure 2.8 Schematic diagram of the PCR process. (Promega, 2002).

For the purposes of many measuring methods, the SDS-protein complexes of different proteins thus differ only in their size and have comparable hydrodynamic qualities (Rehm, 2006).



During SDS electrophoresis, the SDS-protein complex moves in the electric field toward the positive pole. The molecular sieve effect of a porous polyacrylamide matrix separates the SDS protein complexes according to their Stokes radius and thus according to their molecular weight (MW) (Rehm, 2006).

The various SDS gel electrophoresis systems differ among other things in the buffers they use. The discontinuous Lämmli system with Tris-glycine buffers is the most widely used. A stacking gel (Tris-glycine buffer pH 6.8; 3 to 4% acrylamide) is poured over a separation or running gel (Tris-glycine buffer pH 8.8; 5 to 20% acrylamide). The longer the running gel the better the separation. The thinner the gel the nicer the bands and the less can/may be loaded. With 1.5 mm thick gels and 0.5-cm-wide pockets, the upper limit of the load is 1 mg of protein/ pocket.

Fifteen percent separation gels are suited for proteins of an MW of 10 to 60 kd, 10% gels for proteins of an MW of 30 to 120 kd, and 8% gels for proteins of an MW of 50 to 200 kd (Figure 2.6). 18% gels with 7 to 8 M of urea can separate mixtures of small proteins and peptides (MW 1.5 to 10 kd) (Hashimoto et al. 1983). However, urea crystallizes from concentrated solutions and at temperatures less than RT it carbamylizes proteins and interferes with the binding of SDS. The alternative is a Tris in gel system after Schägger and Jagow (1987). It separates peptides between 1 and 100 kd and does not require urea (Figure 2.6).

Gradient gels (e.g., 8 to 15%) have a broader separation range and bands that are slightly more defined. Gradient mixers are suited for pouring linear gradients. However, it is easier to first draw the light solution into a glass pipette using a Peleus ball and then the heavy solution. Allowing a few air bubbles to pass between the two layers transforms them into a gradient that is poured between the glass plates of the electrophoresis apparatus. Perfectionists add another 5% cane sugar and dye to the heavy phase (the higher-percent acrylamide) and visually follow the course and extent of the gradient formation (Rehm, 2006). Smith and Bell's (1986) machine pours good exponential gradients. Gels storage is possible by using gels wrapped in wet tissues can be kept in a sealed plastic bag for up to two weeks.



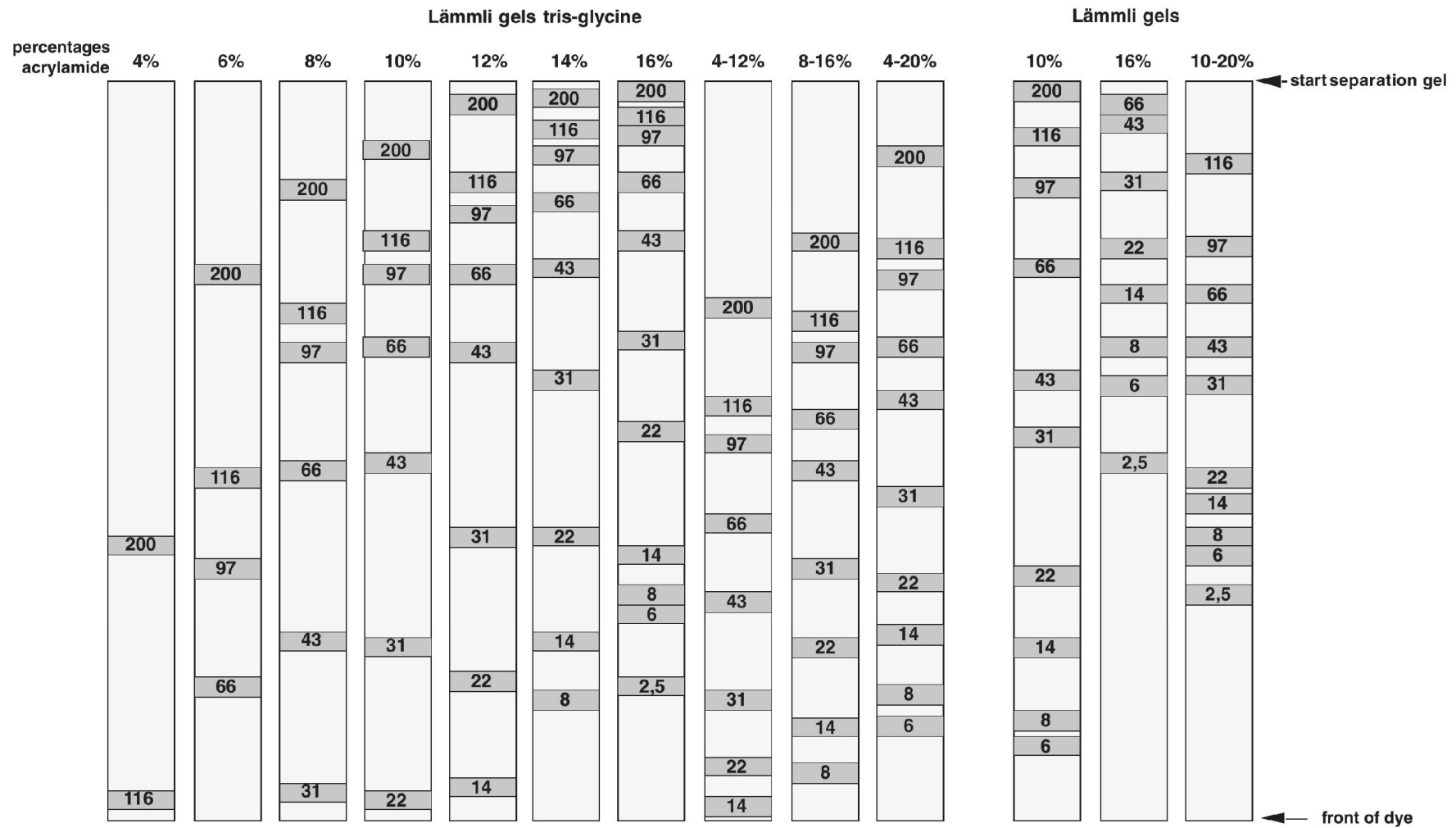


Figure 2.9 Run speed of molecular weight markers in SDS gels. (Lämmli, 1970; Rehm, 2006)

CHAPTER 3

Methodology

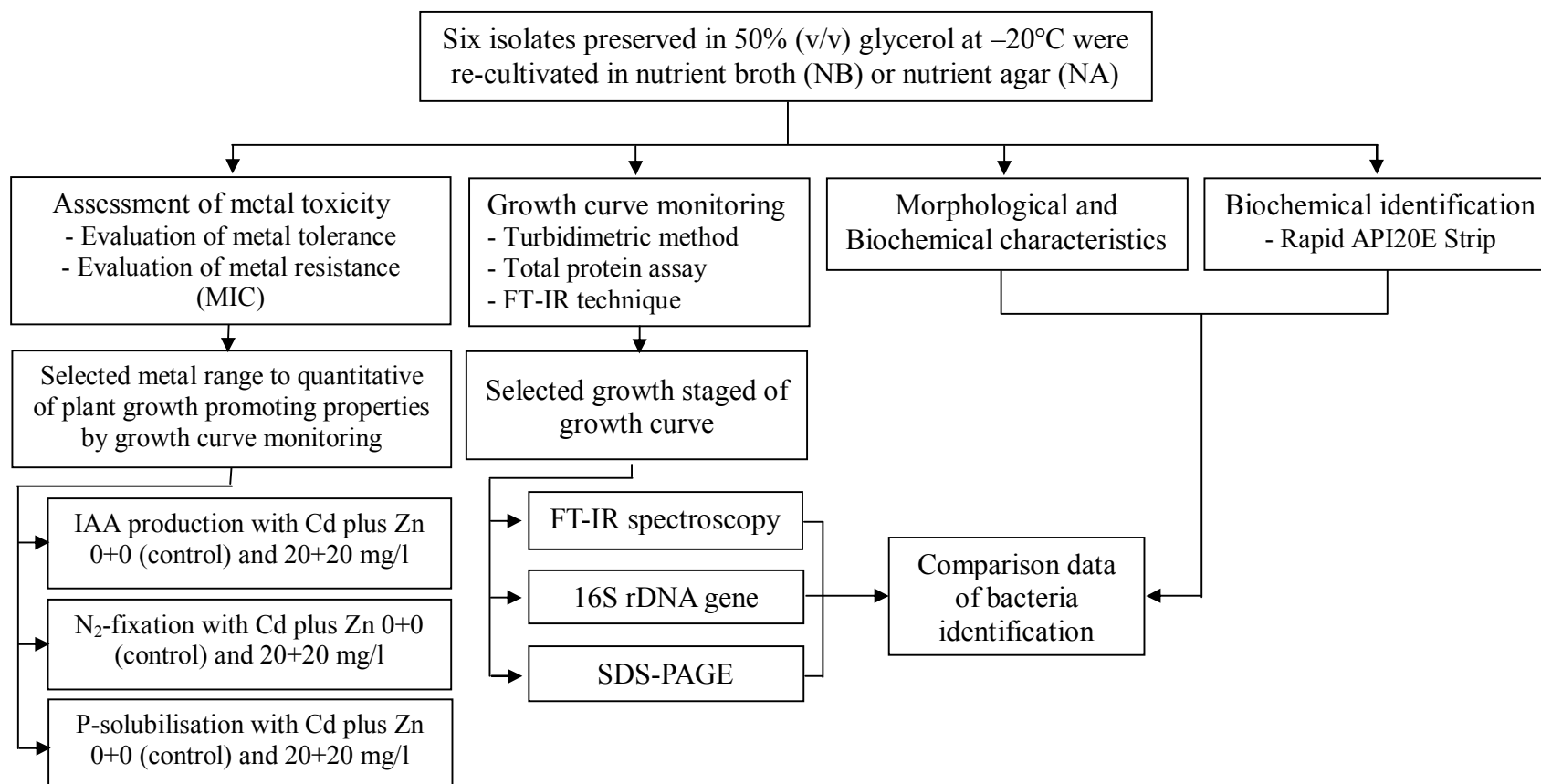
This research was designed as an experimental laboratory to identify six bacterial isolates and compare with three techniques of genotype characteristics of partial 16S rRNA sequence, FT-IR microspectroscopy, and whole cell protein patterns obtained from SDS-PAGE. Zn and/or Cd resistance and characteristic of plant growth promoting properties under metals treatment was investigated.

3.1 Research diagram

3.2 Materials and Methods



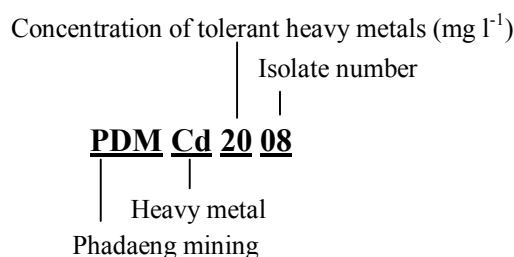
3.1 Research diagram



3.2 Materials and methods

3.2.1 Microorganisms

The bacterial isolates of PDMZn2008, PDMCd0501, PDM Cd2007, PDMCd2008, PDMZnCd1502 and PDMZnCd2003 were studied in this experiment. Meesungnoen, et al. (2009) reported their properties of plant growth promoting and zinc and cadmium tolerance. They were given code names as following:



The six isolates preserved in 50% (v/v) glycerol at -20°C was re-cultivated in nutrient broth (NB) at room temperature ($30\pm 5^{\circ}\text{C}$) for 18-24 h, before cultured and maintained in nutrient agar (NA) slant containing zinc and/or cadmium at their resisted zinc and/or cadmium concentrations of 5, 15 and 20 mg/l. The zinc and cadmium added in nutrient broth (NB) were $\text{ZnSO}_4 \cdot 7\text{H}_2\text{O}$ (Ajax Finechem, Australia) and $\text{CdSO}_4 \cdot 8\text{H}_2\text{O}$ (Ajax Finechem, Australia), respectively.

3.2.2 Morphological, physiological and biochemical characteristics

Bacteria isolated were identified via gram staining, casein hydrolysis, starch hydrolysis, cellulose hydrolysis, a 10 μl of bacterial suspension (OD_{600} of 0.5) was inoculated into starch agar, skimmed-milk agar, and NA containing 1% (w/v) carboxymethyl cellulose (CMC) by drop plate technique. The bacterial plates were incubated for 24-48 hours at $30\pm 5^{\circ}\text{C}$. After incubation, starch hydrolysis was tested with iodine solution. Cellulose hydrolysis was tested by flooding with 1% Congo red solution for 5–10 min, then removal of the remaining Congo red by washing with 1 M NaCl. Casein hydrolysis was detected from the obvious clear zone. A zone of clearing around the growth area was used to determine the solubilization index (SI), which was calculated from the diameter of the clear zone (mm) divided by the diameter of the colony (mm). Conventional biochemical tests; triple sugar iron (TSI) test (Hajna, 1945), and peptone iron agar (PIA) test (Williams and Goodfellow, 1966). All the biochemical



test (urease, lysin decarboxylase, esculin, fermentation, etc.) were done by Rapid API20 Bacterial Identification Strip, through TISTR Microbiological Resources Center, Thailand.

3.2.3 Growth curve of six bacteria isolates

Growth curve of six bacteria isolated of PDMZn2008, PDMCd0501, PDMCd2007, PDMCd2008, PDMZnCd1502 and PDMZnCd2003 was examined. A bacterium was refreshed on nutrient agar slant for 24 hours. One loop full of refreshed bacteria cultures was transferred into 50 ml nutrient broth (Himedia, India), to prepare bacterial starter. A starter was aerobically cultured and shaken at 150 rpm, room temperature ($30\pm 5^{\circ}\text{C}$) for 24 hours to obtain the optical density (OD) at 660 nm for 0.5 units. The 1 ml of the bacterial starter was inoculated into 50 ml nutrient broth (NB), shaken at 150 rpm in room temperature ($30\pm 5^{\circ}\text{C}$). The bacterial growth was monitored every 2 hours from 0-24 hours, every 4 hours from 24-48 hours, and every 6 hours from 48-72 hours. Before sample collection, pH of bacteria cultures was measured by a pH meter (Denver Instrument Model 215, German). Bacteria growth was examined with two method of an optical density at 660 nm by a Vis-spectrophotometer (Thermo Fisher scientific, Spectrolnic Genesys 215, USA) and total protein content by Bradford protein assay. The spectroscopic features of bacterial cells were monitored by FT-IR microspectroscopy. The bacteria cell were collected by refrigerated centrifugation (TOMMY MX-301, USA) and washed twice by deionized water prior to further studies.

3.2.3.1 Spectrophotometric determination

A 1.0 of sample was collected in microcentrifuge tube, before centrifuged at 10,000 rpm, 4°C for 10 minutes and washed twice with 1.0 ml of deionized water. The cell pellet was resuspended and adjusted volume to 1.0 ml before measured the optical density (OD) at 660 nm by the Vis-spectrophotometer.

3.2.3.2 Bradford protein assay

Bradford protein assay were used to determine total protein content to represent the bacterial growth, because EPS produced by the bacteria cell and the composition in nutrient broth might interfere the optical density and dry weight. The bacteria pellets obtained from the refrigerated centrifugation were re-suspended in 600 μl of deionized water. The freezing and thawing technique was used for break cell.



The microcentrifuge tube contained cell suspension was put into liquid nitrogen for 2 minutes, and then rapidly transferred into 85°C water bath for 2 minutes. A 0.1 ml of the lysed cell suspension was mixed with 1.0 ml of Coomassie Brilliant Blue G250 reagent, vortex and incubated for 5 minutes, the sample should be left for more 10 minutes. Then the sample were measured the absorbance at 595 nm by the Vis-spectrophotometer. The protein concentration was calculated against a standard curve of bovine serum albumin (BSA) (Sigma, USA) (Bradford, 1976).

3.2.4 Study on the quantitative of plant growth promoting properties

The plant growth promoting properties of IAA production, nitrogen fixation and phosphate solubilization were examined quantitatively under various Zn and/or Cd concentrations.

3.2.4.1 IAA production

The bacterial isolate was inoculated in trypticase soy broth (TSB) containing 0.2% w/v tryptophan in the absence or presence of Zn plus Cd (20/20 mg/l), and incubated at 30±2°C in the dark by shaking at 150 rpm (Innova 2100 Platform shaker, New Brunswick Scientific, USA). The culture were then centrifuged at 6,000 rpm for 15 minutes at 4°C by a refrigerate centrifuge (TOMMY MX-301, USA). The supernatants were mixed with Salkowski's reagent (ratio 2:1) in the dark for 20 minutes. The optical density was measured at an absorbance of 530 nm (Bric, et al., 1991). The IAA concentration was determined using a standard curve of authentic IAA (Sigma-Aldrich, St. Louis, MO, USA).

3.2.4.2 Nitrogen fixation

The bacteria were cultured in N-free malate medium in the absence or presence of Zn plus Cd (20/20 mg/l), and incubated at 30±5°C at 150 rpm. Ammonia nitrogen (NH₃-N), an inorganic dissolved form of nitrogen in the supernatant was quantitatively analysed with Nessler's reagent as described by Cappuccino and Sherman (1992). The amount of NH₃-H was measured against a standard curve of ammonium chloride (NH₄Cl) (Ajax Finechem Pty Ltd, Australia).

3.2.4.3 Phosphate solubilization

The bacteria were cultivated in the National Botanical Research Institute's phosphate growth (NBRIP) medium containing 0.5% (w/v) tricalcium phosphate, in the absence or presence of Zn plus Cd (20/20 mg/l) and



incubated at $30\pm 5^\circ\text{C}$ at 150 rpm. The bacterial cultures were centrifuged at 6,000 rpm for 15 minutes at 4°C . Soluble phosphate in the supernatant was measured by the modified ascorbic acid method of Clesceri, et al. (1998). The concentration of the soluble phosphate was determined against a standard curve of potassium dihydrogen phosphates (KH_2PO_4) (Ajax Finechem Pty Ltd, Australia).

3.2.5 Fourier transform infrared (FT-IR) microspectroscopy

Biomass samples were collected from medium by centrifugation at 8,000 rpm, 4°C for 5 min. The cell was washed with normal saline 0.85 %, and then washed twice with distilled water to remove any remainder of cultivation medium. Cells were resuspension with distilled water to obtain 10^5 - 10^8 cell ml^{-1} . Each suspension was spotted on IR reflected Kevey slides and vacuum dried at room temperature. FT-IR microscope (HYPERION 2000 Bruker Optics, German) and OPUS/IR software (Bruker, German) were used to analysis the samples. Spectra were measured for each sample spot at different locations, the IR-spectra were recorded in Reflectance mode under the spectral region between 4000 and 700 cm^{-1} , at a resolution of 6 cm^{-1} with 64 scans (Naumann, et al., 1996; Naumann, 2000).

The first and second derivatives of the absorbance spectra were used to evaluate the spectra, and a hierarchical cluster analysis was performed with the OPUS software of one spectrum average from 125 spectra. The algorithm 'standard method' was selected for the calculation of distance matrix. Various spectral ranges between 3000 - 2800 cm^{-1} (W1; the 'fatty acid region'), 1800 - 1500 cm^{-1} (W2; the 'amide region'), 1500 - 1200 cm^{-1} (W3; the 'mixed region') and 1200 - 900 cm^{-1} (W4; the polysaccharide region) were used for calculating distance matrices from biomass spectra. From the distance matrices, the dendrograms were created with the Hierarchical Cluster Analysis (HCA). Spectral distance was calculated as D-value correlation coefficient and the ward's algorithm was applied to determine heretical cluster. Pretreated spectrums were statistically analyzed by multivariate data analysis (principle component analysis; PCA) and the Unscramble 9.7, CAMO software (Helm, et al., 1991b; Naumann, et al., 1996; Naumann, 2000).



3.2.6 Identification of bacteria based on 16S rDNA gene sequence analyses

For molecular characterization, the selected bacterial strains were subjected to 16S rDNA gene sequence analyses. The selected bacterial strains were grown in nitrogen-free agar (NFA) and total genomic DNA of selected isolate was extracted by a modified phenol: chloroform procedure of Sambrook and Russel, (2001). Two primers of fD1 (5'-AGAG TTTGATCCT GGCTCAG-3') and rP2 (5'-ACGGCTACCTT GTTACGACT T-3') (Weisburg et al., 1991) were used for 16S rDNA (ribosomal Deoxyribonucleic acid) amplification. Each 50 µl of polymerase chain reaction (PCR) reaction contained: 100 ng of purified total DNA, 0.2 mM of each diethylnitrophenyl thiophosphate (dNTP), 5 unit of Tag DNA polymerase (Invitrogen, USA) in 5 µL of 10x Tag buffer, 1 mM MgCl₂, 0.2 mM of each primer, and 35 µl sterile deionized water. Thermal cycling program for 16S rDNA amplification consisted of 1 cycle of 94°C for 5 min (denaturation), 57°C for 2 min (annealing for fD1 and rP2) and 72°C for 2 min (extension), and 29 cycles of 94°C for 2 min, 57°C for 30 sec and 72°C for 2 min, with a final elongation cycle of 72°C for 10 min (Wood et al., 1998). The PCR products obtained were purified with a HiYield™ Gel/PCR DNA Fragments extraction kit (Real Biotech Corporation, Taiwan). For molecular technique, the PCR products of their 16S rDNA (ribosomal Deoxyribonucleic acid) were sequenced by a 3730XL DNA sequencer, through Laboratory Information Management System (LIMS), Macrogen Inc, Korea. Sequence data of 16S rDNA (1500 bp) were compared with sequences in the National Center for Biotechnology Information (NCBI) data bank using BLAST program (Altschul, et al., 1997). The multiple sequences were aligned by BioEdit and MEGA software for phylogenetic tree (Kimura, 1980; Tamura et al., 2007).

3.2.7 SDS-PAGE

Crude protein was extracted of bacteria adapted from Sánchez, et al (2003). Cultures grown on tryptic soy agar (TSA) for 24 h were inoculated in 50 ml of tryptic soy broth and incubated at 30±5°C. Late log phase cell pellets were harvested by centrifugation (8000 rpm for 5 min at 4°C) and washed twice in 0.85% (w/v) NaCl. Whole cell extraction from the pellets was optimized on a small number of strains. The freezing and thawing technique was used for break cell. The microcentrifuge tube contained cell suspension was put into liquid nitrogen for 2 minutes, then rapidly



transferred into 85°C water bath for 2 minutes. The 1 ml of SDS treatment buffer (0.0625 M Tris-HCl, pH 6.8; 2% (w/v) SDS; 10% (v/v) glycerol, 5% (v/v) 2-Mercaptoethanol) was added to the tube and the suspension heated at 95°C for 10 min. After cooling on ice and centrifugation (8000 rpm for 5 min at 4°C), the supernatant was separated for protein measurement and storage at -20°C.

Protein concentrations were estimated by the method of Bradford (1976). SDS PAGE was performed as described by Laemmli (1970). In briefly, 40 µg of the sample was loaded in each well in a 5% stacking gel over a separating gel of 12% polyacrylamide, for 2 hours at 20 mA per gel by electrophoresis (MiniVEGE Healthcare Bio-Sciences Corp., USA). The gels were stained with Coomassie Brilliant Blue R-250 staining buffer. Molecular weight of protein band was measured based on the molecular weight of two broad range protein markers of 7.1 kDa to 209 kDa and 10 kDa to 250 kDa (prestained SDS-PAGE standard, broad range, Bio-Rad, USA). The expression of proteins in SDS-PAGE was analysed by Quantity One 1-D analysis software program (Bio-Rad, USA).

3.2.8 Assessment of metal toxicity

Heavy metal resistance for bacterial strain present in various natural habitats such as soil, water, sediments soil. Therefore, the bacteria isolates was tested for its tolerance and resistance properties to Zn and/or Cd in both solid and liquid media, respectively.

3.2.8.1 Evaluation of metal tolerance

The refreshed bacterium was aerobically cultured and shaken at 150 rpm, room temperature (30±2°C) for 18-24 hours to obtain the optical density at 600 nm (OD₆₀₀) of 0.5. To determine metal tolerance, 10 µl of bacterial suspension was inoculated into a nutrient agar plate (NA) containing Zn and/or Cd by the drop plate technique at 35±2°C for 24-48 h. The various Zn and/or Cd concentrations ranged from 5 to 200 mg/l, Cd plus Zn ranged from 5/5 to 200/200 mg/l. After the period of incubation, the effect of Zn and/or Cd on the growing spot of each bacterium was evaluated and indicated as no growth (-), low growth (+), moderate growth (++), and high growth (+++).



3.2.8.2 Evaluation of metal resistance

The MICs of Zn and Cd were evaluated following a modified microtitre plate-based antibacterial assay incorporating resazurin as an indicator of cell growth (Sarker, 2007). Each well contained (1) 50 μ l of Mueller Hinton broth, (2) 50 μ l of Zn/Cd stock solution or sterile water (control), (3) 10 μ l of resazurin solution and (4) 10 μ l of bacterial suspension with the OD₆₀₀ of 0.132 (McFarland No. 0.5, approximate cell density of 1.5×10^8 CFC/ml). The various Zn and/or Cd concentrations ranged from 5 to 400 mg/l, Cd plus Zn ranged from 5/5 to 100/100 mg/l and fixed Cd 20 mg/l plus Zn concentrations ranged from 20 to 2000 mg/l. Plates were prepared under aseptic conditions and incubated at $30 \pm 2^\circ\text{C}$ for 24-48 h. The colour change was then assessed visually. Any colour changes from purple to pink or colourless were recorded as positive. The lowest concentration of the metals inhibiting growth was determined as when the colour changed from dark purple to purple and this was taken as the MIC value. The minimum bactericidal concentration (MBC) of Zn and Cd were determined by streak microbial suspensions that changed resazurin's colour from purple to dark purple, on Mueller Hinton agar plates. The lowest Zn and Cd concentrations with no growth of the bacteria on the agar plate was taken as the MBC value.



CHAPTER 4

Results and Discussion

4.1 Morphological and biochemical characteristics

The morphological characteristics of PDMZn2008, PDMCd0501, PDMCd2007, PDMCd2008, PDMZnCd1502 and PDMZnCd2003 are shown in Table 4.1. Five isolates were Gram negative and one isolate was Gram positive bacteria, and all bacterial isolates were motile. The biochemical characteristics indicated that the six isolates were not able to hydrolyze starch in the starch agar (Table 4.1). PDMZn2008 and PDMZnCd2003 hydrolysed casein with a soluble index (SI) of 1.28 ± 0.08 and 1.45 ± 0.03 , respectively. PDMZnCd2003 hydrolyzed cellulose with a SI of 2.29 ± 0.35 and produced H₂S via an aerobic system as a dark color of ferrous (II) sulfide (FeS) in Tryptone Sugar Iron (TSI) agar and a dark color of FeS on the surface of peptone iron agar (PIA) media. The biochemical analyses of the six bacterial isolates were done by Rapid API20E Bacterial Identification Strip. Based on the API20E, PDMZn2008, PDMCd0501 and PDMCd2007 were identified to nonpigmented *Serratia marcescens*. Whereas, PDMCd2008, PDMZnCd1502 and PDMZnCd2003 were identified to be *Providencia stuartii*, *Providencia stuartii* and *Pseudomonas aeruginosa*, respectively (Appendix B, C).

Environmental stress might cause a high number of Gram-negative bacteria to form complex cell wall structures of Gram-negative bacteria. Most of rhizobacteria belonging to this group and are Gram-negative rods with a lower proportion being Gram-positive rods, cocci or pleomorphic (Ahmad and Kibret, 2014). In addition, major free-living Gram-negative bacteria isolated from rhizospheric soil of different crops (mustard, barseem, wheat, sugarcane, brinjal, onion, cauliflower, cabbage and chick pea) were *Pseudomonas* (Ahmad, et al., 2008).



Table 4.1 Morphological and biochemical characteristics

Microbial characteristics	Isolates					
	PDMZn2008	PDMCd0501	PDMCd2007	PDMCd2008	PDMZnCd1502	PDMZnCd2003
Morphological characteristics						
Colony morphology	Yellowish cream, round with smooth margin	Cream, circular with entire margin and smooth surface	Cream, circular with entire margin and smooth surface	Cream, circular with entire margin and smooth surface	Cream, circular with entire margin and smooth surface	Blue-green, circular with curled margin and rough surface
Gram reaction ^a	+ve, Short rod	-ve, rod	-ve, rod	-ve, Short rod	-ve, Short rod	-ve, coccobacilli
Motility	Motile	Motile	Motile	Motile	Motile	Motile
Biochemical characteristics						
Casein hydrolysis (mm ⁻¹) ^b	1.28±0.08	-	-	-	-	1.45±0.03
Starch hydrolysis (mm ⁻¹) ^b	-	-	-	-	-	-
Cellulose hydrolysis (mm ⁻¹) ^b	-	-	-	-	-	2.29±0.35
Growth on TSI ^c	K/AG	K/A	K/A	K/A	K/A	K/NC, H ₂ S on slant
Growth on PIA ^d	-	-	-	-	-	+

^a+ve =Gram negative bacteria, -ve =Gram positive bacteria

^bSI (Solubilization Index; mm⁻¹); Mean values ($n=2$) ± Standard deviation (S.D.)

^cK/A=Alkaline slant/acid butt; K/AG=Alkaline slant/acid butt with gas, no H₂S; K/NC =Alkaline slant/no change and no gas

^dH₂S production (+)with H₂S; (-)no H₂S

4.2 Growth curve of bacteria isolates

4.2.1 Comparison of two techniques for growth curve of bacteria isolates

The studies of bacterial growth investigated the characteristics of the six bacteria isolates in nutrient broth (NB) without heavy metals. Two techniques, turbidimetric method and total protein assay, were carried out for growth monitoring due to some bacterial isolates producing a large amount of an extracellular polymeric substance (EPS), which led to difficulty when only using one technique (Gu and Pan, 2006; Meesungnoen, et al., 2012).

The system pHs were altered and growth curves of the six bacteria under aerobic conditions in nutrient broth (NB) media are shown in Figure 4.1 and Figure 4.2. The detail data are shown in Appendix D. The growth curves from the turbidimetric method and protein assay were similar, especially in the lag to late-log phase. However, differences in the stationary phase and death phase were found as shown in Table 4.2. Although the protein assay precisely analyses the bacterial growth in the log phase, there is variability in the stationary phase and death phase because of cell death and lysis (Willey et al., 2008). Figure 4.1 shows that the system pHs of the bacterial cultivation in NB gradually increased from 7.3 ± 0.5 (lag phase) to 8.5 ± 0.1 (late log phase) and 9.0 ± 0.1 (death phase). The stable pH values at ~ 9.0 might be caused by the secondary metabolites secreted from bacteria. In the case of PDMZnCd2003, the bacterium secreted a yellow-green pigment, which probably was a fluorescent siderophore affecting the alkaline pH in the culture medium (Meesungnoen, 2012; Chiadò, et al., 2013).

Each phase of the bacterial growth is shown in Table 4.2. Due to the maximum and homogeneous cells in late log phase, the bacterial cells in late-log phase were appropriate for SDS-PAGE and 16S rDNA sequence analysis.



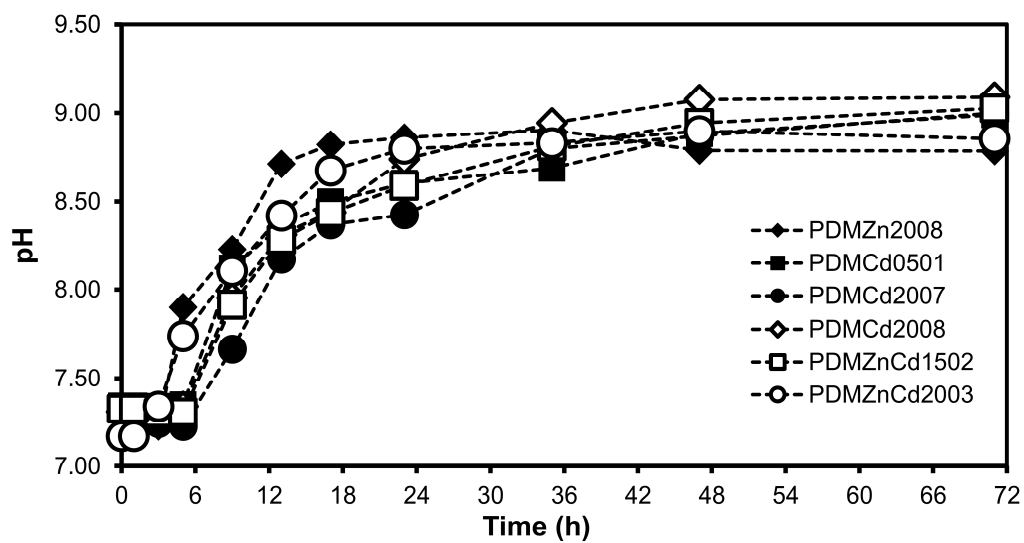


Figure 4.1 System pHs during the cultivation of PDMZn2008, PDMCd0501, PDMCd2007, PDMCd2008, PDMZnCd1502 and PDMZnCd2003 in nutrient broth.



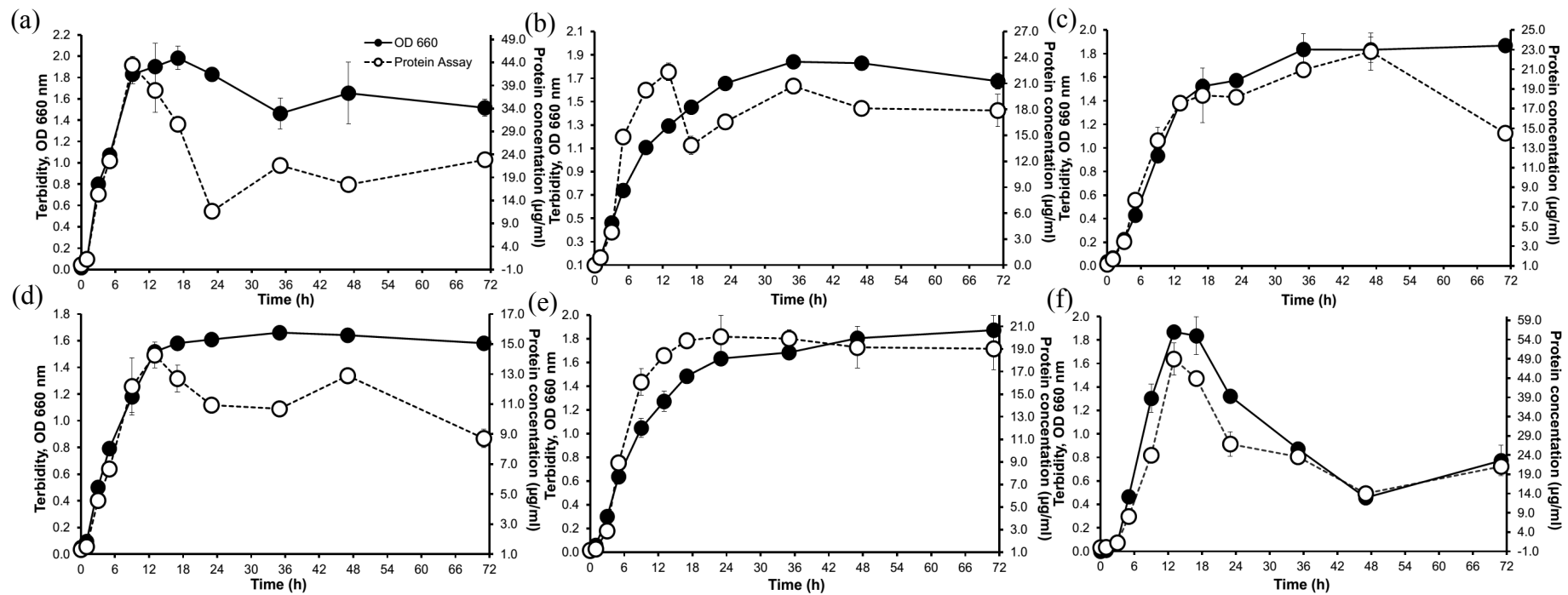


Figure 4.2 Growth curves of six bacteria in nutrient broth, monitored by the turbidimetric method and protein assay: (a) PDMZn2008, (b) PDMCd0501, (c) PDMCd2007, (d) PDMCd2008, (e) PDMZnCd1502 and (f) PDMZnCd2003.

Table 4.2 Growth phase of the bacterial isolates of PDMZn2008, PDMCd0501, PDMCd2007, PDMCd2008, PDMZnCd1502 and PDMZnCd2003 determined by turbidimetric method and Bradford protein assay.

Bacterial isolates	Lag phase	Log phase	Late-log phase	Stationary phase	Death phase
Growth phase (hours)^a					
PDMZn2008	0-1	1-9	9-13	13-23	23-72
PDMCd0501	0-1	1-9	9-13	13-35	47-72
PDMCd2007	0-1	1-13	13-17	17-47	47-72
PDMCd2008	0-1	1-9	9-13	13-47	47-72
PDMZnCd1502	0-1	1-13	13-17	17-47	47-72
PDMZnCd2003	0-3	3-9	9-13	13-17	17-72
Growth phase (hours)^b					
PDMZn2008	0-1	1-9	9-13	13-23	23-72
PDMCd0501	0-1	1-9	9-13	13-35	47-72
PDMCd2007	0-1	1-13	13-17	17-47	47-72
PDMCd2008	0-1	1-9	9-13	13-47	47-72
PDMZnCd1502	0-1	1-13	13-17	17-47	47-72
PDMZnCd2003	0-3	3-9	9-13	13-17	17-72
Growth phase (hours)^c					
PDMZn2008	1	5	11	17	72
PDMCd0501	1	5	13	35	72
PDMCd2007	1	5	13	35	72
PDMCd2008	1	5	13	35	72
PDMZnCd1502	1	5	13	35	72
PDMZnCd2003	1	5	11	17	72

^aTurbidimetric method

^bBradford protein assay

^cSummary data



4.2.2 FT-IR characterization of bacterial growth

FT-IR microspectrometry was used to establish the relationship between the growth of the six bacterial isolates and changes in the cell characteristics. Figure 4.2 shows the growth curve of the six bacterial isolates over a period of 72 hours. The FT-IR spectra in Figures 4.3-4.20 indicated that the spectroscopic features of the six bacterial isolates depending on the physiological conditions during the different growth phases. The characterization of bacterial growth was analyzed following the steps of normalized average spectra, second derivative spectra discriminant and principal component analysis (PCA).

The normalized average FT-IR spectra and second derivative spectra at each growth phase of PDMZn2008 are shown in Figure 4.3 and Figure 4.4, respectively. Through the time period from lag phase to death phase, the normalized spectral features of the whole cells did not show peaks shifting in fatty acid region of $-\text{CH}_3$ and $>\text{CH}_2$ stretching vibrations ($3000\text{-}2800\text{ cm}^{-1}$), whereas the peak height continuously increased from the lag phase to stationary phase in the $-\text{CH}_3$ asymmetric stretching vibrations (2960 cm^{-1}), $>\text{CH}_2$ asymmetric stretching vibrations (2923 cm^{-1}), $-\text{CH}_3$ symmetric stretching vibrations (2874 cm^{-1}) and $>\text{CH}_2$ symmetric stretching vibrations (2852 cm^{-1}). In addition, the peak height in the amide I, II region continuously increased from the lag phase to stationary phase in the amide I of the α -helical structure proteins (1658 cm^{-1}), amide I of the β -sheets proteins (1637 cm^{-1}) and amide II (1552 cm^{-1}). In the cells' death phase, the height of peaks in the amide I, II region, fatty acids region, phospholipids region with $\text{P}=\text{O}$ asymmetric stretching of PO_2 ($1241, 1220\text{ cm}^{-1}$) and polysaccharide region of the carbohydrates ($1120, 1085$ and 1058 cm^{-1}) were decreasing. In addition, the height of the peaks in the fatty acids region, amide I, II region, phospholipids (PO_2) region and polysaccharide (C-O-P) region were the least in the lag phase and log phase.

Multivariate data analysis, in particular Principal Component Analysis (PCA) could be used to distinguish the bacterial growth phase. The PCA provided information of clustering visualization of similar spectra within datasets in scores of plots and identification of variables (spectral bands representing various molecular groups within the samples). The major variability between the spectra can be concentrated into a smaller set of values called principal components (PCs).



The PCA score plot and loading plots of PDMZn2008 are shown in Figure 4.5. The clusters of spectra were separated along PC1 and PC4; PC1 explained nearly 80% of the variance and PC4 explained 4% (Figure 4.5A). The PC1 score plot separated the bacterial lag and log phases from late-log to death phases, the PC4 score plot clustered the death phase from late-log phase and stationary phase. Analysis of PC1 loadings (Figure 4.5 B, C) showed differences in the peak heights in the fatty acid region ($-\text{CH}_3$ and $>\text{CH}_2$ asymmetric stretching (2960 cm^{-1} , 2923 cm^{-1}) and $-\text{CH}_3$ and $>\text{CH}_2$ symmetric stretching (2874 cm^{-1} , 2852 cm^{-1})), amide I, II region (amide I of α -helical proteins (1658 cm^{-1}), amide I of β -sheets proteins (1637 cm^{-1}), amide II of proteins (1552 cm^{-1})), phospholipids region with $\text{P}=\text{O}$ asymmetric stretching of PO_2 (PO_2 of Phospholipids at 1241 and 1220 cm^{-1}) and polysaccharide region ($\text{C}-\text{O}-\text{P}$ of the carbohydrates at 1120 , 1085 and 1058 cm^{-1}). The PC4 loading (Figure 4.5 B, C) indicated differences in the amide I, II region (amide I of α -helical proteins (1658 cm^{-1}), amide I of β -sheets proteins (1637 cm^{-1}), amide II of proteins (1552 cm^{-1})), phospholipids region with $\text{P}=\text{O}$ asymmetric stretching of PO_2 (PO_2 of phospholipids at 1241 and 1220 cm^{-1}) and polysaccharide region ($\text{C}-\text{O}-\text{P}$ of the carbohydrates at 1120 , 1085 and 1058 cm^{-1}). Table 4.4 shows the characteristic functional groups corresponding to wavenumber ranges.



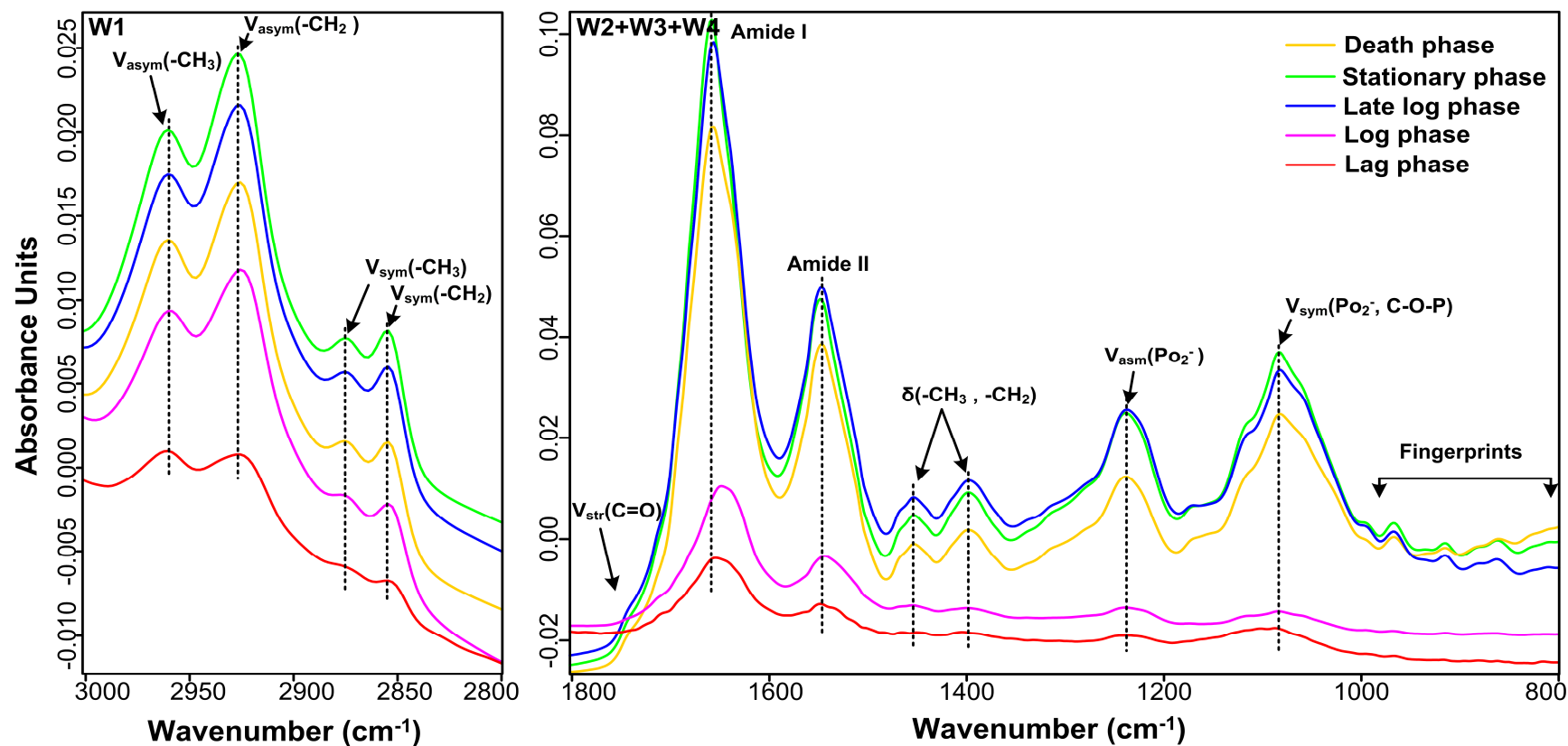


Figure 4.3 Normalized average FT-IR spectra of PDMZn2008 cells at lag phase, log phase, late-log phase, stationary phase and death phase.

The spectral windows are defined according to the classification. Where, W1 is the fatty acid region ($3000-2800\text{ cm}^{-1}$), W2 is the amide region ($1800-1500\text{ cm}^{-1}$), W3 is the mixed region ($1500-1200\text{ cm}^{-1}$) and W4 is the polysaccharide region ($1200-900\text{ cm}^{-1}$). One spectrum was averaged from 100-125 spectra of each growth phase.

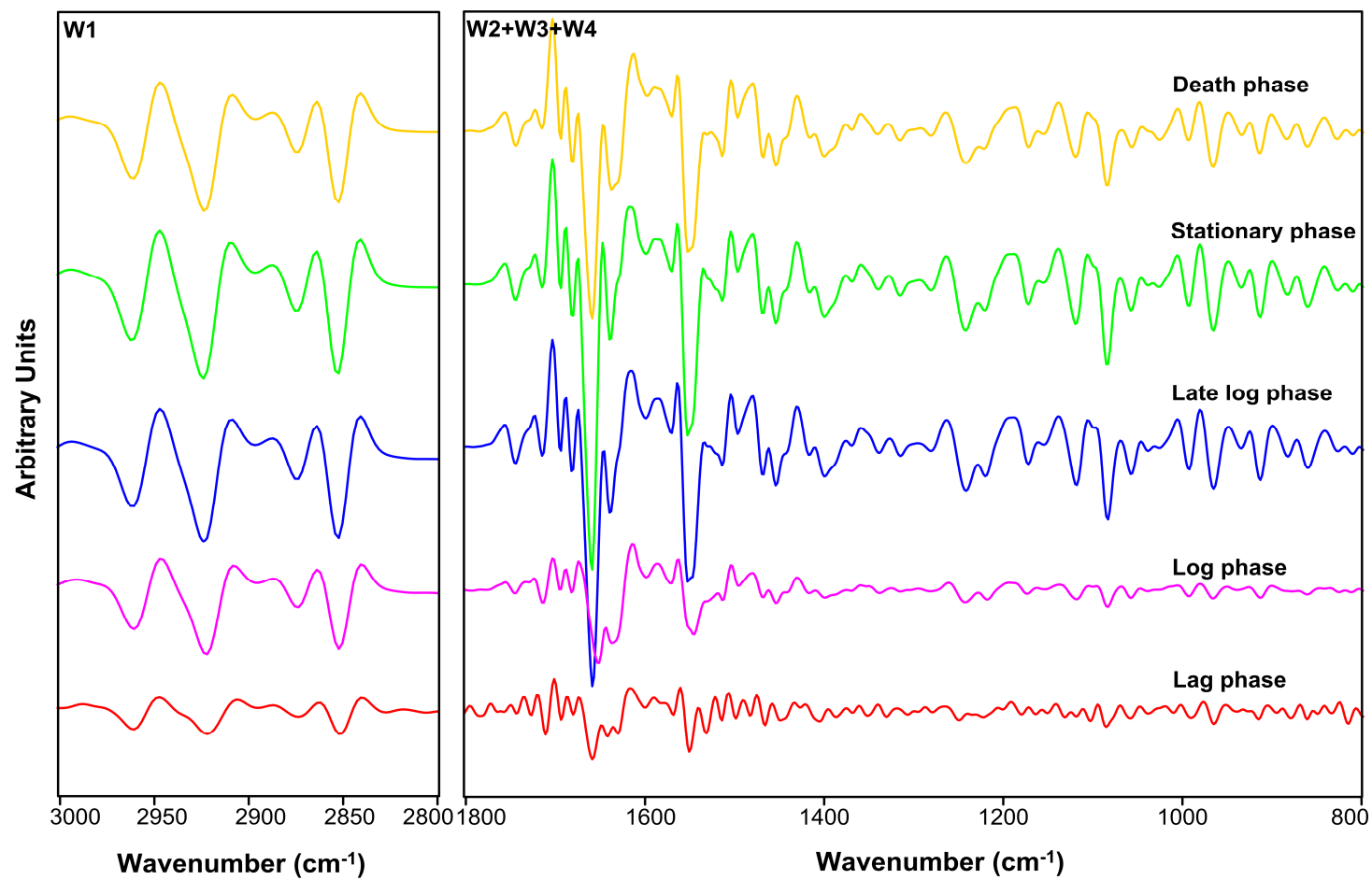


Figure 4.4 Second derivative FT-IR spectra of PDMZn2008 cells at lag phase, log phase, late-log, phase, stationary phase and death phase. The spectral windows are defined according to the classification.

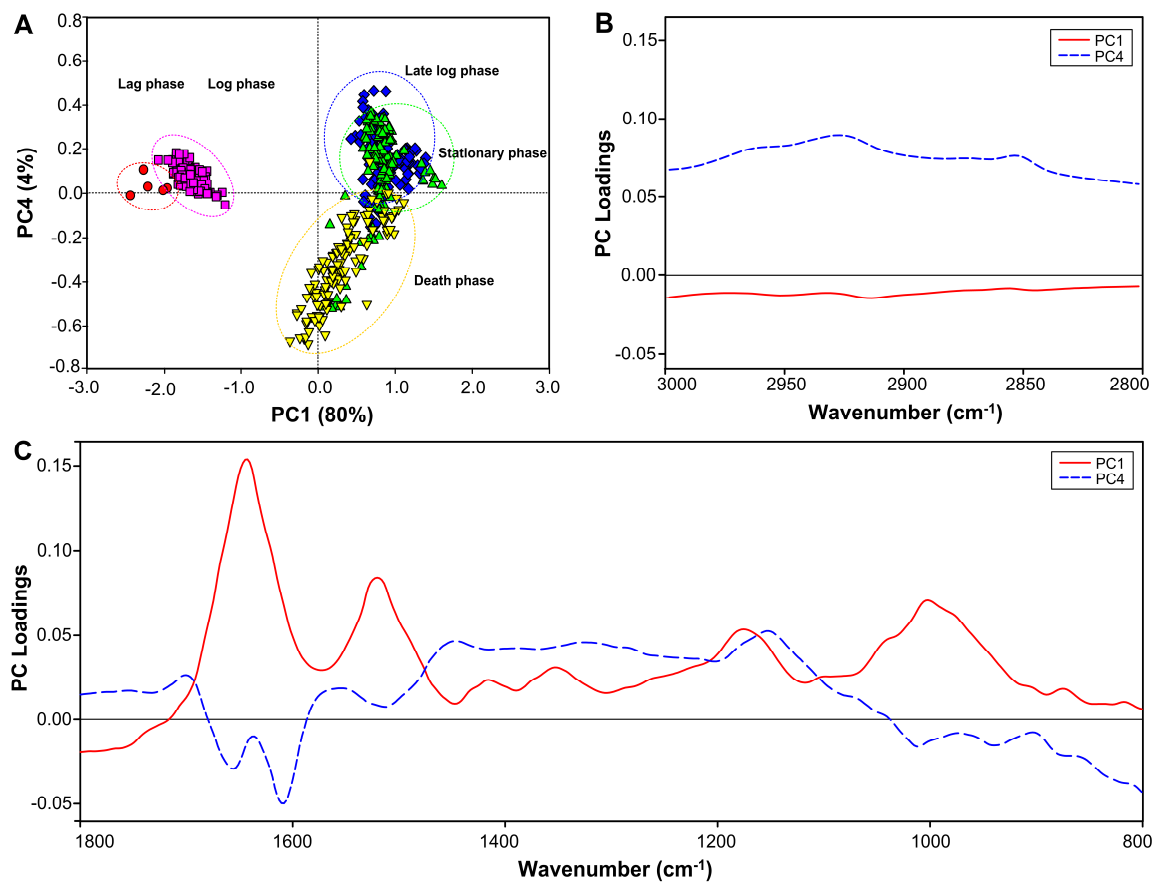


Figure 4.5 Principal component analysis (PCA) applied to FT-IR spectra of PDMZn2008 growth phases. (A) shows the score plots of PC1 and PC4; (B) and (C) show loading plots of PC1 and PC4 in the ranges of 3000-2800 cm⁻¹ and 1800-800 cm⁻¹, respectively.

The normalized average FT-IR spectra and second derivative spectra at each growth phase of PDMCd0501 are shown in Figure 4.6 and Figure 4.7, respectively. Through the time period from lag phase to death phase, the normalized spectral features of the whole cells did not show peaks shifting in the fatty acid region of $-\text{CH}_3$ and $>\text{CH}_2$ stretching ($3000\text{-}2800\text{ cm}^{-1}$), whereas the peak height in the fatty acids region continuously increased from the lag phase to stationary phase by $-\text{CH}_3$ asymmetric stretching (2960 cm^{-1}) and $>\text{CH}_2$ asymmetric stretching (2923 cm^{-1}), $-\text{CH}_3$ symmetric stretching (2874 cm^{-1}) and $>\text{CH}_2$ symmetric stretching (2852 cm^{-1}). The peak height decreased in the fatty acids region during the death phase. The peaks in the amide I, II region (amide I regions of the α -helical structure proteins at 1656 cm^{-1} , β -sheets proteins at 1637 cm^{-1} and amide II at 1550 cm^{-1}) did not shift and change in the late-log phase to death phase of the bacterial growth. The peaks shifting in the amide I regions of the α -helical structure proteins from 1656 to 1650 cm^{-1} occurred in the log phase. The higher peaks in the phospholipids region with $\text{P}=\text{O}$ asymmetric stretching of PO_2 ($1240, 1220\text{ cm}^{-1}$) and polysaccharide region of the carbohydrates ($1122, 1083$ and 1056 cm^{-1}) were found in the death phase. In addition, the lowest amount in the fatty acids region, amide I, II region, phospholipids (PO_2) region and polysaccharide (C-O-P) region were found in lag phase and log phase.

The PCA score plot and loading plots of PDMCd0501 growth phases are shown in Figure 4.8. The spectra of the bacterial cells in the growth phases were clustered along PC1 and PC2, PC1 explained nearly 67% of the variance and PC2 explained 20% (Figure 4.8 A). The PC1 score plot separated the bacterial cell growth in the lag phase and log phase from the late-log to death phase, the PC2 score plot did not separate the growth phase. The PC1 loading plots (Figure 4.8 B, C) showed differences in the peak heights in the amide I, II region (amide I of the α -helical proteins ($1650, 1658\text{ cm}^{-1}$), amide I of the β -sheets proteins (1637 cm^{-1}), amide II of proteins (1550 cm^{-1})), phospholipids region with $\text{P}=\text{O}$ asymmetric stretching of PO_2 (PO_2 of phospholipids at 1240 and 1220 cm^{-1}) and polysaccharide region (C-O-P of the carbohydrates at $1122, 1083$ and 1056 cm^{-1}). The PC2 loading plots (Figure 4.8 B, C) also indicated differences in the amide I, II region (amide I of the α -helical proteins (1658 cm^{-1}), amide I of the β -sheets proteins (1637 cm^{-1}), amide II of proteins (1550 cm^{-1})),



phospholipids region with P=O asymmetric stretching of PO₂ (PO₂ of phospholipids at 1240 and 1220 cm⁻¹) and polysaccharide region (C-O-P of the carbohydrates at 1122, 1083 and 1056 cm⁻¹).



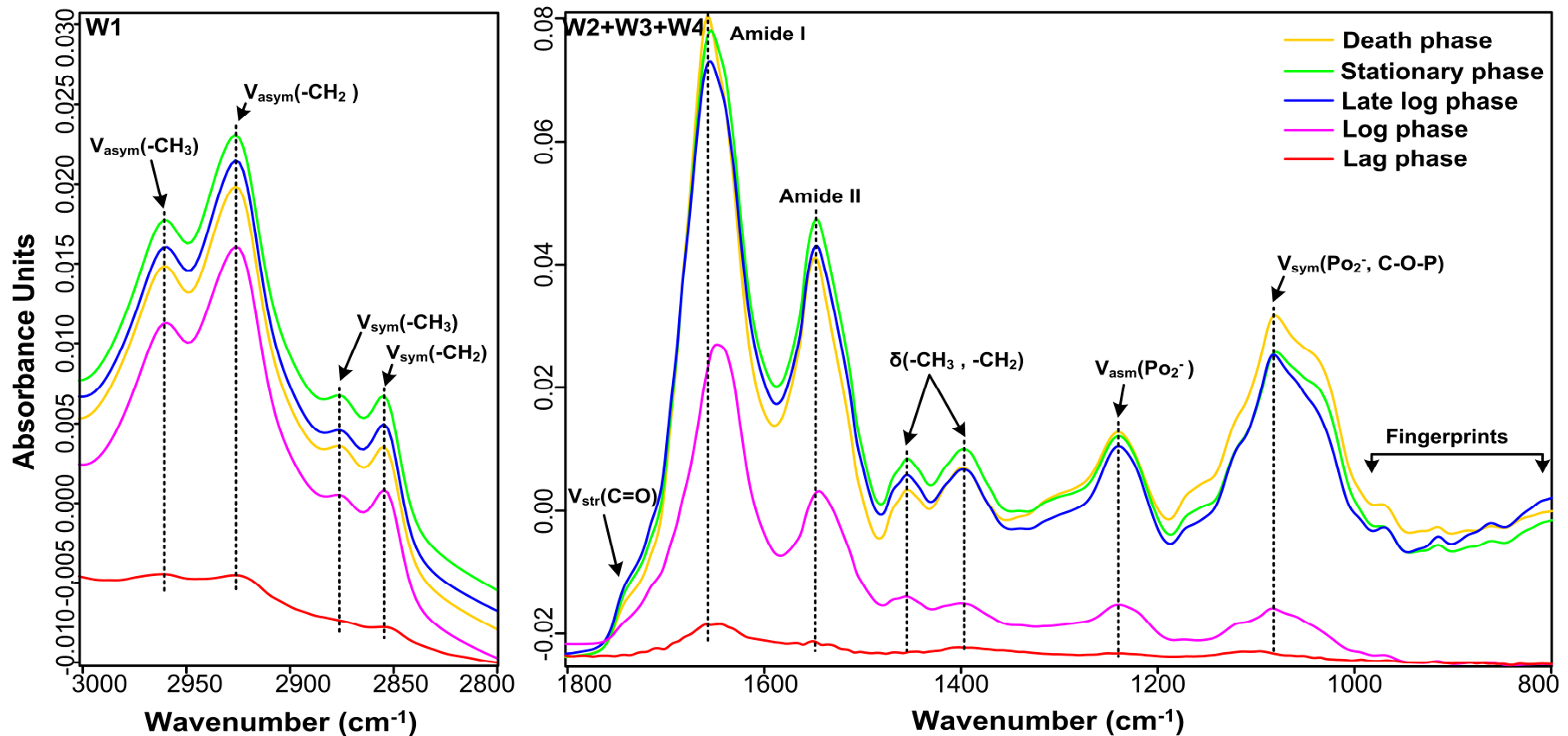


Figure 4.6 Normalized average FT-IR spectra of PDMCd0501 cells at lag phase, log phase, late-log phase, stationary phase and death phase. The spectral windows are defined according to the classification. Where, W1 is the fatty acid region (3000-2800 cm^{-1}), W2 is the amide region (1800-1500 cm^{-1}), W3 is the mixed region (1500-1200 cm^{-1}) and W4 is the polysaccharide region (1200-900 cm^{-1}). One spectrum was averaged from 100-125 spectra of each growth phase.

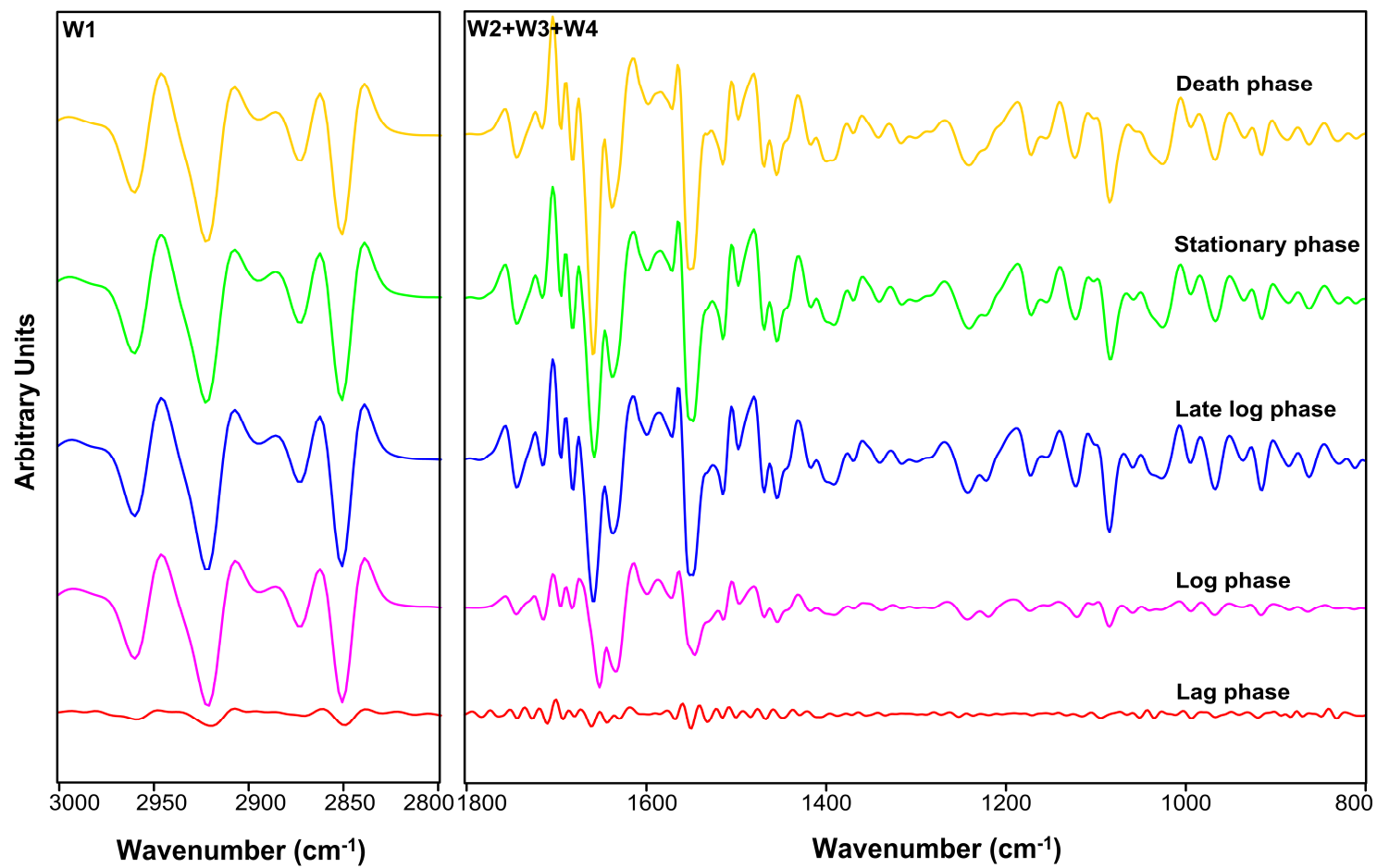


Figure 4.7 Second-derivative FT-IR spectra of PDMCd0501 cells at lag phase, log phase, late-log, phase, stationary phase and death phase. The spectral windows are defined according to the classification.

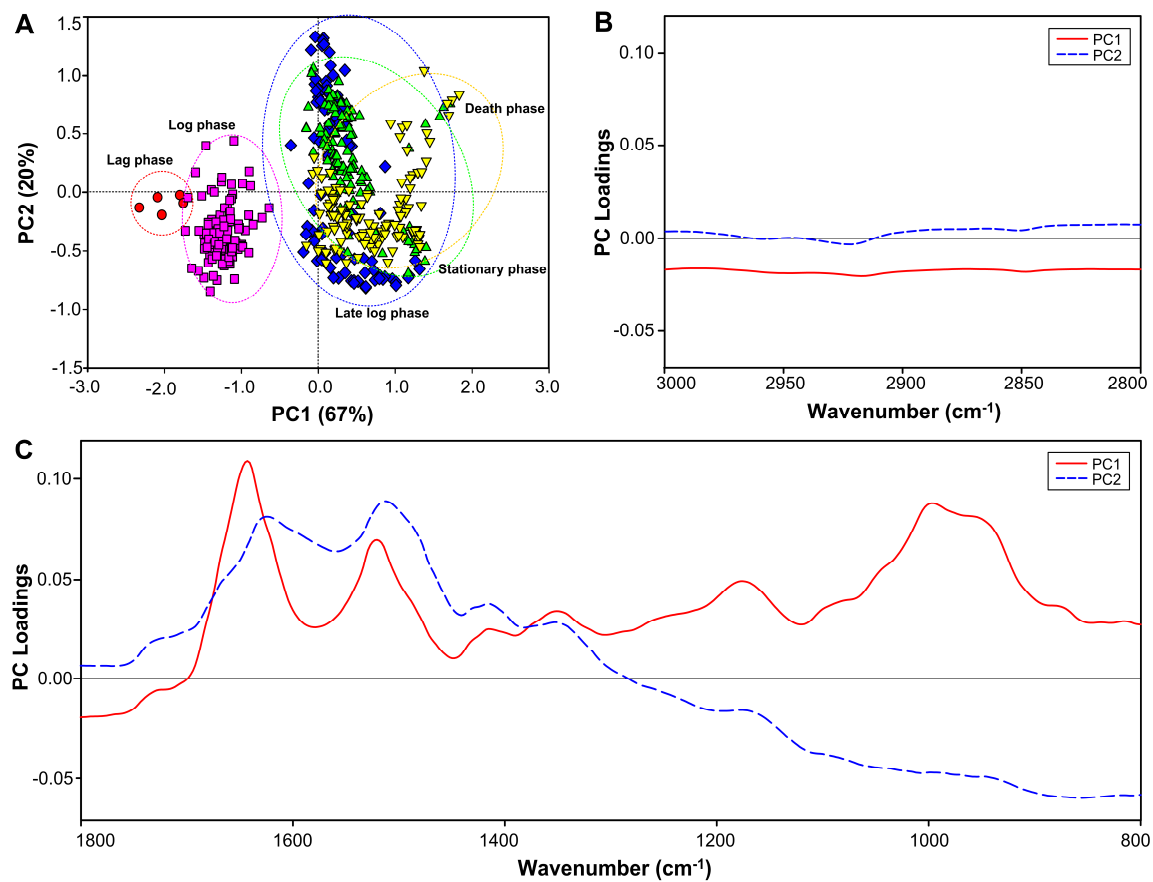


Figure 4.8 Principal component analysis (PCA) applied to FT-IR spectra of PDMCd0501 growth phases. (A) shows the score plots of PC1 and PC2; (B) and (C) show loading plots of PC1 and PC2 in the ranges of 3000-2800 cm⁻¹ and 1800-800 cm⁻¹, respectively.

Normalized average FT-IR spectra and second derivative spectra at each growth phase of PDMCd2007 are shown in Figure 4.9 and Figure 4.10, respectively. Through the time period from lag phase to death phase, the normalized spectral features of the whole cells did not show peaks shifting in the fatty acid region of $-\text{CH}_3$ and $>\text{CH}_2$ stretching, whereas the peak height continuously increased from the lag phase to stationary phase by $-\text{CH}_3$ asymmetric stretching (2960 cm^{-1}), $>\text{CH}_2$ asymmetric stretching (2923 cm^{-1}), $-\text{CH}_3$ symmetric stretching (2873 cm^{-1}) and $>\text{CH}_2$ symmetric stretching (2852 cm^{-1}). Decreasing peaks were found in the fatty acids region in the death phase. In the stationary and death phases, the peaks in the amide I region of the α -helical structure proteins shifted from 1658 to 1652 cm^{-1} and the β -sheets proteins shifted from 1637 to 1630 cm^{-1} . The peak height of the amide I region (amide I regions of α -helical structure proteins at 1652 cm^{-1} , β -sheets proteins at 1630 cm^{-1}) continuously decreased in the stationary phase and death phase. Whereas, there were no differences in the amide II region at 1552 cm^{-1} . The higher peaks, but no shifts in the phospholipids region with $\text{P}=\text{O}$ asymmetric stretching of PO_2 ($1241, 1220\text{ cm}^{-1}$) and polysaccharide region of the carbohydrates ($1120, 1085$ and 1058 cm^{-1}), were in the late-log phase. The lowest peak height in the fatty acids region, amide I, II region, phospholipids (PO_2) region and polysaccharide (C-O-P) region were found in the lag phase and log phase.

The PCA score plot and loading plots for PDMCd2007 growth phases are shown in Figure 4.11. The clusters of spectra were separated along PC1 and PC2; PC1 explained nearly 77% of the variance and PC2 explained 13% (Figure 4.11 A). The PC1 score plot separated the lag phase and log phase from the late-log to death phase; the PC2 score plot did not separate the growth phases. Analysis of PC1 loadings (Figure 4.11 B, C) shows differences in the peak heights in the fatty acid region ($-\text{CH}_3$ and $>\text{CH}_2$ asymmetric stretching ($2960\text{ cm}^{-1}, 2923\text{ cm}^{-1}$), $-\text{CH}_3$ and $>\text{CH}_2$ symmetric stretching ($2873\text{ cm}^{-1}, 2852\text{ cm}^{-1}$)), amide I, II region (amide I of α -helical proteins ($1650, 1658\text{ cm}^{-1}$), amide I of the β -sheets proteins (1637 cm^{-1}), amide II of proteins (1550 cm^{-1}), phospholipids region with $\text{P}=\text{O}$ asymmetric stretching of PO_2 (PO_2 of phospholipids at 1241 and 1220 cm^{-1}) and polysaccharide region (C-O-P of the carbohydrates at $1120, 1085$ and 1058 cm^{-1}). The PC2 loading (Figure 4.11B, C) indicated differences in the phospholipids region with $\text{P}=\text{O}$ asymmetric stretching of



PO₂ (PO₂ of phospholipids at 1241 and 1220 cm⁻¹) and polysaccharide region (C-O-P of the carbohydrates at 1120, 1085 and 1058 cm⁻¹).



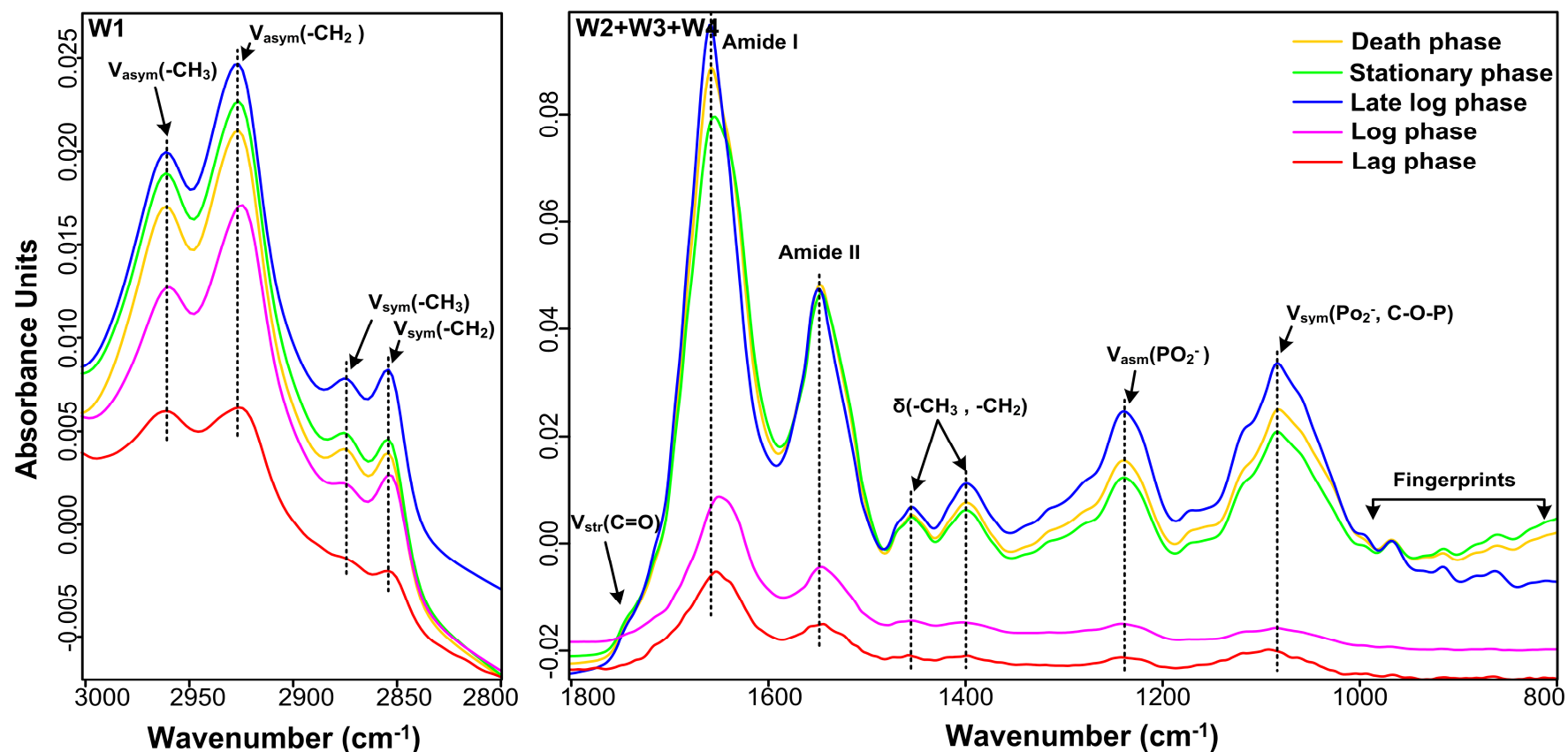


Figure 4.9 Normalized average FT-IR spectra of PDMCd2007 cells at lag phase, log phase, late-log phase, stationary phase and death phase.

The spectral windows are defined according to the classification. Where, W1 is the fatty acid region ($3000-2800\text{ cm}^{-1}$), W2 is the amide region ($1800-1500\text{ cm}^{-1}$), W3 is the mixed region ($1500-1200\text{ cm}^{-1}$) and W4 is the polysaccharide region ($1200-900\text{ cm}^{-1}$). One spectrum was averaged from 100-125 spectra of each growth phase.

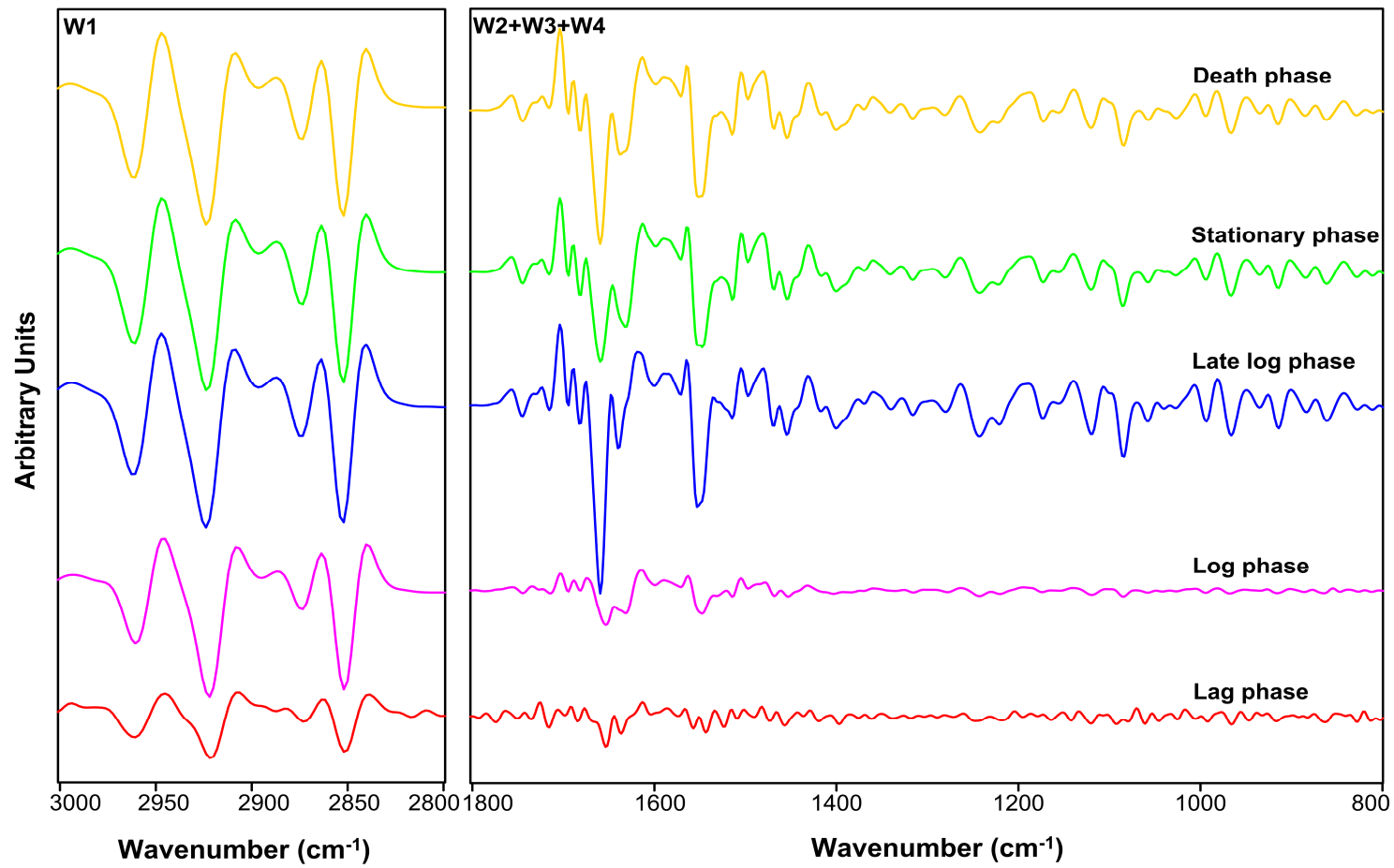


Figure 4.10 Second-derivative FT-IR spectra of PDMCd2007 cells at lag phase, log phase, late-log, phase, stationary phase and death phase. The spectral windows are defined according to the classification.

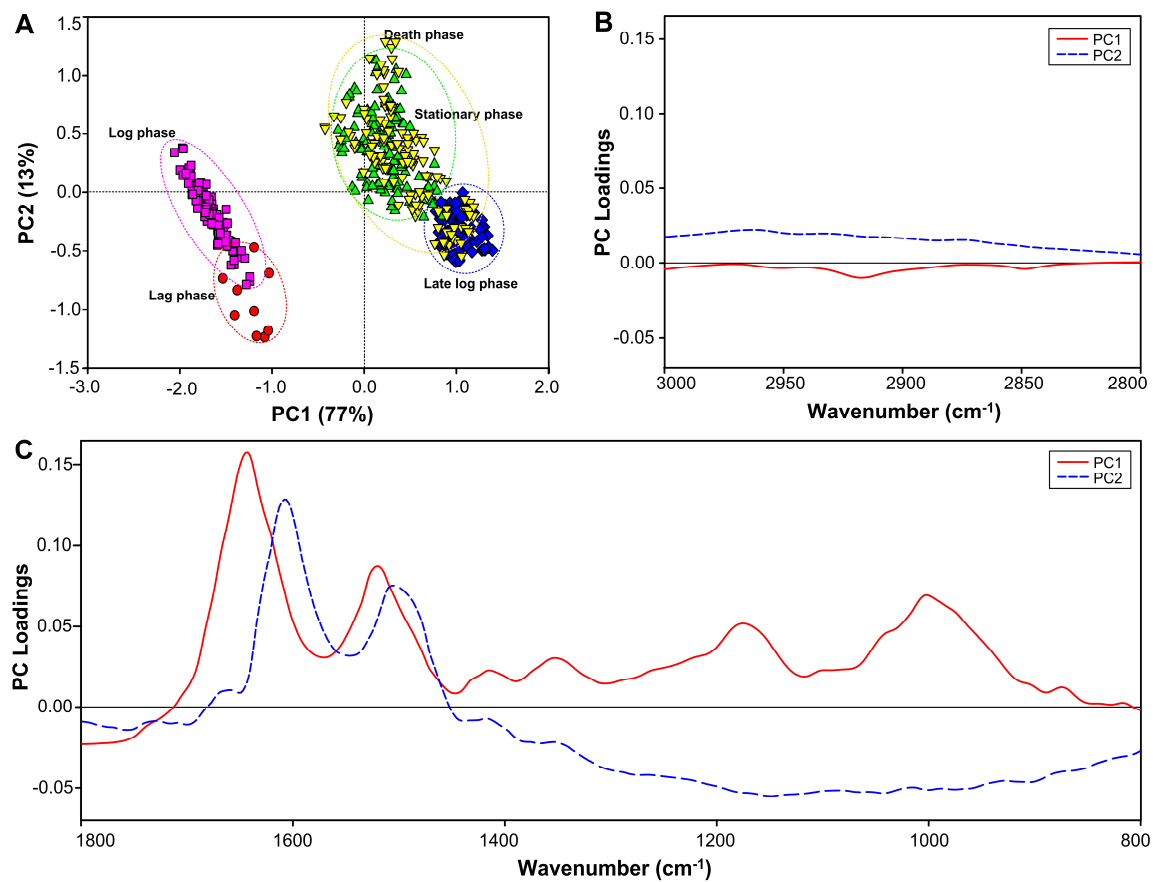


Figure 4.11 Principal component analysis (PCA) applied to FT-IR spectra of PDMCd2007 growth phases. (A) shows the score plots of PC1 and PC2; (B) and (C) show loading plots of PC1 and PC2 in the ranges of 3000-2800 cm⁻¹ and 1800-800 cm⁻¹, respectively

Normalized average FT-IR spectra and second derivative spectra at each growth phase of PDMCd2008 are shown in Figure 4.12 and Figure 4.13, respectively. Through the time period from the lag phase to death phase, the normalized spectral features of the whole cells did not show peaks shifting in the fatty acid region of -CH_3 and >CH_2 stretching. The height of peaks in the fatty acid region were highest in the stationary phase, and the peaks continuously decreased in the death phase and late-log phase by -CH_3 asymmetric stretching (2960 cm^{-1}), >CH_2 asymmetric stretching (2923 cm^{-1}), -CH_3 symmetric stretching (2873 cm^{-1}) and >CH_2 symmetric stretching (2852 cm^{-1}). In addition, the peaks in the amide I, II region from of amide I regions of the α -helical structure proteins ($1658, 1652, 1650\text{ cm}^{-1}$), amide I of the β -sheets proteins ($1639, 1638, 1635\text{ cm}^{-1}$) and amide II (1545 cm^{-1}) continuously increased from lag phase to stationary phase, but the peaks of the amide I, II region were decreasing in the death phase. The highest peaks in the amide I, II region of the α -helical structure proteins (1652 cm^{-1}), amide I of the β -sheets proteins (1638 cm^{-1}) and amide II (1545 cm^{-1}) were in the late-log phase, and the peaks shifted in the amide I region (amide I regions of the α -helical structure proteins from 1650 to 1652 cm^{-1} , the β -sheets proteins from 1635 to 1639 cm^{-1}). The peaks in the amide I region of the stationary and death phases shifting as the α -helical structure proteins from 1650 to 1658 cm^{-1} and the β -sheets proteins from 1635 to 1638 cm^{-1} . The highest peaks in the phospholipids region with P=O asymmetric stretching of PO_2 ($1240, 1219\text{ cm}^{-1}$) and polysaccharide region of the carbohydrates ($1118, 1083$ and 1056 cm^{-1}) were in the stationary phase. In addition, the lowest peaks in the fatty acids region, amide I, II region, phospholipids (PO_2) region and polysaccharide (C-O-P) region were in the lag phase and log phase.

The PCA score plot and loading plots for PDMCd2008 growth phases are shown in Figure 4.14. The cluster of spectra were separated along PC1 and PC2; PC1 explained nearly 70% of the variance and PC2 explained 13% (Figure 4.14 A). The PC1 score plot separated the growth of the lag phase and log phase from the late-log to death phase; the PC2 score plot did not separate the growth phases. Analysis of PC1 loading plots (Figure 4.14 B, C) explained the differences in the amide I, II region (amide I of α -helical proteins ($1658, 1652\text{ cm}^{-1}$), amide I of β -sheets proteins ($1639, 1638\text{ cm}^{-1}$), amide II of proteins (1545 cm^{-1})), phospholipids region with P=O asymmetric stretching of PO_2 (PO_2 of Phospholipids at $1240, 1219\text{ cm}^{-1}$) and polysaccharide region



(C-O-P of the carbohydrates at 1118, 1083, 1056 cm^{-1}). The PC2 loading plots (Figure 4.14B, C) showed differences in the fatty acid region ($-\text{CH}_3$ and $>\text{CH}_2$ asymmetric stretching (2960 cm^{-1} , 2923 cm^{-1}) and $-\text{CH}_3$ and $>\text{CH}_2$ symmetric stretching (2873 cm^{-1} , 2852 cm^{-1})), amide I, II region (amide I of α -helical proteins (1658, 1652, 1650 cm^{-1}), amide I of β -sheets proteins (1639, 1638, 1635 cm^{-1}), amide II of proteins (1545 cm^{-1})), phospholipids region with P=O asymmetric stretching of PO_2 (PO_2 of Phospholipids at 1240, 1219 cm^{-1}) and polysaccharide region (C-O-P of the carbohydrates at 1118, 1083, 1056 cm^{-1}).



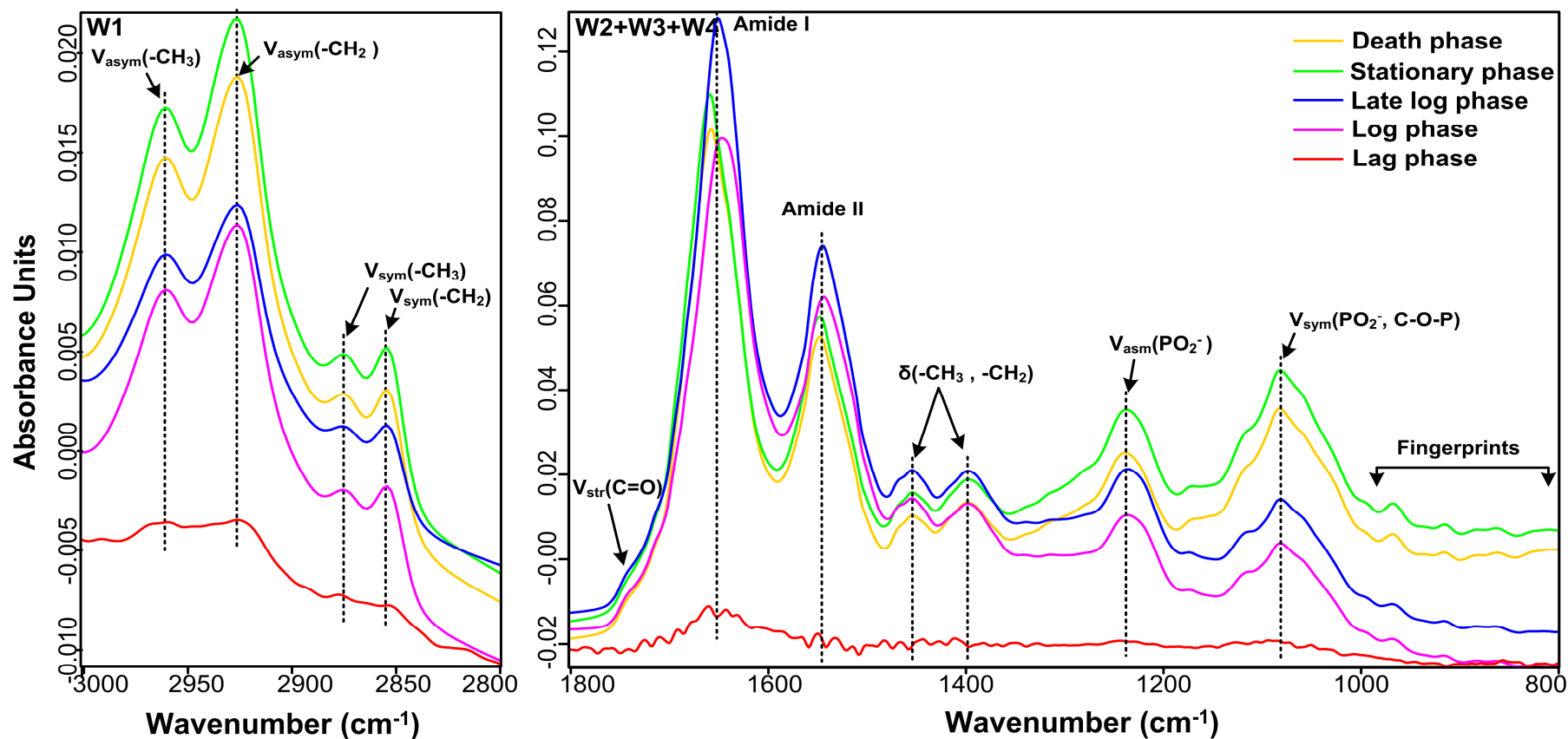


Figure 4.12 Normalized average FT-IR spectra of PDMCd2008 cells at lag phase, log phase, late-log phase, stationary phase and death phase. The spectral windows are defined according to the classification. Where, W1 is the fatty acid region (3000-2800 cm^{-1}), W2 is the amide region (1800-1500 cm^{-1}), W3 is the mixed region (1500-1200 cm^{-1}) and W4 is the polysaccharide region (1200-900 cm^{-1}). One spectrum was averaged from 100-125 spectra of each growth phase.

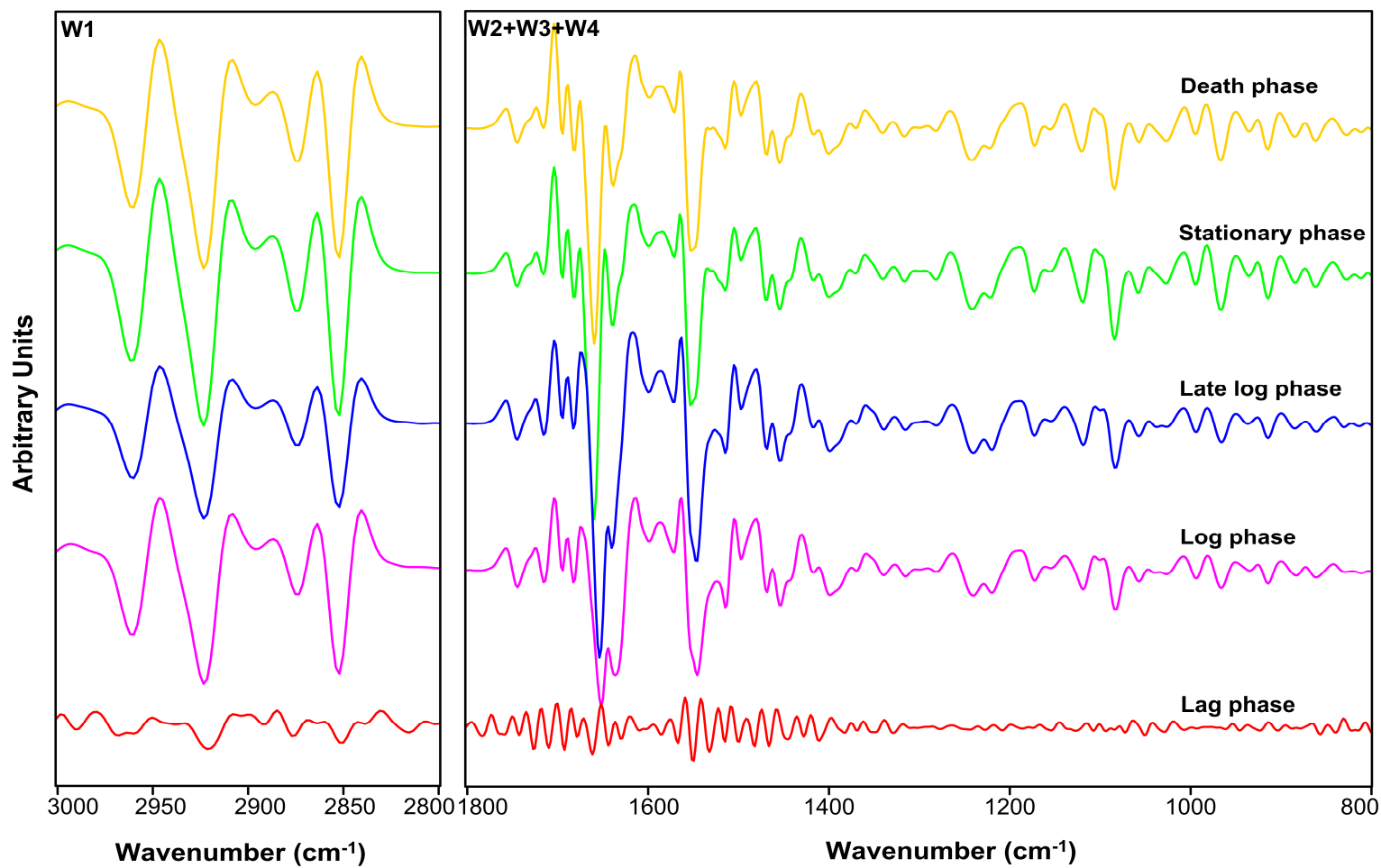


Figure 4.13 Second-derivative FT-IR spectra of PDMCd2008 cells at lag phase, log phase, late-log, phase, stationary phase and death phase. The spectral windows are defined according to the classification.

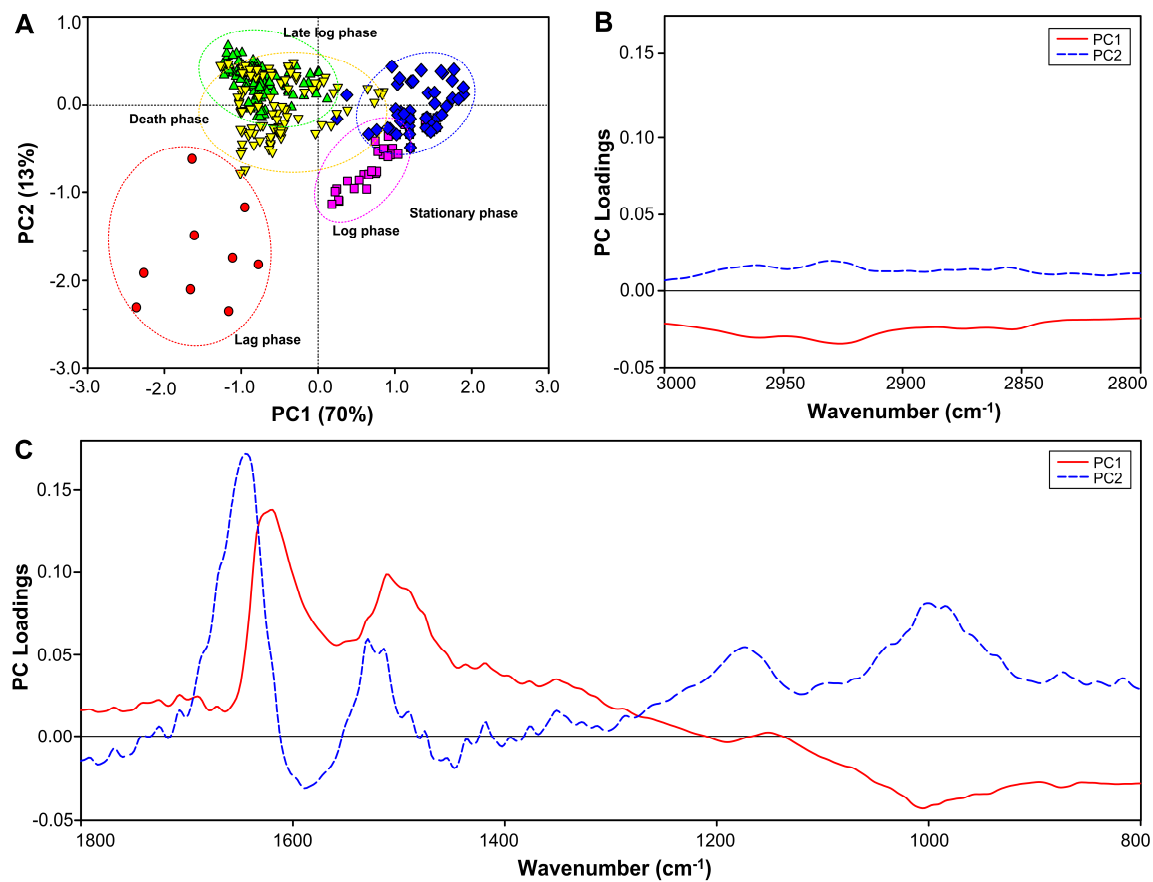


Figure 4.14 Principal component analysis (PCA) applied to FT-IR spectra of PDMCd2008 growth phases. (A) shows the score plots of PC1 and PC2; (B) and (C) show loading plots of PC1 and PC2 in the ranges of 3000-2800 cm^{-1} and 1800-800 cm^{-1} , respectively.

Normalized average FT-IR spectra and second derivative spectra at each growth phase of PDMZnCd1502 are shown in Figure 4.15 and Figure 4.16, respectively. Through the time period from the lag phase to death phase, the normalized spectral features of the whole cells did not show peak shifts in the fatty acid region of $-\text{CH}_3$ and $>\text{CH}_2$ stretching. The height of peaks in the fatty acids region of $-\text{CH}_3$ asymmetric stretching vibrations (2960 cm^{-1}), $>\text{CH}_2$ asymmetric stretching vibrations (2923 cm^{-1}), $-\text{CH}_3$ symmetric stretching vibrations (2873 cm^{-1}) and $>\text{CH}_2$ symmetric stretching vibrations (2852 cm^{-1}) continuously increased in the lag phase to stationary phase, and decreased in the death phase. The height of peaks in the amide I, II region of the amide I regions of the α -helical structure proteins ($1658, 1653\text{ cm}^{-1}$), amide I of the β -sheets proteins ($1638, 1629\text{ cm}^{-1}$) and amide II (1550 cm^{-1}) continuously increased in the lag to death phases, and the peaks decreased in the stationary phase. The highest peaks in the amide I, II region of the α -helical structure proteins (1658 cm^{-1}), amide I of the β -sheets proteins (1638 cm^{-1}) and amide II (1550 cm^{-1}) were in the death phase. The shift peaks in the amide I region of the α -helical structure proteins from 1653 to 1658 cm^{-1} and the β -sheets proteins from 1629 to 1638 cm^{-1} were in the late-log to death phases. The shift peaks in the phospholipids region with $\text{P}=\text{O}$ asymmetric stretching of PO_2 (phospholipids region with $\text{P}=\text{O}$ asymmetric stretching of PO_2 from 1240 to 1242 cm^{-1} and from 1219 to 1220 cm^{-1}) and the polysaccharide region of the carbohydrates (polysaccharide region of C-O-P from 1118 to $1119, 1083$ to 1085 and 1056 to 1058 cm^{-1}) were in the death phase. The highest peaks in the phospholipids region with $\text{P}=\text{O}$ asymmetric stretching of PO_2 ($1240, 1220\text{ cm}^{-1}$) and the polysaccharide region of the carbohydrates ($1118, 1083$ and 1056 cm^{-1}) were in the late-log phase. The lowest peaks in the fatty acids region, amide I, II region and phospholipids (PO_2) region and polysaccharide (C-O-P) region were in the lag phase and log phase.

The PCA score plot and loading plots for PDM ZnCd1502 growth phases are shown in Figure 4.17. The cluster of spectra were separated along PC1 and PC3; PC1 explained nearly 79% of the variance and PC3 explained 7% (Figure 4.17A). The PC1 score plot separated the lag phase and log phase from the late-log to death phase, the PC3 score plot separated the death phase from the late-log to stationary phase. Analysis of PC1 loading plots (Figure 4.17B, C) showed differences in the fatty acid region ($-\text{CH}_3$ and $>\text{CH}_2$ asymmetric stretching ($2960\text{ cm}^{-1}, 2923\text{ cm}^{-1}$))



and $-\text{CH}_3$ and $>\text{CH}_2$ symmetric stretching (2873 cm^{-1} , 2852 cm^{-1}), amide I, II region (amide I of α -helical proteins (1658 , 1653 cm^{-1}), amide I of the β -sheets proteins (1638 , 1629 cm^{-1}), amide II of proteins (1550 cm^{-1})), phospholipids region with $\text{P}=\text{O}$ asymmetric stretching of PO_2 (PO_2 of phospholipids at 1240 , 1242 cm^{-1} and 1219 , 1220 cm^{-1}) and polysaccharide region (C-O-P of the carbohydrates at 1118 , 1119 and 1083 , 1085 and 1056 , 1058 cm^{-1}). The PC3 loading plots (Figure 4.17 B, C) explained differences in the amide I, II region (amide I of the α -helical proteins (1658 cm^{-1}), amide I of the β -sheets proteins (1638 cm^{-1}), amide II of proteins (1550 cm^{-1})), phospholipids region with $\text{P}=\text{O}$ asymmetric stretching of PO_2 (PO_2 of phospholipids at 1240 cm^{-1} , 1220 cm^{-1}) and polysaccharide region (C-O-P of the carbohydrates at 1118 , 1083 , 1056 cm^{-1}).



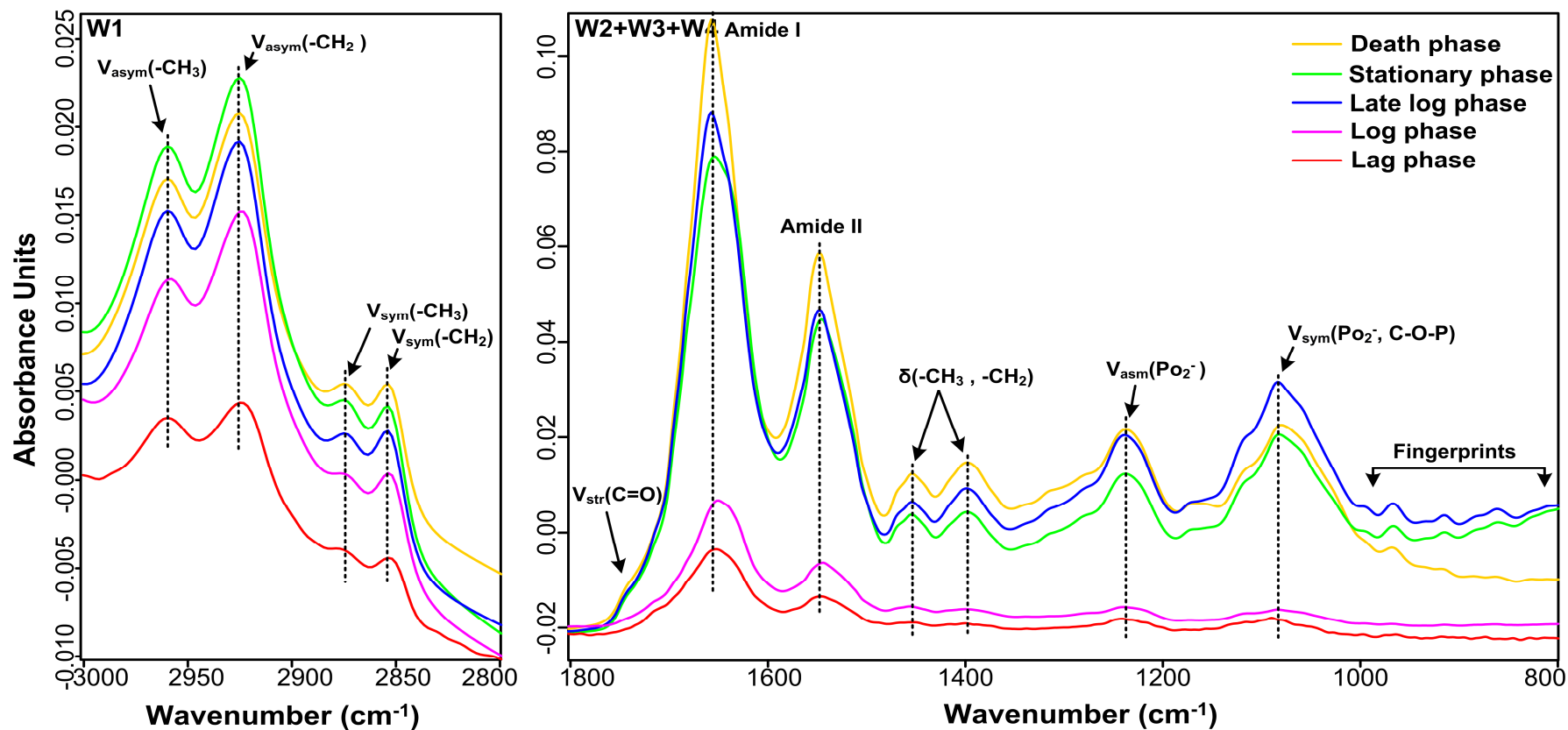


Figure 4.15 Normalized average FT-IR spectra of PDMZnCd1502 cells at lag phase, log phase, late-log phase, stationary phase and death phase. The spectral windows are defined according to the classification. Where, W1 is the fatty acid region (3000-2800 cm^{-1}), W2 is the amide region (1800-1500 cm^{-1}), W3 is the mixed region (1500-1200 cm^{-1}) and W4 is the polysaccharide region (1200-900 cm^{-1}). One spectrum was averaged from 100-125 spectra of each growth phase.

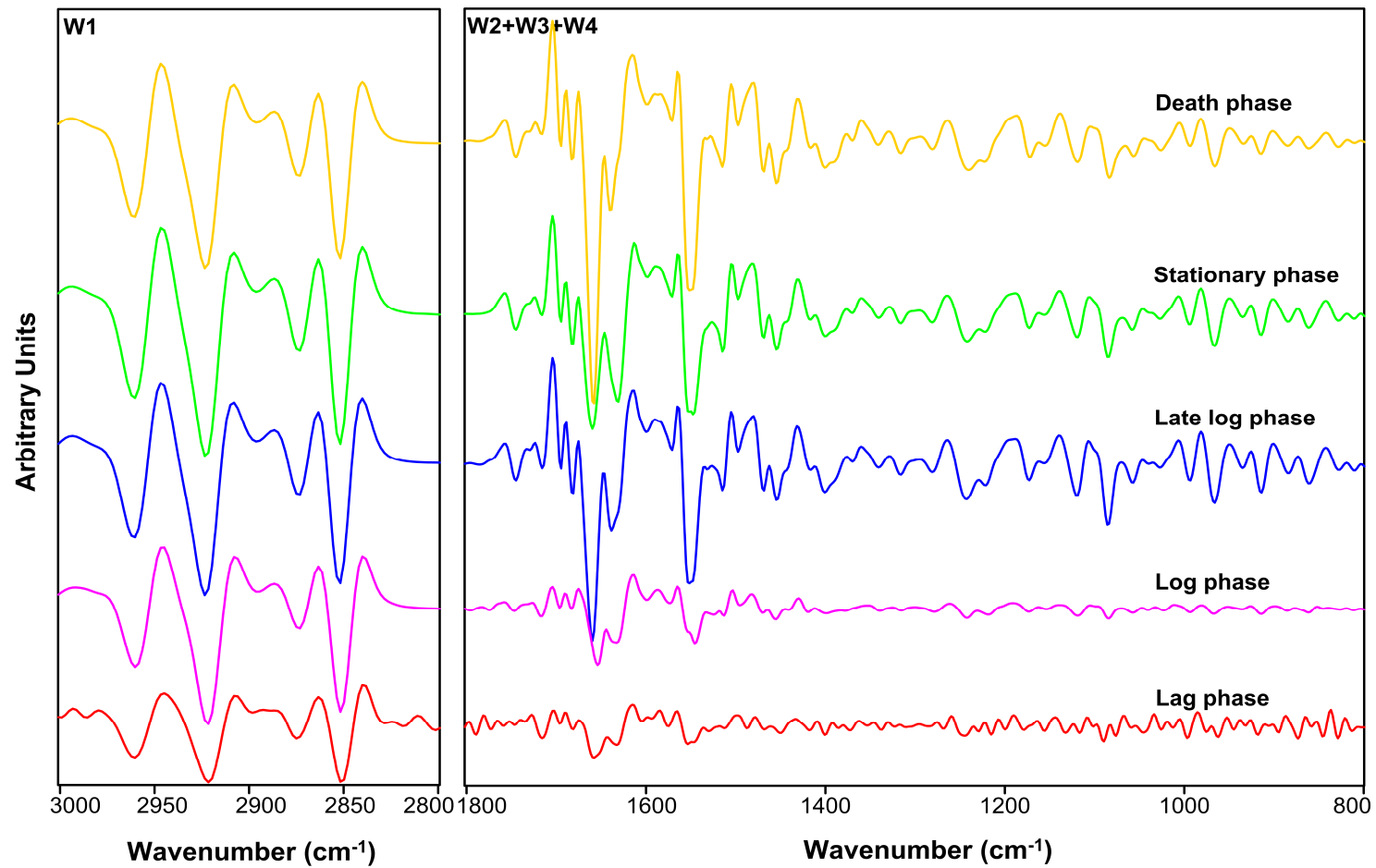


Figure 4.16 Second-derivative FT-IR spectra of PDMZnCd1502 cells at lag phase, log phase, late-log phase, stationary phase and death phase. The spectral windows are defined according to the classification.

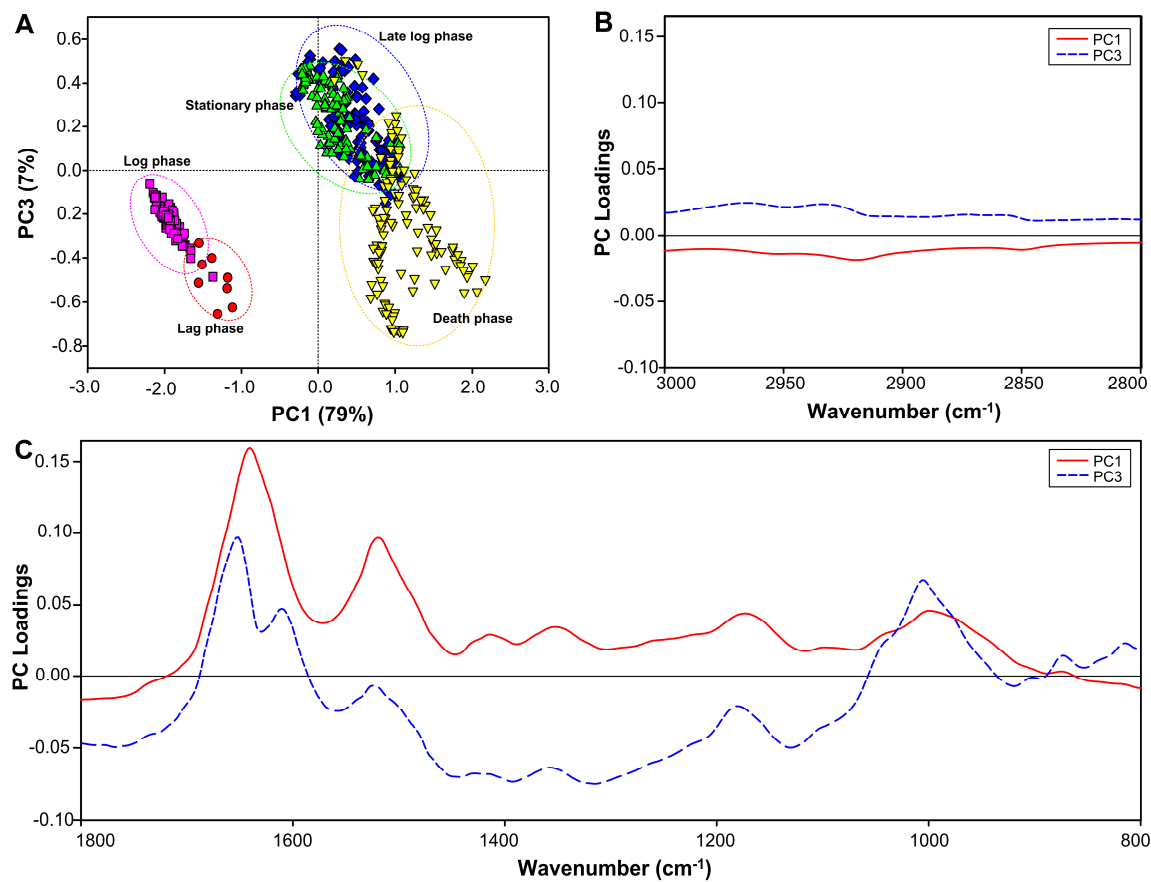


Figure 4.17 Principal component analysis (PCA) applied to FT-IR spectra of PDMZnCd1502 growth phases. (A) shows the score plots of PC1 and PC2; (B) and (C) show loading plots of PC1 and PC2 in the ranges of 3000-2800 cm⁻¹ and 1800-800 cm⁻¹, respectively.

Normalized average FT-IR spectra and second derivative spectra at each growth phase of PDMZnCd2003 are shown in Figure 4.18 and Figure 4.19, respectively. Through the time period from the lag phase to death phase, the normalized spectral features of the whole cells did not show peak shifts in the fatty acid region -CH₃ and >CH₂ stretching. The height of the peaks in the fatty acids region of -CH₃ asymmetric stretching vibrations (2960 cm⁻¹), >CH₂ asymmetric stretching vibrations (2923 cm⁻¹), -CH₃ symmetric stretching vibrations (2873 cm⁻¹) and >CH₂ symmetric stretching vibrations (2852 cm⁻¹) continuously increased from the lag phase to stationary phase, and decreased in the death phase. The height of the peaks in the amide I, II region of the amide I regions of the α -helical structure proteins (1655, 1651 cm⁻¹), amide I of the β -sheets proteins (1639, 1635 cm⁻¹) and amide II (1545 cm⁻¹) continuously increased in the lag phase to death phase. The highest peaks of the amide I, II region of the α -helical structure proteins (1651 cm⁻¹), amide I of the β -sheets proteins (1639 cm⁻¹) and amide II (1545 cm⁻¹) were in the death phase. In the stationary phase, the peaks shifted in the amide I region were in the amide I regions of the α -helical structure proteins from 1655 to 1651 cm⁻¹, the β -sheet proteins from 1625 to 1639 cm⁻¹ of the stationary phase. There were no shifts in the peaks in the phospholipids and polysaccharide region. The highest peaks in the phospholipids region with P=O asymmetric stretching of PO₂ (1240, 1218 cm⁻¹) and the polysaccharide region of the carbohydrates (C-O-P) (1118, 1084 and 1057 cm⁻¹) were in the late-log phase. The lowest peaks in the fatty acids region, amide I, II region and phospholipids (PO₂) region and polysaccharide (C-O-P) region were in the lag phase and log phase.

The PCA score plot and loading plots for PDMZnCd2003 growth phases are shown in Figure 4.20. The cluster of spectra were separated along PC1 and PC2; PC1 explained nearly 74% of the variance and PC2 explained 22% (Figure 4.20A). The PC1 score plot separated the lag phase and log phase from the late-log to death phase; the PC2 score plot did not separate the growth phases. Analysis of the PC1 loading plots (Figure 4.20 B, C) explained the difference in the fatty acid region (-CH₃ and >CH₂ asymmetric stretching (2960 cm⁻¹, 2923 cm⁻¹) and -CH₃ and >CH₂ symmetric stretching (2873 cm⁻¹, 2852 cm⁻¹)), amide I, II region (amide I of α -helical proteins (1655, 1651 cm⁻¹), amide I of the β -sheets proteins (1639, 1635 cm⁻¹), amide II of proteins (1545 cm⁻¹)), phospholipids region with P=O asymmetric stretching of PO₂ (1240, 1218 cm⁻¹))



and polysaccharide region of the carbohydrates (C-O-P) (1118, 1084 and 1057 cm^{-1}). The PC2 loading plots (Figure 4.20 B, C) showed differences in the amide I, II region (amide I of the α -helical proteins (1655, 1651 cm^{-1}), amide I of the β -sheets proteins (1639, 1635 cm^{-1}), amide II of the proteins (1545 cm^{-1})), phospholipids region with P=O asymmetric stretching of PO_2 (1240, 1218 cm^{-1}) and polysaccharide region of the carbohydrates (C-O-P) (1118, 1084 and 1057 cm^{-1}).

The FT-IR spectra and data analysis of the six bacterial isolates (Figures 4.3-4.20) indicated that the spectroscopic features of the bacterial cells depended on their growth phases. The cell components in the lag and log phases seemed to be not stable, whereas the cells in the stationary and death phases started death and lysis. Therefore, the bacterial cells in the late-log phase were the best representative cells for bacterial identification by the 16S rDNA sequence and the bacterial classification with whole cell protein patterns and normalized FT-IR spectral features of the whole cell.



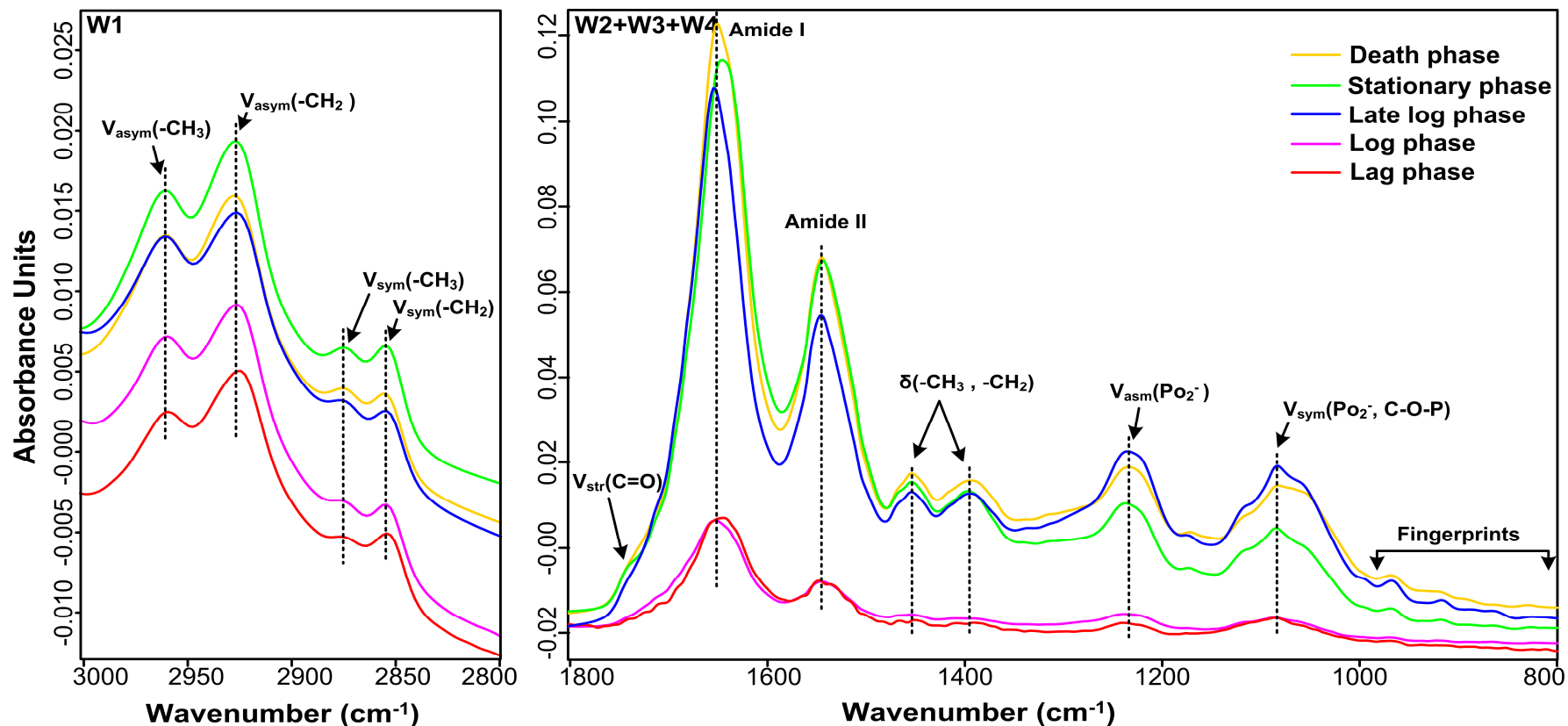


Figure 4.18 Normalized average FT-IR spectra of PDMZnCd2003 cells at lag phase, log phase, late-log phase, stationary phase and death phase. The spectral windows are defined according to the classification. Where, W1 is the fatty acid region (3000-2800 cm^{-1}), W2 is the amide region (1800-1500 cm^{-1}), W3 is the mixed region (1500-1200 cm^{-1}) and W4 is the polysaccharide region (1200-900 cm^{-1}). One spectrum was averaged from 100-125 spectra of each growth phase.

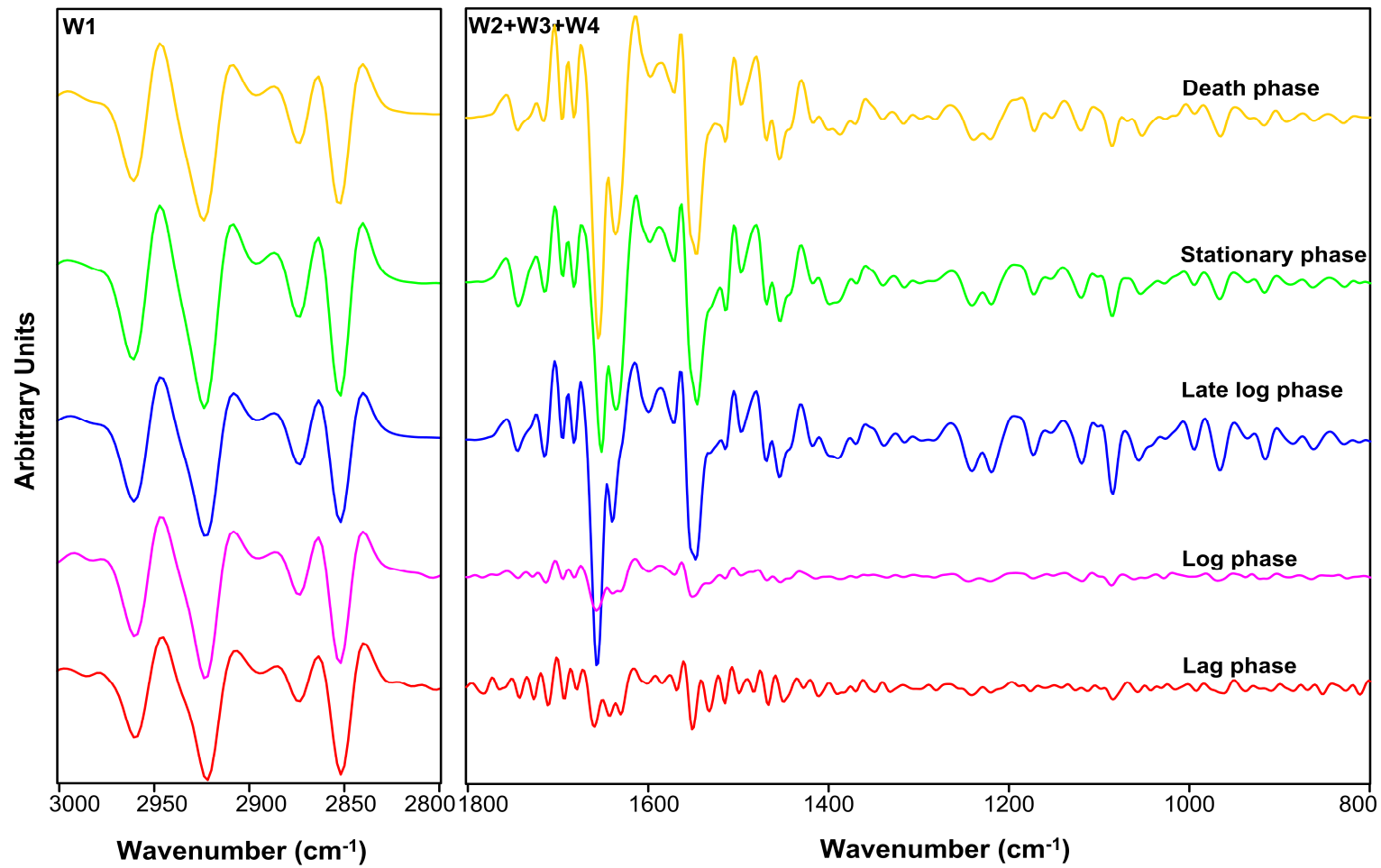


Figure 4.19 Second-derivative FT-IR spectra of PDMZnCd2003 cells at lag phase, log phase, late-log phase, stationary phase and death phase. The spectral windows are defined according to the classification.

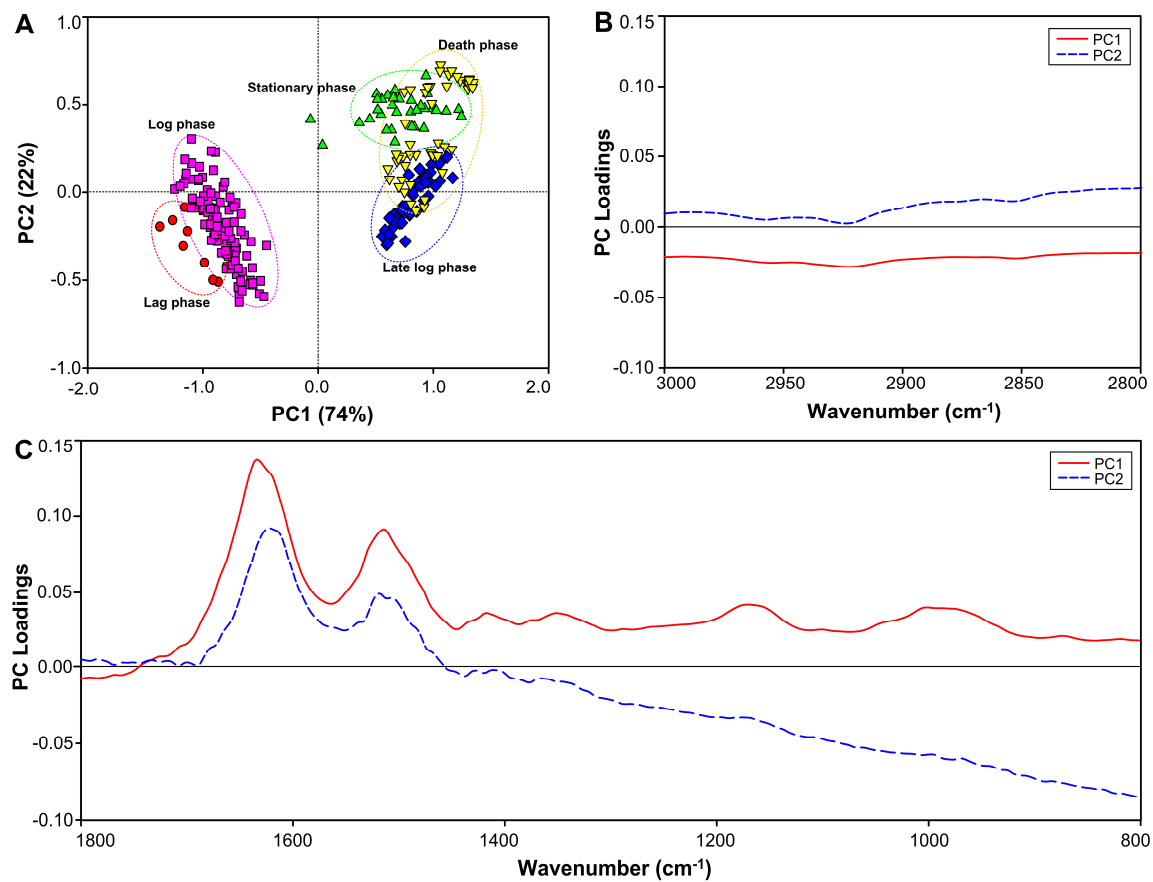


Figure 4.20 Principal component analysis (PCA) applied to FT-IR spectra of PDMZnCd2003 growth phases. (A) shows the score plots of PC1 and PC2; (B) and (C) show loading plots of PC1 and PC2 in the ranges of 3000-2800 cm⁻¹ and 1800-800 cm⁻¹, respectively.

4.3 Identification and classification of bacterial isolates

The bacterial isolates were identified and classified with three techniques of genotype characteristics of partial 16S rDNA sequence, whole cell protein patterns obtained by Sodium Dodecyl Sulphate Polyacrylamide Gel Electrophoresis (SDS-PAGE) and normalized spectral features of the whole cells obtained by Fourier Transform Infrared spectroscopy (FT-IR) microspectroscopy.

4.3.1 Identification by 16S rDNA sequences

The 16S rDNA sequencing data of the six bacterial isolates were matched with the available sequences in the GenBank database. They belonged to 2 phyla, 3 families and 4 different genera. Figure 4.21 shows the phylogenetic relationship between different members of the *Brevibacterium* genus, *Serratia* genus, *Providencia* genus and *Pseudomonas* genus and our bacterial isolates. The identification by genotype characteristics of the partial 16S rDNA sequence indicated that bacterial isolates of PDMZn2008 showed 99% similarity with *Brevibacterium epidermidi*. PDMCd0501 and PDMCd2007 exhibited 99% and 98%, respectively, similarity with *Serratia marcescens*. PDMCd2008 and PDMZnCd1502 exhibited 99% and 99%, respectively, similarity with *Providencia vermicola*. PDMZnCd2003 revealed 99% similarity with *Pseudomonas aeruginosa*. The GenBank accession numbers and the corresponding strain numbers are: KF781536 (PDMZn2008), JX193587 (PDMCd0501), JX193588 (PDMCd2007), KF781537 (PDMCd2008), KF781538 (PDMZnCd1502) and JX193586 (PDMZnCd2003).

The results of the genetic distance between the pairwise 26 populations of 16S rDNA for all taxa examined are shown in Table 4.3. The distance of the 26 taxa of the 16S rDNA indicated that bacterial isolates of PDMZn2008 showed *Brevibacterium* genus genetic distances in the range of 1.2-5.7% and a species genetic distance of 0.9% with the *B. epidermidis*. PDMCd0501 and PDMCd2007 exhibited *Serratia* genus genetic distances in the range of 1.6-3.7% and species genetics distances of 0.5% and 1.2% with *S. marcescens* respectively. PDMCd2008 and PDMZnCd1502 exhibited *Providencia* genus genetic distances in the range of 0.3-2.1% and species genetics distances of 0.7% and 0.6% with *P. vermicola*, respectively. PDMZnCd2003



revealed *Pseudomonas* genus genetic distances in the range of 3.2-7.4% and a species genetic distance of 2.0% with *P. aeruginosa*.

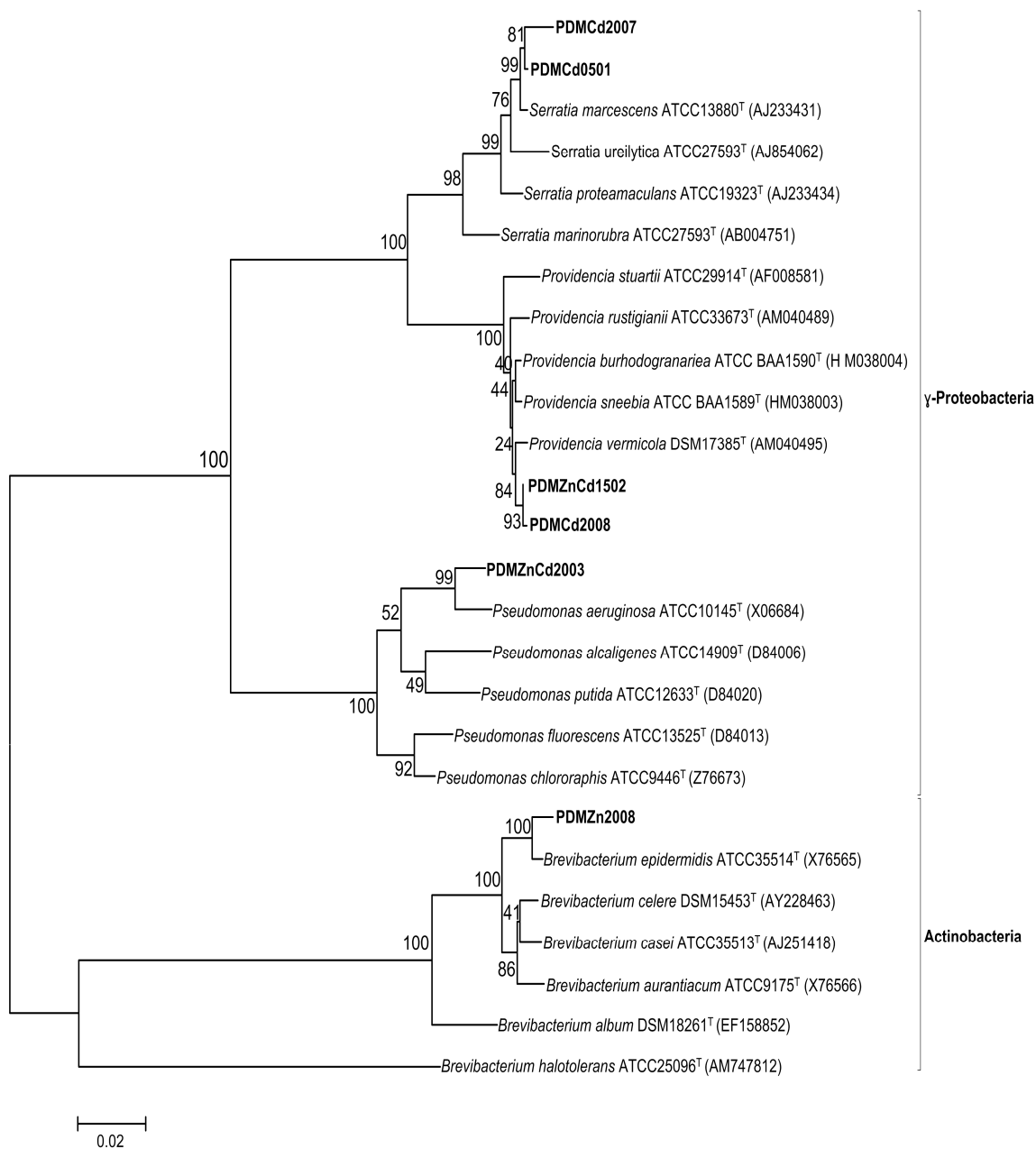


Figure 4.21 Phylogenetic tree of 16S rDNA phylotypes based on the algorithm of the neighbor-joining method as determined by distance using Kimura's two-parameter correction. Scale bar represents 2% estimated distance.



Table 4.3 Kimura 2-parameter genetic distances between F_{ST} pairwise 26 populations for 16S rDNA of the taxa examined.

Population	1	2	3	4	5	6	7	8	9	10	11	12	13	14	15	16	17	18	19	20	21	22	23	24	25	26
1.PDMzn2008	-																									
2.PDMcd0501	0.308	-																								
3.PDMcd2007	0.319	0.009	-																							
4.PDMcd2008	0.315	0.067	0.075	-																						
5.PDMzncd1502	0.313	0.067	0.075	0.001	-																					
6.PDMzncd2003	0.294	0.158	0.167	0.162	0.162	-																				
7. <i>S. marcescens</i> ^T	0.306	0.005	0.012	0.067	0.067	0.158	-																			
8. <i>S. proteamaculans</i> ^T	0.296	0.016	0.023	0.066	0.066	0.152	0.016	-																		
9. <i>S. ureilytica</i> ^T	0.299	0.016	0.023	0.075	0.075	0.152	0.016	0.019	-																	
10. <i>S. marinorubra</i> ^T	0.299	0.027	0.034	0.059	0.057	0.163	0.027	0.029	0.037	-																
11. <i>B. casei</i> ^T	0.026	0.303	0.313	0.311	0.312	0.301	0.301	0.289	0.294	0.301	-															
12. <i>B. celere</i> ^T	0.021	0.301	0.312	0.311	0.312	0.303	0.299	0.289	0.292	0.296	0.012	-														
13. <i>B. epidermidis</i> ^T	0.009	0.303	0.313	0.313	0.311	0.301	0.303	0.292	0.296	0.298	0.025	0.021	-													
14. <i>B. aurantiacum</i> ^T	0.030	0.299	0.310	0.315	0.315	0.305	0.298	0.289	0.291	0.298	0.016	0.013	0.025	-												
15. <i>B. album</i> ^T	0.053	0.286	0.296	0.299	0.297	0.282	0.284	0.285	0.284	0.287	0.057	0.051	0.051	0.051	-											
16. <i>B. halotolerans</i> ^T	0.246	0.276	0.284	0.276	0.276	0.266	0.276	0.274	0.274	0.283	0.230	0.235	0.243	0.233	0.234	-										
17. <i>P. sneebia</i> ^T	0.315	0.072	0.080	0.008	0.007	0.164	0.072	0.071	0.080	0.060	0.309	0.309	0.313	0.313	0.296	0.279	-									
18. <i>P. stuartii</i> ^T	0.318	0.075	0.083	0.017	0.016	0.168	0.075	0.074	0.083	0.065	0.320	0.317	0.317	0.320	0.297	0.281	0.014	-								
19. <i>P. vermicola</i> ^T	0.317	0.074	0.081	0.007	0.006	0.162	0.074	0.072	0.082	0.061	0.315	0.311	0.315	0.318	0.297	0.284	0.006	0.017	-							
20. <i>P. burhodogranariae</i> ^T	0.313	0.071	0.079	0.007	0.006	0.161	0.071	0.070	0.079	0.061	0.311	0.311	0.315	0.315	0.297	0.277	0.003	0.015	0.007	-						
21. <i>P. rustigiani</i> ^T	0.311	0.070	0.077	0.010	0.009	0.155	0.070	0.069	0.078	0.062	0.310	0.310	0.310	0.313	0.292	0.276	0.009	0.021	0.010	0.008	-					
22. <i>Ps. aeruginosa</i> ^T	0.310	0.157	0.165	0.162	0.162	0.020	0.159	0.154	0.155	0.164	0.305	0.310	0.298	0.305	0.289	0.275	0.164	0.168	0.162	0.164	0.155	-				
23. <i>Ps. alcaligenes</i> ^T	0.312	0.162	0.171	0.164	0.164	0.040	0.164	0.159	0.158	0.170	0.305	0.305	0.301	0.300	0.293	0.263	0.162	0.166	0.164	0.162	0.156	0.040	-			
24. <i>Ps. chlororaphis</i> ^T	0.290	0.147	0.155	0.145	0.145	0.052	0.147	0.141	0.144	0.153	0.281	0.283	0.286	0.288	0.276	0.243	0.144	0.151	0.145	0.144	0.141	0.058	0.040	-		
25. <i>Ps. fluorescens</i> ^T	0.278	0.152	0.161	0.151	0.150	0.065	0.152	0.147	0.147	0.153	0.276	0.274	0.276	0.283	0.274	0.256	0.148	0.154	0.149	0.148	0.145	0.074	0.055	0.017	-	
26. <i>Ps. putida</i> ^T	0.303	0.152	0.161	0.162	0.162	0.059	0.155	0.149	0.152	0.164	0.296	0.295	0.298	0.300	0.286	0.264	0.161	0.168	0.162	0.161	0.158	0.064	0.035	0.032	0.041	-

The consistent results of the consensus phylogeny (Figure 4.21) and genetics pairwise distance (Table 4.3) were clearly demonstrated for this sample of 26 taxa. The distances between species were always higher, and usually much higher than the levels of diversity segregating within species. A prokaryotic species is practically considered to be a group of strains that are characterized by a certain degree of phenotypic consistency, which shows 70% DNA–DNA binding and over 97% 16S rDNA sequence identity (Vandamme, et al., 1996).

The identified species of our six bacteria isolates, which had Zn/Cd tolerant and PGPB properties, corresponded with past references. *Brevibacterium* sp. HZM-1 containing a zinc resistance was isolated from an abandoned zinc mining area (Taniguchi, et al., 2000), and *B. epidermidis* RS15 was isolated from a halophytic plant's rhizosphere and had plant growth promoting properties (Siddikee, et al., 2010). A *Serratia* sp. was found in arsenic-contaminated soil and it had the ability to promote the growth of plants (Chopra, et al., 2007). A *Providencia* sp. UTDM314 had great potential for bioremediation of Cr(VI) containing wastes, and it exhibited multiple heavy metal (Ni, Zn, Hg, Pb, Co) tolerances (Thacker et al., 2006). In addition, a *Providencia* sp. isolated from wheat plants was reported to be a plant growth promoting bacterium (Rana, et al., 2011). In addition, *Pseudomonas* sp. have been reported on heavy metals and to have chemical stress characteristics, while the bacterium has been suggested for improving the phytoremediation process previously (Roane and Pepper, 2000; Robinson et al., 2001; Farwell et al., 2007; Rajkumar and Freitas, 2008a, b; Abou-Shanab, et al., 2008; Braud, et al., 2009a, b; Nakbanpote, et al 2010; Meesungnoen, et al., 2012; Siripornadulsil and Siripornadulsil, 2013). *Ps. Aeruginosa*, showed uranium accumulation by both passive diffusion and translocation processes (Strandberg, et al., 1981; Hughes and Poole, 1989) and a *Pseudomonas* sp. was isolated and found to have Cd²⁺-resistance (Horitsu, et al., 1986).

4.3.2 SDS-PAGE

Whole-cell protein profiles of the six bacteria isolates obtained by SDS-PAGE are shown in Figure 4.22 A. The characteristic protein bands of PDMZn2008, PDMCd0501, PDMCd2007, PDMCd2008, PDMZnCd1502 and PDMZnCd2003 were shown in lines A, B, C, D, E and F, respectively. The protein bands of the PDMCd0501 and PDMCd2007 isolates (lines B and C) had similar patterns. While, the protein bands



of the PDMCd2008 and PDMZnCd1502 isolates (lines D and E) had alike patterns. Moreover, the protein bands of PDMZn2008 and PDMZnCd2003 (lines A and F) obviously differed from the other bacteria isolates. A dendrogram produced after numerical analysis of the whole-cell protein profiles using the Pearson product-moment correlation coefficient and unweighted pair group method with arithmetic averages algorithm (UPGMA) is shown in Figure 4.22B. Numerical analysis clearly revealed two distinct clusters at a similarity level of 42% as shown in the dendrogram. Cluster 1 included two isolates of PDMZn2008 and PDMZnPd2003. The similarity levels of 47% belonged to PDMZn2008 and PDMZnCd2003. The strains of the cluster 2 were clearly separated from cluster 1 by numerical analysis. Cluster 2 comprised four isolates at similarity levels that altered between 67% and 100% and belonged to PDMCd0501, PDMCd2007, PDMCd2008 and PDMZnCd1502. As seen from Figure 4.22A and 4.22B, the isolates of PDMCd0501 and PDMCd2007 formed an electrophoretically homogeneous cluster with a 100% similarity level. The same was true for the PDMCd2008 and PDMZnCd1502 isolates at the similarity level of 100%. In addition, previous research work has already demonstrated that numerical analysis of one-dimensional protein electrophoretic patterns might be useful in bacterial taxonomy studies.

Numerical analysis of one-dimensional protein electrophoretic patterns may be useful in bacterial taxonomy studies. The conventional tests based on the phenotypic characteristics can clearly lead to misclassification in some bacterial taxa (Berber, 2004). The electrophoretic technique is necessary for integrated use of phenotypic characters in identification of bacterial genera (Clink and Pennington, 1987; Murray et al 1990; Khan et al., 1996). Previous research work already demonstrated that numerical analysis of one-dimensional protein electrophoretic patterns is very useful for the identification of bacteria at the species level (Kerstens, et al., 1994). The SDS-PAGE database of whole-cell proteins also proved to be of great value for the identification of new isolates from environmental samples (Vancanneyta, et al., 1996), and protein electrophoresis has been of great value for the delineation of numerous bacterial taxa (Costas, 1992).



It was also found that protein patterns can be applied to study the diversity, characterization and identification of natural microbial species, and this thus suggests

that protein patterns may be useful in bacterial taxonomy studies (Jackman and Pelczynska, 1986; Adwan, 1999; Zamfira, et al., 2006). In addition, protein profiles of whole-cell and extracellular proteins are good enough to distinguish most of bacterial genera at the species level (Cokmus and Yousten, 1987; Costas, et al., 1993; Saçilik, et al., 2000; Berber, et al., 2003; Berber, 2004; Piraino, et al 2006).



4.3.3 FT-IR characteristics of bacteria

The normalized average original spectra and second derivative spectra are shown in Figure 4.23A and 4.23B, respectively. The spectra were identified by visual inspection of the spectra regions W1, W2, W3 and W4. The region between W2 and W3 ($1800\text{-}1400\text{ cm}^{-1}$) showed the majority of the variations. When the six bacterial spectra were compared, the most evident differences appeared in the W1 and W2 regions. Well-defined peaks emerged in the PDMZn2008, PDMCd0501, PDMCd2007 and PDMZnCd1502 spectra of 2923 , 2852 , 1658 and 1639 cm^{-1} , and in the PDMCd2008 and PDMZnCd2003 spectra of 1656 , 1657 and 1639 cm^{-1} , which were the structures of the fatty acid region -CH_3 and >CH_2 stretching vibrations and amide I of the α -helical and the β -pleated sheet structures of proteins and peptides. Table 4.4 shows characteristic functional groups contributing to the formation of absorption peaks at the wavenumber ranges.

The FT-IR spectra of the bacterial isolates were statistically analyzed by multivariate data analysis, in particular Principal Component Analysis (PCA). The PCA score plots and loading plots are shown in Figure 4.24. In Figure 4.24A, the PCA score plot clustered the bacterial isolates along PC1 and PC2; PC1 explained nearly 62% of the variance and PC2 explained 28%. Analysis of PC1 loadings (Figure 4.24 B-D) explained differences in the fatty acids structure with predominant C-H asymmetric and symmetric stretching of >CH_2 (2923 cm^{-1} , 2852 cm^{-1}) and the amide I and amide II bands of the proteins and peptides (1648 cm^{-1} , 1540 cm^{-1}). The PC1 was able to separate only three isolates, PDMCd0501, PDMCd2008 and PDMZnCd2003, and could not distinguish the three isolates of PDMZn2008, PDMCd2007 and PDMZnCd1502 because of few different functional groups. Therefore, the three isolates were repeatedly analyzed for distinction.

The repeated PCA score plots of PDMCd2008, PDMZnCd2003 and PDMCd0501 were clustered along PC1 and PC2 (Figure 4.24 E); PC1 explained 35% of the variance and PC2 explained 28%. Analysis of PC1 loadings plots (Figure 4.24 F-H) showed differences in the fatty acids region with predominant C-H asymmetric and symmetric stretching of >CH_2 (2923 cm^{-1} , 2852 cm^{-1}) and the amide I, II region of proteins and peptides (1648 cm^{-1} , 1540 cm^{-1}). However, the PC1 of Figure 4.24



(E) could separate only three bacterial isolates (PDMCd0501, PDMCd2008 and PDMZnCd2003).

The repeated PCA score plot shows that the spectra from the bacterial isolates of PDMCd2007, PDMZnCd1502 and PDMZn2008 were clustered along PC1 and PC6 (Figure 4.24 I); PC1 explained nearly 68% of the variance and PC6 explained 1%. PC1 and PC6 clearly separated the three isolates. Analysis of PC1 loading plots in Figure 4.24 J-L explain the different peaks in the amide I, II region of the proteins and peptides (1660 cm^{-1} , 1648 cm^{-1} , 1631 cm^{-1} and 1540 cm^{-1}). The PC6 loading plots in Figure 4.24 J-L indicated the difference between the bacteria isolates from the C=O of the ester and RNA/DNA, phospholipids structure with P=O symmetric stretching of PO_2 (1714 , 1081 and 1060 cm^{-1}).

The Hierarchical Cluster Analysis (HCA) method was used for direct comparison to clarify spectra based on similarities and differences in the macromolecule chemistry of the different cells. HCA analysis included the average spectra of spectral clusters (100-125 spectra) and was based on calculating the multidimensional Ward linkage with Euclidean distance. The metric was then applied to the spectral data to compare within sample and between sample spectral variability. The HCA dendrogram in Figure 4.25 was constructed from the averaged whole cell spectra of the six bacterial isolates using the best combination of derivative and region, i.e. a second derivative (9-point) and region of W_1 , W_2 , W_3 and W_4 . The HCA indicated that the bacteria have been the basic components of each separate group, and each cluster might be closed together in one class. The results of HCA in the regions of W_1 , W_2 , W_3 and W_4 (Figure 4.25 A-D) showed that all bacteria were clearly separated into six groups, which corresponded to the HCA results of all region. Figure 4.25E clearly separates the six bacterial isolates into two main clusters of 1 and 2. Cluster 1 consisted of the isolates of PDMZn2008, PDMCd0501, PDMCd2007 and PDMZnCd1502, and cluster 2 consisted of the isolates of PDMCd2008 and PDMZnCd2003.

Cluster analysis is one of the methods used for identifying bacteria on the basis of FT-IR spectra. However, the application of this analysis is limited, and the results obtained are sometimes unsatisfactory. Apart from being a discriminative method, the technique may provide information on the phylogeny of bacteria. Therefore, the FT-IR spectroscopy technique combined with chemometrics can be



helpful to study the differentiation, classification and discrimination of bacterial strains based on the biochemical component. Previous references demonstrated that FT-IR can differentiate between bacteria strains (Al-Holya, et al., 2006). FT-IR spectroscopy is a reliable whole-organism fingerprinting tool capable of monitoring structural and quantitative changes in biomacromolecules (Garip, et al., 2009). Several authors have established these spectral zones as a fingerprint for bacterial characterization and differentiation (Bouhedja, et al., 1997; Amiel, et al., 2000; Garip, et al., 2007); hence, the region-selection methodology used in this work ($900\text{--}1350\text{ cm}^{-1}$) was accurate. The relationships between carbohydrates and phospholipid bands of DNA, RNA or cell membranes could be a potential marker for differentiating the study bacteria (San-Blas et al., 2012). The spectroscopic fingerprints of microbial cells obtained by the microspectroscopic approach provide important structural and compositional information of microbial cells, and can be used to differentiate these microorganisms down to the strain level (Yu and Irudayaraj, 2005). FT-IR is a very powerful method for discriminating bacteria at the species to subspecies levels (Naumann, et al., 1991; Naumann, et al. 1988). Moreover, the advantages of this technique regarding other phenotypic or genotypic methods are its swiftness, easiness and high through put capacity at low cost (Guibet, et al., 2003). Therefore, overall this has demonstrated a new application for FT-IR ellipsometry for the detection and identification of microorganisms (Garcia-Caurel, et al., 2004).



Table 4.4 Characteristic functional groups contributing to the formation of absorption bands at the wavenumber ranges of 3000–2800 cm^{-1} , 1800–1500 cm^{-1} , 1500–1400 cm^{-1} and 1200–900 cm^{-1} .

Vibration group	Frequency (cm^{-1})	Bond/remarks
<i>Alkane</i>		
Aromatic-CH ₃	2930-2920 (m)	Asymmetric C-H stretch
	2870-2860 (m)	Symmetric C-H stretch
-CH ₂ -	2936-2915 (vs)	Scissoring bending or deformation
	2965-2840 (vs)	
Lipids, Proteins	1475-1445 (m-s)	
Lipids esters, RNA/DNA	1741, 1715	C=O str of esters
	~1695	Amide I band components
	~1685	Resulting from antiparallel
	~1675	Pleated sheets and b-turns of proteins
<i>Proteins</i>	~1655	Amide I of α -helical structures
	~1637	Amide I of β -pleated sheet structures
	1548	Amide II
	1515	Tyrosine band
<i>Carbonyl bands</i>		
Acid anhydrides [-CO-O-CO-]	1300–1050 (s)	CO stretching
Esters and lactones [-CO-O-]	1300–1050 (s)	CO stretching
<i>Ethers</i>		
CH ₂ -O-CH ₂	1150–1060 (vs)	Asymmetric C-O-C stretch
CH ₂ =CH-O-	890–820 (w)	Symmetric C-O-C stretch
Ph-O-C	1050–1010 (s)	Symmetric C-O-C stretch
	850–810 (w)	Symmetric C-O-C stretch
Aromatic ethers (aryl-alkyl)	1050–1010 (s)	O-CH ₂ or O-CH ₃ stretch
<i>Phosphorus compounds</i>		
PH and PH ₂	1090–1080 (m-s)	Scissors bending or deformation
P=O	1250–1220 (s)	
	, 1085	
P-OH	1040–910 (s)	Asymmetric of stretch of $>\text{PO}_2$ -
P-O-P	1025–870 (s)	Symmetric stretch of $>\text{PO}_2$ -
P-O-C:		P-O
Aliphatic	1050–970 (vs)	Asymmetric P-O-C stretch
Phenyl	1260–1160 (s)	P-O-Ph

** *w=weak, m = moderate, m-s = moderate to strong, s = strong, vs = very strong.*

Note: These groups are derived from Dean's analytical chemistry handbook (Patnaik, 2004) and adapted from Naumann, et al., 1991; Yu and Irudayaraj, 2005.



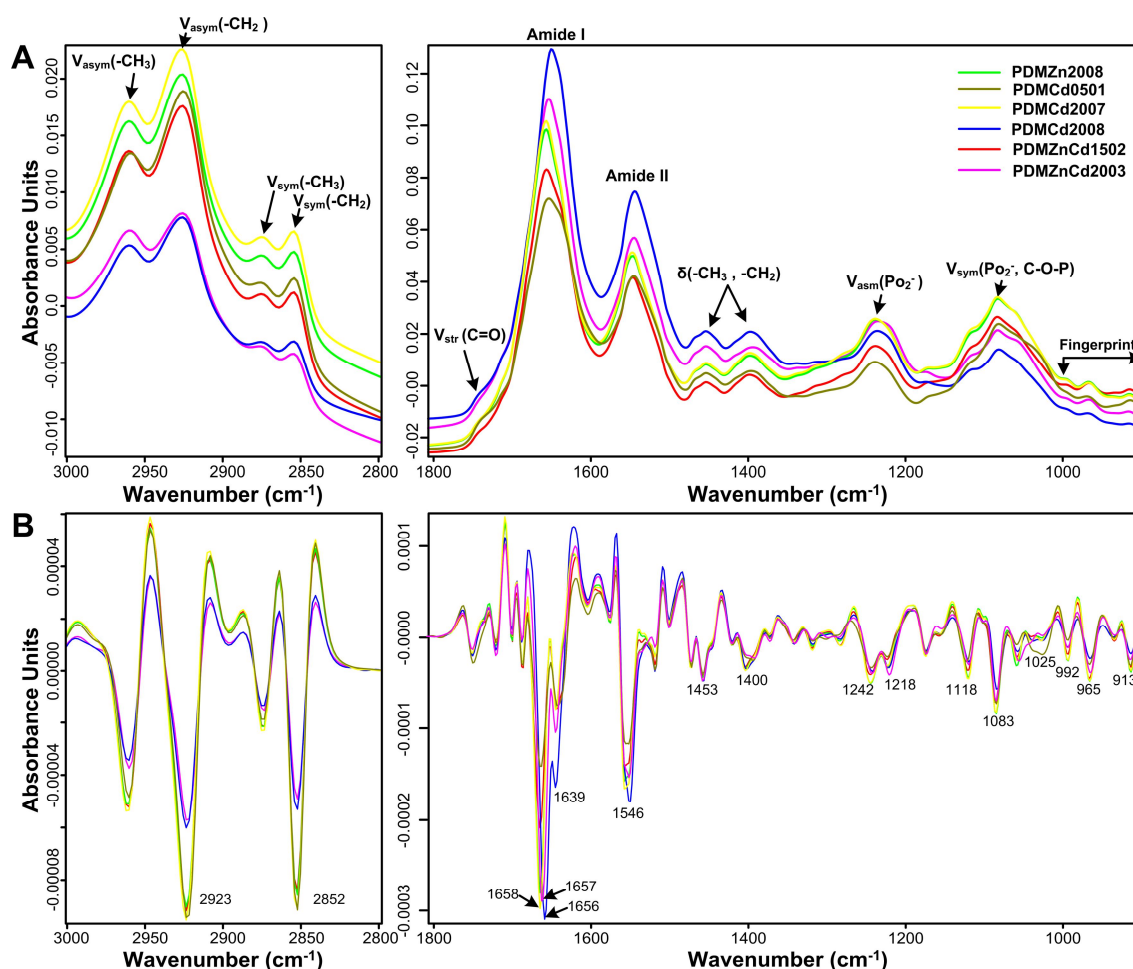


Figure 4.23 (A) Normalized average FT-IR spectra and (B) second-derivative FT-IR spectra of six bacterial isolates: PDMZn2008, PDMCd0501, PDMCd2007, PDMCd2008, PDMZnCd1502 and PDMZnCd2003, depicted in the most-discriminatory spectral windows. The spectral windows are defined according to the classification as follows: W1, the ‘fatty acid region’ (3000-2800 cm^{-1}); W2, the ‘amide region’ (1800-1500 cm^{-1}); W3, the ‘mixed region’ (1500-1200 cm^{-1}); and W4, the polysaccharide region (1200-900 cm^{-1}), dominated by the fingerprint-like absorption bands of the carbohydrates present within the cell wall. (One spectrum was averaged from 100-125 spectra of sample.)



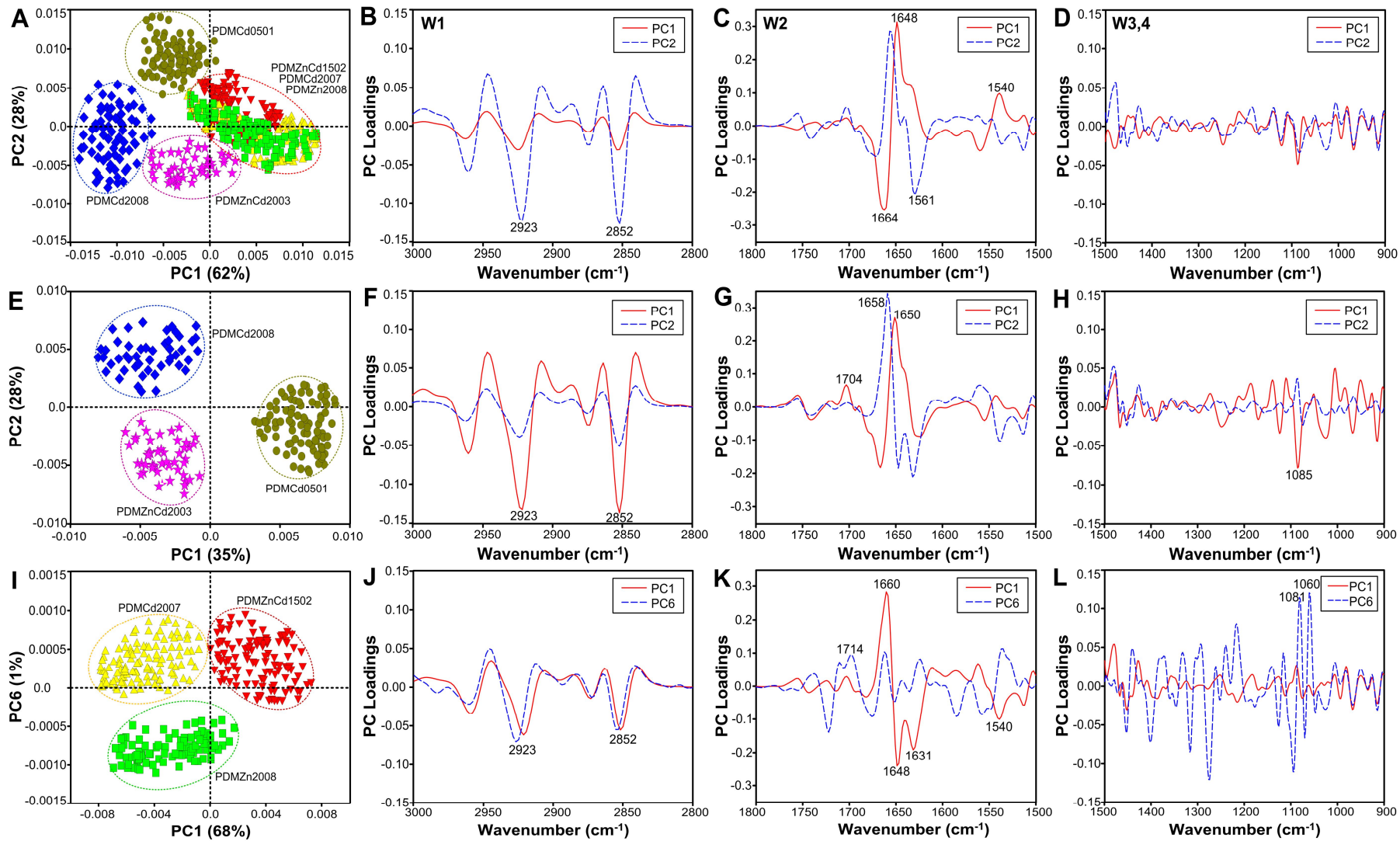


Figure 4.24 PCA score plots and loading plots for six bacterial classifications. (A) shows the PCA score plot for classification of the spectral data of six bacterial isolates: PDMZn2008, PDMCd0501, PDMCd2007, PDMCd2008, PDMZnCd1502 and PDMZnCd2003, (B-D) represent the loading plots of (A) in the PC1 and PC2 space, (E) shows the PCA scores plot for classification of PDMCd2008, PDMZnCd2003 and PDMCd0501, (F-H) represent the loading plots of (E) in the PC1 and PC2 space, (I) shows the PCA score plot for classification of PDMCd2007, PDMZnCd1502 and PDMZn2008 and (J-L) represent the loading plots of (I) in the PC1 and PC6. The classification is as follows: W1, the 'fatty acid region' (3000-2800 cm^{-1}); W2, the 'amide region' (1800-1500 cm^{-1}); W3, the 'mixed region' (1500-1200 cm^{-1}); and W4, the polysaccharide region (1200-900 cm^{-1}). (One spectrum was averaged from 100-125 spectra of each growth phase.)

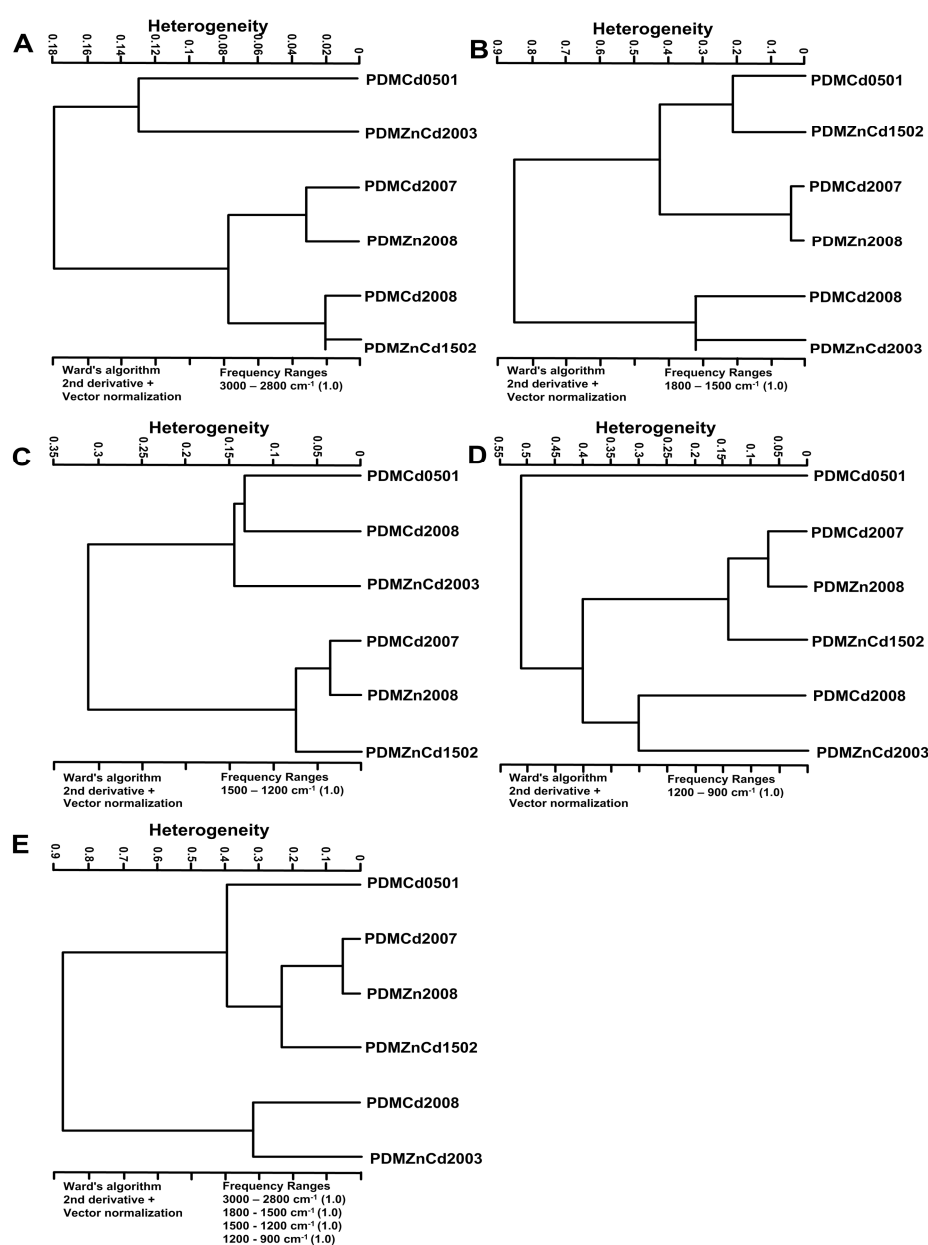


Figure 4.25 Dendrogram of bacterial classification based on FT-IR data of six isolates: PDMZn2008, PDMCd0501, PDMCd2007, PDMCd2008, PDMZnCd1502 and PDMZnCd2003. Hierarchical cluster analysis (HCA) method was performed by second derivative and vector normalized of the spectra, considering the spectral ranges (weighting factors in parentheses) of (A) $3000\text{--}2800\text{ cm}^{-1}$, (B) $1800\text{--}1500\text{ cm}^{-1}$, (C) $1500\text{--}1200\text{ cm}^{-1}$, (D) $1200\text{--}900\text{ cm}^{-1}$ and (E) $3000\text{--}2800\text{ cm}^{-1}$, $1800\text{--}1500\text{ cm}^{-1}$, $1500\text{--}1200\text{ cm}^{-1}$ and $1200\text{--}900\text{ cm}^{-1}$. All spectral ranges were equally weighted Ward's algorithm (second derivative + vector normalization)



4.3.4 Comparison of bacterial classification between FT-IR spectroscopy, protein pattern (SDS-PAGE) and 16S rDNA sequence analysis

The identification by genotype characteristics of the partial 16S rDNA sequence indicated that bacterial the isolates of PDMZn2008, PDMCd0501, PDMCd2007, PDMCd2008, PDMZnCd1502 and PDMZnCd2003 were the closest relative strain of *B. epidermidis*, *S. marcescens*, *S. marcescens*, *P. vermicola*, *P. vermicola* and *P. aeruginosa*, respectively. The six isolates obtained from cultures similar ages and quality of nutrient solutions were differentiated in phenotype characteristics by SDS-PAGE and FT-IR techniques. The FT-IR spectra clarified the functional groups of bacterial whole cells and statistical analysis by the HCA method separated the bacteria into six groups. However, the dendrogram of classifications was based on the FT-IR data set of spectral ranges (Figure 4.25) and does not correspond with the phylogenetic tree (Figure 4.2). In addition, the dendrogram based on the unweighted pair group method of whole-cell protein profiles also separated the six isolates into six groups (Figure 4.22), which did not corresponding to the phylogenetic tree (Figure 4.2).

16S rDNA sequence comparison is considered to be the current gold standard for elucidating bacterial phylogeny (Amann et al., 1994; Ludwig et al., 1998; Ludwig and Schleifer, 1999). The diversity of 16S rDNA sequences and the micro-evolutionary change of the cellular overall characters measured by FT-IR spectroscopy and SDS-PAGE appear not to be coupled. Previous references indicated that FT-IR spectroscopy could not be used to assess the evolutionary relationships of strains within *Actinomycece* species, and could not be used to establish taxonomic relationships between different genera of yeasts (Kummerle et al., 1998). In the case of bacteria, however, FT-IR spectroscopy showed very high efficiency for distinguishing different of bacterial strains (Oberreuter et al., 2002; Yu and Irudayaraj, 2005), with the advantages of swiftness, easiness and low cost of this technique regarding other phenotypic or genotypic methods (Guibet et al., 2003). Therefore, although the branching pattern of the bacterial differentiation obtained from the FT-IR technique did not corresponded with the patterns from SDS-PAGE and 16S rDNA sequences, FT-IR provides a potential alternative to conventional typing methods for bacterial monitoring in a bioaugmentation process.



4.4 Assessment of metal toxicity

Heavy metal resistance in bacterial strains present in various natural habitats such as soil, water and soil sediments. Therefore, the six bacteria were tested for their tolerance and resistance properties to Zn and/or Cd in both solid and liquid media.

4.4.1 Evaluation of metal tolerance

The bacterial isolates' tolerances to NA (solid medium) contaminated with various concentrations of Zn, Cd and Zn plus Cd are shown in Table 4.5. The results showed that the effects of the metals on growth inhibition depended on the metal concentrations and properties of the bacterial isolates. Table 4.5 shows that the separate treatment with a Zn concentration of 200 mg/l resulted in (+) low growth and (++) moderate growth of all bacterial isolates. Treatment with 50 mg/l Cd affected the growth of PDMZn2008, whereas 100 mg/l of Cd started to inhibit the growth of PDMCd0501, PDMCd2007, PDMCd2008 and PDMZnCd1502.

Although Zn and Cd are periodic table group II metals, Zn is an essential micronutrient but Cd is not an essential element (Prasad, 1995; Das et al., 1997; Deckert, 2005). However, supra-optimal Zn concentrations might affect bacterial growth (Chaney, 1993; Barceloux, 1999; Broadley et al., 2007). In addition, the biochemical mechanisms of Zn plus Cd are not clearly understood. The effects of Zn plus Cd treatment on the six bacterial growths are shown in Table 4.5. The Zn plus Cd at 40+40 mg/l affected PDMZn2008, whereas the bacterial isolates of PDMCd0501, PDMCd2007, PDMCd2008 and PDMZnCd1502 tolerated Zn plus Cd at 50+50 mg/l. Among the six bacterial isolates, PDMZnCd2003 was able to tolerate the highest concentrations of Zn, Cd and Zn plus Cd treatments of 200 mg/l, 200 mg/l and 50+50 mg/l, respectively.



Table 4.5 The bacterial isolates' tolerance to NA (solid medium) contaminated with various concentrations of Zn, Cd and Zn plus Cd.

Isolates	5	10	15	20	30	40	50	100	200
Zinc (mg/l)*									
PDMZn2008	+++	+++	+++	+++	+++	+++	+++	++	+
PDMCd0501	+++	+++	+++	+++	+++	+++	+++	++	+
PDMCd2007	+++	+++	+++	+++	+++	+++	+++	++	+
PDMCd2008	+++	+++	+++	+++	+++	+++	+++	++	+
PDMZnCd1502	+++	+++	+++	+++	+++	+++	+++	++	+
PDMZnCd2003	+++	+++	+++	+++	+++	+++	+++	+++	++
Cadmium (mg/l)*									
PDMZn2008	+++	+++	+++	+++	+++	++	+	-	-
PDMCd0501	+++	+++	+++	+++	+++	++	++	+	-
PDMCd2007	+++	+++	+++	+++	+++	++	++	+	-
PDMCd2008	+++	+++	+++	+++	+++	+++	++	+	-
PDMZnCd1502	+++	+++	+++	+++	+++	+++	++	+	-
PDMZnCd2003	+++	+++	+++	+++	+++	+++	+++	++	++
Zinc+Cadmium (mg/l)*									
PDMZn2008	+++	+++	+++	+++	++	+	-	-	-
PDMCd0501	+++	+++	+++	+++	++	++	+	-	-
PDMCd2007	+++	+++	+++	+++	++	++	+	-	-
PDMCd2008	+++	+++	+++	+++	++	++	+	-	-
PDMZnCd1502	+++	+++	+++	+++	++	++	+	-	-
PDMZnCd2003	+++	+++	+++	+++	+++	+++	+++	-	-

*(-) indicates no growth; (+) low growth; (++) moderate growth; (+++) high growth



4.4.2 Evaluation of metal resistance

The bacterial isolates' resistance to NB (liquid medium) contaminating various concentrations of Zn, Cd and Zn plus Cd could be determined as a minimum inhibitory concentration (MIC). The metal-binding capacity of the microorganisms, chelation to various components of the media and formation of complexes can cause a reduction in the activities of free metals (Augle and Chaney, 1989). Table 4.6 shows the MICs of Zn, Cd, Zn plus Cd and fixed Cd plus Zn. The isolates of PDMZn2008, PDMCd0501, PDMCd2007, PDMCd2008, PDMZnCd1502 and PDMZnCd2003 resisted Zn, Cd and Zn plus Cd concentrations of 150, 50 and 30/30 mg/l, respectively. The MICs for PDMZnCd2003 were the highest at Zn, Cd and Zn plus Cd of 150, 70 and 60/60 mg/l, respectively. The MIC of the fixed Cd plus Zn treatments for PDMCd0501, PDMCd2007 and PDMCd2008 were 20/60 mg/l, whereas the treatments for PDMZnCd1502 and PDMZnCd2003 were 20/100 and 20/150 mg/l, respectively.

The minimum bactericidal concentration (MBC) of Zn and Cd were determined by streak microbial suspensions that changed resazurin's colour from purple to dark purple, which were determined as the MICs, on Mueller Hinton agar plates. The lowest Zn and Cd concentrations with no growth of the bacteria on the agar plate were taken as the MBC value. None of the MBCs for the six bacterial isolates were found under the treatments with various Zn concentrations (Table 4.7). The MBCs of the separate Cd treatments were 200 to 300 mg/l. Comparison between the six bacteria showed that PDMZn2008 could not resist Cd, Zn plus Cd and fixed Cd plus Zn of 250, 70/70 and 20/170 mg/l. The highest concentration of fixed Cd plus Zn that inhibited the growth of PDMCd0501, PDMCd2007, PDMCd2008 and PDMZnCd1502 was 20/1000 mg/l. In addition, the MBCs for PDMZnCd2003 under Zn plus Cd treatments were not determined.



Table 4.6 Minimal inhibitory concentrations (MICs) of zinc and/or cadmium

Isolates	MIC of heavy metals*			
	Zinc	Cadmium	Zinc+Cadmium	Fixed Cadmium+Zinc
PDMZn2008	150	50	30/30	20/20
PDMCd0501	150	50	30/30	20/60
PDMCd2007	150	50	30/30	20/60
PDMCd2008	100	50	30/30	20/60
PDMZnCd1502	150	50	30/30	20/100
PDMZnCd2003	150	70	60/60	20/150

*Minimal inhibitory concentration (MIC) expressed in mg/liter.

Table 4.7 Minimal bactericidal concentrations (MBCs) of zinc and/or cadmium

Isolates	MBC of heavy metals*			
	Zinc	Cadmium	Zinc + Cadmium	Fixed Cadmium+Zinc
PDMZn2008	-	250	70/70	20/170
PDMCd0501	-	250	-	20/1000
PDMCd2007	-	250	-	20/1000
PDMCd2008	-	200	90/90	20/1000
PDMZnCd1502	-	200	-	20/1000
PDMZnCd2003	-	300	-	-

*Minimal bactericidal concentration (MBC) expressed in mg/liter. (-) no MBC determined

Most of the isolates in the present study showed multiple tolerances of heavy metals. A heavy metal resistant organism could be a potential agent for bioremediation of heavy metal pollution. The microbial resistance to heavy metal is attributed to a variety of detoxifying mechanisms developed by resistant microorganisms such as complexation by exopolysaccharides, binding with bacterial cell envelopes, metal reduction and metal efflux etc. These mechanisms are sometimes encoded in the plasmid genes facilitating the transfer of toxic metal resistance from one



cell to another (Silver, 1996). Viti and Giovannetti (2003) have compared the MIC of bacterial strains to various heavy metals and reported that different isolates exhibited different levels of metal tolerance. Similarly, *Ochrobactrum tritici* 5bv11 also showed resistance to various heavy metals like Ni(II), Co(II), Cd(II) and Zn(II), in which the presence of Zn(II) did not affect the growth but the other metals decreased the growth rate (Branco, et al., 2004). Filali, et al. (1999) studied wastewater bacterial isolates of *Ps. aeruginosa*, *Klebsiella pneumoniae*, *Proteus mirabilis* and *Staphylococcus* resistant to heavy metals. Sharma et al. (2000) isolated highly Cd resistant *Klebsiella* that was found to precipitate significant amount of CdS. Much research has reported that the MICs of separate Zn and Cd treatments against *Pseudomonas* strains were 13-130 mg/l and 16-281 mg/l, respectively (Hassen, et al., 1998; Dell, et al., 2008; Kuffner, et al., 2008; Poirier, et al., 2008; Sinha and Mukherjee, 2008; Mastretta, et al., 2009; Siripornadulsil and Siripornadulsil, 2013). They corresponded to the Zn/Cd tolerance properties of PDMZnCd2003. The tolerance properties are due to the functional groups of thiol, carbonyl and amine in its structure, EPS and siderophore (Meesungnoen, et al., 2012).

4.5 Plant-growth promoting properties of bacteria isolates

The plant growth promoting properties of IAA production, nitrogen fixation and phosphate solubilization were examined quantitatively under heavy metal stress. In addition, the extractable amounts of Zn and Cd leached from the Zn/Cd contaminated soil in an agricultural area by diethylene triamine pentaacetic acid (DTPA) ranged from 30-120 mg/kg dry wt. and 1-10 mg/kg dry wt., respectively. Therefore, Zn plus Cd at the concentration of 20+20 mg/l, which had no Zn/Cd precipitation, was supplied to the media to study their effect on plant growth promoting properties.

4.5.1 Indole-3-acetic acid (IAA) production

The six bacterial isolates' growth and IAA production were studied under the conditions of absence and presence of Zn plus Cd (20+20 mg/l). Figure 4.26 shows the growth and system pHs, and Figure 4.27 shows IAA production. A high cell density and EPS production was obtained when culturing in the complete medium of TSB. The growth curves of the six bacteria isolates were slightly different, and the pHs of the



bacterial cultivation in TSB gradually increasing from 7.0 ± 0.5 to approximately 8.5 ± 0.1 to $\sim 9.0 \pm 0.1$. Although the amounts of IAA increased with the growth of bacteria, the presence of Zn plus Cd (20+20 mg/l) decreased the IAA production.

The period of maximum IAA production of the six bacteria under the absence and presence of Zn plus Cd (20+20 mg/l) was at 13-17 hours as shown in Figure 4.28. The maximum IAA production by PDMZn2008, PDMCd0501, PDMCd2007, PDMCd2008, PDMZnCd1502 and PDMZnCd2003, without metal treatments, were 977, 25, 637, 603, 535 and 250 $\mu\text{g/ml}$, respectively. The maximum IAA production by PDMZn2008, PDMCd0501, PDMCd2007, PDMCd2008, PDMZnCd1502 and PDMZnCd2003 under the Zn plus Cd treatments were 289, 23, 260, 488, 333 and 234 $\mu\text{g/ml}$, respectively. The Zn plus Cd had negative effects on IAA production after the stationary phase. A negative effect of metal cations (Fe^{3+} , Al^{3+} , Cd^{2+} , Cu^{2+} and Ni^{2+}) on auxin production has been significantly demonstrated (Acuña, et al., 2011; Dimkpa, et al., 2008). Deshwal and Kumar (2013) evaluated the effect of metals (Cu, Cr, Ni and Cd) on growth and IAA production of *P. aeruginosa*. Seiderophores may reduce the toxic effect of metal cations by chelation (Dimkpa et al., 2008). In addition, Ananthalakshmi, et al (2013) reported the formation of IAA-metal complexes that possibly led to decreasing amounts of free IAA.

The decrease in the specific growth rate and prolonged lag-phase responding to high concentrations of Zn and Cd happened to *P. fluorescens* BA3d12 and *Pseudomonas* spp. strains KKU25000-4 to KKU2500-24 (Poirier et al., 2008; Siripornadulsil and Siripornadulsil, 2013). The increase of the system's pH to ~ 9.0 might be caused by the secondary metabolites secreted in the cultured media (Wendenbaum, et al., 1983; Khamna, et al., 2010; Acuña, et al., 2011; Patil, et al., 2011). The alkaline pHs in TSB during the growth of PDMZn2008 and PDMZnCd2003 might be due to protein utilized aerobically. The protein digestions to ammonia (NH_4^+) under aerobic conditions were shown in the biochemical testing of TSI (Table 4.1). In case of *P. aeruginosa* PDMZnCd2003, the secretion of yellow-green fluorescent pigment, which probably was pyoverdine siderophore, might affect the alkaline pH in the culture medium as found in *P. fluorescens* (Chiadò, et al., 2013).



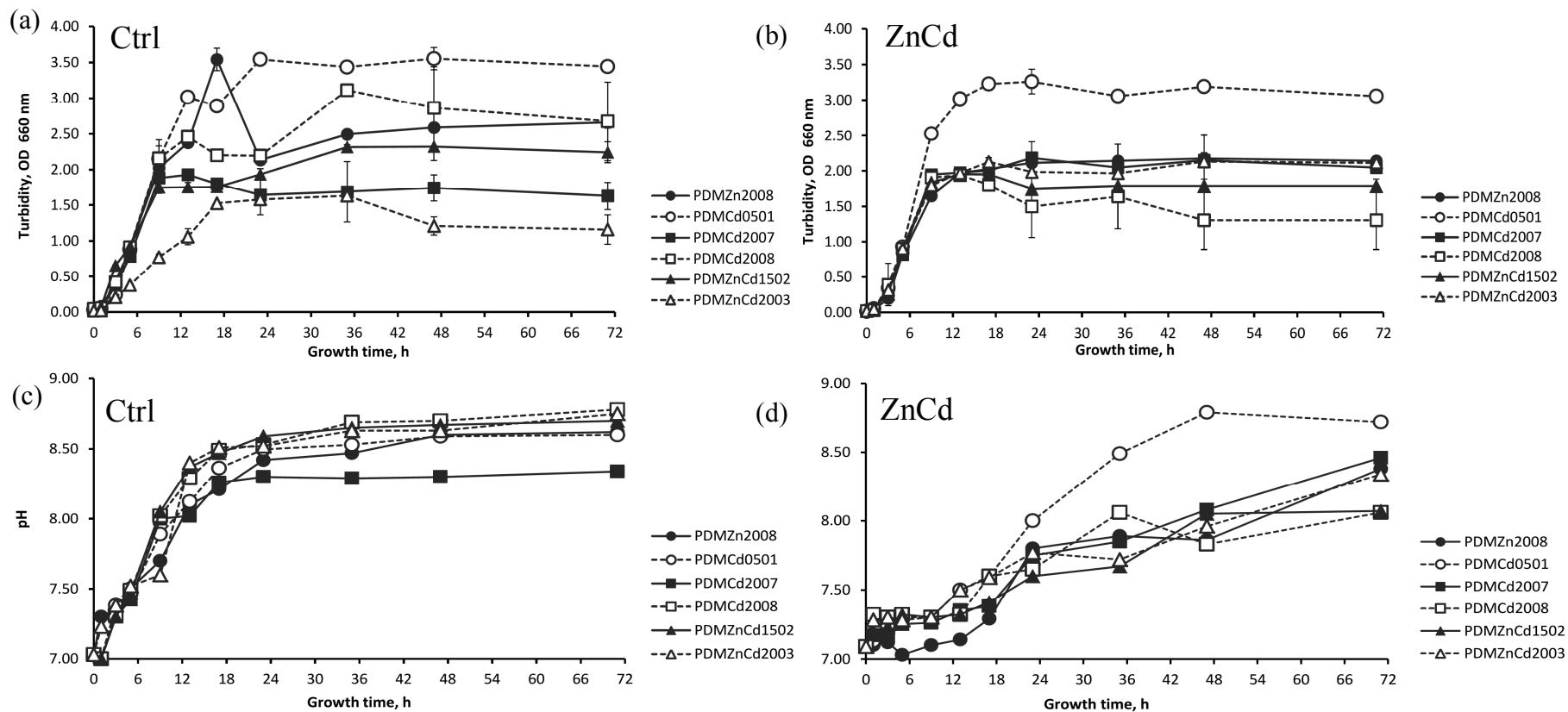
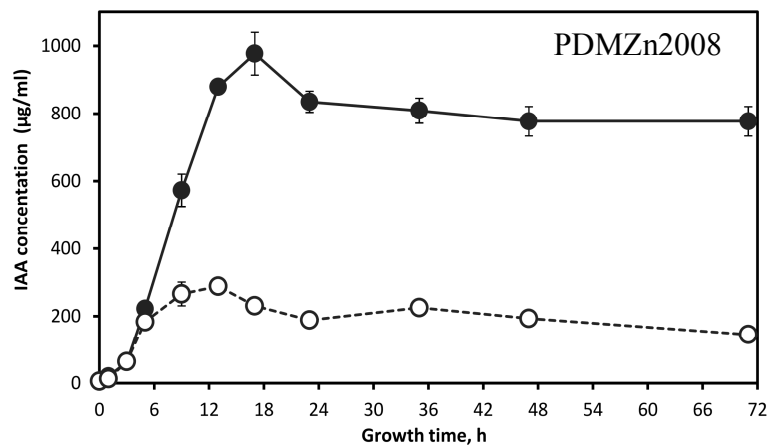
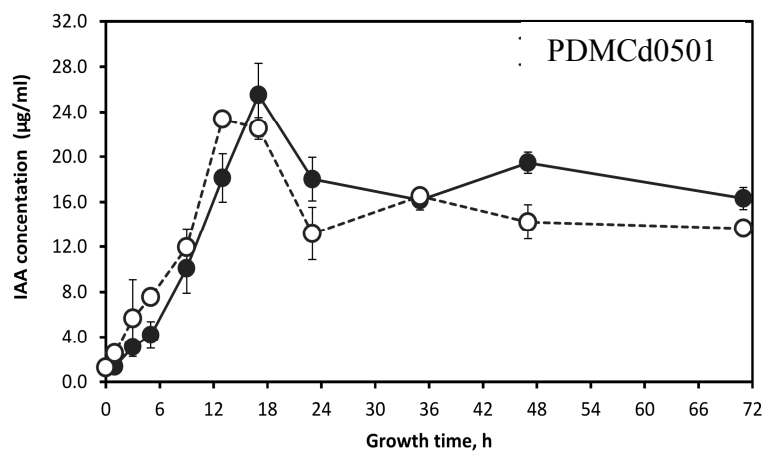


Figure 4.26 Growth and pH change of PDMZn2008, PDMCd0501, PDMCd2007, PDMCd2008, PDMZnCd1502 and PDMZnCd2003 under cultivation in Trypticase soy broth (TSB), with the absence and presence of Zn plus Cd (20+20 mg/l). (a) bacterial growth in TSB, (b) bacterial growth in the presence of Zn plus Cd, (c) pH change in TSB and (d) pH change in the presence of Zn plus Cd.

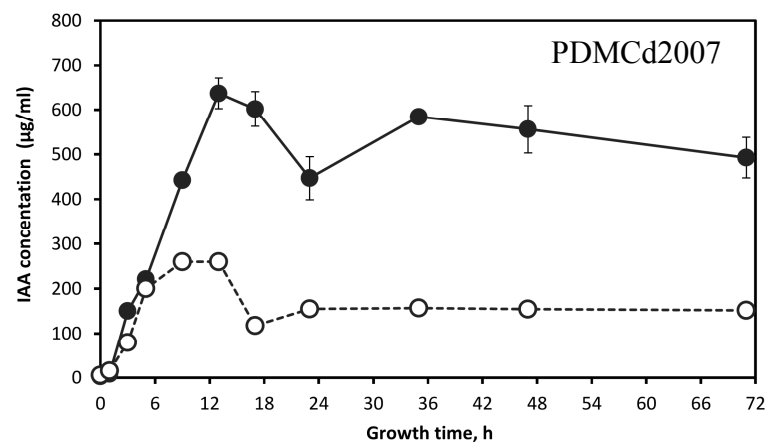
(a)



(b)



(c)



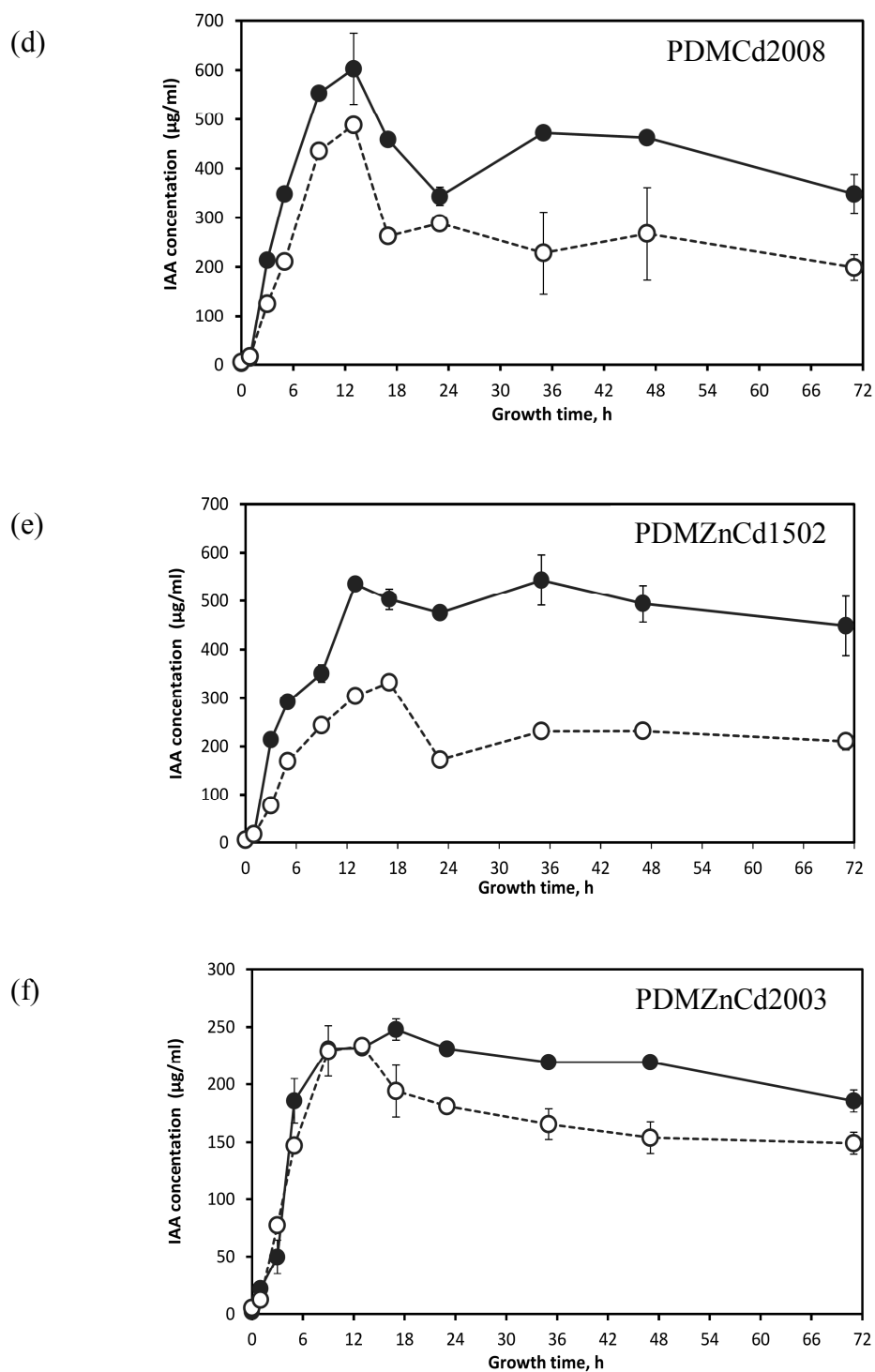


Figure 4.27 IAA production of (a) PDMZn2008, (b) PDMCd0501, (c) PDMCd2007, (d) PDMCd2008, (e) PDMZnCd1502 and (f) PDMZnCd2003 under cultivation in Trypticase soy broth (TSB), with the absence and presence of Zn plus Cd (20+20 mg/l). (—●— control, and - -○- - Zn+Cd 20 mg/l)



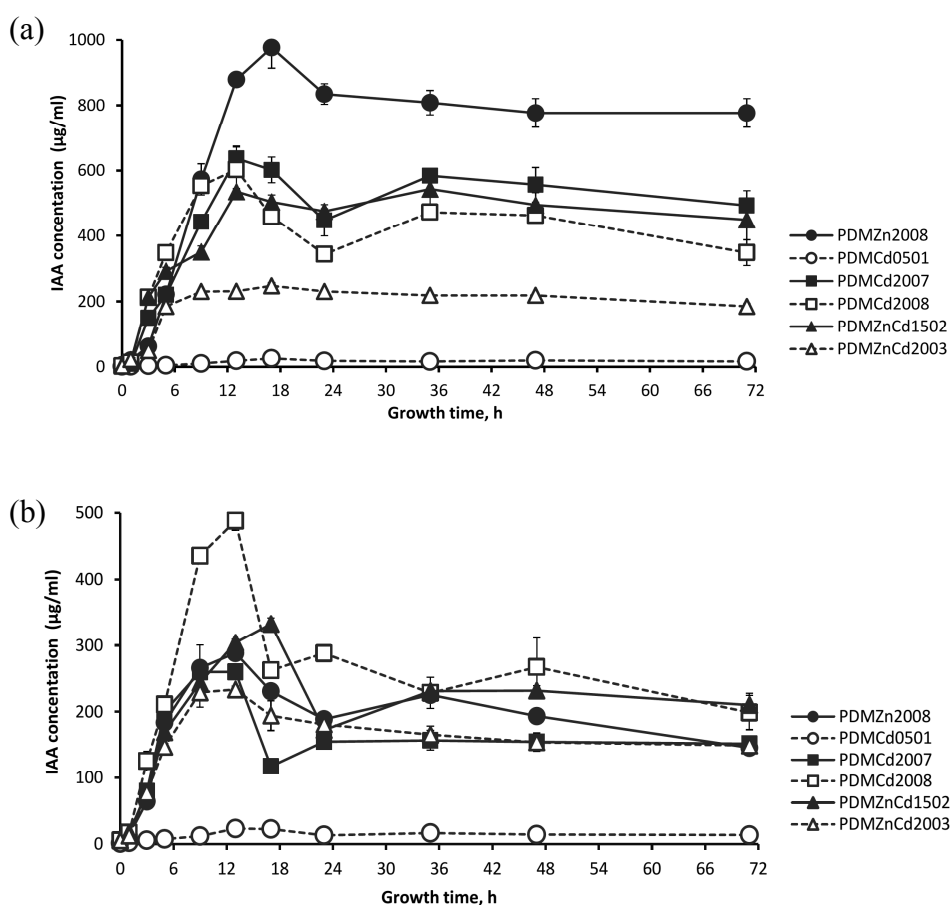


Figure 4.28 Comparison of IAA production by PDMZn2008, PDMCd0501, PDMCd2007, PDMCd2008, PDMZnCd1502 and PDMZnCd2003 under cultivation in Trypticase soy broth (TSB) under the (a) absence and (b) presence of Zn plus Cd (20+20 mg/l).

4.5.2 Nitrogen fixation

The PGPB properties in nitrogen fixation of the six isolates were studied in N-free malate media, under the absence and presence of Zn plus Cd (20+20 mg/l). Figure 4.29 shows the growth and system pH in the N-free malate media, and Figure 4.30 shows nitrogen fixations, which were detected by $\text{NH}_3\text{-N}$ production. The $\text{NH}_3\text{-N}$ productions do not correspond with the bacterial growth. The growth curves of the six bacteria isolates in N-free malate media with the absence and presence of Zn plus Cd (20+20 mg/l) were slightly different as shown in Figure 4.29 (a) and (b).



The pHs of bacterial cultivation gradually increased from 7.0 ± 0.5 to alkaline pHs of 8.5 ± 0.1 to $\sim 9.0 \pm 0.1$ (Figure 4.29 (c) and (d)). The presence of Zn plus Cd (20+20 mg/l) tended to decrease $\text{NH}_3\text{-N}$ production (Figure 4.30).

The periods of maximum $\text{NH}_3\text{-N}$ production of the five bacteria, except PDMCd0501, under the absence and presence of Zn plus Cd (20+20 mg/l) were at 10-15 hours as shown in Figure 4.31. The maximum $\text{NH}_3\text{-N}$ productions of PDMZn2008, PDMCd0501, PDMCd2007, PDMCd2008, PDMZnCd1502 and PDMZnCd2003 under the absence of Zn plus Cd were 66.0, 10.4, 7.9, 12.3, 8.6 and 7.0, respectively.

Whereas, the maximum $\text{NH}_3\text{-N}$ productions of PDMZn2008, PDMCd0501, PDMCd2007, PDMCd2008, PDMZnCd1502 and PDMZnCd2003 under the presence of Zn plus Cd (20+20 mg/l) were 11.1, 5.3, 6.7, 8.1, 6.4 and 6.3, respectively.

The increase in the alkaline pHs in the N-free malate medium was probably caused by nitrogen fixation into ammonium (NH_4^+) (Yan, et al., 2010). The decrease of nitrogen fixation after 17 hours might be due to the optimal rates of nitrogenase activity occurring at an alkaline pH (6.5 to 7.0) (Baldani, et al., 1986; Peng, et al., 1987; Valiente and Leganes, 1989). In addition, an excess of ammonium in the growth medium may result in immediate repression of the *nif* gene transcription (Yan, et al., 2010).



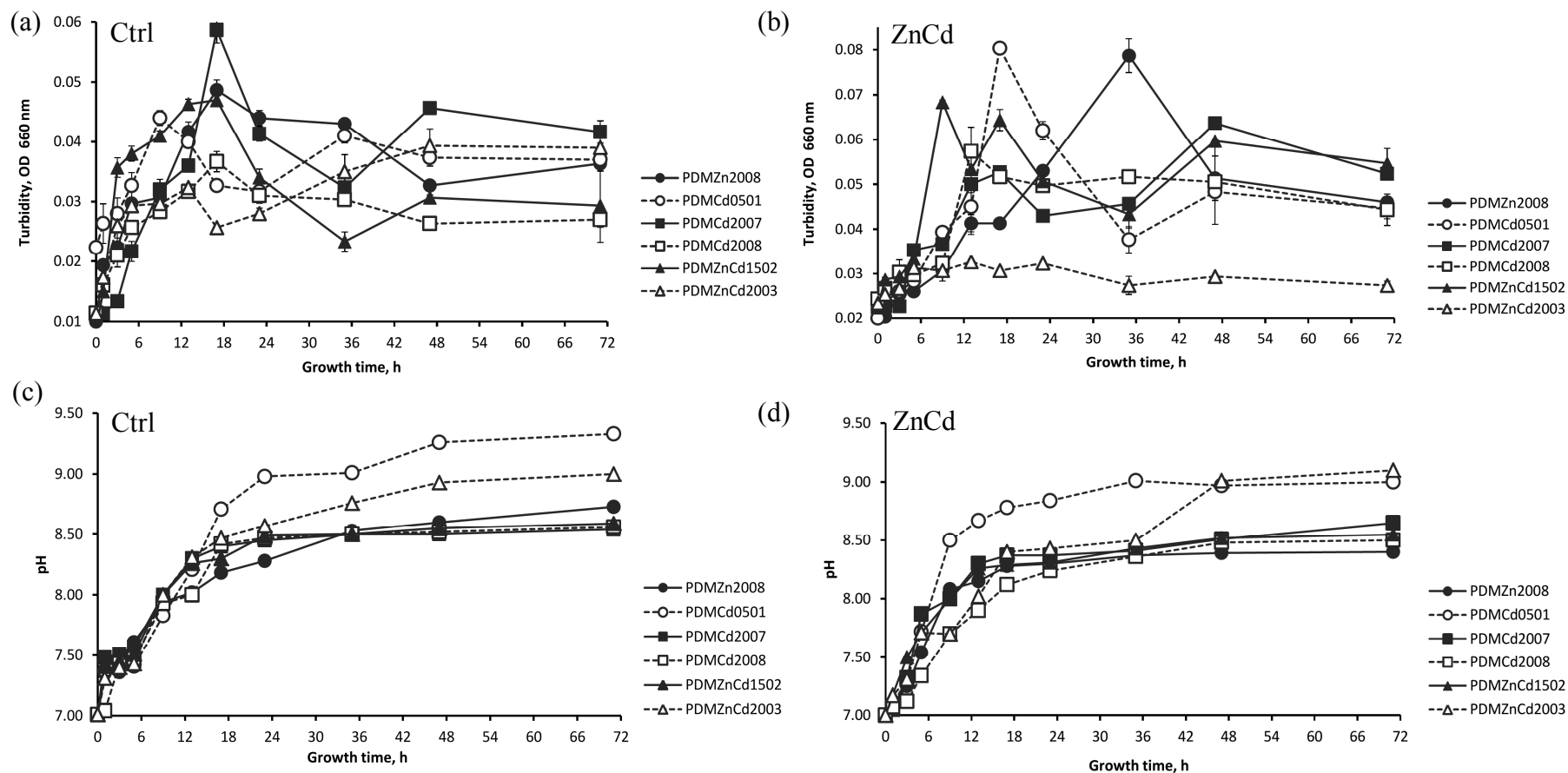
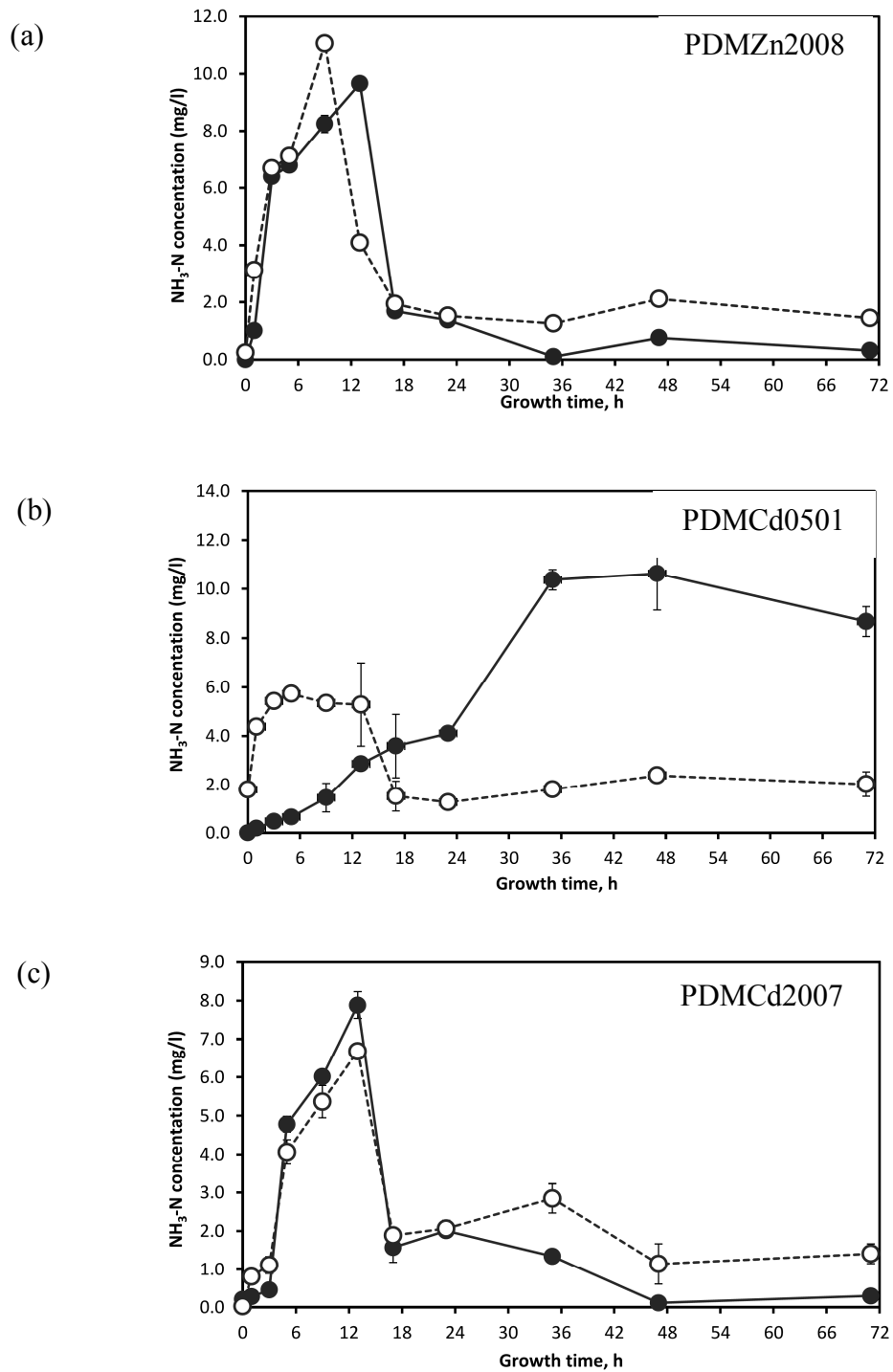


Figure 4.29 Growth and pH change of PDMZn2008, PDMCd0501, PDMCd2007, PDMCd2008, PDMZnCd1502 and PDMZnCd2003 under cultivation in N-free malate medium, with the absence and presence of Zn plus Cd (20+20 mg/l). (a) bacterial growth in the N-free medium, (b) bacterial growth in the presence of Zn plus Cd, (c) pH change in the N-free medium and (d) pH change in the presence of Zn plus Cd.



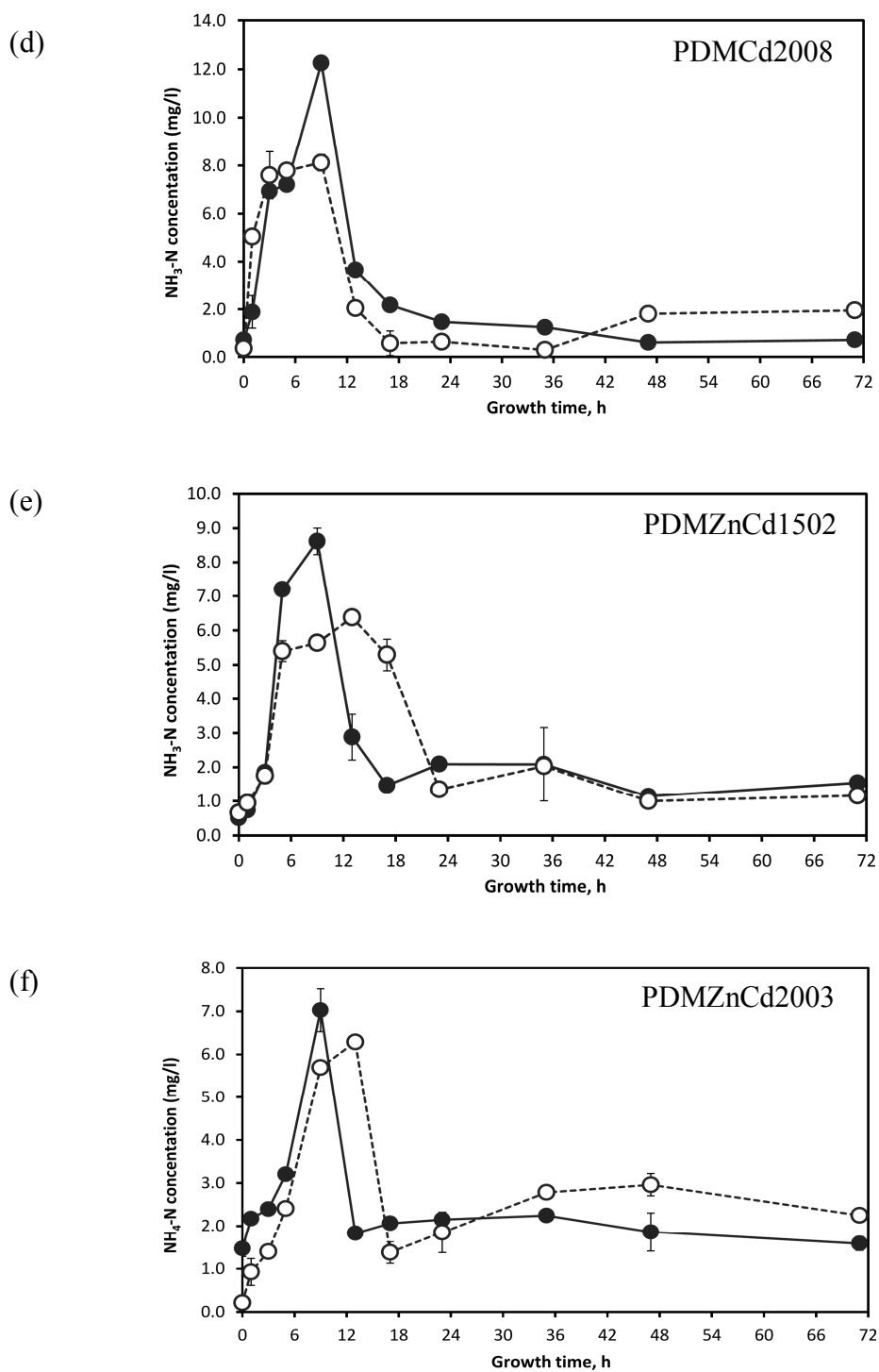


Figure 4.30 $\text{NH}_3\text{-N}$ production of (a) PDMZn2008, (b) PDMCd0501, (c) PDMCd2007, (d) PDMCd2008, (e) PDMZnCd1502 and (f) PDMZnCd2003 under cultivation in N-free malate medium, with the absence and presence of Zn plus Cd (20+20 mg/l). (—●— control, and - -○- - Zn+Cd 20 mg/l)



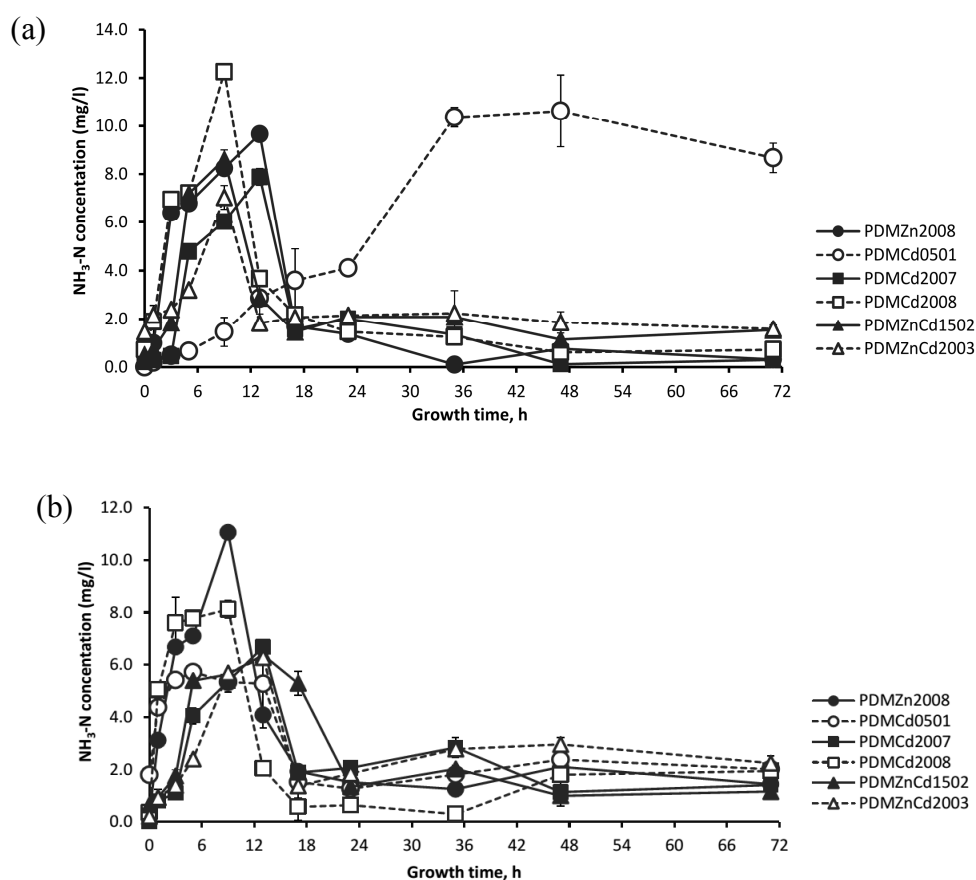


Figure 4.31 Comparison of $\text{NH}_3\text{-N}$ production by PDMZn2008, PDMCd0501, PDMCd2007, PDMCd2008, PDMZnCd1502 and PDMZnCd2003 under cultivation in N-free malate medium, under the (a) absence and (b) presence of Zn plus Cd (20+20 mg/l).

4.5.3 Phosphate solubilization

The PGPB properties in the phosphate solubilization of the six isolates were studied in NBRIP (National Botanical Research Institute's phosphate growth) medium consisting of 0.5% w/v tricalcium phosphate, under the absence and presence of Zn plus Cd (20+20 mg/l). Figure 4.32 shows the growth and system pH in the NBRIP medium, and Figure 4.33 shows the phosphate solubilization, which was detected by the $\text{PO}_4^{3-}\text{-P}$ concentration.



The growth curves of the six bacteria isolates in the NBRIP medium with the absence and presence of Zn plus Cd (20+20 mg/l) were different as shown in Figure 4.32 (a) and (b). The pH of the bacterial cultivation gradually decreased from 7.0 ± 0.5 to acidic pHs of 6.5 ± 0.1 to $\sim 5.0 \pm 0.1$ (Figure 4.32 (c) and (d)). The presence of Zn plus Cd (20+20 mg/l) caused a decrease in the P-solubilization (Figure 4.33).

The periods of maximum PO_4^{3-} -P concentration of the six bacteria under the absence and presence of Zn plus Cd (20+20 mg/l) were at 13-17 hours as shown in Figure 4.34. The maximum PO_4^{3-} -P concentrations of PDMZn2008, PDMCd0501, PDMCd2007, PDMCd2008, PDMZnCd1502 and PDMZnCd2003 under the absence of Zn and Cd were 288, 298, 283, 209, 219 and 376 mg/l, respectively. The maximum PO_4^{3-} -P concentrations of PDMZn2008, PDMCd0501, PDMCd2007, PDMCd2008, PDMZnCd1502 and PDMZnCd2003 with the presence of Zn plus Cd were 262, 261, 208, 210, 202 and 261 mg/ml, respectively.

The acidic pHs of the bacterial cultivation in NBRIP might be caused by the secretion of acid phosphatase in the cultured media as found in *Pseudomonas* sp. and *Serratia marcescens* (Rodríguez, et al., 1999; Hwangbo, et al., 2003; Chen, et al., 2006). The production of organic acids by phosphate solubilizing bacteria has been well documented. The hydroxyl and carboxyl groups of organic acids can chelate the cations bound to phosphate, thereby converting mineral phosphate into soluble forms (Rodríguez, and Fraga, 1999; Chen, et al., 2006). Among them, gluconic acid was reported as the principal organic acid produced by *Pseudomonas* sp. (Illmer and Schinner, 1992). In addition, the effect of metals (Cu, Cr, Ni, Cd) on PO_4^{3-} -P production were reported in *Pseudomonas* (Deshwal and Kumar, 2013).



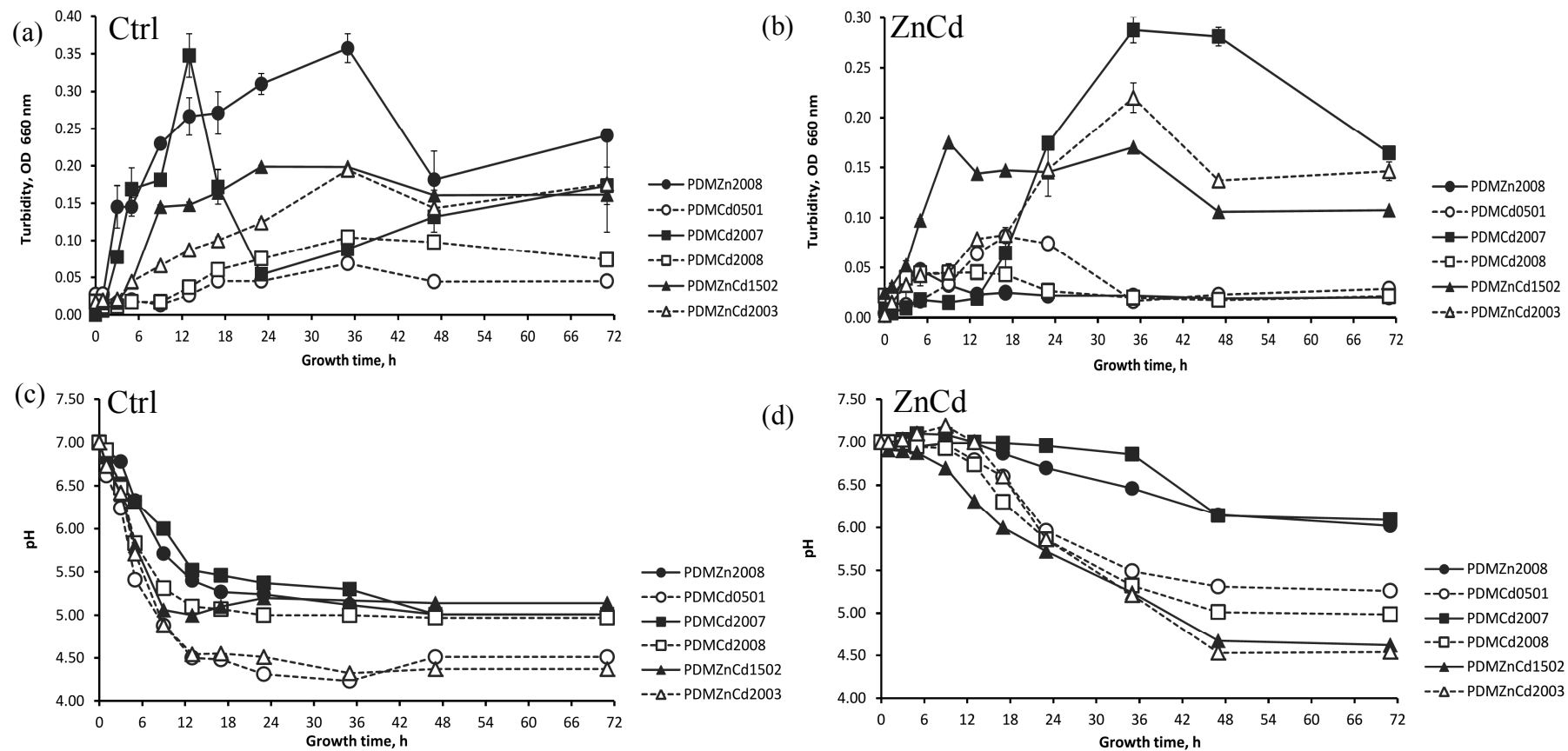
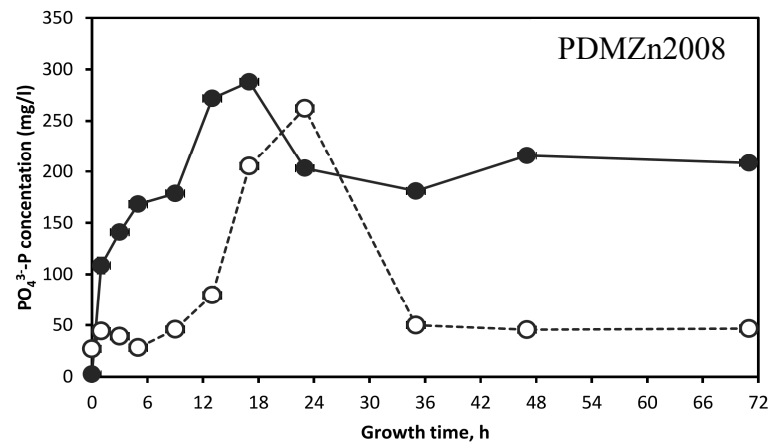
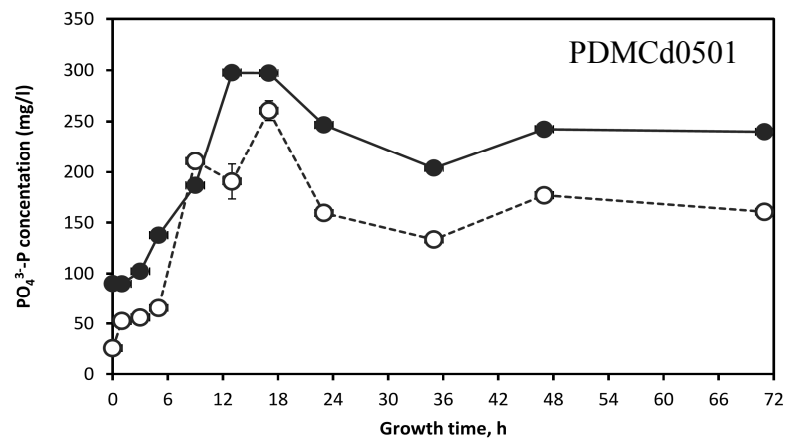


Figure 4.32 Growth and pH change of PDMZn2008, PDMCd0501, PDMCd2007, PDMCd2008, PDMZnCd1502 and PDMZnCd2003 under cultivation in NBRIP medium consisting of 0.5% w/v tricalcium phosphate, with the absence and presence of Zn plus Cd (20+20 mg/l). (a) bacterial growth in the NBRIP medium, (b) bacterial growth in the presence of Zn plus Cd, (c) pH change in the NBRIP medium and (d) pH change in the presence of Zn plus Cd.

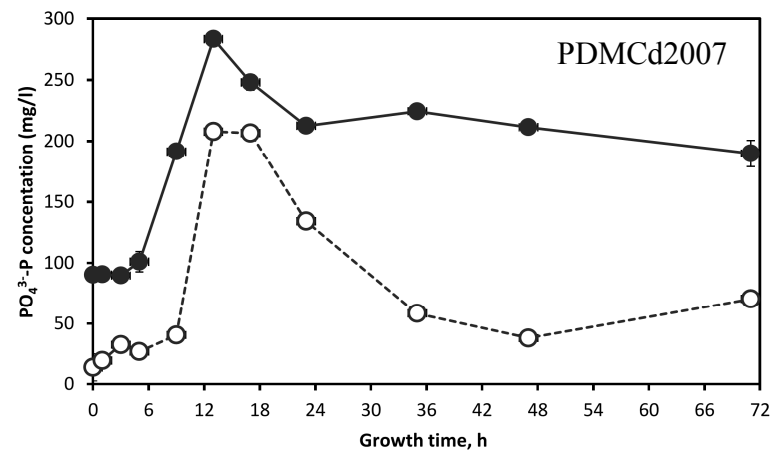
(a)



(b)



(c)



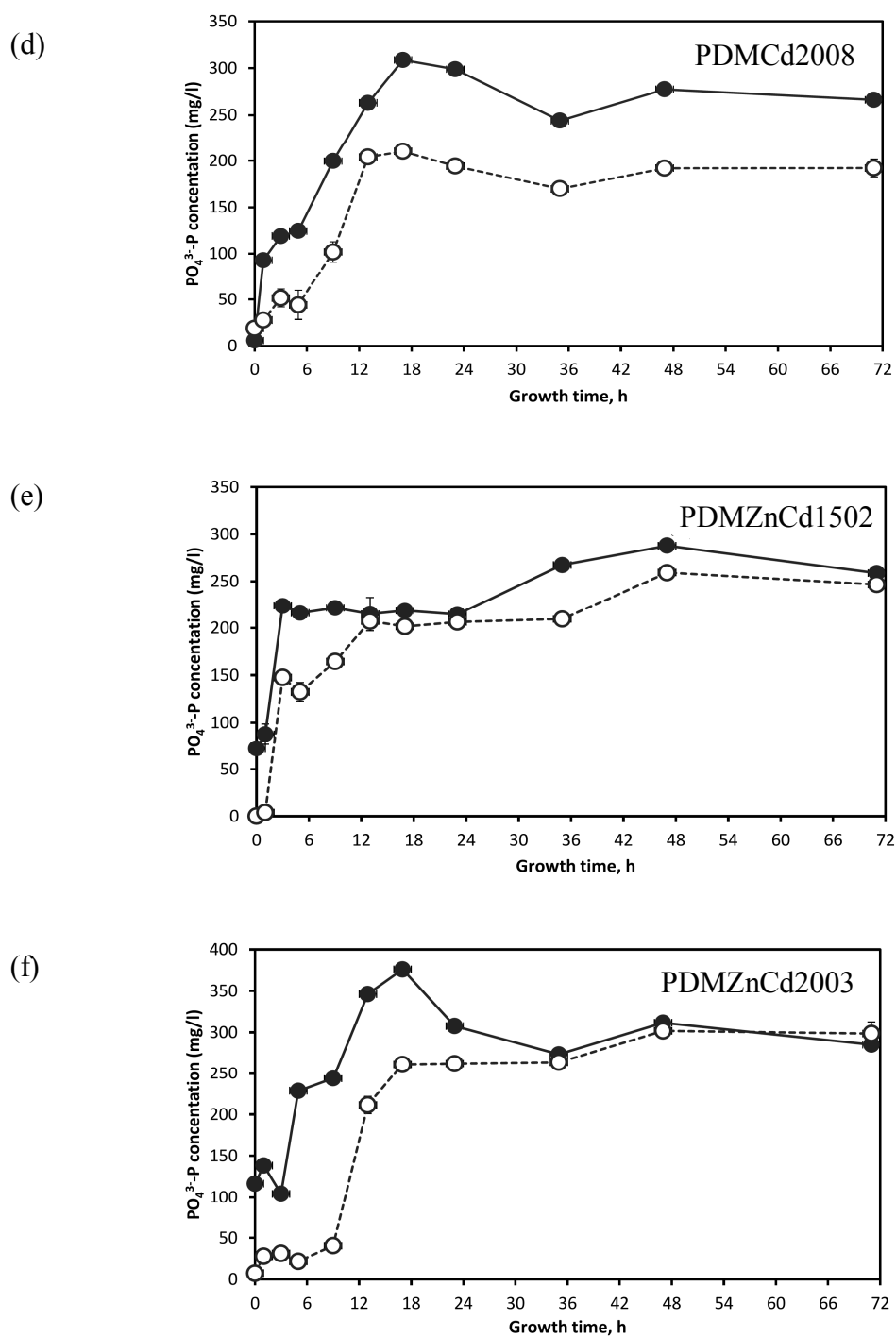


Figure 4.33 Phosphate solubilization of (a) PDMZn2008, (b) PDMCd0501, (c) PDMCd2007, (d) PDMCd2008, (e) PDMZnCd1502 and (f) PDMZnCd2003 under cultivation in NBRIP medium consisting of 0.5% w/v tricalcium phosphate, with the absence and presence of Zn plus Cd (20+20 mg/l). (—●— control, and - -○- - Zn+Cd 20 mg/l)



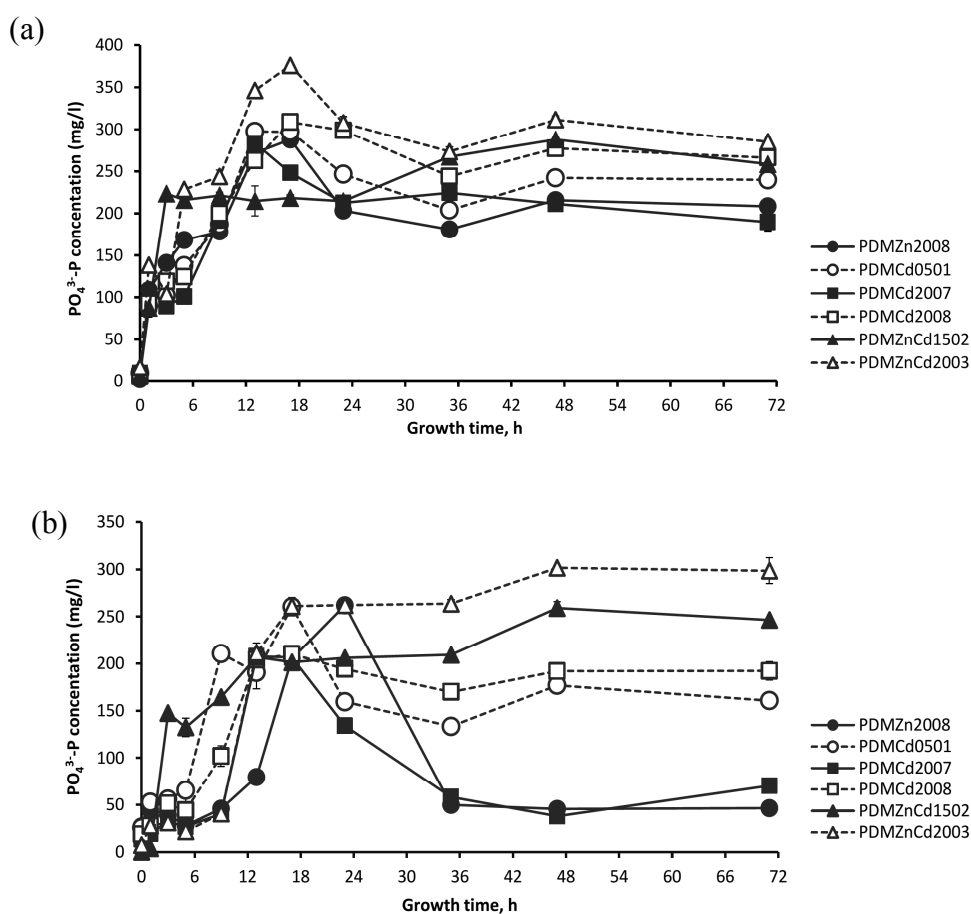


Figure 4.34 Comparison of phosphate solubilization by PDMZn2008, PDMCd0501, PDMCd2007, PDMCd2008, PDMZnCd1502 and PDMZnCd2003 under cultivation in NBRIP medium consisting of 0.5% w/v tricalcium phosphate, under the (a) absence and (b) presence of Zn plus Cd (20+20 mg/l).

The beneficial effects of bacterial inoculants can be realized only if they survive competitively in the rhizosphere. In this study, the bacterial isolates of PDMCd2008, PDMCd0501, PDMZnCd1502 and PDMZnCd2003 were able to withstand Zn and/or Cd concentrations of 20+20 mg/l. However, the metal stress affected the growth of the bacteria and decreased some properties of IAA production, N_2 fixation and P solubilization.



CHAPTER 5

Conclusion and suggestion

5.1 Conclusion

This research studied six bacteria isolated from the rhizosphere of *Gynura pseudochina* (L.) DC., a Zn/Cd hyperaccumulative plant, growing in a Zn mining. PDMCd0501, PDMCd2007, PDMCd2008, PDMZnCd1502 and PDMZnCd2003 were Gram negative bacteria, and PDMZn2008 was a Gram positive bacteria. They were motile and could not hydrolyze starch. PDMZn2008 and PDMZnCd2003 hydrolysed casein, PDMZnCd2003 hydrolysed cellulose and produced H₂S via an aerobic system. Based on the biochemical testing of API20E, PDMZn2008, PDMCd0501, PDMCd2007 were identified as nonpigmented *Serratia marcescens*. Whereas, PDMCd2008, PDMZnCd1502 and PDMZnCd2003 were identified to be *Providencia stuartii*, *Providencia stuartii* and *Pseudomonas aeruginosa*, respectively.

The FT-IR spectroscopic features of the bacterial cells depended on their growth phases. The bacterial cells in the late-log phase were the best representative cells for study of the bacterial identification by the 16S rDNA sequence and the bacterial classification with whole cell protein patterns and normalized FT-IR spectral features of whole cells. The identification by genotype characteristics of the partial 16S rDNA sequence indicated that the bacterial isolates of PDMZn2008, PDMCd0501, PDMCd2007, PDMCd2008, PDMZnCd1502 and PDMZnCd2003 were the closest relative strains to *Brevibacterium epidermidis*, *Serratia marcescens*, *Serratia marcescens*, *Providencia vermicola*, *Providencia vermicola* and *Pseudomonas aeruginosa*, respectively. The six isolates obtained from cultures of the same age and qualities of nutrient solution were different in the phenotype characterized by SDS-PAGE and FT-IR techniques. The dendrogram of classifications based on the FT-IR data set did not corresponded with the phylogenetic tree. In addition, the dendrogram based on the whole-cell protein of SDS-PAGE could separate the six isolates, but it did not corresponding to the phylogenetic tree.



There is heavy metal resistance in bacterial strains present in various natural habitats such as soil, water, sediments soil. Therefore, the six bacteria were tested for their tolerance and resistance properties to Zn and/or Cd in both solid and liquid media. Among the six bacterial isolates, PDMZnCd2003 was able to grow on nutrient agar (NA) containing Zn (200 mg/l), Cd (200 mg/l) and Zn plus Cd (50+50 mg/l). The bacterial isolates' resistance to NB (liquid medium) containing various concentrations of Zn and/or Cd could be determined as the minimum inhibitory concentration (MIC). The isolates of PDMZn2008, PDMCd0501, PDMCd2007, PDMCd2008, PDMZnCd1502 and PDMZnCd2003 were able to resist Zn, Cd and Zn plus Cd concentrations of 150, 50 and 30/30 mg/l, respectively. The MICs for PDMZnCd2003 were the highest for Zn, Cd and Zn plus Cd at 150, 70 and 60/60 mg/l, respectively. The MIC of the fixed Cd plus Zn treatment for PDMCd0501, PDMCd2007 and PDMCd2008 was 20/60 mg/l, whereas for the treatment of PDMZnCd1502 and PDMZnCd2003 it was 20/100 and 20/150 mg/l, respectively. The minimum bactericidal concentrations (MBC) of Zn and Cd were determined by streak microbial suspensions that changed resazurin's color from purple to dark purple. PDMZn2008 could not resist Cd, Zn plus Cd and fixed Cd plus Zn levels of 250, 70/70 and 20/170 mg/l. The highest concentration of fixed Cd plus Zn that inhibited the growth of PDMCd0501, PDMCd2007, PDMCd2008 and PDMZnCd1502 was 20/1000 mg/l. In addition, there were no MBCs detected for PDMZnCd2003 under our Zn plus Cd treatments. A heavy metal resistant organism could be a potential agent for bioremediation of heavy metal pollution.

The beneficial effects of bacterial inoculants can be realized only if they survive competitively in the rhizosphere. In this study, the bacterial isolates of PDMCd2008, PDMCd0501, PDMZnCd1502 and PDMZnCd2003 were able to withstand Zn and/or Cd concentrations of 20+20 mg/l. However, the metal stress affected the growth of the bacteria and decreased some properties of IAA production, N₂ fixation and P solubilization. The use of purified IAA and/or N, P fertilizer to enhance plant growth may be expensive, and therefore unsustainable for large-scale phytoremediation, especially in resource-poor countries. Therefore, the Zn/Cd tolerant



bacteria with PGPB properties, especially *aeruginosa*, *P. PDMZnCd2003*, could serve as an efficient biofertilizer candidate for microbe assisted phytoremediation in Zn/Cd contaminated areas.

5.2 Suggestions

1. *aeruginosa*, *P. PDMZnCd2003* should be studied as a bacterium for bioaugmentation to support phytoremediation in Zn/Cd contaminated sites.
2. The bioaugmentation processes requires bacteria monitoring to detect if any of the bacteria applied in the soil remains. Therefore, FT-IR spectroscopy should be studied *in vitro* and *in vivo* for physicochemical properties to enable bacteria monitoring in a bioaugmentation process.
3. This research studied the PGPB properties under one concentration of Zn and Cd of 20+20 mg /l, which was lower than the MICs of Zn and/or Cd for the six bacteria. Therefore, the effect of Zn/Cd on the expression of PGPB properties should be studied under separate treatments with high concentrations of Zn and Cd.



REFERENCES



References

- Abou-Shanab, R.A., Ghanem, K., Ghanem, N. and Al-Kolaibe, A. (2008). The role of bacteria on heavy-metal extraction and uptake by plants growing on multi-metal-contaminated soils. *World Journal of Microbiology and Biotechnology*, 24(2), 253-262.
- Acuña J.J., Jorquera, M.A., Martínez, O.A., Menezes-Blackburn, D., Fernández, M.T., Marschner, P., Greiner, R. and Mora, M.L. (2011). Indole acetic acid and phytase activity produced by rhizosphere bacilli as affected by pH and metals. *Journal of Soil Science and Plant Nutrition*, 11(3), 1-12.
- Adwan, K. (1999). Brief Report: The Use of SDS Polyacrylamide Gel Electrophoresis of Periplasmic Proteins to Subtype *Pseudomonas aeruginosa* Pyocin Type 10/b Clinical Isolates. *Infection*, 27(1), 39-41.
- Ahmad, F., Ahmad, I. and Khan, MS. (2008). Screening of free-living rhizospheric bacteria for their multiple plant growth promoting activities. *Microbiological Research*, 163(2), 173-181.
- Ahemad, M. and Kibret, M. (2014). Mechanisms and applications of plant growth promoting hizobacteria: Curren perspective. *Journal of King Saud University–Science*, 26, 1–20.
- Al-Holya, M.A., Lin, M., Cavinato, A.G. and Rasco, B.A. (2006). The use of fourier transform infrared spectroscopy to differentiate *Escherichia coli*O157:H7 from other bacteria inoculated into apple juice. *Food Microbiology*, 23(2), 162–168.
- Alloway B.J. (1995). *Heavy Metals in Soils*. 2nd edition. Glasgow: Blackie Academic and Professional.
- Altschul, S.F., Madden, T.L., Schaffer, A.A., Zhang, J., Zhang, Z., Miller, W. and Lipman, D.J. (1997). Gapped BLAST and PSI-BLAST: a new generation of protein database search programs. *Nucleic acids Research*, 25(17), 3389-3402.
- Alvarez, P.J.J. and Illman, W.A. (2006). *Bioremediation and natural attenuation: process fundamentals and mathematical models*, Hoboken, New Jersey: John Wiley and Sons.



- Amann, R., Ludwig, W. and Schleifer, K.-H. (1994). Identification of uncultured bacteria: a challenging task for molecular taxonomists. *ASM News*, 60, 360-365.
- Amersham, P.B. (1999). *Protein purification handbook*. Sweden: Amersham Pharmacia Biotech AB.
- Amiel, C., Mariey, L., Curk-Daubie, M-C., Pichon, P. and Travert, J. (2000). Potentiality of Fourier transform infrared spectroscopy (FTIR) for discrimination and identification of dairy lactic acid bacteria. *Lait*, 80(4), 445-459.
- Ananthalakshmi, S., Punitha, J.T. and Gowri, M. (2013) Complexation behaviour of 3-indole acetic acid with dipositive metal ions and the characterization of the complexes. *International Journal of Pharmaceutical and Life Sciences*, 4, 2638-2643.
- Angle, J.S. and Chaney, R.L. (1989). Cadmium resistance screening in nitrolotriacetate-buffered minimal media. *Applied and Environmental Microbiology*, 55(8), 2101-2104.
- Anjum, M.A., Sajjad, M.R., Akhtar, N., Qureshi, M.A., Iqbal, A., Jami A.R. and Hasan, M. (2007). Response of cotton to plant growth promoting Rhizobacteria (PGPR) inoculation under different levels of nitrogen. *Journal of Agricultural Research*, 45, 135-143.
- Asghar, H.N., Zahir, Z.A. and Arshad, M. (2004). Screening rhizobacteria for improving the growth, yield, and oil content of canola (*Brassica napus* L). *Australian Journal of Agricultural Research*, 55(2), 187-194.
- Babich, H. and Stotzky, G. (1978). Toxicity of Zinc to Fungi, Bacteria, and Coliphages: Influence of Chloride Ions. *Applied and Environmental Microbiology*, 36(6), 906-914.
- Baker, A.J., Ewart, M., K., Hendry, G.A.F., Thorpe, P.C. and Walker, P.L. (1990). The evolutionary basis of cadmium tolerance in higher plants. in: Barcelo, J. (Ed.) *Proceeding of the 4th International Conference on Environmental Contamination*, Barcelona, p. 23–29. CEP Consultants Ltd, Edinburgh.
- Baldani, J.I., Baldani, V.L.D., Seldin, L. and Dobereiner, J. (1986). Characterization of *Herbaspirillum seropedicae* gen. nov. sp. nov. a Root- Associated Nitrogen-Fixing Bacterium. *International Journal of Systematic Bacteriology*, 36, 86-93.



- Bano, A. and Fatima, M. (2009). Salt tolerance in *Zea mays* (L). following inoculation with *Rhizobium* and *Pseudomonas*. *Biology Fertilizer Soils*, 45(4), 405–413.
- Barceloux, DG (1999). Zinc. *Journal of toxicology-clinical toxicology*, 37(2), 279-292.
- Barth, A. (2007). Infrared spectroscopy of proteins. *Biochimica et Biophysica Acta*, 1767(9), 1073–1101.
- Belimov, A.A., Hontzeas, N., Safronova, V.I., Demchinskaya S.V., Piluzza, G., Bullitta, S. and Glick, B.R. (2005). Cadmium-tolerant plant growth-promoting bacteria associated with the roots of Indian mustard (*Brassica juncea* L. Czern.). *Soil Biology and Biochemistry*, 37, 241–250.
- Berber, I. (2004). Characterization of *Bacillus* species by numerical analysis of their SDS-PAGE protein profiles. *Journal of Cell and Molecular Biology*, 3(1), 33-37.
- Berber, I., Cokmus, C. and Atalan, E. (2003). Characterization of *Staphylococcus* species by SDS-PAGE of whole-cell and extracellular proteins. *Microbiology*, 72(1), 42–47.
- Bermejo-Alvarez, P., Rizos, D., Rath, D., Lonergan, P. and Gutierrez-Adan, A. (2008). Can bovine in vitro-matured oocytes selectively process X- or Y-sorted sperm differentially. *Biology of Reproduction*, 79(4), 594–597.
- Bhattacharyya, P.N. and Jha, D.K. (2012). Plant growth-promoting rhizobacteria (PGPR): emergence in agriculture. *World Journal of Microbiology and Biotechnology*, 28(4), 1327–1350.
- Bolan, N., Kunhikrishnan, A., Thangarajan, R., Kumpiene, J., Park, J., Makino, T., Kirkham, M.B. and Scheckel, K. (2014). Remediation of heavy metal(loid)s contaminated soils-To mobilize or to immobilize. *Journal of Hazardous Materials*, 266, 141-166.
- Bouhedja W., Sockalingum, G.D., Pina, P., Allouch, P., Bloy, C., Labia, R., Millot, J.M. and Manfait, M. (1997). ATR-FTIR spectroscopic investigation of *E. coli* transconjugants beta-lactams-resistance phenotype. *FEBS Letters*, 412(1), 39–42.
- Bradford, M.M. (1976). A rapid and sensitive method for the quantitation of microgram quantities of protein utilizing the principle of protein-dye binding. *Analytical Biochemistry*, 72, 248-254.



- Branco, R., Alpoim, M.C. and Morais, P.V. (2004). Ochrobactrum triticistrain 5bv11 characterization of a Cr(VI)-resistant and Cr(VI)-reducing strain. *Canadian Journal of Microbiology*, 50(9), 697–703.
- Braud, A., Jézéquela, J., Bazota, S. and Lebeau, T. (2009a). Enhanced phytoextraction of an agricultural Cr and Pb contaminated soil by bioaugmentation with siderophore-producing bacteria. *Chemosphere*, 74(2), 280-286.
- Braud, A., hannauer, M., Mislin, G.L.A. and Schalk, I.J. (2009b). The *Pseudomonas aeruginosa* pyochelin-iron uptake pathway and its metal specificity. *Journal of Bacteriology*, 191, 3517-3525.
- Braun, V., Mahren, S. and Ogierman, M. (2003). Regulation of the FecI-type ECF sigma factor by transmembrane signalling. *Current Opinion in Microbiology*, 6(2), 173–180.
- Bric, J.M., Bostock, R.M. and Silversone, S.E. (1991). Rapid in situ assay for indole acetic acid production by bacteria immobilization on a nitrocellulose membrane. *Applied and Environmental Microbiology*, 57(2), 535–538.
- Broadley, M.R., White, P.J., Hammond, J.P., Zelko, I. and Lux, A. (2007). Zinc in plants. *New Phytologist*, 173(4), 677-702.
- Brookes, P.C., Heijnen, C.E., McGrath, S.P. and Vance, E.D. (1986) Soil microbial biomass estimates in soils contaminated with metals. *Soil Biology and Biochemistry*, 18(4), 383–388.
- Buxbaum, E. (2007). *fundamental of protein structure and function*. New York: springer Science and Business Media Inc.
- Burr, T. J., Caesar, A.M. and Schrolh, N. (1984). Beneficial plant bacteria. *Critical Reviews in Plant Sciences*, 2(1), 1–20.
- Cappuccino, J.G. and Sherman, N. (1999). *Microbiology: A Laboratory Manual*. 5th ed. New York: Benjamin/cummings Science Publishing.
- Campbell, P.G.C. (2006). Cadmium-A priority pollutant. *Environmental Chemistry*, 3(6), 387–388.
- Chaney R.L. (1993). Zinc phytotoxicity, in: A.D. Robson (Ed.), *Zinc in Soils and Plants*. Dordrecht: Kluwer Academic Publishers.



- Chaney, R.L., Angle, J., Broadhurst, C. and Peters, C.A. (2007). Improved Understanding of Hyperaccumulation Yields Commercial Phytoextraction and Phytomining Technologies. *Journal of Environmental Quality*, 36(5), 1429-1443.
- Chen, Y.P., Rekha, P.D., Arun, A.B., Shen, F.T., Lai, W.A., Young, C.C., (2006). Phosphate solubilizing bacteria from subtropical soil and their tricalcium phosphate solubilizing abilities. *Applied Soil Ecology*, 34, 33–41.
- Chen, Y.X., Wang, Y.P., Lin, Q. and Luo, Y.M. (2005). Effect of copper-tolerant rhizosphere bacteria on mobility of copper in soil and copper accumulation by *Elsholtzia splendens*. *Environment International*, 31(6), 861-866.
- Chess, B. (2009). *Laboratory applications in microbiology: a case study approach*. New York: McGraw-Hill.
- Chiadò, A., Varani, L., Bosco, F. and Marmo, L. (2013). Opening study on the development of a new biosensor for metal toxicity based on *Pseudomonas fluorescens pyoverdine*. *Biosensors*, 3(4), 385-399.
- Collins, Y.E. and Stotzky, G. (1989). Factors affecting the toxicity of heavy metals to microbes. In: *Metal Ions and Bacteria*. Beveridge, T.J., Doyle, R.J. (Eds.), New York: Wiley. p. 31–90.
- Cox, C.D., K.L. Rinehart, M.L. and Moore, Jr. and Cook, Jr. J.C. (1981). Pyochelin: novel structure of an iron-chelating growth promoter for *Pseudomonas aeruginosa*. *The Proceedings of the National Academy of Sciences of the United States of America*. 78(7), 4256–4260.
- Chopra, B.K., Chopra, S. B., Mikheenko, I.P., Xua, Z., Yanga, Y., Luo, X., Chend, H., van. Zwieten, L, Lilleya, R. M. and Zhang, R. (2007). The characteristics of rhizosphere microbes associated with plants in arsenic-contaminated soils from cattle dip sites. *Science of The Total Environment*, 378(3), 331-342.
- Clesceri, L.S., Greenberg, A.E. and Eaton, A.D. (1998). *Standard methods for the examination of water and wastewater*, 7th ed. Washington, DC: American Public Health Association.
- Clink, J. and Pennington, T.H. (1987). Staphylococcal whole-cell polypeptide analysis: evaluation as a taxonomic and typing tool. *Journal of Medical Microbiology*, 23(1), 41-44.



- Cokmus, C. and Yousten, A.A. (1987). Characterization of *Bacillus sphaericus* strains by SDS-PAGE. *Journal of Invertebrate Pathology*, 64, 267-268.
- Costas, M. (1992). Classification, identification, and typing of bacteria by the analysis of their one-dimensional polyacrylamide gel electrophoretic protein patterns. *Advances in electrophoresis*, eds Chambrach A., Dunn M. J., Radola B. J. (VCH Verlagsgesellschaft, Weinheim, Germany), 5, 351-408.
- Costas, M, Holmes, B, Frith, K.A, Riddle, C. and Hawkey, P.M. (1993). Identification and typing of *Proteus penneri* and *Proteus vulgaris* biogroups 2 and 3, from clinical sources, by computerized analysis of electrophoretic protein patterns. *Journal of Applied Bacteriology*, 75(5), 489-498.
- Curk, M.C., Peledan, F. and Hubert, J.C. (1994). Fourier Transform infrared (FT-IR) spectroscopy for identifying Lactobacillus species. *FEMS Microbiology Letters*, 123(3), 241-248.
- Dar, G.H. (1996). Effects of cadmium and sewage-sludge on soil microbial biomass and enzyme activities. *Bioresource Technology*, 56, 141-145.
- Das, P., Samantaray, S. and Rout, G.R. (1997). Studies on cadmium toxicity in plants: a review. *Environmental Pollution*, 98(1), 29-36.
- Deckert, J. (2005). Cadmium Toxicity in Plants: Is There any Analogy to its Carcinogenic Effect in Mammalian Cells. *BioMetals*, 18(5), 475-481.
- Dell, A.E., Cavalca, L. and Andreoni, V. (2008). Improvement of *Brassica napus* growth under cadmium stress by cadmium-resistant rhizobacteria. *Soil Biology and Biochemistry*, 40, 74-84.
- Deshwal, V.K. and Kumar, P. (2013). Effect of Heavy metals on Growth and PGPR activity of Pseudomonads. *Journal of Academia and Industrial Research*, 2(5), 286-290.
- Dhungana, S., Ratledge, C. and Crumbliss, A.L. (2004). Iron Chelation Properties of an Extracellular Siderophore Exochelin MS. *Inorganic Chemistry*, 43(20), 6274-6283.
- Diem, M., Boydston-White, S. and Luis, C. (1999). Infrared spectroscopy of cells and tissues: shining light onto a novel subject. *Applied Spectroscopy*, 53(4), 148A-161A.



- Dimkpa, CO., Merten, D., Svatoš, A., Büchel, G. and Kothe, E. (2009). Metal-induced oxidative stress impacting plant growth in contaminated soil is alleviated by microbial siderophores. *Soil Biology and Biochemistry*, 41(1), 154–162.
- Dimkpa, C.O., Svatos, A., Dabrowska, P., Schmidt, A., Boland, W. and Kothe, E. (2008). Involvement of siderophores in the reduction of metal-induced inhibition of auxin synthesis in *Streptomyces* spp. *Chemosphere*, 74(1), 19-25.
- Dobereiner, J., Day, J.M. and Dart, P.J. (1972). Nitrogenase Activity and Oxygen Sensitivity of the *Paspalum notatum*-*Azotobacter paspali* Association. *Journal of General Microbiology*, 71, 103-116.
- Dobereiner, J. and Day, J.M. (1975). Nitrogen fixation in rhizosphere of grasses. In *Nitrogen Fixation by Free-Living Microorganisms*. Edited by Stewart WDP Cambridge: Cambridge University Press. pp. 39–56.
- Duffus, J. H. (2002). “Heavy metals” a meaningless term? (IUPAC Technical Report). *Pure and Applied Chemistry*, 74, 793–807.
- Duygu, D., Baykal, T., Acilk, A.I. and Yildizi, K. (2009). Fourier Transform Infrared (FT-IR) Spectroscopy for Biological Studies. *G.U. Journal of Science*, 22(3), 117-121.
- Dziuba, B., Babuchowski, A., Nałęcz, D. and Niklewicz, M. (2007). Identification of lactic acid bacteria using FTIR spectroscopy and cluster analysis. *International Dairy Journal*, 17, 183–189.
- Egamberdiyeva, D. (2007). The effect of plant growth promoting bacteria on growth and nutrient uptake of maize in two different soils. *Applied Soil Ecology*, 36(2), 184–189.
- Eisler, R. (1993). *Zinc Hazard to Fish, Wildlife, and Invertebrates: A Synoptic Review*. Laurel, MD: U.S. Department of the Interior, Fish and Wildlife Service.
- Ensley, B.D. (2000). Rationale for Use of Phytoremediation. In *Phytoremediation of Toxic Metals: Using Plants to Clean Up the Environment*, ed. I. Raskin and B.D. Ensley, Hoboken, NJ: John Wiley & Sons, Inc. pp. 3-11.
- EPA, U.S. (1987) *Ambient water quality criteria for zinc*. [Online]. Available from: <http://spokaneriver.net/wp-content/uploads/2011/03/Zinc-1987.pdf> [accessed 9 July 2013].



- Farwell, A.J., Vesely, S., Nero, V., Rodriguez, H., McCormack, K., Shah, S., Dixon, D.G. and Glick, B.R. (2007). Tolerance of transgenic canola plants (*Brassica napus*) amended with plant growth-promoting bacteria to flooding stress at a metal-contaminated field site. *Environmental Pollution*, 147(3), 540-545.
- Filali, B.K., Taoufik, J., Zeroual, Y., Dzairi, F.A.Z., Talbi, M. and Blaghen, M. (1999). Waste water bacterial isolates resistant to heavy metals and antibiotics. *Current Microbiology*, 41(3), 151-156.
- Fosmire, G.J. (1990). Zinc toxicity. *American Journal of Clinical Nutrition*, 51(2), 225–227.
- Frostegard, A., Tunlid, A. and Baath, E. (1993). Phospholipid fatty acid composition, biomass, and activity of microbial communities from 2 soil types experimentally exposed to different heavy metals. *Applied and Environmental Microbiology*, 59(11), 3605–3617.
- Garcia-Caurel, E., Nguyen, J., Schwartz, L. and Drevillon, B. (2004). Application of FTIR ellipsometry to detect and classify microorganisms. *Thin Solid Films*, 455-456, 722–725.
- Garip, S., A. Gozen, C. and Severcan, F. (2009). Use of Fourier transform infrared spectroscopy for rapid comparative analysis of *Bacillus* and *Micrococcus* isolates. *Food Chemistry*, 113(4), 1301–1307.
- Garip, S., Bozoglu, F. and Severcan F., (2007). Differentiation of mesophilic and thermophilic bacteria with Fourier transform infrared spectroscopy. *Applied Spectroscopy*, 61(2), 186 -192.
- Ghosh, M. and Singh, S.P. (2005). A review on phytoremediation of heavy metals and utilization of its by products. *Applied and ecology and environmental research*, 3(1), 1-18.
- Glick, B.R., Penrose, D.M. and Li, J.P. (1998) A model for the lowering of plant ethylene concentration by Plant Growth Promoting Bacteria. *Journal of Theoretical Biology*, 190(1), 63-68.
- Glick, B.R., Patten, C.L., Holguin, G. and Penrose, D.M. (1999). *Biochemical and Genetic Mechanisms Used by Plant Growth Promoting Bacteria*. London, UK: Imperial College Press.



- Glick, B.R. (2003). Phytoremediation: synergistic use of plants and bacteria to clean up the environment. *Biotechnology Advances*, 21(5), 383-393.
- . (2012). *Plant Growth-Promoting Bacteria: Mechanisms and Applications*. Canada: University of Waterloo.
- . (2010). Using soil bacteria to facilitate phytoremediation. *Biotechnology Advances*, 28(3), 367–274.
- Gomez, M.A., Perez, M.A.B. and Gil, F.J.M. (2003). Identification of species of *Brucella* using Fourier transform infrared spectroscopy. *Journal of Microbiological Methods*, 55, 121-131.
- Greger, M., 2004. Metal availability, uptake, transport and accumulation in plants. In: Prasad, M.N.V.(ed.), *Heavy Metal Stress in Plants: From Biomolecules and Ecosystems*, p. 1–27. Heidelberg: Springer-Verlag.
- Griffiths, B.S., Diaz-Ravina, M., Ritz, K., McNicol, J.W., Ebbelwhite, N. and Baath, E. (1997). Community DNA hybridisation and %G+C profiles of microbial communities from heavy metal polluted soils. *FEMS Microbiology Ecology*, 24(2), 103–112.
- Guibet, F., Amiel, C., Cadot, P., Cordevant, C., Desmonts, M.H., Lange, M., Marecat, A., Travert, J., Denis, C. and Mariey, L. (2003). Discrimination and classification of Enterococci by Fourier transform infrared (FT-IR) spectroscopy. *Vibrational Spectroscopy*, 33(1), 133–142.
- Gu, J-D. and Pan, L. (2006). Comparing the growth characteristics of three bacteria involved in degrading rubbers. *Journal of Polymers and the Environment*, 14(3), 273–279.
- Hajna, A.A. (1945). Triple-Sugar Iron Agar Medium for the Identification of the Intestinal Group of Bacteria. *Journal of Bacteriology*, 49(5), 516–517.
- Hameeda, B., Rupela, O., Reddy, G. and Satyavani, K. (2006). Application of plant growth -promoting bacteria associated with composts and macrofauna for growth promotion of Pearl millet (*Pennisetum glaucum* L). *Biology and Fertility of Soils*, 43(2), 221-227.



- Hashimoto, F., Horigome, T., Kanbayashi, M., Yoshida, K. and Sugano, H. (1983). An improved method for separation of low-molecular weight polypeptides by electrophoresis in sodium dodecyl sulfate-polyacrylamide gels. *Analytical Biochemistry*, 129(1), 192–199.
- Hassen, A., Said, N., Cherif, M., and Boudabous, A. (1998). Resistance of environmental bacteria to heavy metals. *Bioresource Technology*, 64, 7-15.
- Helm, D, Labischinski, H. and Naumann, D. (1991a). Elaboration of a procedure for identification of bacteria using Fourier-Transform IR spectral libraries: a stepwise correlation approach. *Journal of Microbiological Methods*, 14, 127–142.
- Helm, D., Labischinski, H., Schallehn, G. and Naumann, D. (1991b). Classification and identification of bacteria by Fourier transform infrared spectroscopy. *Journal of General Microbiology*, 137(1), 69–79.
- Hoegy, F., Lee, X., Noël, S., Mislin, G.L., Rognan, D., Reimann, C. and Schalk, I.J. (2009). Stereospecificity of the siderophore pyochelin outer membrane transporters in fluorescent Pseudomonads. *The Journal of Biological Chemistry*, 284(22), 14949–14957.
- Hogan, C.M. (2010). *Heavy metal*. Encyclopedia of Earth. National Council for Science and the Environment. eds. E. Monosson and C. Cleveland. Washington DC: Encyclopedia of Earth.
- Honma, M. and Shimomura, T. (1978). Metabolism of 1-aminocyclopropane-1-carboxylic acid. *Agricultural Biology and Chemistry*, 42, 1825-1831.
- Holleman, A.F., Wiberg, E. and Wiberg, N. (1985). *Lehrbuch der anorganischen Chemie*. Berlin: Walter de Gryter.
- Horitsu, H., Yamamoto, K., Wachi, S., Kawai, K. and Fukuchi, A. (1986). Plasmid-determined cadmium resistance in *Pseudomonas putida* GAM-1 isolated from soil. *Journal of Bacteriology*, 165(1), 334-335.
- Hughes, M.N. and Poole, R.K. (1989). *Metals and Microorganisms*. New York: Chapman & Hall.
- Hwangbo, H., Park, R.D., Kim, Y.W., Rim, Y.S., Park, K. H., Kim, T.H., Suh, J. S. and Kim, K.Y. (2003). 2-Ketogluconic Acid Production and Phosphate Solubilization by *Enterobacter* intermedium. *Current Microbiology*, 47(2), 87–92.



- Illmer, P. and Schinner, F. (1992). Solubilization of inorganic phosphates by microorganisms isolated from forest soil. *Soil Biology and Biochemistry*, 24, 389-395.
- Indiragandhi, P., Anandham, R., Madhaiyan, M. and Sa, T.M. (2008), Characterization of plant growth-promoting traits of bacteria isolated from larval guts of diamondback moth *Plutella xylostella* (Lepidoptera: Plutellidae). *Current Microbiology*, 56(4), 327–333.
- Jackman, P. J. H. and Pelczynska, S. (1986). Characterization of *Corynebacterium* Group JK by Whole-cell Protein Patterns. *Journal of General Microbiology*, 132(7), 1911-1 915.
- Jing, Y., He, Z. and Yang, X. (2007). Role of soil rhizobacteria in phytoremediation of heavy metal contaminated soil. *Journal of Zhejiang University Science*, 8, 192-207.
- Kang, B.G., Kim, W.T., Yun, H.S. and Chang, S.C. (2010). Use of plant growth-promoting rhizobacteria to control stress responses of plant roots. *Plant biotechnology reports*, 4, 179–183.
- Kansiza, M., Heraud, P., Wood, B., Burden, F. Beardall, J. and McNaughton, D. (1999). Fourier Transform Infrared microspectroscopy and chemometrics as a tool for the discrimination of cyanobacterial strains. *Phytochemistry*, 52(3), 407-417.
- Karakurt, H., Aslantas, R., Ozkan, G. and Guleryuz, M. (2009). Effects of indol–3-butyrac acid (IBA), plant growth promoting rhizobacteria (PGPR) and carbohydrates on rooting of hardwood cutting of MM106 Apple rootstock. *African Journal of Agricultural Research*, 4(2), 60-64.
- Kerstens, K., Pot, B., Dewettinck, D., Torck, U., Vancanneyt, M., Vauterin, L. and Vandamme, P. (1994). Identification and typing of bacteria by protein electrophoresis. *Bacterial Diversity and Systematics*, 75, 51-66.
- Khan, I.A., Rattan, A., Fatima, T., Khan, F.G. and Kalia, A. (1996). Application of Whole Cell Protein Analysis by SDS-PAGE to Establish the Source of *Salmonella typhimurium*. *Journal of Infection*, 33(3), 169-171.
- Khan, K.S., Xie, Z.M. and Huang, C.Y. (1997). Effect of anions on toxicity of cadmium applied to microbial biomass in red soil. *Pedosphere*, 7(3), 231–235.



- Khan, M.S., Zaidi, A. and Wani, P.A. (2006). Role of phosphate solubilizing microorganisms in sustainable agriculture—a review. *Sustainable Agriculture*, 27, 29–43.
- Khan, M.S., Zaidi, A., Wani, P.A. and Oves, M. (2009). Role of plant growth promoting rhizobacteria in the remediation of metal contaminated soils. *Environmental Chemistry Letters*, 7, 1–19.
- Khamna S., Yokota, A., Peberdy, J.F., Lumyong, S. (2010). Indole-3-acetic acid production by *Streptomyces* sp. isolated from some Thai medicinal plant rhizosphere soils. *EurAsian Journal of BioSciences*, 4, 23-32.
- Khaokaew, S., Chaney, R.L., Landrot, G., Ginder-Vogel, M., Donald, L. and Sparks, D. (2011). Speciation and release kinetics of cadmium in an alkaline paddy soil under various flooding periods and draining conditions. *Environmental Science and Technology*, 45(10), 4249-4255.
- Kim, J. and Rees, D.C. (1994). Nitrogenase and biological nitrogen fixation. *Biochemistry*, 33(2), 389–397.
- Kimura, M. (1980). A simple method for estimating evolutionary rates of base substitutions through comparative studies of nucleotide sequences. *Journal Molecular Evolution*, 16(2), 111–120.
- Kiss, T. and Farkas, E. (1998). Metal-binding ability of desferrioxamine B. *Journal of Inclusion Phenomena and Macrocyclic Chemistry*, 32(2-3), 385–403.
- Klumpp, C., Burger, A., Mislin, G.L. and Abdallah, M.A. (2005). From a total synthesis of cepabactin and its 3:1 ferric complex to the isolation of a 1:1:1 mixed complex between iron (III), cepabactin and pyochelin. *Bioorganic and Medicinal Chemistry Letters*, 15(6), 1721–1724.
- Kuffner, M., Puschenreiter, M., Wieshammer, G., Gorfer, M. and Sessitsch, A. (2008). Rhizosphere bacteria affect growth and metal uptake of heavy metal accuulating willows. *Plant and Soil*, 304, 35-44.
- Kummerle, M., Scherer, S. and Seiler, H. (1998). Rapid and reliable identification of fermentative yeasts by Fourier transform infrared spectroscopy. *Applied and Environmental Microbiology*, 64(6), 2207-2214.



- Ladha, J.K., De Bruijn, F.J. and Malik, K.A. (1997). Introduction: assessing opportunities for nitrogen fixation in rice-a frontier project. *Plant Soil*, 124(1-2), 1–10.
- Laemmli, UK. (1970). Cleavage of structural proteins during assembly of the head of bacteriophage T4. *Nature*, 227(5259), 680-685.
- Leong, S.A., and Winkelmann, G. (1998). Molecular biology of iron transport in fungi. *Metal ions in biological systems*, 35, 147–186.
- Lipkus, A.H., K.K. Chittur and S.J. Vesper (1990) Evolution of infrared spectroscopy as a bacterial identification method. *Journal Industrial Microbiology*, 6: 71-75.
- Ludwig, W. and Schleifer, K.-H. (1999). Phylogeny of Bacteria beyond the 16S rRNA standard. *ASM News*, 65, 752-757.
- Ludwig, W., Strunk, O., Klugbauer, S., Klugbauer, N., Weizenegger, M., Neumaier, J. and Bachleitner, M. (1998). Bacterial phylogeny based on comparative sequence analysis. *Electrophoresis*, 19(4), 554-568.
- Ma Y., Rajkumar, M. and Freitas, H. (2009a). Improvement of plant growth and nickel uptake by nickel resistant-plant growth promoting bacteria. *Journal of Hazardous Materials*, 166(2-3), 1154–1161.
- Ma Y., Rajkumar, M. and Freitas, H. (2009b). Isolation and characterization of Ni mobilizing PGPB from serpentine soils and their potential in promoting plant growth and Ni accumulation by *Brassica* spp. *Chemosphere*, 75(6), 719–275.
- Ma Y, Prasad, MNV., Rajkumar, M. and Freitas, H. (2011). Plant growth promoting rhizobacteria and endophytes accelerate phytoremediation of metalliferous soils. *Biotechnology Advances*, 29(2), 248–258.
- Malik, K.A., Bilal, R., Mehnaz, S., Rasul, G., Mirza, M.S. and Ali, S. (1997). Association of nitrogen-fixing, plant-growth-promoting rhizobacteria (PGPR) with kallar grass and rice. *Plant and Soil*, 194(1-2), 37–44.
- Maquelin, K. and Kirschner, C. (2002). Identification of medically relevant microorganisms by vibrational spectroscopy. *Journal of Microbiological Methods*, 51(3), 255-271.
- Margarita, P. and Quinteiro, R. (2000). Fourier Transform Infrared (FT-IR) Technology for the Identification of Organisms, *Clinical Microbiology Newsletter*, 22(8), 57–61.



- Mastretta, C., Taghavi, S., Lelie, D., Mengoni, A., Galardi, F., Gonnelli, C., Barac, T., Boulet, J., Weyens, N. and Vangronsveld, J. (2009). Endophytic bacteria from seeds of *Nicotiana tabacum* can reduce cadmium phytotoxicity. *International Journal of Phytoremediation*, 11, 251–267.
- McGrath, S.P., Zhao, J. and Lombi, E. (2002). Phytoremediation of metals, metalloids, and radionuclides. *Advances in Agronomy*, 75, 1–56.
- McKenzie, R.H. and Roberts, T.L. (1990). Soil and fertilizers phosphorus update. In: *Proceedings of Alberta Soil Science Workshop Proceedings*, February. 20–22, Edmonton, Alberta, pp. 84–104.
- Meesungnoen, O., Nakbanpote, W., Thiwthong, R. and Thumanu, K. (2009). Plant growth promoting properties of heavy metal tolerant bacteria isolated from *Gynura pseudochina* (L.) DC.'s rhizosphere. *Proceeding of International Conference on Green and Sustainable Innovation (ICGSI)*. December 2 - 4, 2009, Chiang Rai, Thailand. p. 7.
- Meesungnoen, O., Nakbanpote, W., Thiwthong, R. and Thumanu, K. (2012). Zinc and Cadmium Resistance Mechanism of *Pseudomonas aeruginosa* PDMZnCd2003. *Research Journal of Biological Sciences*, 7(1), 4-13.
- Miransari, M. (2011). Hyperaccumulators, arbuscular mycorrhizal fungi and stress of heavy metals. *Biotechnology Advances*, 29(6), 645–653.
- Mueller, J. G., Cerniglia, C. E. and Pritchard, P. H. (1996). *Bioremediation of environments contaminated by polycyclic aromatic hydrocarbons*. In *bioremediation: Principles and applications*, p. 125–194. Cambridge: Cambridge University Press.
- Murray, RGE., Brenner, DJ., Colwell, RR., Devos, P., Goodfellow, M., Grimont, PAD., Pfennig, N., Stackebrandt, E. and Zavarzin, GA. (1990). Report of the ad hoc committee on approaches to taxonomy within the prokaryotes. *International Journal of Systematic Bacteriology*. 40(2), 213-215.
- Muysen, B.T.A., De Schampelaere, K.A.C. and Janssen, C.R. (2006). Mechanisms of chronic waterborne Zn toxicity in *Daphnia magna*. *Aquatic Toxicology*, 77(4), 393–401.



- Nakbanpote, W., Panitlertumpai, N., Sukadeetad, K., Meesungneon, O. and Noisa-nguan, W. (2010). Chapter 20: Advances in Phytoremediation Research: A Case Study of *Gynura pseudochina* (L.) DC. In: *Advanced Knowledge Application in Practice*. Igor Furstner (Editor). ISBN 978-953-307-141-1 InTech, Croatia, pp. 353-378.
- Nannipieri, P. (1994). The potential use of soil enzymes as indicators of productivity, sustainability and pollution. In: *Pankhurst, C.E., Doube, B.M., Gupta, V.V.S.R., Grace, P.R. (Eds.), Soil Biota, Management in Sustainable Farming Systems*. CSIRO Publications, Australia, pp. 238–244.
- Naumann, D. (1998). Infrared and NIR Raman spectroscopy in medical microbiology. In: H H Mantsch and M Jackson (eds), *Infrared spectroscopy: new tool in medicine*, Proceedings of SPIE Vol. 3257. Washington: Bellingham, pp. 245-257.
- Naumann, D. (2000). Infrared Spectroscopy in Microbiology. in *Encyclopedia of Analytical Chemistry*. p. 102-131. R.A. Meyers (Ed), London: John Wiley & Sons Ltd.
- Naumann, D., Helm, D. and Labischinski, H. (1991). Microbiological characterizations by FT-IR spectroscopy. *Nature*, 351, 81–82.
- Nauman, D., Fijala, V. and Labischinski, H. (1988). The Differentiation and Identification of Pathogenic Bacteria Using FT-IR and Multivariate Statistical. *Mikrochim. Acta [Wien]*, 1, 373-377.
- Naumann, D., Schultz, C.P. and Helm, D. (1996). What can Infrared Spectroscopy Tell us about the Structure and Composition of Intact Bacterial Cells. In *Infrared Spectroscopy of Biomolecules*, H.H. Mantsch and D. Chapman editor. New York: Wiley-Liss. pp. 279-310.
- Neilands, J.B. (1995). Siderophores: structure and function of microbial iron transport compounds. *The Journal of Biological Chemistry*, 270(45), 26723–26726.
- Neubauer, U., Furrer, G., Kayser, A. and Schulin, R. (2000). Siderophores, NTA, and citrate: potential soil amendments to enhance heavy metal mobility in phytoremediation. *International Journal of Phytoremediation*, 2(4), 353–368.
- Nickerson, W.J. (1946). Inhibition of fungus respiration: a metabolic bioassay method. *Science*, 103, 484-486.



- Nies, D.H. (1999). Microbial heavy-metal resistance. *Applied Microbiology and Biotechnology*, 51(6), 730-750.
- Oberreuter, H., Charzinski, J. and Scherer, S. (2002). Intraspecific diversity of *Brevibacterium linens*, *Corynebacterium glutamicum* and *Rhodococcus erythropolis* based on partial 16S rDNA sequence analysis and Fourier-transform infrared (FT-IR) spectroscopy. *Microbiology*, 148 (Pt 5), 1523–1532.
- Oliveira, A. and Pampuha, M.E. (2006). Effects of long-term heavy metal contamination on soil microbial characteristic. *Journal of Bioscience and Bioengineering*, 102(3), 157-161.
- Ojeda, J.J., Romero-Gonzalez, M.E., Pouran, H.M. and Banwart, S.A. (2008). In situ monitoring of the biofilm formation of *Pseudomonas putida* on hematite using flow-cell ATR-FTIR spectroscopy to investigate the formation of inner-sphere bonds between the bacteria and the mineral. *Mineralogical Magazine*, 72(1), 101–106.
- Pancholy, S.K., Rice, E.L. and Turner, J.A. (1975). Soil factors preventing revegetation of a denuded area near an abandoned zinc smelter in Oklahoma. *Journal of Applied Ecology*, 12(1), 337–342.
- Paniltertumpaia, N., Nakbanpote, W., Sangdee, A., Thumanu, K., Nakai, I. and Hokura, A. (2013). Zinc and/or cadmium accumulation in *Gynura pseudochina* (L.) DC. studied in vitro and the effect on crude protein. *Journal of Molecular Structure*, 1036, 279–291.
- Patil, N.B., Gajbhiye, M., Ahiwale, S.S., Gunjal, A.B. and Kapadnis, B.P. (2011). Optimization of Indole 3-acetic acid (IAA) production by *Acetobacter diazotrophicus* L1 isolated from Sugarcane. *International Journal of Environmental Sciences*, 2(1), 295-302.
- Patnaik, P. (2004). *Dean's Analytical Chemistry Handbook*. 2nd edition. New York: McGraw-Hill.
- Patten, C.L. and Glick, B.R. (1996). Bacterial biosynthesis of indole-3-acetic acid. *Canadian Journal Microbiology*, 42(3), 207–220.
- Peer, W.A., Baxter, I.R., Richards, E.L., Freeman, J.L. and Murphy, A.S. (2005). Phytoremediation and hyperaccumulator plants. *Topics in Current Genetics*, 14, 299-340.



- Peng, J.F., Song, Y.H., Yuan, P., Cui, X.Y. and Qiu, G.L. (2009). The remediation of heavy metals contaminated sediment. *Journal of Hazardous Materials*, 161(2-3), 633–640.
- Peng, Y., Stevens, P., De Vos, P. and De Ley, J. (1987). Relation between pH, Hydrogenase and Nitrogenase Activity, NH_4^+ Concentration and Hydrogen Production in Cultures of *Rhodobacter sulfidophilus*. *Journal of General Microbiology*, 133, 1243-1247.
- Piraino, P., Ricciardi, A., Salzano, G., Zotta, T. and arente, E. P (2006). Use of unsupervised and supervised artificial neural networks for the identification of lactic acid bacteria on the basis of SDS-PAGE patterns of whole cell proteins. *Journal of Microbiological Methods*, 66(2),336–346.
- Poirier, I., Jean, N., Guary, J.C. and Bertrand, M. (2008). Responses of the marine bacterium *Pseudomonas fluorescens* to an excess of heavy metals: Physiological and biochemical aspects. *Science of The Total Environment*, 406(1-2), 76-87.
- Prasad, A.S. (1995). Zinc: An overview. *Nutrition*, 11(1 Suppl), 93-99.
- Prasad, M.N.V. (1995). Cadmium toxicity and tolerance in vascular plants. *Environmental and Experimental Botany*, 35(4), 525–545.
- Prasad, M.N.V. (2004). *Heavy metal stress in plants from biomolecules to ecosystems*. India: Springer, New Delhi.
- Promega Corporation (2002). Nucleic Acid Amplification: In *Protocols and Applications Guide*. Wisconsin: Promega Corporation.
- Rajkumar, M. and Freitas, H. (2008a). Influence of metal resistant-plant growth-promoting bacteria on the growth of *Ricinus communis* in soil contaminated with heavy metals. *Chemosphere*, 71(5), 834-842.
- . (2008b). Effects of inoculation of plant-growth promoting bacteria on Ni uptake by Indian mustard. *Bioresource Technology*, 99(9), 3491–3498.
- Rajkumar, M., Prasad, M.N.V., Freitas, H. and Ae, N. (2009). Biotechnological applications of serpentine soil bacteria for phytoremediation of trace metals. *Critical Reviews in Biotechnology*, 29(2), 120–130.



- Rajkumar, M., Ae, N., Prasad, M.N.V. and Freitas, H. (2010). Potential of siderophore-producing bacteria for improving heavy metal phytoextraction. *Trends Biotechnology*, 28(3), 142–149.
- Rajkumar M, Sandhya, S., Prasad, M.N.V. and Freitas, H. (2012). Perspectives of plant associated microbes in heavy metal phytoremediation. *Biotechnology Advances*, 30(6), 1562–1574.
- Ramamoorthy, V., Viswanathan, R., Raguchander, T., Prakasam, V. and Samiyappan, R. (2001). Induction of systemic resistance by plant growth promoting rhizobacteria in crop plants against pests and diseases. *Crop Protection*, 20(1), 1-11.
- Ramette, A., Moenne-Loccoz, Y. and Defago, G. (2003). Prevalence of Fluorescent pseudomonads producing antifungal phloroglucinols and/or hydrogen cyanide in soils naturally suppressive or conducive to tobacco black root rot. *FEMS Microbiology Ecology*, 44(1), 35-43.
- Rana, A., Saharan, B., Joshi, M., Prasanna, R., Kumar, K. and Nain, L. (2011). Identification of multi-trait PGPR isolates and evaluating their potential as inoculants for wheat. *Annals of Microbiology*, 61(4), 893-900
- Raskin, I., Smith, R.D. and Salt, D. E. (1997). Phytoremediation of metals: using plants to remove pollutants from the environment. *Plant Biotechnology*, 8(2), 221–226.
- Raskin, I. and Ensley, B.D. (2000). *Phytoremediation of Toxic Metals: Using Plants to Clean up the Environment*, New York: John Wiley and Sons.
- Raymond, K.N., Dertz, E.A. and Kim, S.S. (2003). Enterobactin: an archetype for microbial iron transport. *Proceedings of the National Academy of Sciences of the United States of America*, 100(7), 3584–3588.
- Raymond, J., Siefert, J.L., Staples, C.R. and Blankenship, R.E. (2004). The natural history of nitrogen fixation. *Molecular Biology and Evolution*, 21(3), 541–554.
- Rodríguez, H. and Fraga, R. (1999) Phosphate solubilizing bacteria and their role in plant growth promotion. *Biotechnology Advances*, 17(4-5), 319–339.
- Reeves, R.D. and Brooks, R.R. (1983). Hyperaccumulation of lead and zinc by two metallophytes from mining areas of Central Europe. *Environmental Pollution Series A, Ecological and Biological*, 31(4), 277-285.



- Rehm, H. (2006) *Protein Biochemistry and Proteomics*. California: Academic Press.
- Riddle, J.W., Kabler, P.W., Kenner, B.A., Bordner, R.H, Rockwood, S.W. and Stevenson, H.J.R. (1956). Bacterial identification by infrared spectrophotometry. *Journal of Bacteriology*, 72(5), 593-603.
- Roane, T.M., Pepper, I.L. and Miller, R.M. (1996). Microbial remediation of metals. In: *Bioremediation: Principles and applications*, Crawford, R.L., and Crawford, D.L., editor. Cambridge, UK: Cambridge University Press. p. 312-340.
- Rubio, L.M. and Ludden, P.W. (2008). Biosynthesis of the iron-molybdenum cofactor of nitrogenase. *Annual Review of Microbiology*, 62, 93–111.
- Robinson, B., Russell, C., Hedley, M. and Clothier, B. (2001). Cadmium adsorption by rhizobacteria: implications for New Zealand pastureland. *Agriculture, Ecosystems and Environment*, 87(3), 315-321.
- Rohlf, F. J. (2000). *NTSYS-pc: numerical taxonomy and multivariate analysis system, version 2.1*. New York: Exeter Software.
- Ryu, C., Farag, M.A., Hu, C., Reddy, M.S., Wei, H., Paré, P.W. and Kloepper, J.W. (2003). Bacterial volatiles promote growth in Arabidopsis. *Proceedings of the National Academy of Sciences*, 100(8), 4927-4932.
- Saçilik, S. C., Osmanağaoğlu, Ö., Gündüz, U. and Çökmüş, C. (2000). Availability of use of Total Extracellular Proteins in SDS-PAGE for Characterization of Gram-Positive Cocci. *Turkey Journal Biology*, 24(4), 817–823.
- Sacksteder, C. and Barry, B.A. (2001). Fourier Transform Infrared Spectroscopy: A Molecular Approach to an Organism Question, *Journal of Phycology*, 37(2), 197-199.
- Saharan, B.S. and Nehra, V. (2011). Plant Growth Promoting Rhizobacteria: A Critical Review. *Life Sciences and Medicine Research*, 21, 1-31.
- Saiki, R., Scharf, S., Faloona, F., Mullis, K.B., Horn, G.T., Erlich, H.A. and Arnheim, N. (1985). Enzymatic amplification of beta-globin genomic sequences and restriction site analysis for diagnosis of sickle cell anemia. *Science*, 230(4732), 1350–1354.
- Salt, D.E., Smith, R.D. and Raskin, I. (1998). PHYTOREMEDIATION. *Annual Review of Plant Physiology and Plant Molecular Biology*, 49, 643-668.



- Sambrook, J. and Russell, D.W. (2001). *Molecular cloning: a laboratory manual*. 3rd. ed. Cold Spring Harbor, N.Y.: Cold Spring Harbor Laboratory.
- San-Blas, E., Cubillán, N., Guerrac, M., Portillo, E. and Esteves, I. (2012). Characterization of *Xenorhabdus* and *Photorhabdus* bacteria by Fourier transform mid-infrared spectroscopy with attenuated total reflection (FT-IR/ATR). *Spectrochimica Acta Part A: Molecular and Biomolecular Spectroscopy*, 93, 58–62.
- Sánchez, I., Seseña, S. and Palop, L. (2003). Identification of lactic acid bacteria from spontaneous fermentation of ‘Almagro’ eggplants by SDS-PAGE whole cell protein fingerprinting. *International Journal of Food Microbiology*, 82(2), 181–189.
- Santner, A., L.I.A. Calderon-Villalobos and M. Estelle (2009) Plant hormones are versatile chemical regulators of plant growth. *Nature Chemical Biology*, 5(5), 301–307.
- Saraf, M., Pandya, U. and Thakkar, A. (2014). Role of allelochemicals in plant growth promoting rhizobacteria for biocontrol of phytopathogens. *Microbiological Research*, 169(1), 18-29.
- Sarker, S.D., Nahar, L. and Kumarasamy, Y. (2007). Microtitre plate-based antibacterial assay incorporating resazurin as an indicator of cell growth, and its application in the *in vitro* antibacterial screening of phytochemicals. *Methods*, 42(4), 321–324.
- Schägger, H. and Jagow, G. (1987). Tricine-sodium-dodecylsulfate Polyacrylamide Gel Electrophoresis for the Separation of Proteins in the Range from 1–100 kDa. *Analytical Biochemistry*, 166(2), 368–379.
- Schnoor, J.L. (1997). Phytoremediation, GWRTAC Technology Evaluation Report TE-98-01, Pittsburgh, PA: Ground-Water Remediation Technologies Analysis Center.
- Schuster, K.C., Mertens, F. and Gapes, J.R. (1999). FTIR spectroscopy applied to bacterial cells as a novel method for monitoring complex biotechnological processes. *Vibrational Spectroscopy*, 19(2), 467-477.



- Shahzad, S.M., Khalid, A., Arshad, M., Khalid, M. and Mehboob, I. (2008). Integrated use of plant growth promoting bacteria and Penriched compost for improving growth, yield and nodulating of Chickpea. *Pakistan Journal of Botany*, 40(4), 1735-1441.
- Sharma, K.P., Frenkel, A. and Balkwill, L.D. (2000). A new *Klebsiella planticola* strain (cd-1) grows anaerobically at high cadmium concentrations and precipitates cadmium sulphide. *Applied and Environmental Microbiology*, 66, 3083-3087.
- Sheng, X.F. and Xia, J.J. (2006). Improvement of rape (*Brassica napus*) plant growth and cadmium uptake by cadmium-resistant bacteria. *Chemosphere*, 64(6), 1036-1042.
- Siddiquee, M.A., Chauhan, P.S., Anandham, R., Gwang-Hyun, H. and Tongmin, Sa. (2010). Isolation, Characterization, and Use for Plant Growth Promotion Under Salt Stress, of ACC Deaminase-Producing Halotolerant Bacteria Derived from Coastal Soil. *Journal Microbiology Biotechnology*, 20(11), 1577–1584.
- Siebert, F. (1995), Infrared spectroscopy applied to biochemical and biological problems, In: Sauer, K. (Ed), *Biochemical Spectroscopy. Methods in Enzymology*, 246, 501-526.
- Silver, S. (1996). Bacterial resistances to toxic metal ions-a review. *Gene*, 179(1), 9-19.
- Simmons, R.W., Pongsakul, P., Saiyasitpanich, D. and Klinphoklap, S. (2005). Elevated levels of cadmium and zinc in paddy soils and elevated levels of cadmium in rice grain downstream of a zinc mineralized area in Thailand: implications for public health. *Environmental Geochemistry and Health*, 27(5-6), 501-511.
- Sinha, S. and Mukherjee, S.K. (2008). Cadmium-induced siderophore production by a high Cd-resistant bacterial strain relieved Cd toxicity in plants through root colonization. *Current Microbiology*, 56(1), 55-60.
- Siripornadulsil, S. and Siripornadulsil, W. (2013). Cadmium-tolerant bacteria reduce the uptake of cadmium in rice: Potential for microbial bioremediation. *Ecotoxicology and Environmental Safety*, 94, 94–103.
- Smith, T. and Bell, J. (1986). An Exponential Gradient Maker for Use with Minigel Polyacrylamide Electrophoresis Systems. *Analytical Biochemistry*, 152(1), 74–77.



- Smith, W. H., Staskawicz, B.J. and Harkov, R.S. (1978). Trace-metal pollutants and urban-tree leaf pathogens. *Transactions of the British Mycological Society*, 70(1), 29-33.
- Somers, E. (1961). The fungi toxicity of metal ions. *Annals of Applied Biology*, 49(2), 246-253.
- Spaepen, S., Vanderleyden, J. and Remans, R. (2007). Indole- 3-acetic acid in microbial and microorganism-plant signaling. *FEMS Microbiology Review*, 31(4), 425–448.
- Spaepen, S. and Vanderleyden, J. (2011). Auxin and plant-microbe interactions. *Cold Spring Harbor Perspectives in Biology*, 3(4), 1-24.
- Staniszewska, I., Sariyer, I.K., Lecht, S., Brown, M.C., Walsh, E.M., Tuszyński, G.P., Safak, M., Lazarovici, P. and Marcinkiewicz, C. (2008). Integrin alpha9 beta1 is a receptor for nerve growth factor and other neurotrophins. *Journal of Cell Science*, 121(4), 504–513.
- Strandberg, G.W., Shumate, S.E. and Parrott, J.R. (1981). Microbial cells as biosorbents for heavy metals: accumulation of uranium by *Saccharomyces cerevisiae* and *Pseudomonas aeruginosa*. *Applied and Environmental Microbiology*, 41,(1), 237-245.
- Suresh, B. and Ravishankar, G.A. (2004) Phytoremediation-A novel and promising approach for environmental clean-up. *Critical Reviews in Biotechnology*, 24(2-3), 97-124
- Swaddiwudhipong, W., Limpatanachote, P., Mahasakpan, P., Krintratun, S. and Padungtod, C. (2007). Cadmium-exposed population in Mae Sot District, Tak Province: 1. Prevalence of high urinary cadmium levels in the adults. *Journal of the Medical Association of Thailand*, 92(10), 1345-1353.
- Swaddiwudhipon, W., Limpatanachote, P., Mahasakpan, P., Krintratun, S., Punta, B. and Funkhiew, T. (2012). Progress in cadmium-related health effects in persons with high environmental exposure in northwestern Thailand: A five-year follow up. *Environmental Research*, 112,194-198.
- Tamura, K., Dudley, J., Nei, M. and Kumar, S. (2007). MEGA4: molecular evolutionary genetics analysis (MEGA) software version 4.0. *Molecular Biology and Evolution*, 24(8), 1596-1599.



- Taniguchi, J., Hemmi, H., Tanahashi, K., Amano, N., Nakayama, T and Nishino, T. (2000). Zinc biosorption by a zincresistant bacterium, *Brevibacterium* sp. strain HZM1. *Application Microbiology Biotechnology*, 54(4), 581-588.
- Tao, G.C., Tian, S.J., Cai, M.Y. and Xie, G.H. (2008). Phosphate solubilizing and - mineralizing abilities of bacteria isolated from. *Pedosphere*, 18, 515–523.
- Thacker, U., Parikh, b.R., Shouche, Y. and Madamwar, D. (2006), Hexavalent chromium reduction by *Providencia* sp. *Process Biochemistry*, 41(6), 1332–1337.
- Tucker, R.K. and Shaw, J.A. (2000). Phytoremediation and public acceptance, In: *Phytoremediation of Toxic Metals: Using Plants to Clean up the Environment*. Raskin, L. and Ensley, R.D. (Ed.), 33-49, New York: John Wiley and Sons.
- Ueshima, M., Ginn, B.R., Haack, E.A., Szymanowski, J.E.S. and Fein, J.B. (2008). Cd adsorption onto *Pseudomonas putida* in the presence and absence of extracellular polymeric substances. *Geochimica et Cosmochimica Acta*, 72(24), 5885–5895.
- Valiente, E.F. and Leganes, L. (1989). Regulatory effect of pH and Incident Irradiance on the levels of Nitrogenase activity in the cyanobacterium *Nostoc* sp. UAM205. *Journal of Plant Physiology*, 135, 623-627.
- Vancanneyta, M., Torck, U., Dewettinck, D., Vaerewijck, M. and Kersters, K. (1996). Grouping of *Pseudomonads* by SDS-PAGE of Whole-cell Proteins. *Systematic and Applied Microbiology*, 19(4), 556-568.
- Vandamme, P., Pot, B., Gillis, M., Vos, P de., Kersters, K. and Swings, J. (1996). Polyphasic taxonomy, a consensus approach to bacterial systematics. *Microbiology Review*, 60(2), 407–438.
- Vidali, M. (2001). Bioremediation: An overview. *Pure and Applied Chemistry*, 73(7), 1163–1172
- Viti, C., Pace, A. and Giovannetti, L. (2003). Characterization of Cr (VI) resistant bacteria isolated from chromium contaminated soil by tannery activity. *Current Microbiology*, 46(1), 1–5.
- Weisburg, W.G., Barns, S.M., Pelletier, D.A. and Lane, D.J. (1991). 16s ribosomal DNA Amplify- cation for phylogenetic study. *Journal of Bacteriology*, 173(2), 697-703.



- Wendenbaum, S., Demange, P., Dell, A., Meyer, J.M. and Abdallah, M.A. (1983). The structure of pyoverdine *Pa*, the siderophore of *Pseudomonas aeruginosa*. *Tetrahedron Letters*, 24(44), 4877–4880.
- Willey, J.M., Sherwood, L.M. and Woolverton, C.J. (2008). *Prescott, Harley and Klevin's Microbiology 8th Edition*. New York: McGraw-Hill.
- Williams, S.T. and Goodfellow, M. (1966). Use of Peptone Iron Agar for the Detection of Hydrogen Sulfide. *Journal of Bacteriology*, 91(2), 907-A.
- Winslow, C.-E. A. and Haywood, E.T. (1931). The specific potency of certain cations with reference to their effect on bacterial viability. *Journal of Bacteriology*, 22(1), 49-69.
- Wood, J., Scott, K.P., Avgustin, G., Newbold, C.J. and Flint, H.J. (1998). Estimation of the relative abundance of different *Bacteroides* and *Prevotella ribotypes* in gut samples by restriction enzyme profiling of PCR-amplified 16S rRNA gene sequences. *Applied and Environmental Microbiology*, 64(10), 3683–3689.
- Wuana, R.A. and Okieimen, F.E. (2011). Heavy Metals in Contaminated Soils: A Review of Sources, Chemistry, Risks and Best Available Strategies for Remediation. *International Scholarly Research Network ISRN Ecology*, [Online]. Available from: <http://dx.doi.org/10.5402/2011/402647> [accessed 9 July 2013].
- Yan, Y., Ping, S., Peng, J., Han, Y., Li, L., Yang, J., Dou, Y., Li, Y., Fan, H., Fan, Y., Li, D., Zhan, Y., Chen, M., Lu, W., Zhang, W., Cheng, Q., Jin, Q., and Lin, M. (2010). Global transcriptional analysis of nitrogen fixation and ammonium repression in root-associated *Pseudomonas stutzeri* A1501. *BMC Genomics*, 11(11), 1-13.
- Yasmin, F., Othman, R., Sijam, K. and Saad, M.S. (2009). Characterization of beneficial properties of plant growth-promoting rhizobacteria isolated from sweet potato rhizosphere. *African Journal of Microbiology Research*, 3(11), 815-821.
- Yoch, D.C. and Gotfo, J.W. (1982). Effect of Light Intensity and Inhibitors of Nitrogen Assimilation on NH_4^+ Inhibition of Nitrogenase Activity in *Rhodospirillum rubrum* and *Anabaena* sp. *Journal of Bacteriology*, 151(2), 800-806.



- Youard, Z.A., Mislin, G.L., Majcherczyk, P.A., Schalk, I.J. and Reimann, C. (2007). *Pseudomonas fluorescens* CHA0 produces enantio-pyochelin, the optical antipode of the *Pseudomonas aeruginosa* siderophore pyochelin. *The Journal of Biological Chemistry*, 282(49), 35546–35553.
- Yu, C. and Irudayaraj, J. (2005). Spectroscopic Characterization of Microorganisms by Fourier Transform Infrared Microspectroscopy. *Biopolymers*, 77(6), 368-377.
- Yue, W.W., Grizot, S. and Buchanan, S.K. (2003). Structural evidence for iron-free citrate and ferric citrate binding to the TonB-dependent outer membrane transporter FecA. *Journal of Molecular Biology*, 332(2), 353–368.
- Zaidi, A., Khan, M.S., Ahemad, M., and Oves, M. (2009). Plant growth promotion by phosphate solubilizing bacteria. *Acta Microbiologica et Immunologica Hungarica*, 56(3), 263–284.
- Zamfira, M., Vancanneyt, M., Makras, L., Vaningelgem, F., Lefebvre, K., Pot, B., Swings, J. and De Vuyst, L. (2006). Biodiversity of lactic acid bacteria in Romanian dairy products. *Systematic and Applied Microbiology*, 29(6), 487–495.



APPENDICES



Appendix A

Bacterial media



A-1 Nutrient Agar (NA)-Metal Free (per liter)

Beef extract	3.00	grams
Peptone	5.00	grams
Agar	18.00	grams
pH 7.0		

A-2 Nutrient Agar (NA) contained Zn

Beef extract	3.00	grams
Peptone	5.00	grams
Agar	18.00	grams
ZnSO ₄ .7H ₂ O (1,000 ppm) 5, 10, 15 and 20 mg/l		
pH 7.0		

A-3 Nutrient Agar (NA) contained Cd

Beef extract	3.00	grams
Peptone	5.00	grams
Agar	18.00	grams
3CdSO ₄ .8H ₂ O (1,000 ppm) 5, 10, 15 and 20 mg/l		
pH 7.0		

A-4 Nutrient Agar (NA) contained Zn+Cd

Beef extract	3.00	grams
Peptone	5.00	grams
Agar	18.00	grams
ZnSo ₄ .7H ₂ O (1,000 ppm) 5, 10, 15 and 20 mg/l		
3CdSo ₄ .8H ₂ O (1,000 ppm) 5, 10, 15 and 20 mg/l		
pH 7.0		

A-5 Nutrient Broth (NB)-Metal Free (per liter)

Beef extract	3.00	grams
Peptone	5.00	grams
pH7.0		



A-6 Nutrient Broth (NB) contained Zn

Beef extract	3.00	grams
Peptone	5.00	grams
ZnSO ₄ .7H ₂ O (1,000 ppm)	5, 10, 15 and 20	mg/l
pH 7.0		

A-7 Nutrient Broth (NB) contained Cd

Beef extract	3.00	grams
Peptone	5.00	grams
3CdSO ₄ .8H ₂ O (1,000 ppm)	5, 10, 15 and 20	mg/l
pH 7.0		

A-8 Nutrient Broth (NB) contained Zn+Cd

Beef extract	3.00	grams
Peptone	5.00	grams
ZnSO ₄ .7H ₂ O (1,000 ppm)	5, 10, 15 and 20	mg/l
3CdSO ₄ .8H ₂ O (1,000 ppm)	5, 10, 15 and 20	mg/l
pH 7.0		

A-9 LB media (Luria-Bertani media)

Bacto-Tryptone	10.00	grams
Bacto-yeast extract	5.00	grams
NaCl	10.00	grams
pH 7.0		

A-10 Trypticase soy broth (per liter)

Casein	17.00	grams
Sodium Chloride	5.00	grams
Dipotassium Phosphate	2.50	grams
Glucose (Dextrose)	2.50	grams
pH 7.0		



A-11 Nitrogen-Free medium (per liter)

Malic acid	5.00	grams
K ₂ HPO ₄	0.50	grams
MgSO ₄ .7H ₂ O	0.20	grams
NaCl	0.10	grams
CaCl ₂ .2H ₂ O	0.02	grams
NaMO ₄ .2H ₂ O	0.002	grams
FeCl ₃ .6H ₂ O	0.01	grams
Bromothymol Blue	0.025	grams
Yeast nitrogen base w/o amino acid	0.25	grams
Agar	12.00	grams
pH	7.0	

A-12 National Botanical research Institute's phosphate growth medium (NBRIP) (per liter)

Glucose	10.00	grams
Ca ₃ (PO ₄) ₂	5.00	grams
MgCl ₂ .6HO	5.00	grams
MgSO ₄ .7H ₂ O	0.25	grams
KCl	0.20	grams
(NH ₄) ₂ SO ₄	0.10	grams
Agar	20.00	grams
pH	7.0	

A-12 Salkowski's reagent

0.5 M FeCl ₃	2.00	milliliters
35% HClO ₄	98.00	milliliters

Add 0.5 M FeCl₃ and 35% HClO₄ mixed in ratio 1:49 when mixed, use immediately.

A-13 Nessler's reagent

Dissolved HgI₂ 25 g and KI 17.5 g in 15 ml distilled water and added to the previous post in this slowly into the cold solution of NaOH 40 g in 125 ml distilled water to 250 ml. Diluted to 250 mL in a brown bottle.



Appendix B

Morphological and biochemical characteristics



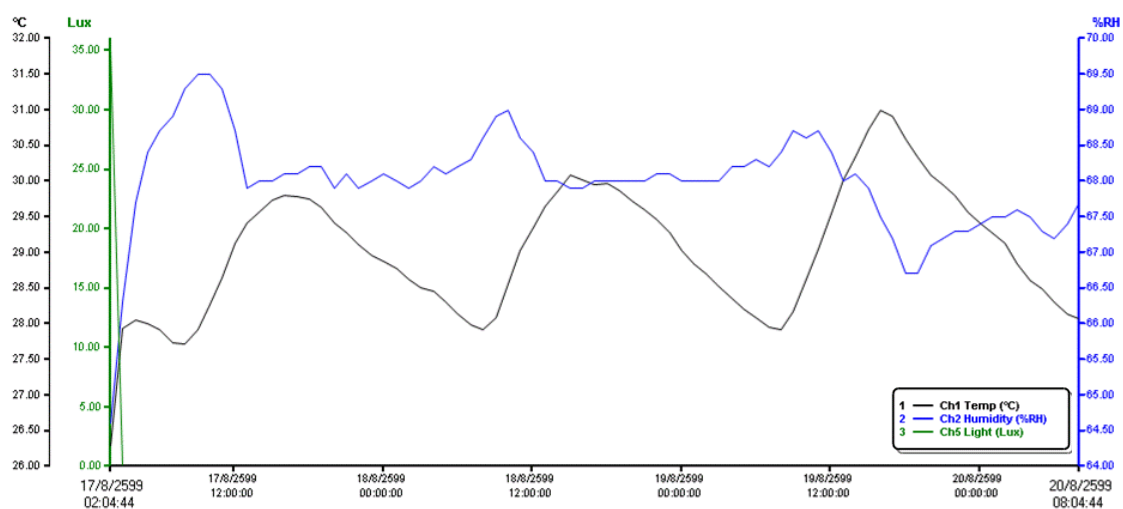


Figure B-1 Profiles of temperature, humidity and light intensity during bacterial cultivation

Table B-1 Average temperature, humidity and light intensity of the bacterial cultured Condition

Statistics	Temperature (°C)	Humidity (%RH)	Light (Lux)
Minimum	26.28	64.6	0
Maximum	30.99	69.5	0
Average	29.019	67.992	0.443
Standard derivation	0.885	0.701	3.913



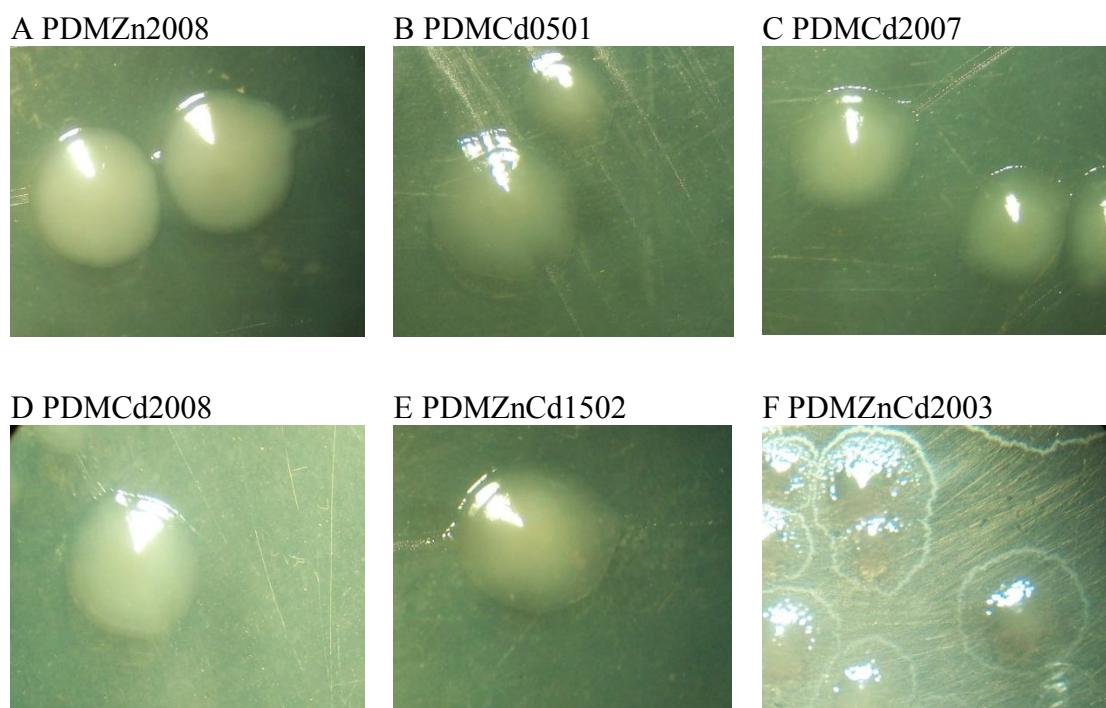
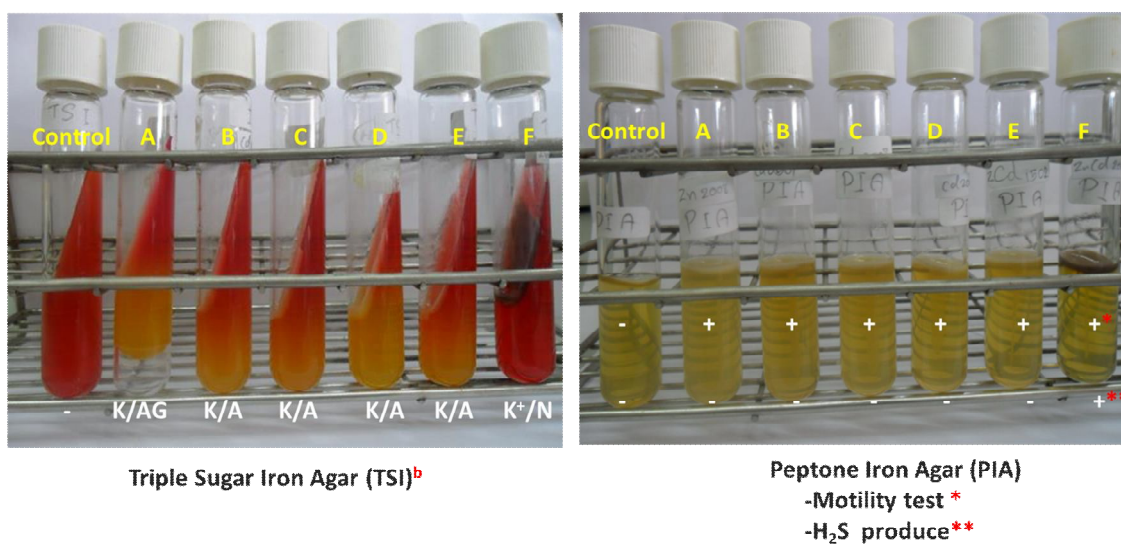


Figure B-2 Colony morphology characteristics of the six bacterial isolates growing on nutrient agar (NA) plates for 48 hours



Note

A = Zn2008 , B = Cd0501 C = Cd2007, D = Cd02008,E = ZnCd1502, F = ZnCd2003

K/A=Alkaline slant / acid butt; K/AG=Alkaline slant / acid butt with gas, no H₂S, K/AG=Alkaline slant / acid butt with gas, with H₂S ; (+) Indicates Positive; (-) indicates Negative

Figure B-3 Biochemical characteristics of the six bacterial isolates on triple sugar iron (TSI) agar and peptone iron agar (PIA), cultivated for 48 hours.



Appendix C

Biochemical identification





๖๖.

คำขอบริการที่ 2552/059

ที่ ผวช.

รายงานผลการทดสอบและวิเคราะห์

ให้แก่

ภาควิชาชีววิทยา คณะวิทยาศาสตร์ มหาวิทยาลัยมหาสารคามการทดสอบ / วิเคราะห์ จัดจำแนกสายพันธุ์แบคทีเรียวิธีทดสอบ / วิเคราะห์ ระบบจัดจำแนกชนิดจุลินทรีย์ เอ พี ไอ (API)ภาวะการทดสอบ / วิเคราะห์ : อุณหภูมิ 30 และ 37 °Cวันที่ทดสอบ / วิเคราะห์ 23 ธันวาคม 2551

ผลการทดสอบ / วิเคราะห์

ผลการจัดจำแนกสายพันธุ์แบคทีเรีย จำนวน 3 สายพันธุ์ ดังนี้

NA-Cd 5 (1) : *Serratia marcescens*NA-Cd 20 (7) : *Serratia marcescens*NA-Zn+Cd 20 (3): *Pseudomonas aeruginosa*

(รายละเอียดดังตาราง)

ผู้ทดสอบ / วิเคราะห์

น.ส.พิริวารรณ ศรีศิลป์

ผู้ตรวจสอบ

(น.ส.สุกมล ปาลกะวงค์ ณ อุชฺชา)

ผู้รับรอง

(นายสุภรพ อัจฉริยะศรีพงษ์)

ผู้อำนวยการฝ่ายวิทยาศาสตร์ชีวภาพ

วันที่ ๕ มกราคม ๒๕๕๒

ผลการทดสอบ หรือ วิเคราะห์นี้ รับรองเฉพาะตัวอย่าง หรือ รายการที่ได้รับไปเท่านั้น การแก้ไขรายงานนี้ถือเป็นความผิดทางกฎหมาย
 การนำรายงานนี้ไปโฆษณา คัดถ่ายหรือการนำผลงานส่วน ไปเผยแพร่ต่อสาธารณะต้องได้รับอนุญาตเป็นลายลักษณ์อักษรจากผู้ว่าการ วว.

แก้ไขครั้งที่ : 0

แบบฟอร์มประกาศใช้วันที่ 16 ตุลาคม 2551

FM-BSD-WI-10-02 (ไทย)

สถาบันวิจัยวิทยาศาสตร์และเทคโนโลยีแห่งประเทศไทย

๓๕ หมู่ ๓ เทคโนโลยีธานี ต.คลองห้า อ.คลองหลวง จ.ปทุมธานี ๑๒๑๒๐
 โทร. (๐๒) ๐ ๒๕๘๗๗ ๕๐๐๐ โทรสาร ๐ ๒๕๘๗๗ ๕๐๐๗
 E-mail : tistr@tistr.or.th Website : www.tistr.or.th



คำขอบริการที่ 2552 / 059



วว.

รายละเอียดการตรวจวิเคราะห์

Table 1. Characteristics of the bacterial strain NA-Cd 5 (1): *Serratia marcescens*

Characteristics	Reaction
Gram reaction	-ve
β -galactosidase production (ortho-nitro-phenyl- β -D-galactopyranoside)	-
Arginine dihydrolase production	-
Lysine decarboxylase production	+
Ornithine decarboxylase production	-
Citrate utilization	+
H ₂ S production	-
Urease production	-
Tryptophane deaminase production	-
Indole production of tryptophane	-
Acetoin production	+
Hydrolysis of gelatin	+
Fermentation or oxidation of:	
- Glucose	+
- Mannitol	+
- Inositol	+
- Sorbitol	+
- Rhamnose	-
- Sucrose	+
- Melibiose	+
- amygdalin	+
- Arabinose	-
Cytochrome oxidase	-

Remark : - ve = Gram negative bacteria

+ = Positive reaction

- = Negative reaction

ผลการทดสอบ หรือ วิเคราะห์นี้ รับรองผลเฉพาะตัวอย่าง หรือ รายการที่ได้รับระบุไว้เท่านั้น การแก้ไขรายงานนี้ถือเป็นการคิดทางกฎหมาย
การนำรายงานนี้ไปโฆษณา คัดลอกหรือการนำผลบางส่วน ไปเผยแพร่ต่อสาธารณะต้องได้รับอนุญาตเป็นลายลักษณ์อักษรจากผู้ว่ากร วว.

สถาบันวิจัยวิทยาศาสตร์และเทคโนโลยีแห่งประเทศไทย

๓๕ หมู่ ๓ เทคโนธานี ต.คลองห้า อ.คลองหลวง จ.ปทุมธานี ๑๒๑๒๐
โทร. (๖๖) ๐ ๒๕๗๗ ๙๐๐๐ โทรสาร ๐ ๒๕๗๗ ๙๐๐๙
E-mail : tistr@tistr.or.th Website : www.tistr.or.th

หน้า 2 ข



คำขอบริการที่ 2552 / 059



วว.

รายละเอียดการตรวจวิเคราะห์

Table 2. Characteristics of the bacterial strain NA-Cd 20 (7): *Serratia marcescens*

Characteristics	Reaction
Gram reaction	-ve
β -galactosidase production (ortho-nitro-phenyl- β -D-galactopyranoside)	-
Arginine dihydrolase production	-
Lysine decarboxylase production	+
Ornithine decarboxylase production	-
Citrate utilization	+
H ₂ S production	-
Urease production	-
Tryptophane deaminase production	-
Indole production of tryptophane	-
Acetoin production	+
Hydrolysis of gelatin	+
Fermentation or oxidation of:	
- Glucose	+
- Mannitol	+
- Inositol	+
- Sorbitol	+
- Rhamnose	-
- Sucrose	+
- Melibiose	+
- amygdalin	+
- Arabinose	-
Cytochrome oxidase	-

Remark : - ve = Gram negative bacteria
+ = Positive reaction
- = Negative reaction

ผลการทดสอบ หรือ วิเคราะห์นี้ รับรองเฉพาะตัวอย่าง หรือ รายการที่ได้ระบุไว้เท่านั้น การแก้ไขรายงานนี้ถือเป็นความผิดทางกฎหมาย
การนำรายงานนี้ไปโฆษณา คัดลอกหรือการนำผลบางส่วน ไปเผยแพร่ต่อสาธารณะต้องได้รับอนุญาตเป็นลายลักษณ์อักษรจากผู้ว่าการ วว.

สถาบันวิจัยวิทยาศาสตร์และเทคโนโลยีแห่งประเทศไทย

๓๕ หมู่ ๓, เทคโนโลยีธานี ต.คลองห้า อ.คลองหลวง จ.ปทุมธานี ๑๒๑๒๐
โทร. (๒๖) ๐ ๒๕๗๗ ๙๐๐๐ โทรสาร ๐ ๒๕๗๗ ๙๐๐๙
E-mail : tistr@tistr.or.th Website : www.tistr.or.th

หน้า 3 ของ 4



คำขอบริการที่ 2552/059



วว.

รายละเอียดการตรวจวิเคราะห์

Table 3. Characteristics of the bacterial strain NA-Zn+Cd 20 (3): *Pseudomonas aeruginosa*

Characteristics	Reaction
Gram reaction	-ve
Reduction of nitrate	+
Indole production of tryptophane	-
Fermentative of acid from glucose	-
Arginine dihydrolase	+
Urease production	-
Hydrolysis of esculin	-
Hydrolysis of gelatin	+
β -galactosidase production (p-nitro phenyl- β -galactopyranoside)	-
Assimilation of:	
- Glucose	+
- Arabinose	-
- Mannose	-
- Mannital	+
- N-acetyl-glucosamine	+
- Maltose	-
- Gluconate	+
- Caprate	+
- Adipate	+
- Malate	+
- Citrate	+
- Phenyl-acetate	-
Cytochrome oxidase	+

Remark : - ve = Gram negative bacteria
 + = Positive reaction
 - = Negative reaction

ผลการทดสอบ หรือ วิเคราะห์นี้ รับรองเฉพาะตัวอย่าง หรือ รายการที่ได้ระบุไว้เท่านั้น การแก้ไขรายงานนี้ถือเป็นการผิดทางกฎหมาย
 การนำรายงานนี้ไปโฆษณา คัดลอกหรือการนำผลบางส่วน ไปเผยแพร่ต่อสาธารณะต้องได้รับอนุญาตเป็นลายลักษณ์อักษรจากผู้ว่าการ วว.

สถาบันวิจัยวิทยาศาสตร์และเทคโนโลยีแห่งประเทศไทย
 ๓๕ หมู่ ๓๓ เขตอินทนนท์ ต.คลองห้า อ.คลองหลวง จ.ปทุมธานี ๑๒๑๒๐
 โทร. (๖๖) ๐ ๒๕๕๗๗ ๙๐๐๐ โทรสาร ๐ ๒๕๕๗๗ ๙๐๐๙
 E-mail : tistr@tistr.or.th Website : www.tistr.or.th

หน้า 4 ของ 4





คำขอบริการที่ 2551/185

ที่ ผวช.

รายงานผลการทดสอบและวิเคราะห์

ให้แก่

ภาควิชาชีววิทยา คณะวิทยาศาสตร์ มหาวิทยาลัยมหาสารคาม

การทดสอบ / วิเคราะห์ จัดจำแนกสายพันธุ์แบคทีเรีย

วิธีทดสอบ / วิเคราะห์ ระบบจัดจำแนกชนิดจุลินทรีย์ เอ พี ไอ (API)

ภาวะการทดสอบ / วิเคราะห์ : อุณหภูมิ 37 °C

วันที่ทดสอบ / วิเคราะห์ 9 กันยายน 2551

ผลการทดสอบ / วิเคราะห์

ผลการจัดจำแนกสายพันธุ์แบคทีเรีย จำนวน 1 สายพันธุ์ ดังนี้

Cd-20 (3): *Pseudomonas aeruginosa*

(รายละเอียดดังตาราง)

ผู้ทดสอบ / วิเคราะห์

น.ส.พิราวรรณ ศรีศิลป์

ผู้ตรวจสอบ

(น.ส.สุตภา ปาลกะวงศ์ ณ อยุธยา)

ผู้รับรอง

(นายสุภาเพ็ อัจฉริยศรีพงศ์)

ผู้อำนวยการฝ่ายวิทยาศาสตร์ชีวภาพ

วันที่ 16 กันยายน 2551

ผลการทดสอบ / วิเคราะห์นี้ รับรองผลเฉพาะตัวอย่างที่ได้ทำการทดสอบ / วิเคราะห์เท่านั้น

ห้ามนำผลการทดสอบ / วิเคราะห์ไปโฆษณาโดยมิได้รับอนุญาตเป็นลายลักษณ์อักษรจาก วว.

สถาบันวิจัยวิทยาศาสตร์และเทคโนโลยีแห่งประเทศไทย

๓๕ หมู่ ๓ เทคโนโลยีธานี ต.คลองห้า อ.คลองหลวง จ.ปทุมธานี ๑๒๑๒๐

โทร. (๖๖) ๐ ๒๕๗๗ ๙๐๐ โทรสาร ๐ ๒๕๗๗ ๙๐๐๙

E-mail: tistr@tistr.or.th Website: www.tistr.or.th





รายละเอียดการตรวจวิเคราะห์

Table 1. Characteristics of the bacterial strain Cd-20 (3): *Pseudomonas aeruginosa*

Characteristics	Reaction
Gram reaction	-ve
Reduction of nitrate	+
Indole production of tryptophane	-
Fermentative of acid from glucose	-
Arginine dihydrolase	+
Urease production	-
Hydrolysis of esculin	-
Hydrolysis of gelatin	+
β -galactosidase production (p-nitro phenyl- β -galactopyranoside)	-
Assimilation of:	
- Glucose	+
- Arabinose	-
- Mannose	-
- Manni	+
- N-acetyl-glucosamine	+
- Maltose	-
- Gluconate	+
- Caprate	+
- Adipate	+
- Malate	+
- Citrate	+
- Phenyl-acetate	-
Cytochrome oxidase	+

Remark : - ve = Gram negative bacteria
 + = Positive reaction
 - = Negative reaction

ผลการทดสอบ / วิเคราะห์นี้ รับรองผลเฉพาะตัวอย่างที่ได้ทำการสอบ / วิเคราะห์เท่านั้น
 ห้ามนำผลการทดสอบ / วิเคราะห์ไปโฆษณาโดยมิได้รับอนุญาตเป็นลายลักษณ์อักษรจาก วว.

สถาบันวิจัยวิทยาศาสตร์และเทคโนโลยีแห่งประเทศไทย

๓๕ หมู่ ๓๓ เขตในธานี ต.คลองห้า อ.คลองหลวง จ.ปทุมธานี ๑๒๑๒๐
 โทร. (๒๖) ๐ ๒๕๗๗ ๙๐๐๐ โทรสาร ๐ ๒๕๗๗ ๙๐๐๗
 E-mail : tistr@tistr.or.th Website : www.tistr.or.th





Request No. I 122/56

At Bioscience Department

REPORT ON TESTING AND ANALYSIS
FOR
Faculty of Science, Maharakham University

Testing / Analysis of Identification of bacteriaMethod of testing / analysis Biochemical test for identification of microorganisms
(API Identification system)Condition of testing / analysis: Temperature 37 °C Relative humidity %Date of testing / analysis September 19, 2013

Result of testing / analysis

Identification result 3 strains of bacteria

Cd 2008*:	<i>Providencia stuartii</i>	99.9% Identification
Zn 2002*:	<i>Serratia marcescens</i>	98.9% Identification
ZnCd 1502*:	<i>Providencia stuartii</i>	99.9% Identification

(Please see attached documents)

Remark: * Fresh culture

Tested / analyzed by
Ms. Pirawan SrisinExamined by (2)
B. Wannissorn
(Ms. Bhusita Wannissorn)Examined by (1)
Lawan Chatanon
(Ms. Lawan Chatanon)Approved by
Chantara Phoosiri
(Ms. Chantara Phoosiri)
Director of Bioscience Department
Date Oct. 11, 2013

The above results are valid exclusively for tests or analyzed samples as mentioned in this report. Changed data in this report is illegal.
 Publish or advertisement of the results on testing or analysis is prohibited unless written permission from the Governor of TISTR.

แก้ไขครั้งที่ : 1

แบบฟอร์มประกาศใช้วันที่ 22 ตุลาคม 2555

FM-BSD-WI-10-02 (อังกฤษ)



Request No. J 122/56



TISTR

Analytical Results

Table 1. Characteristics of the bacterial strain Cd 2008: *Providencia stuartii*
99.9% Identification

Characteristics	Reaction
Gram reaction	-ve
Fermentative production of acid from:	
Glycerol	+
Erythritol	-
D-arabinose	-
L-arabinose	-
D-ribose	+
D-xylose	-
L-xylose	-
D-adonitol	-
Methyl-βD-xylopyranoside	-
D-galactose	+
D-glucose	+
D-fructose	+
D-mannose	+
L-sorbose	-
L-rhamnose	-
Dulcitol	-
Inositol	+
D-mannitol	-
D-sorbitol	-
Methyl-αD-mannopyranoside	-
Methyl-αD-glucopyranoside	-
N-acetylglucosamine	+
Amygdaline	-
Arbutine	-

Remark : -ve = Gram negative bacteria
+ = Positive reaction
- = Negative reaction



TISTR

The above results are valid exclusively for tests or analyzed samples as mentioned in this report. Changed data in this report is illegal.
Publish or advertisement of the results on testing or analysis is prohibited unless written permission from the governor of TISTR.

Thailand Institute of Scientific and Technological Research
35 Moo 3, Technopolis Tambon Khlong 5 Amphoe Khlong Luang Pathum Thani 12120 Thailand
Tel. (66) 0 2577 9000 Fax 0 2577 9009
E-mail : tistr@tistr.or.th Website : www.tistr.or.th

Page 2 o



Request No. | 122/56



Analytical Results

Table 1. (continued) Characteristics of the bacterial strain Cd 2008: *Providencia stuartii*
99.9% Identification

Characteristics	Reaction
Fermentative production of acid from: (continued)	
Esculine ferric citrate	-
Salicine	-
D-cellobiose	-
D-maltose	-
D-lactose (bovine origin)	-
D-melibiose	-
D-saccharose (sucrose)	+
D-trehalose	+
Inuline	-
D-melezitose	-
D-raffinose	-
Amidon (starch)	-
Glycogene	-
Xylitol	+
Gentiobiose	-
D-turanose	-
D-lyxose	+
D-tagatose	-
D-fucose	-
L-fucose	-
D-arabitol	-
L-arabitol	-
Potassium gluconate	+
Potassium 2-ketogluconate	-
Potassium 5-ketogluconate	-

Remark : -ve = Gram negative bacteria
+ = Positive reaction
- = Negative reaction



The above results are valid exclusively for tests or analyzed samples as mentioned in this report. Changed data in this report is illegal.
Publish or advertisement of the results on testing or analysis is prohibited unless written permission from the governor of TISTR.

Page 3 of 8

Thailand Institute of Scientific and Technological Research
35 Moo 3, Technopolis Tambon Khlong 5 Amphoe Khlong Luang Pathum Thani 12120 Thailand
Tel. (66) 0 2577 9000 Fax 0 2577 9009
E-mail : tistr@tistr.or.th Website : www.tistr.or.th



Request No. I 122/56



TISTR

Analytical Results

Table 1. (continued) Characteristics of the bacterial strain Cd 2008: *Providencia stuartii*
99.9% Identification

Characteristics	Reaction
β -galactosidase (ortho-nitro-phenyl- β D-galactopyranoside)	-
Arginine dihydrolase	-
Lysine decarboxylase	-
Ornithine decarboxylase	-
Citrate utilization	+
H ₂ S production	-
Urease	+
Tryptophane deaminase	+
Indole production	-
Acetoin production of sodium pyruvate (voges proskauer)	-
Gelatinase	-

Remark : - ve = Gram negative bacteria
+ = Positive reaction
- = Negative reaction



The above results are valid exclusively for tests or analyzed samples as mentioned in this report. Changed data in this report is illegal.
Publish or advertisement of the results on testing or analysis is prohibited unless written permission from the governor of TISTR.

Thailand Institute of Scientific and Technological Research
35 Moo 3, Technopolis Tambon Khlong 5 Amphoe Khlong Luang Pathum Thani 12120 Thailand
Tel. (66) 0 2577 9000 Fax 0 2577 9009
E-mail : tistr@tistr.or.th Website : www.tistr.or.th

Page 4 of 8



Request No. I 122/56



TISTR

Analytical Results

Table 2. Characteristics of the bacterial strain Zn 2002: *Serratia marcescens*
98.9% Identification

Characteristics	Reaction
Gram reaction	-ve
β -galactosidase (ortho-nitro-phenyl- β D-galactopyranoside)	-
Arginine dihydrolase	-
Lysine decarboxylase	+
Ornithine decarboxylase	-
Citrate utilization	+
H ₂ S production	-
Urease	-
Tryptophane deaminase	-
Indole production	-
Acetoin production of sodium pyruvate (voges proskauer)	+
Gelatinase	+
Fermentation or oxidation of:	
D-glucose	+
D-mannital	+
Inositol	+
D-sorbitol	+
D-rhamnose	-
D-saccharose (sucrose)	+
D-melibiose	-
Amygdalin	+
L-arabinose	-
Cytochrome oxidase	-

Remark : -ve = Gram negative bacteria
+ = Positive reaction
- = Negative reaction



The above results are valid exclusively for tests or analyzed samples as mentioned in this report. Changed data in this report is illegal.
Publish or advertisement of the results on testing or analysis is prohibited unless written permission from the governor of TISTR.

Thailand Institute of Scientific and Technological Research
35 Moo 3, Technopolis Tambon Khlong 5 Amphoe Khlong Luang Pathum Thani 12120 Thailand
Tel. (66) 0 2577 9000 Fax 0 2577 9009
E-mail : tistr@tistr.or.th Website : www.tistr.or.th

Page 5 of 8



Request No. | 122/56



TISTR

Analytical Results

Table 3. Characteristics of the bacterial strain ZnCd 1502: *Providencia stuartii*
99.9% Identification

Characteristics	Reaction
Gram reaction	-ve
Fermentative production of acid from:	
Glycerol	+
Erythritol	-
D-arabinose	-
L-arabinose	-
D-ribose	+
D-xylose	-
L-xylose	-
D-adonitol	-
Methyl-βD-xylopyranoside	-
D-galactose	+
D-glucose	+
D-fructose	+
D-mannose	+
L-sorbose	-
L-rhamnose	-
Dulcitol	-
Inositol	+
D-mannitol	-
D-sorbitol	-
Methyl-αD-mannopyranoside	-
Methyl-αD-glucopyranoside	-
N-acetylglucosamine	+
Amygdaline	-
Arbutine	-

Remark : - ve = Gram negapositive bacteria
+ = Positive reaction
- = Negative reaction



The above results are valid exclusively for tests or analyzed samples as mentioned in this report. Changed data in this report is illegal.
Publish or advertisement of the results on testing or analysis is prohibited unless written permission from the governor of TISTR.

Thailand Institute of Scientific and Technological Research
35 Moo 3, Technopolis Tambon Khlong 5 Amphoe Khlong Luang Pathum Thani 12120 Thailand
Tel. (66) 0 2577 9000 Fax 0 2577 9009
E-mail : tistr@tistr.or.th Website : www.tistr.or.th

Page 6 of 8



Request No. J 122/56



TISTR

Analytical Results

Table 3. (continued) Characteristics of the bacterial strain ZnCd 1502: *Providencia stuartii*
99.9% Identification

Characteristics	Reaction
Fermentative production of acid from: (continued)	
Esculine ferric citrate	-
Salicine	-
D-cellobiose	-
D-maltose	-
D-lactose (bovine origin)	-
D-melibiose	-
D-saccharose (sucrose)	-
D-trehalose	+
Inuline	-
D-melezitose	-
D-raffinose	-
Amidon (starch)	-
Glycogene	-
Xylitol	+
Gentiobiose	-
D-turanose	-
D-lyxose	+
D-tagatose	-
D-fucose	-
L-fucose	-
D-arabitol	-
L-arabitol	-
Potassium gluconate	+
Potassium 2-ketogluconate	-
Potassium 5-ketogluconate	-

Remark : - ve = Gram negative bacteria
+ = Positive reaction
- = Negative reaction



The above results are valid exclusively for tests or analyzed samples as mentioned in this report. Changed data in this report is illegal.
Publish or advertisement of the results on testing or analysis is prohibited unless written permission from the governor of TISTR.

Thailand Institute of Scientific and Technological Research
35 Moo 3, Technopolis Tambon Khlong 5 Amphoe Khlong Luang Pathum Thani 12120 Thailand
Tel. (66) 0 2577 9000 Fax 0 2577 9009
E-mail : tistr@tistr.or.th Website : www.tistr.or.th

Page 7 of 8



Request No. I 122/56



TISTR

Analytical Results

Table 3. (continued) Characteristics of the bacterial strain ZnCd 1502: *Providencia stuartii*
99.9% Identification

Characteristics	Reaction
β -galactosidase (ortho-nitro-phenyl- β D-galactopyranoside)	-
Arginine dihydrolase	-
Lysine decarboxylase	-
Ornithine decarboxylase	-
Citrate utilization	+
H ₂ S production	-
Urease	+
Tryptophane deaminase	+
Indole production	-
Acetoin production of sodium pyruvate (voges proskauer)	-
Gelatinase	-

Remark : - ve = Gram negative bacteria
+ = Positive reaction
- = Negative reaction



The above results are valid exclusively for tests or analyzed samples as mentioned in this report. Changed data in this report is illegal.
Publish or advertisement of the results on testing or analysis is prohibited unless written permission from the governor of TISTR.

Thailand Institute of Scientific and Technological Research
35 Moo 3, Technopolis Tambon Khlong 5 Amphoe Khlong Luang Pathum Thani 12120 Thailand
Tel. (66) 0 2577 9000 Fax 0 2577 9009
E-mail : tistr@tistr.or.th Website : www.tistr.or.th

Page 8 of 8



Appendix D

Growth curve monitoring



Table D-1 System pHs and growth curves of PDMZn2008 in nutrient broth, monitored by the turbidimetric method and protein assay

Time (hour)	Protein (µg/ml)			Mean	SD	Optical density (660 nm)			Mean	SD	pH			Mean	SD
	I	II	III			I	II	III			I	II	III		
0	0.00	0.00	0.00	0.00	0.00	0.025	0.036	0.033	0.016	0.005	7.200	7.200	7.200	7.200	0.000
1	1.25	1.02	1.40	1.22	0.16	0.106	0.091	0.085	0.094	0.009	7.220	7.200	7.180	7.200	0.016
3	15.10	16.06	14.97	15.37	0.49	0.757	0.840	0.806	0.801	0.034	7.250	7.230	7.200	7.227	0.021
5	23.37	23.91	20.59	22.62	1.45	1.101	1.100	1.015	1.072	0.040	7.940	7.880	7.880	7.900	0.028
9	46.03	40.72	43.50	43.42	2.17	1.710	1.920	1.860	1.830	0.088	8.270	8.240	8.180	8.230	0.037
13	31.10	39.70	42.99	37.93	5.02	1.620	1.940	2.150	1.903	0.218	8.720	8.700	8.710	8.710	0.008
17	31.86	30.59	29.32	30.59	1.03	2.070	1.830	2.050	1.983	0.109	8.830	8.830	8.800	8.820	0.014
23	11.48	10.79	12.69	11.65	0.79	1.740	1.870	1.880	1.830	0.064	8.870	8.860	8.850	8.860	0.008
35	21.88	20.82	22.16	21.62	0.58	1.610	1.270	1.510	1.463	0.143	8.900	8.910	8.900	8.903	0.005
47	17.32	17.96	17.12	17.47	0.36	1.490	1.410	2.060	1.653	0.289	8.580	8.900	8.880	8.787	0.146
71	22.54	24.26	21.78	22.86	1.04	1.630	1.450	1.470	1.517	0.081	8.780	8.780	8.790	8.783	0.005

*SD: Standard derivation

Table D-2 System pHs and growth curves of PDMCd0501 in nutrient broth, monitored by the turbidimetric method and protein assay

Time (hour)	Protein ($\mu\text{g/ml}$)			Mean	SD	Optical density (660 nm)			Mean	SD	pH			Mean	SD
	I	II	III			I	II	III			I	II	III		
0	0.00	0.00	0.00	0.00	0.00	0.100	0.108	0.101	0.103	0.004	7.340	7.350	7.340	7.343	0.005
1	0.79	0.88	0.91	0.86	0.05	0.164	0.147	0.183	0.165	0.015	7.330	7.290	7.300	7.343	0.017
3	3.83	3.86	3.74	3.81	0.05	0.460	0.445	0.482	0.462	0.015	7.360	7.370	7.290	7.340	0.036
5	14.78	14.41	15.29	14.83	0.36	0.737	0.739	0.741	0.739	0.002	7.370	7.350	7.330	7.350	0.016
9	20.88	18.76	21.07	20.24	1.05	1.105	1.108	1.110	1.108	0.002	8.110	8.130	8.130	8.123	0.009
13	22.77	20.22	23.98	22.32	1.57	1.320	1.308	1.248	1.292	0.031	8.360	8.410	8.320	8.363	0.037
17	14.02	11.83	15.72	13.85	1.59	1.456	1.498	1.406	1.453	0.038	8.470	8.520	8.500	8.497	0.021
23	16.93	15.84	16.90	16.56	0.51	1.674	1.664	1.630	1.656	0.019	8.600	8.580	8.620	8.600	0.016
35	20.88	20.67	20.55	20.70	0.14	1.866	1.876	1.784	1.842	0.041	8.660	8.700	8.700	8.687	0.019
47	17.94	17.39	19.06	18.13	0.70	1.844	1.870	1.776	1.830	0.040	8.880	8.900	8.870	8.883	0.012
71	14.20	19.33	20.09	17.88	2.62	1.606	1.654	1.768	1.676	0.068	8.990	8.990	8.990	8.990	0.000

*SD: Standard derivation

Table D-3 System pHs and growth curves of PDMCd2007 in nutrient broth, monitored by the turbidimetric method and protein assay

Time (hour)	Protein ($\mu\text{g/ml}$)			Mean	SD	Optical density (660 nm)			Mean	SD	pH			Mean	SD
	I	II	III			I	II	III			I	II	III		
0	0.00	0.00	0.00	0.00	0.00	0.029	0.039	0.038	0.035	0.004	7.300	7.330	7.350	7.327	0.021
1	0.43	0.64	0.35	0.47	0.13	0.056	0.083	0.063	0.067	0.011	7.410	7.400	7.400	7.327	0.005
3	3.38	3.63	3.38	3.46	0.11	0.219	0.225	0.227	0.224	0.003	7.270	7.240	7.220	7.243	0.021
5	7.96	6.77	8.31	7.68	0.66	0.496	0.378	0.412	0.429	0.050	7.290	7.190	7.200	7.227	0.045
9	15.55	14.30	11.38	13.74	1.75	0.882	1.008	0.910	0.933	0.054	7.650	7.660	7.690	7.667	0.017
13	17.61	17.18	17.91	17.56	0.30	1.420	1.380	1.348	1.383	0.029	8.170	8.190	8.160	8.173	0.012
17	19.24	13.92	21.89	18.35	3.31	1.604	1.452	1.512	1.523	0.062	8.360	8.390	8.360	8.370	0.014
23	17.61	17.56	19.34	18.17	0.83	1.547	1.556	1.614	1.572	0.030	8.440	8.410	8.430	8.427	0.012
35	20.78	21.00	21.08	20.95	0.13	1.836	1.998	1.672	1.835	0.133	8.760	8.800	8.830	8.797	0.029
47	20.29	25.96	22.19	22.81	2.35	1.924	1.892	1.682	1.833	0.107	8.860	8.850	8.900	8.870	0.022
71	15.96	14.38	13.17	14.50	1.14	1.820	1.866	1.918	1.868	0.040	9.000	9.000	9.000	9.000	0.000

*SD: Standard derivation

Table D-4 System pHs and growth curves of PDMCd2008 in nutrient broth, monitored by the turbidimetric method and protein assay

Time (hour)	Protein (µg/ml)			Mean	SD	Optical density (660 nm)			Mean	SD	pH			Mean	SD
	I	II	III			I	II	III			I	II	III		
0	0.00	0.00	0.00	0.00	0.00	0.049	0.065	0.037	0.050	0.011	7.350	7.320	7.260	7.310	0.037
1	0.09	0.43	0.56	0.30	0.28	0.086	0.151	0.049	0.095	0.042	7.260	7.290	7.300	7.310	0.017
3	4.38	5.01	4.36	4.58	0.30	0.551	0.470	0.484	0.502	0.035	7.330	7.330	7.310	7.323	0.009
5	6.55	6.85	6.63	6.68	0.13	0.773	0.835	0.768	0.792	0.030	7.370	7.310	7.340	7.340	0.024
9	8.91	14.49	13.11	12.17	2.37	1.018	1.230	1.294	1.181	0.118	7.990	7.990	7.880	7.953	0.052
13	15.90	12.92	14.01	14.28	1.23	1.514	1.492	1.548	1.518	0.023	8.330	8.270	8.340	8.313	0.031
17	14.28	11.13	12.70	12.70	1.28	1.562	1.616	1.568	1.582	0.024	8.450	8.400	8.470	8.440	0.029
23	10.56	11.19	11.05	10.93	0.27	1.638	1.584	1.606	1.609	0.022	8.700	8.610	8.900	8.737	0.121
35	10.64	10.75	10.67	10.69	0.05	1.638	1.634	1.712	1.661	0.036	8.930	8.920	8.980	8.943	0.026
47	13.06	12.19	13.44	12.89	0.52	1.662	1.654	1.610	1.642	0.023	9.090	9.070	9.070	9.077	0.009
71	10.08	8.18	7.88	8.71	0.97	1.574	1.616	1.554	1.581	0.026	9.100	9.090	9.080	9.090	0.008

*SD: Standard derivation

Table D-5 System pHs and growth curves of PDMCd1502 in nutrient broth, monitored by the turbidimetric method and protein assay

Time (hour)	Protein (µg/ml)			Mean	SD	Optical density (660 nm)			Mean	SD	pH			Mean	SD
	I	II	III			I	II	III			I	II	III		
0	0.00	0.00	0.00	0.00	0.00	0.010	0.030	0.021	0.020	0.008	7.520	7.390	7.560	7.490	0.073
1	0.22	0.43	0.10	0.15	0.27	0.056	0.058	0.061	0.058	0.002	7.500	7.530	7.450	7.490	0.033
3	3.36	3.00	2.35	4.36	0.42	0.270	0.304	0.330	0.301	0.025	7.410	7.380	7.320	7.370	0.037
5	8.75	9.59	8.45	13.39	0.48	0.672	0.692	0.552	0.639	0.062	7.360	7.370	7.290	7.340	0.036
9	15.41	14.55	18.23	24.10	1.57	0.988	1.164	0.993	1.048	0.082	7.850	7.900	7.930	7.893	0.033
13	17.85	18.61	18.80	27.63	0.41	1.316	1.350	1.152	1.273	0.086	8.390	8.220	8.370	8.327	0.076
17	19.78	20.18	19.26	29.61	0.38	1.466	1.510	1.480	1.485	0.018	8.430	8.510	8.470	8.470	0.033
23	15.69	22.62	21.97	30.14	3.13	1.644	1.674	1.584	1.634	0.037	8.640	8.780	8.610	8.677	0.074
35	19.18	21.57	19.02	29.88	1.16	1.686	1.690	1.678	1.685	0.005	8.740	8.800	8.760	8.767	0.025
47	15.98	20.10	21.35	28.72	2.29	1.750	1.886	1.778	1.805	0.059	8.740	8.800	8.740	8.760	0.028
71	23.90	16.01	17.15	28.53	3.48	1.740	2.040	1.840	1.873	0.125	9.010	8.980	8.990	8.993	0.012

*SD: Standard derivation

Table D-6 System pHs and growth curves of PDMZnCd2003 in nutrient broth, monitored by the turbidimetric method and protein assay

Time (hour)	Protein ($\mu\text{g/ml}$)			Mean	SD	Optical density (660 nm)			Mean	SD	pH			Mean	SD
	I	II	III			I	II	III			I	II	III		
0	0.00	0.00	0.00	0.00	0.00	0.000	0.000	0.000	0.000	0.000	7.150	7.190	7.170	7.170	0.016
1	0.06	0.11	0.01	0.06	0.04	0.009	0.008	0.011	0.009	0.001	7.600	7.550	7.560	7.170	0.022
3	1.75	1.05	0.94	1.25	0.36	0.078	0.077	0.060	0.072	0.008	7.000	7.500	7.520	7.340	0.241
5	8.01	8.56	7.65	8.08	0.38	0.426	0.500	0.472	0.466	0.031	7.780	7.780	7.660	7.740	0.057
9	21.98	23.75	26.26	24.00	1.76	1.430	1.340	1.140	1.303	0.121	8.120	8.130	8.070	8.107	0.026
13	42.74	52.87	51.35	48.99	4.46	1.830	1.940	1.840	1.870	0.050	8.330	8.480	8.450	8.420	0.065
17	44.77	42.74	44.26	43.92	0.86	1.800	1.620	2.090	1.837	0.194	8.630	8.710	8.680	8.673	0.033
23	31.35	22.74	26.54	26.88	3.52	1.333	1.321	1.311	1.322	0.009	8.780	8.800	8.810	8.797	0.012
35	23.25	24.51	22.99	23.59	0.66	0.820	0.870	0.930	0.873	0.045	8.860	8.820	8.810	8.830	0.022
47	13.98	13.88	14.21	14.02	0.14	0.406	0.501	0.465	0.457	0.039	8.900	8.890	8.900	8.897	0.005
71	20.18	21.53	21.50	21.07	0.63	0.588	0.869	0.863	0.773	0.131	8.900	8.850	8.810	8.853	0.037

*SD: Standard derivation

Appendix E

SDS-PAGE



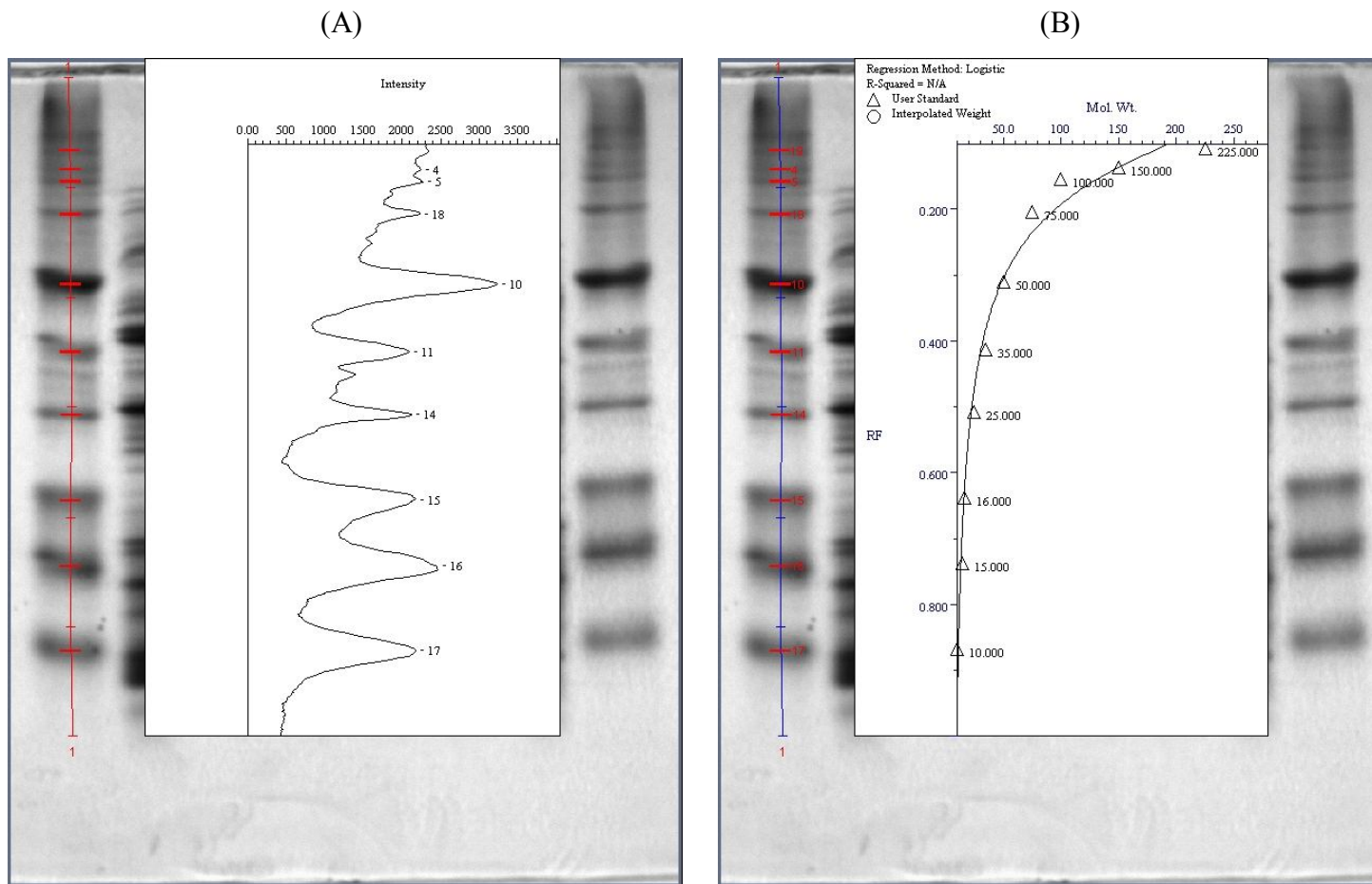
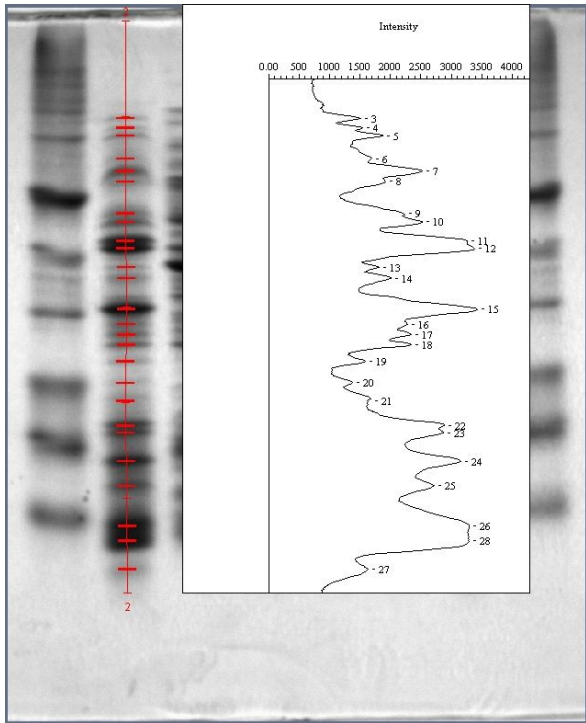
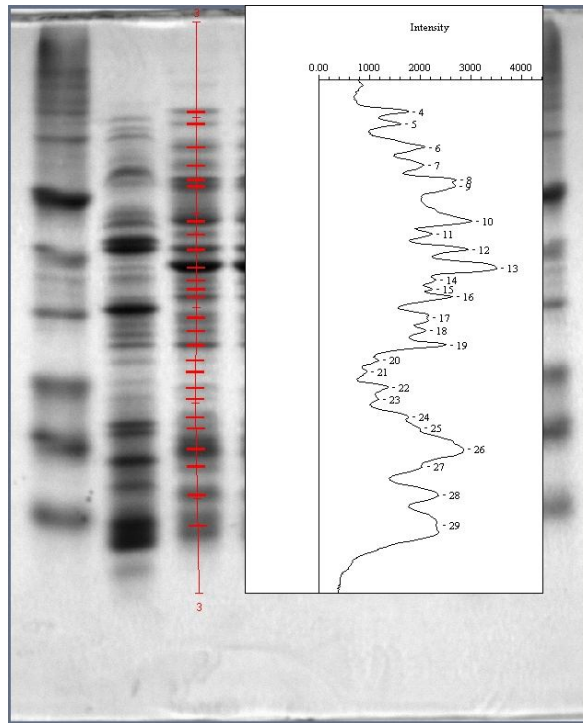


Figure E-1 Intensity (A) and molecular weight (B) of whole-cell protein profile obtained by SDS-PAGE, determined by Quantity One Version 4 (Bio-Rad)

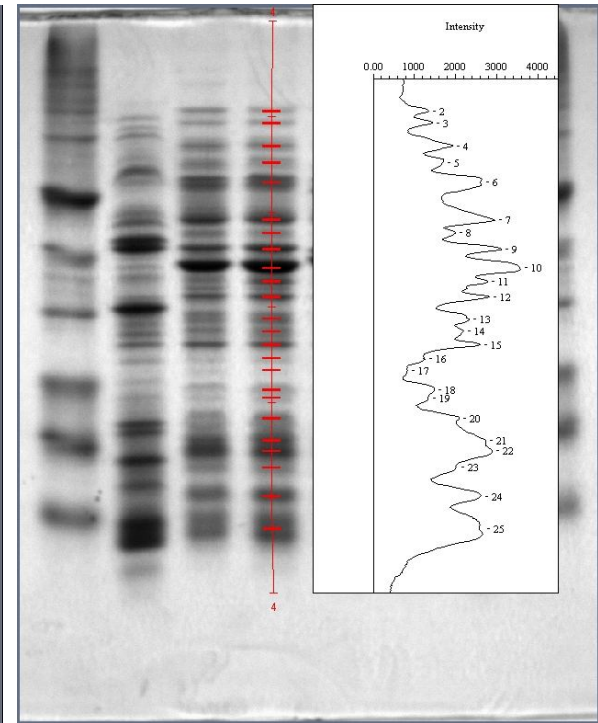
(A)



(B)



(C)



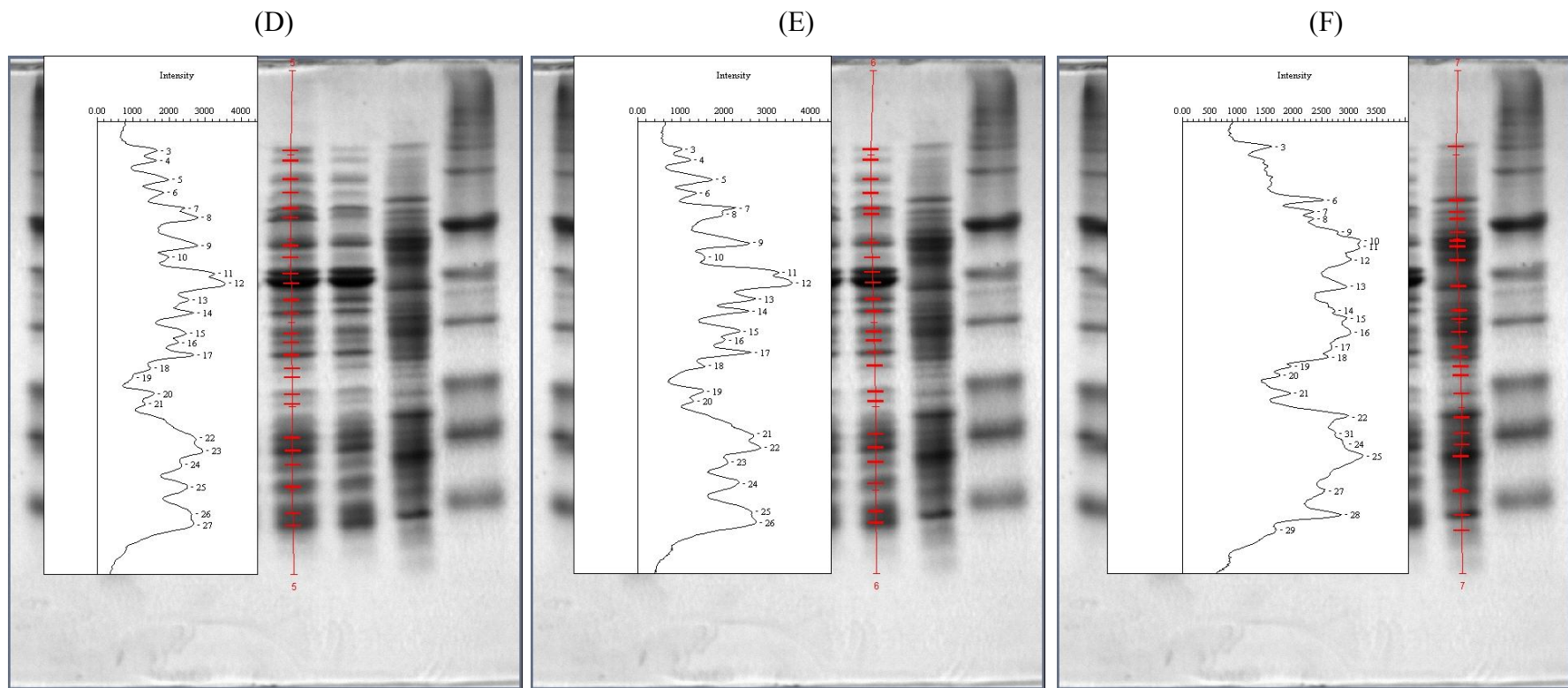
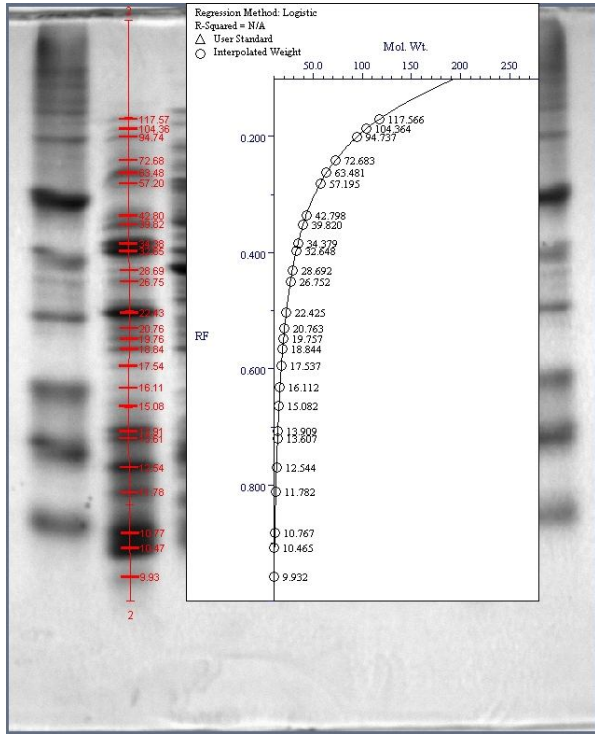
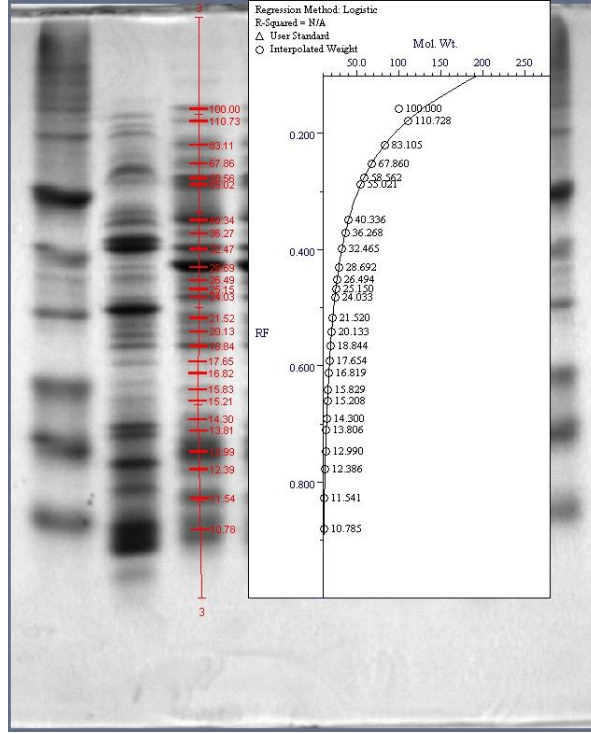


Figure E-2 Intensity of whole-cell protein profiles of (A) PDMZn2008, (B) PDMCd 0501, (C) PDMCd2007, (D) PDMCd2008, (E) PDMZnCd1502 and (F) PDMZnCd2003, obtained by SDS-PAGE and determined by quantity One version 4 (Bio-Rad)

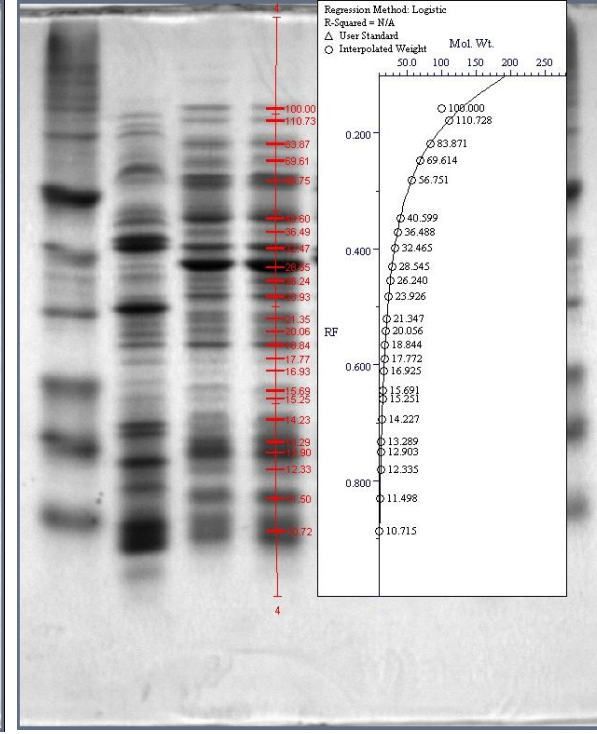
(A)



(B)



(C)



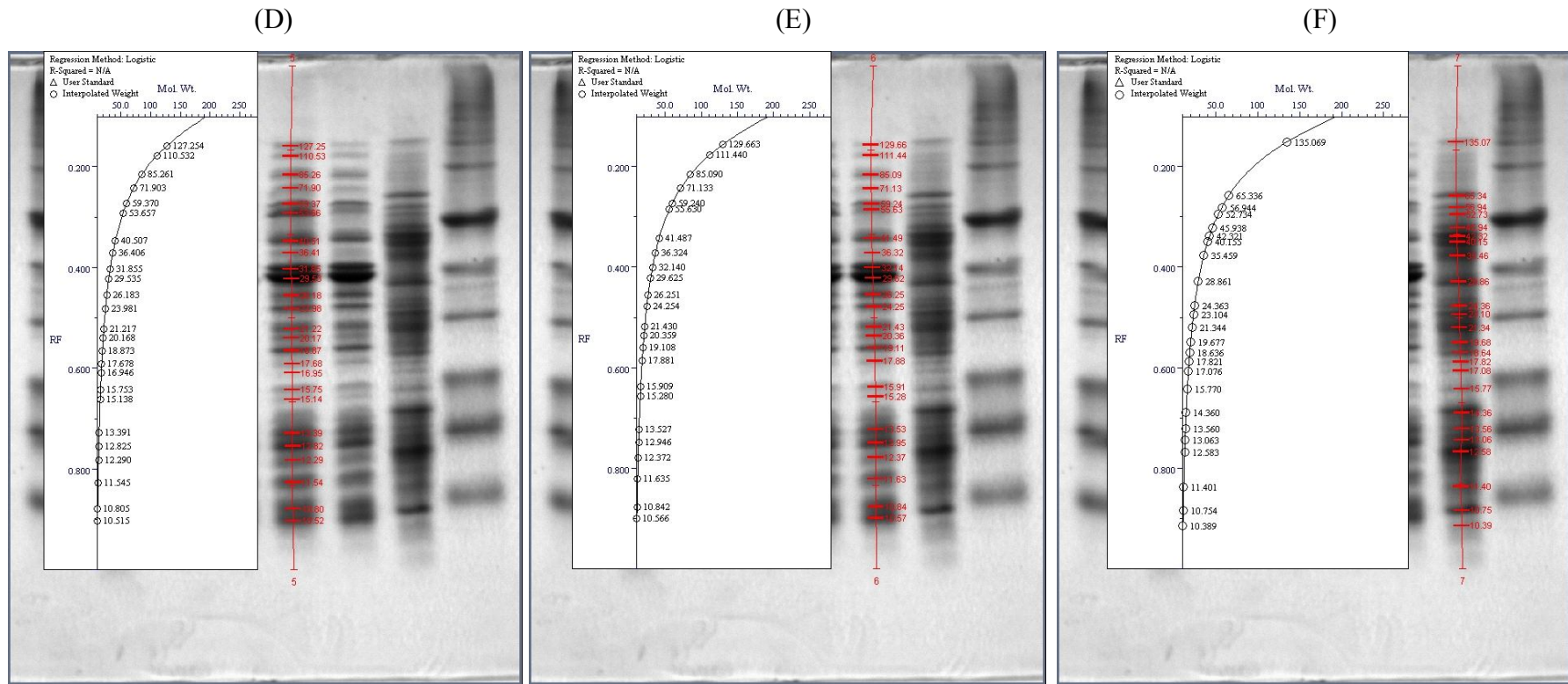


Figure E-3 Molecular weight of whole-cell protein profiles of (A) PDMZn2008, (B) PDMCd 0501, (C) PDMCd2007, (D) PDMCd2008, (E) PDMZnCd1502 and (F) PDMZnCd2003, obtained by SDS-PAGE and determined by quantity One version 4 (Bio-Rad)

Appendix F

Assessment of metal toxicity; MIC



Table F-1 Experimental design for study the minimum inhibitory concentration (MIC) of zinc, cadmium and zinc plus cadmium.

Treatments	Concentrations of zinc and/or cadmium (mg/l)											
	1	2	3	4	5	6	7	8	9	10	11	12
Zinc	400	300	250	200	150	100	70	50	20	15	10	5
Cadmium	400	300	250	200	150	100	70	50	20	15	10	5
Zinc +	100	90	80	70	60	50	40	30	20	10	15	5
Cadmium	+100	+90	+80	+70	+60	+50	+40	+30	+20	+10	+15	+5
Control	+	+	x	-	-							

Table F-2 Experimental design for study the minimum inhibitory concentration (MIC) of 20 mg/l cadmium plus various concentrations of zinc

Treatments	Various concentrations of Zn (mg/l), plus 20 mg/l of Cd											
	1	2	3	4	5	6	7	8	9	10	11	12
Bacteria	2000	1000	500	300	200	170	150	100	80	60	40	20
Bacteria	2000	1000	500	300	200	170	150	100	80	60	40	20
Bacteria	2000	1000	500	300	200	170	150	100	80	60	40	20
Control	+	+	+	x	-	-	-	x				



	1	2	3	4	5	6	7	8	9	10	11	12
Zinc	A											
	B											
Cadmium	C											
	D											
Zinc + Cadmium	E											
	F											
Control ←	G			X				X				
	H											

Negative control
Positive control

Figure F-1 Experimental design for microtiter plate with 96 wells of the minimum inhibitory concentration (MIC) of zinc, cadmium and zinc plus cadmium



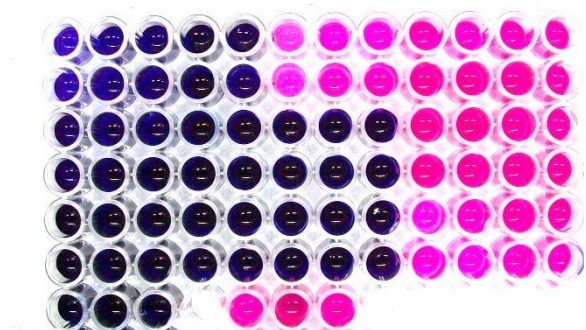
	1	2	3	4	5	6	7	8	9	10	11	12
Bacteria A	A											
	B											
Bacteria B	C											
	D											
Bacteria C	E											
	F											
Control	G			X				X				
	H											
	Negative control			Positive control								

	1	2	3	4	5	6	7	8	9	10	11	12
Bacteria D	A											
	B											
Bacteria E	C											
	D											
Bacteria F	E											
	F											
Control	G			X				X				
	H											
	Negative control			Positive control								

Figure F-2 Experimental design for microtiter plate with 96 wells of the minimum inhibitory concentration (MIC) of the fixed 20 mg/l of cadmium plus various concentrations of zinc



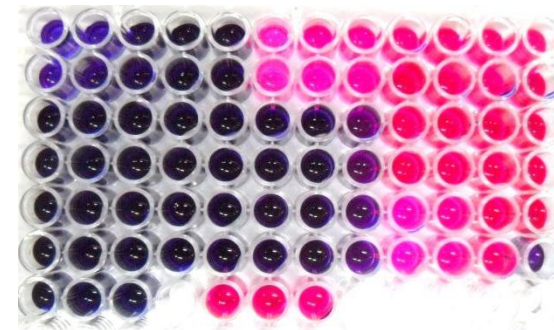
A PDMZn2008



B PDMCd0501



C PDMCd2007



D PDMCd2008



E PDMZnCd1502



F PDMZnCd2003

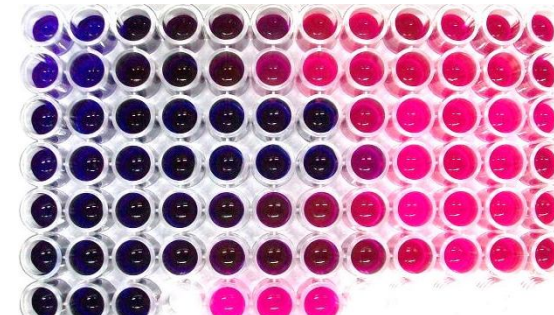


Table F-3 Plates after 24 hours in the modified resazurin assay. Pink colour indicates growth and blue means inhibition of growth; these are taken as the minimum inhibitory concentration (MIC) values for zinc, cadmium, and zinc plus cadmium treatment.

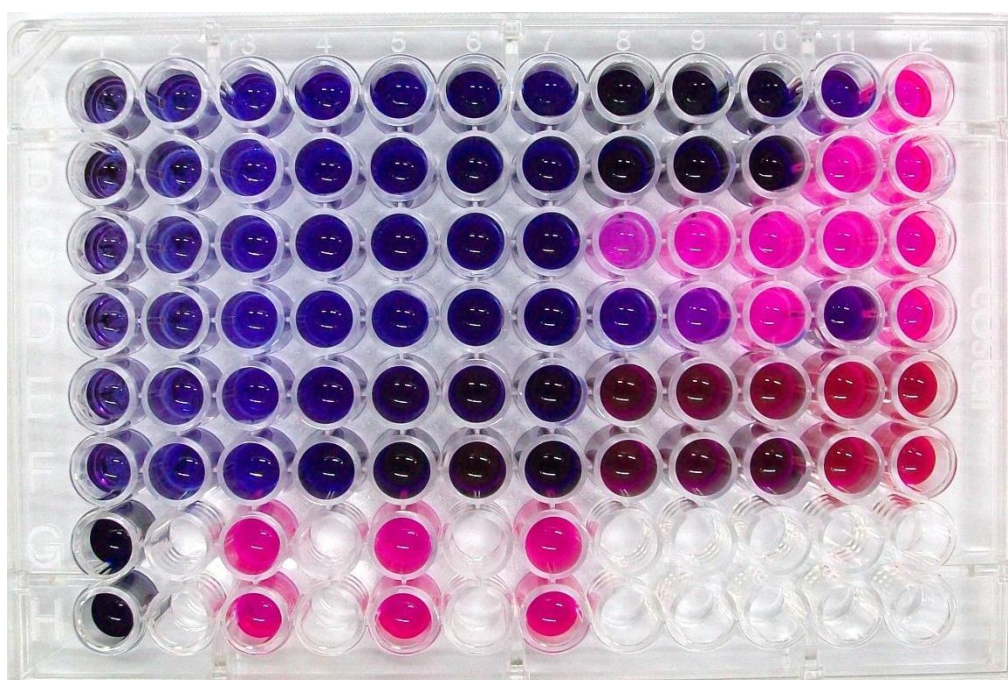
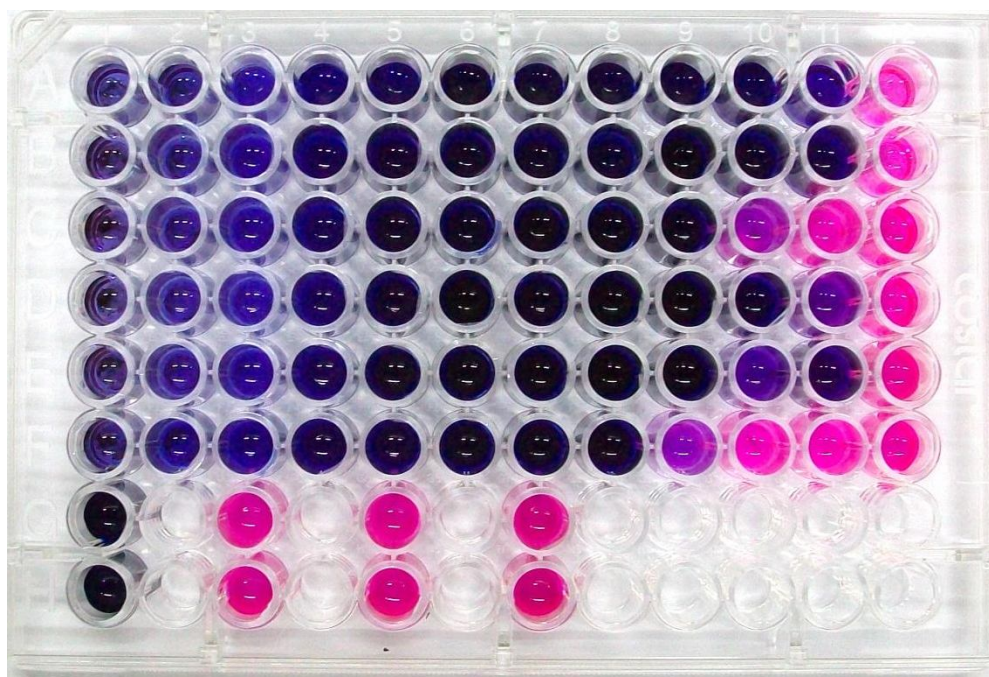


Table F-4 Plates after 24 hours in the modified resazurin assay. Pink colour indicates growth and blue means inhibition of growth; these are taken as the minimum inhibitory concentration (MIC) values for fixed 20 mg/l of cadmium plus various concentrations of zinc treatment



Appendix G

Plant growth promoting properties



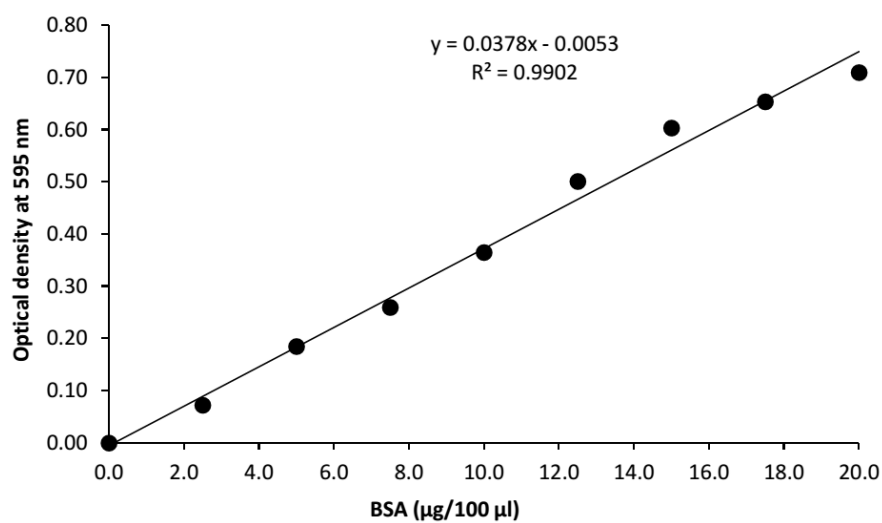


Figure G-1 Standard curve of bovine serum albumin for Bradford protein assay

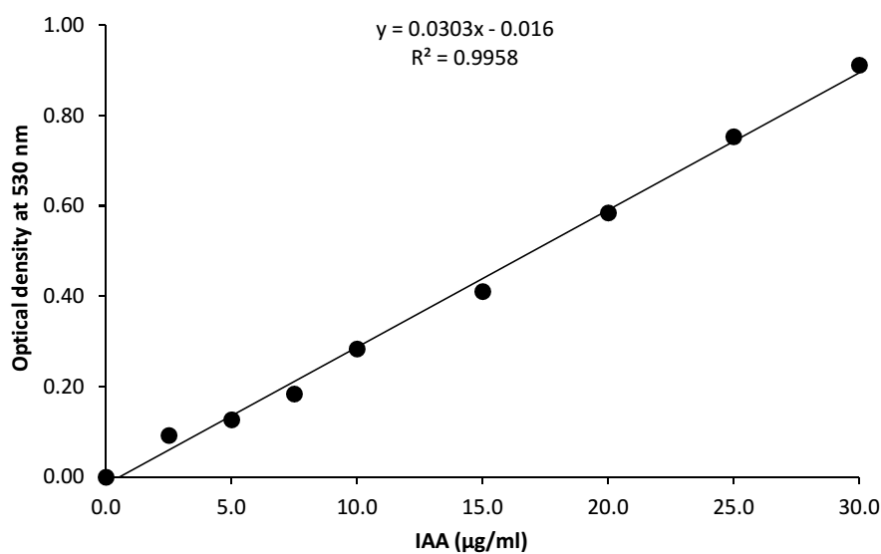


Figure G-2 Standard curve for indole-3-acetic acid (IAA) quantitative analysis



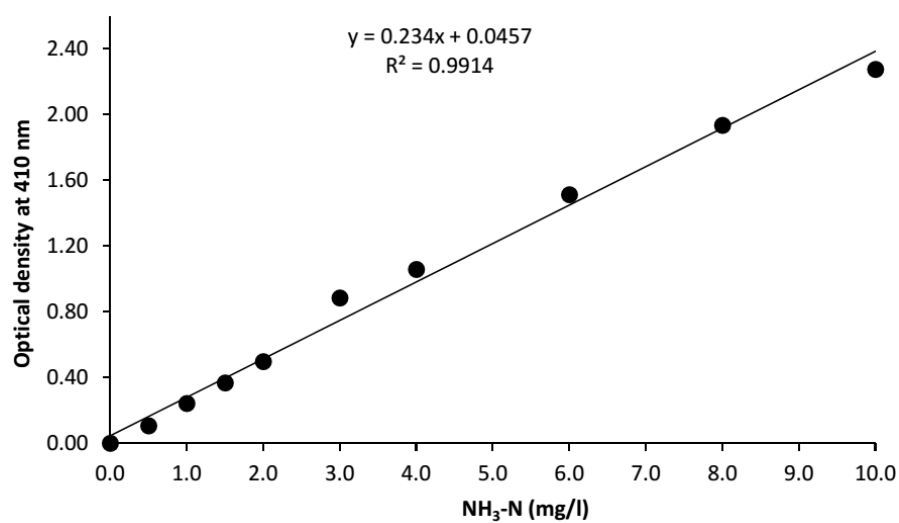


Figure G-3 Standard curve of NH_3^+-N for quantitative analysis of nitrogen fixation

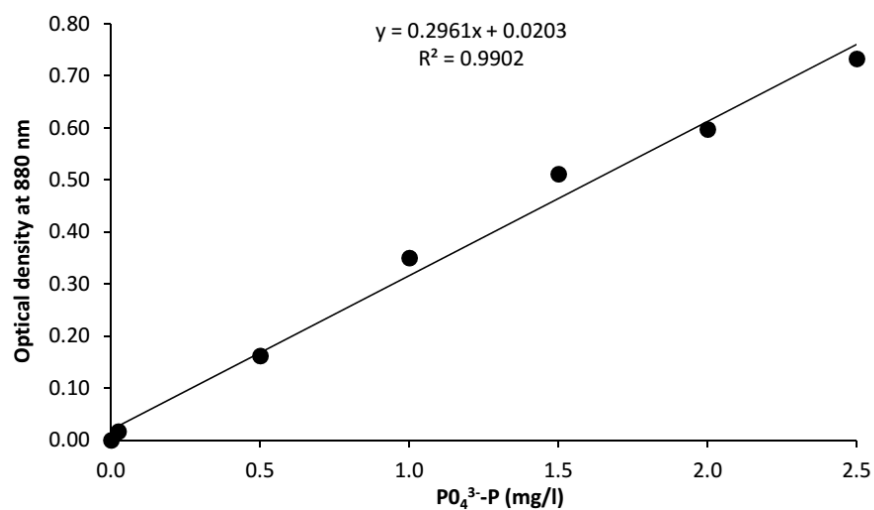


Figure G-4 Standard curve of potassium dihydrogen phosphates for quantitative analysis of soluble phosphate



Plant growth promoting properties of indole-3-acetic acid (IAA) production

Table G-1 Indole-3-acetic acid (IAA) production, system pHs and growth, monitored by the turbidimetric method at 660 nm, of PDMZn2008 in trypticase soy broth (TSB) containing 0.2% w/v tryptophan

Time (hour)	IAA ($\mu\text{g/ml}$)			Mean	SD	Optical density (660 nm)			Mean	SD	pH			Mean	SD
	I	II	III			I	II	III			I	II	III		
0	6.76	6.08	5.07	5.97	0.85	0.040	0.036	0.033	0.036	0.003	7.040	7.020	7.030	7.030	0.008
1	20.47	20.64	20.57	20.56	0.09	0.085	0.079	0.085	0.083	0.003	7.320	7.300	7.280	7.300	0.016
3	64.19	62.26	62.06	62.84	1.17	0.340	0.417	0.385	0.381	0.032	7.350	7.310	7.400	7.353	0.037
5	225.34	218.92	222.94	222.40	3.24	0.859	0.991	0.915	0.922	0.054	7.540	7.480	7.480	7.500	0.028
9	521.28	615.88	581.32	572.83	47.87	2.030	2.020	2.023	2.024	0.004	7.700	7.740	7.680	7.707	0.025
13	873.31	903.72	861.49	879.50	21.79	2.310	2.420	2.404	2.378	0.049	8.120	8.100	8.100	8.107	0.009
17	905.41	1023.65	1001.69	976.91	62.89	3.330	3.700	3.600	3.543	0.156	8.200	8.219	8.220	8.213	0.009
23	831.08	805.74	868.24	835.02	31.44	2.110	2.170	2.130	2.137	0.025	8.370	8.460	8.450	8.427	0.040
35	777.03	849.66	798.99	808.56	37.25	2.500	2.530	2.460	2.497	0.029	8.400	8.510	8.490	8.467	0.048
47	802.36	726.35	802.50	777.07	43.93	2.640	2.580	2.550	2.590	0.037	8.580	8.620	8.588	8.596	0.017
71	802.36	726.35	802.50	777.07	43.93	2.690	2.740	2.550	2.660	0.080	8.630	8.600	8.659	8.630	0.024

*SD: Standard derivation

Table G-2 Indole-3-acetic acid (IAA) production, system pHs and growth, monitored by the turbidimetric method at 660 nm, of PDMZn2008 in trypticase soy broth (TSB) containing 0.2% w/v tryptophan in the presence of Zn plus Cd (20/20 mg/l)

Time (hour)	IAA ($\mu\text{g/ml}$)			Mean	SD	Optical density (660 nm)			Mean	SD	pH			Mean	SD
	I	II	III			I	II	III			I	II	III		
0	6.52	6.35	5.07	5.98	0.79	0.019	0.020	0.013	0.017	0.003	7.040	7.020	7.030	7.090	0.008
1	11.35	13.55	13.82	12.91	1.35	0.039	0.040	0.035	0.038	0.002	7.320	7.300	7.280	7.100	0.016
3	65.98	64.90	62.06	64.31	2.02	0.209	0.199	0.185	0.198	0.010	7.350	7.310	7.400	7.120	0.037
5	191.22	170.95	189.16	183.77	11.16	0.818	0.830	0.815	0.821	0.006	7.540	7.480	7.480	7.030	0.028
9	306.08	248.31	243.48	265.96	34.83	1.640	1.690	1.623	1.651	0.028	7.700	7.740	7.680	7.100	0.025
13	296.96	281.76	287.16	288.63	7.71	2.000	1.950	1.960	1.970	0.022	7.120	7.100	7.100	7.140	0.009
17	229.73	238.18	224.66	230.86	6.83	1.970	2.010	2.100	2.027	0.054	7.200	7.219	7.220	7.290	0.009
23	188.85	184.46	192.57	188.63	4.06	2.110	2.100	2.130	2.113	0.012	7.370	7.860	7.450	7.800	0.215
35	229.39	222.30	224.66	225.45	3.61	2.170	2.100	2.160	2.143	0.031	7.400	7.510	7.490	7.890	0.048
47	193.58	192.23	194.39	193.40	1.09	2.177	2.191	2.160	2.176	0.013	7.580	7.620	7.588	7.860	0.017
71	145.27	144.93	147.09	145.77	1.16	2.170	2.100	2.160	2.143	0.031	8.630	8.600	8.659	8.380	0.024

*SD: Standard derivation

Table G-3 Indole-3-acetic acid (IAA) production, system pHs and growth, monitored by the turbidimetric method at 660 nm, of PDMCd0501 in trypticase soy broth (TSB) containing 0.2% w/v tryptophan

Time (hour)	IAA ($\mu\text{g/ml}$)			Mean	SD	Optical density (660 nm)			Mean	SD	pH			Mean	SD
	I	II	III			I	II	III			I	II	III		
0	1.45	1.11	1.25	1.27	0.17	0.028	0.034	0.030	0.031	0.002	7.030	7.020	7.030	7.027	0.005
1	1.42	1.32	1.32	1.35	0.06	0.046	0.054	0.045	0.048	0.004	7.000	7.003	7.000	7.001	0.001
3	3.14	2.91	3.28	3.11	0.19	0.246	0.250	0.235	0.244	0.006	7.350	7.390	7.400	7.380	0.022
5	5.41	3.04	4.05	4.17	1.19	0.875	0.893	0.883	0.884	0.007	7.540	7.480	7.450	7.490	0.037
9	12.16	10.24	7.80	10.07	2.18	2.490	1.830	2.131	2.150	0.270	7.890	7.870	7.880	7.880	0.008
13	16.08	17.91	20.37	18.12	2.15	3.090	2.960	3.000	3.017	0.054	8.120	8.100	8.100	8.107	0.009
17	24.16	23.65	28.72	25.51	2.79	2.870	2.950	2.850	2.890	0.043	8.350	8.390	8.350	8.363	0.019
23	19.59	18.58	15.88	18.02	1.92	3.540	3.590	3.500	3.543	0.037	8.490	8.484	8.490	8.488	0.003
35	16.89	15.20	16.42	16.17	0.87	3.460	3.440	3.410	3.437	0.021	8.550	8.510	8.549	8.536	0.019
47	18.58	20.44	19.36	19.46	0.93	3.360	3.740	3.563	3.554	0.155	8.580	8.620	8.588	8.596	0.017
71	15.20	16.96	16.79	16.32	0.97	3.560	3.370	3.400	3.443	0.083	8.600	8.600	8.659	8.620	0.028

*SD: Standard derivation

Table G-4 Indole-3-acetic acid (IAA) production, system pHs and growth, monitored by the turbidimetric method at 660 nm, of PDMCd0501 in trypticase soy broth (TSB) containing 0.2% w/v tryptophan in the presence of Zn plus Cd (20/20 mg/l)

Time (hour)	IAA ($\mu\text{g/ml}$)			Mean	SD	Optical density (660 nm)			Mean	SD	pH			Mean	SD
	I	II	III			I	II	III			I	II	III		
0	1.69	0.84	1.25	1.26	0.42	0.015	0.016	0.014	0.015	0.001	7.030	7.020	7.030	7.090	0.005
1	2.60	2.33	2.67	2.53	0.18	0.052	0.049	0.045	0.049	0.003	7.000	7.003	7.000	7.130	0.001
3	9.56	4.12	3.28	5.65	3.41	0.420	0.370	0.235	0.342	0.078	7.350	7.390	7.400	7.240	0.022
5	7.77	7.43	7.43	7.55	0.20	0.956	0.939	0.883	0.926	0.031	7.540	7.480	7.450	7.300	0.037
9	13.85	10.81	11.18	11.95	1.66	2.510	2.550	2.531	2.530	0.016	7.890	7.870	7.880	7.300	0.008
13	22.97	23.31	23.75	23.34	0.39	2.970	3.080	3.000	3.017	0.046	7.120	7.400	7.600	7.500	0.197
17	21.96	23.65	21.96	22.52	0.98	3.290	3.290	3.100	3.227	0.090	7.350	7.390	7.350	7.600	0.019
23	11.82	11.82	15.88	13.18	2.34	3.180	3.100	3.500	3.260	0.173	8.490	8.484	8.490	8.000	0.003
35	17.23	15.88	16.42	16.51	0.68	3.010	3.060	3.100	3.057	0.037	8.550	8.510	8.549	8.490	0.019
47	13.18	13.51	15.98	14.22	1.53	3.310	3.160	3.100	3.190	0.088	8.580	8.620	8.588	8.790	0.017
71	13.61	13.38	13.95	13.65	0.29	3.010	3.060	3.100	3.057	0.037	8.600	8.600	8.659	8.720	0.028

*SD: Standard derivation

Table G-5 Indole-3-acetic acid (IAA) production, system pHs and growth, monitored by the turbidimetric method at 660 nm, of PDMCd2007 in trypticase soy broth (TSB) containing 0.2% w/v tryptophan

Time (hour)	IAA ($\mu\text{g/ml}$)			Mean	SD	Optical density (660 nm)			Mean	SD	pH			Mean	SD
	I	II	III			I	II	III			I	II	III		
0	2.67	1.77	2.28	2.24	0.45	0.031	0.029	0.034	0.031	0.002	7.030	7.020	7.030	7.027	0.005
1	8.11	8.58	8.24	8.31	0.24	0.041	0.043	0.045	0.043	0.002	7.000	7.003	7.000	7.001	0.001
3	153.04	149.66	148.34	150.35	2.42	0.383	0.372	0.369	0.375	0.006	7.310	7.300	7.300	7.303	0.005
5	222.64	225.00	215.88	221.17	4.73	0.804	0.767	0.793	0.788	0.016	7.420	7.419	7.420	7.420	0.000
9	436.82	447.97	442.67	442.49	5.58	1.840	1.920	1.890	1.883	0.033	8.000	8.000	8.080	8.027	0.038
13	634.97	672.40	603.72	637.03	34.39	1.900	1.940	1.950	1.930	0.022	8.020	8.100	8.020	8.047	0.038
17	645.27	569.26	591.11	601.88	39.13	1.830	1.780	1.800	1.803	0.021	8.350	8.139	8.260	8.250	0.086
23	486.49	393.58	460.98	447.02	48.00	1.250	1.820	1.860	1.643	0.279	8.290	8.340	8.290	8.307	0.024
35	576.01	584.46	592.23	584.23	8.11	1.090	1.980	2.000	1.690	0.424	8.250	8.340	8.290	8.293	0.037
47	597.97	496.62	574.32	556.31	53.02	1.500	1.780	1.950	1.743	0.186	8.280	8.320	8.288	8.296	0.017
71	480.07	454.73	542.80	492.53	45.34	1.570	1.890	1.430	1.630	0.193	8.360	8.290	8.290	8.313	0.033

*SD: Standard derivation

Table G-6 Indole-3-acetic acid (IAA) production, system pHs and growth, monitored by the turbidimetric method at 660 nm, of PDMCd2007 in trypticase soy broth (TSB) containing 0.2% w/v tryptophan in the presence of Zn plus Cd (20/20 mg/l)

Time (hour)	IAA ($\mu\text{g/ml}$)			Mean	SD	Optical density (660 nm)			Mean	SD	pH			Mean	SD
	I	II	III			I	II	III			I	II	III		
0	5.03	5.91	5.66	5.53	0.45	0.023	0.020	0.024	0.022	0.002	7.030	7.020	7.030	7.090	0.005
1	14.59	16.96	15.00	15.52	1.26	0.045	0.043	0.045	0.044	0.001	7.000	7.003	7.000	7.170	0.001
3	72.53	85.47	80.78	79.59	6.55	0.267	0.270	0.369	0.302	0.047	7.310	7.300	7.300	7.160	0.005
5	188.18	196.62	215.88	200.23	14.20	0.834	0.799	0.793	0.809	0.018	7.420	7.419	7.420	7.250	0.000
9	254.39	254.39	271.28	260.02	9.75	1.950	2.000	1.890	1.947	0.045	7.700	7.740	7.680	7.260	0.025
13	254.39	254.39	271.28	260.02	9.75	1.990	1.980	1.950	1.973	0.017	7.120	7.100	7.100	7.350	0.009
17	116.55	118.24	118.14	117.65	0.95	2.100	2.110	1.800	2.003	0.144	7.200	7.219	7.220	7.380	0.009
23	151.01	157.09	156.93	155.01	3.46	2.340	2.350	1.860	2.183	0.229	7.370	7.860	7.450	7.750	0.215
35	144.26	173.31	153.04	156.87	14.90	2.090	2.050	2.000	2.047	0.037	7.400	7.510	7.490	7.850	0.048
47	143.24	151.01	169.26	154.50	13.35	2.100	2.050	2.300	2.150	0.108	8.490	8.484	8.490	8.080	0.003
71	157.77	158.78	138.51	151.69	11.42	2.090	2.050	2.000	2.047	0.037	8.360	8.290	8.290	8.460	0.033

*SD: Standard derivation

Table G-7 Indole-3-acetic acid (IAA) production, system pHs and growth, monitored by the turbidimetric method at 660 nm, of PDMCd2008 in trypticase soy broth (TSB) containing 0.2% w/v tryptophan

Time (hour)	IAA ($\mu\text{g/ml}$)			Mean	SD	Optical density (660 nm)			Mean	SD	pH			Mean	SD
	I	II	III			I	II	III			I	II	III		
0	4.26	1.72	1.49	2.49	1.54	0.046	0.044	0.041	0.044	0.002	7.030	7.029	7.030	7.030	0.000
1	12.94	13.75	13.45	13.38	0.41	0.054	0.058	0.055	0.056	0.002	7.000	7.003	7.000	7.001	0.001
3	219.59	216.89	203.48	213.32	8.63	0.419	0.440	0.406	0.422	0.014	7.310	7.300	7.300	7.303	0.005
5	347.64	352.70	344.32	348.22	4.22	0.924	0.896	0.915	0.912	0.012	7.420	7.419	7.420	7.420	0.000
9	547.30	562.50	550.00	553.27	8.11	1.940	2.360	2.180	2.160	0.172	8.000	8.000	8.080	8.027	0.038
13	562.50	685.81	560.03	602.78	71.92	2.490	2.450	2.440	2.460	0.022	8.020	8.100	8.020	8.047	0.038
17	464.53	454.39	456.08	458.33	5.43	2.190	2.220	2.200	2.203	0.012	8.350	8.139	8.260	8.250	0.086
23	322.64	358.11	349.70	343.48	18.54	2.210	2.180	2.200	2.197	0.012	8.290	8.340	8.290	8.307	0.024
35	466.22	479.73	470.27	472.07	6.93	3.140	3.200	3.000	3.113	0.084	8.250	8.340	8.290	8.293	0.037
47	464.53	457.77	463.99	462.09	3.75	3.220	3.320	2.050	2.863	0.577	8.700	8.680	8.720	8.700	0.016
71	312.50	342.91	389.86	348.42	38.98	2.590	3.390	2.050	2.677	0.550	8.580	8.900	8.880	8.787	0.146

*SD: Standard derivation

Table G-8 Indole-3-acetic acid (IAA) production, system pHs and growth, monitored by the turbidimetric method at 660 nm, of PDMCd2008 in trypticase soy broth (TSB) containing 0.2% w/v tryptophan in the presence of Zn plus Cd (20/20 mg/l)

Time (hour)	IAA ($\mu\text{g/ml}$)			Mean	SD	Optical density (660 nm)			Mean	SD	pH			Mean	SD
	I	II	III			I	II	III			I	II	III		
0	5.61	5.30	4.86	5.26	0.37	0.020	0.019	0.021	0.020	0.001	7.030	7.029	7.030	7.090	0.000
1	17.23	16.22	16.82	16.76	0.51	0.035	0.030	0.035	0.033	0.002	7.000	7.003	7.000	7.320	0.001
3	108.58	131.76	135.91	125.42	14.73	0.176	0.186	0.806	0.389	0.295	7.310	7.300	7.300	7.300	0.005
5	210.81	212.50	209.19	210.83	1.66	0.878	0.905	0.915	0.899	0.016	7.420	7.419	7.420	7.320	0.000
9	438.18	440.20	428.38	435.59	6.32	1.910	1.870	1.937	1.906	0.028	7.290	7.190	7.200	7.300	0.045
13	500.00	472.09	492.47	488.19	14.44	1.970	1.900	1.944	1.938	0.029	7.290	7.190	7.200	7.320	0.045
17	260.14	273.65	253.38	262.39	10.32	1.780	1.810	1.820	1.803	0.017	7.650	7.660	7.690	7.600	0.017
23	292.91	289.53	282.13	288.19	5.51	2.120	1.180	1.200	1.500	0.438	7.900	7.340	7.290	7.650	0.277
35	270.61	282.09	132.43	228.38	83.29	1.910	2.010	1.000	1.640	0.454	8.250	8.340	8.290	8.060	0.037
47	176.35	364.19	261.28	267.27	94.06	1.910	1.010	1.000	1.307	0.427	7.700	8.680	7.720	7.830	0.457
71	169.26	216.89	209.80	198.65	25.70	1.910	1.010	1.000	1.307	0.427	8.580	8.900	8.880	8.060	0.146

*SD: Standard derivation

Table G-9 Indole-3-acetic acid (IAA) production, system pHs and growth, monitored by the turbidimetric method at 660 nm, of PDMZnCd1502 in trypticase soy broth (TSB) containing 0.2% w/v tryptophan

Time (hour)	IAA ($\mu\text{g/ml}$)			Mean	SD	Optical density (660 nm)			Mean	SD	pH			Mean	SD
	I	II	III			I	II	III			I	II	III		
0	6.52	3.16	5.07	4.92	1.69	0.030	0.029	0.023	0.027	0.003	7.030	7.029	7.030	7.030	0.000
1	18.28	16.82	17.24	17.45	0.75	0.065	0.071	0.079	0.072	0.006	7.000	7.003	7.000	7.001	0.001
3	212.84	208.78	219.49	213.70	5.41	0.669	0.647	0.656	0.657	0.009	7.310	7.300	7.300	7.303	0.005
5	280.74	292.91	303.18	292.27	11.23	0.978	0.865	0.934	0.926	0.047	7.420	7.419	7.420	7.420	0.000
9	340.54	340.88	371.42	350.95	17.73	1.820	1.630	1.800	1.750	0.085	8.050	8.000	8.080	8.043	0.033
13	525.34	543.92	536.15	535.14	9.33	1.660	1.830	1.770	1.753	0.070	8.390	8.410	8.380	8.393	0.012
17	479.73	521.96	508.78	503.49	21.61	1.730	1.750	1.790	1.757	0.025	8.450	8.439	8.460	8.450	0.009
23	467.91	483.11	474.66	475.23	7.62	2.010	1.970	1.830	1.937	0.077	8.590	8.580	8.590	8.587	0.005
35	496.62	599.66	533.45	543.24	52.21	2.360	2.300	2.290	2.317	0.031	8.650	8.640	8.690	8.660	0.022
47	526.01	452.16	504.46	494.21	37.98	2.440	2.480	2.050	2.323	0.194	8.670	8.680	8.672	8.674	0.004
71	383.45	457.77	504.46	448.56	61.03	2.280	2.400	2.050	2.243	0.145	8.580	8.690	8.880	8.717	0.124

*SD: Standard derivation

Table G-10 Indole-3-acetic acid (IAA) production, system pHs and growth, monitored by the turbidimetric method at 660 nm, of PDMZnCd1502 in trypticase soy broth (TSB) containing 0.2% w/v tryptophan in the presence of Zn plus Cd (20/20 mg/l)

Time (hour)	IAA ($\mu\text{g/ml}$)			Mean	SD	Optical density (660 nm)			Mean	SD	pH			Mean	SD
	I	II	III			I	II	III			I	II	III		
0	6.35	5.47	5.07	5.63	0.65	0.021	0.020	0.023	0.021	0.001	7.030	7.029	7.030	7.090	0.000
1	16.72	17.94	17.24	17.30	0.61	0.059	0.064	0.069	0.064	0.004	7.000	7.003	7.000	7.200	0.001
3	78.04	68.75	84.36	77.05	7.85	0.250	0.280	0.256	0.262	0.013	7.310	7.300	7.300	7.230	0.005
5	175.00	164.53	168.04	169.19	5.33	0.902	0.931	0.914	0.916	0.012	7.320	7.320	7.320	7.320	0.000
9	239.19	255.41	236.28	243.63	10.30	1.820	1.880	1.800	1.833	0.034	7.300	7.300	7.300	7.300	0.000
13	310.47	302.70	299.66	304.28	5.58	1.980	1.905	1.970	1.952	0.033	7.320	7.320	7.200	7.320	0.057
17	336.15	322.64	339.86	332.88	9.07	2.000	2.060	1.790	1.950	0.116	7.410	7.410	7.100	7.410	0.146
23	176.01	170.95	170.61	172.52	3.03	1.900	1.510	1.830	1.747	0.170	7.600	7.600	7.460	7.600	0.066
35	233.45	230.74	229.39	231.19	2.06	1.790	1.670	1.900	1.787	0.094	7.670	7.670	7.567	7.670	0.049
47	237.50	223.65	234.19	231.78	7.23	1.790	1.670	1.900	1.787	0.094	8.670	8.680	8.672	8.050	0.004
71	229.73	206.08	194.93	210.25	17.77	1.790	1.670	1.900	1.787	0.094	8.580	8.690	8.880	8.070	0.124

*SD: Standard derivation

Table G-11 Indole-3-acetic acid (IAA) production, system pHs and growth, monitored by the turbidimetric method at 660 nm, of PDMZnCd2003 in trypticase soy broth (TSB) containing 0.2% w/v tryptophan

Time (hour)	IAA ($\mu\text{g/ml}$)			Mean	SD	Optical density (660 nm)			Mean	SD	pH			Mean	SD
	I	II	III			I	II	III			I	II	III		
0	1.79	2.20	1.96	1.98	0.20	0.014	0.020	0.017	0.017	0.002	7.030	7.029	7.030	7.030	0.000
1	21.96	20.61	22.97	21.85	1.19	0.018	0.022	0.020	0.020	0.002	7.000	7.003	7.000	7.001	0.001
3	33.78	52.03	63.18	49.66	14.84	0.195	0.218	0.206	0.206	0.009	7.310	7.300	7.300	7.303	0.005
5	201.35	191.22	164.19	185.59	19.21	0.363	0.409	0.363	0.378	0.022	7.420	7.419	7.420	7.420	0.000
9	231.76	229.39	231.76	230.97	1.37	0.820	0.710	0.790	0.773	0.046	8.050	8.000	8.080	8.043	0.033
13	265.54	265.54	266.89	265.99	0.78	1.180	0.910	1.090	1.060	0.112	8.390	8.410	8.380	8.393	0.012
17	297.30	282.43	299.32	293.02	9.22	1.530	1.510	1.540	1.527	0.012	8.450	8.439	8.460	8.450	0.009
23	265.61	263.51	265.88	265.00	1.29	1.640	1.520	1.580	1.580	0.049	8.590	8.580	8.590	8.587	0.005
35	263.51	270.95	262.84	265.77	4.50	1.690	1.602	1.605	1.632	0.041	8.650	8.640	8.690	8.660	0.022
47	269.59	266.22	263.51	266.44	3.05	1.360	1.220	1.050	1.210	0.127	8.670	8.680	8.672	8.674	0.004
71	185.81	202.70	201.69	196.73	9.47	1.015	1.013	1.450	1.159	0.206	8.580	8.690	8.880	8.717	0.124

*SD: Standard derivation

Table G-12 Indole-3-acetic acid (IAA) production, system pHs and growth, monitored by the turbidimetric method at 660 nm, of PDMZnCd2003 in trypticase soy broth (TSB) containing 0.2% w/v tryptophan in the presence of Zn plus Cd (20/20 mg/l)

Time (hour)	IAA ($\mu\text{g/ml}$)			Mean	SD	Optical density (660 nm)			Mean	SD	pH			Mean	SD
	I	II	III			I	II	III			I	II	III		
0	5.61	4.93	5.34	5.29	0.34	0.023	0.020	0.017	0.020	0.002	7.030	7.029	7.030	7.090	0.000
1	12.03	12.94	12.43	12.47	0.46	0.051	0.047	0.045	0.048	0.002	7.000	7.003	7.000	7.280	0.001
3	76.69	80.41	74.96	77.35	2.78	0.298	0.341	0.306	0.315	0.019	7.310	7.300	7.300	7.300	0.005
5	141.55	148.31	151.55	147.14	5.10	0.893	0.915	0.863	0.890	0.021	7.420	7.419	7.420	7.280	0.000
9	252.70	208.78	225.88	229.12	22.14	1.780	1.820	1.790	1.797	0.017	7.420	7.419	7.420	7.300	0.000
13	236.49	236.15	228.04	233.56	4.78	1.957	1.970	1.970	1.966	0.006	7.290	7.190	7.200	7.500	0.045
17	177.36	219.59	185.34	194.10	22.44	2.100	2.210	2.070	2.127	0.060	7.420	7.419	7.420	7.590	0.000
23	178.04	179.73	185.34	181.04	3.82	2.010	1.960	1.980	1.983	0.021	7.650	7.660	7.690	7.770	0.017
35	177.36	167.57	151.35	165.43	13.14	2.110	2.380	1.405	1.965	0.411	7.900	7.340	7.290	7.720	0.277
47	168.58	141.89	151.35	153.94	13.53	2.410	2.380	1.605	2.132	0.373	7.970	7.660	7.690	7.960	0.140
71	138.18	155.41	153.72	149.10	9.50	2.110	2.180	2.050	2.113	0.053	8.450	8.439	8.460	8.340	0.009

*SD: Standard derivation

Plant growth promoting properties of NH₃⁺-N production

Table G-13 NH₃⁺-N production, system pHs and growth, monitored by the turbidimetric method at 660 nm, of PDMZn2008 in N-free malate medium

Time (hour)	NH ₃ ⁺ -N (mg/l)			Mean	SD	Optical density (660 nm)			Mean	SD	pH			Mean	SD
	I	II	III			I	II	III			I	II	III		
0	0.00	0.00	0.00	0.000	0.000	0.010	0.011	0.009	0.010	0.001	7.000	7.010	7.020	7.010	0.008
1	0.91	1.08	1.00	0.999	0.086	0.020	0.023	0.015	0.019	0.003	7.300	7.400	7.370	7.350	0.042
3	6.48	6.48	6.20	6.390	0.161	0.022	0.022	0.023	0.022	0.000	7.350	7.370	7.360	7.360	0.008
5	7.09	6.48	6.78	6.784	0.302	0.030	0.031	0.028	0.030	0.001	7.540	7.580	7.600	7.610	0.025
9	8.33	8.20	8.21	8.247	0.076	0.029	0.033	0.030	0.031	0.002	7.700	7.940	7.880	7.940	0.102
13	9.65	9.65	9.67	9.658	0.007	0.040	0.044	0.041	0.042	0.002	8.120	8.020	8.100	8.020	0.043
17	1.64	1.64	1.77	1.686	0.077	0.047	0.050	0.049	0.049	0.001	8.200	8.183	8.220	8.183	0.015
23	1.09	1.52	1.51	1.373	0.246	0.044	0.045	0.043	0.044	0.001	8.370	8.280	8.450	8.280	0.069
35	0.03	0.03	0.24	0.100	0.121	0.043	0.043	0.043	0.043	0.000	8.400	8.530	8.490	8.530	0.054
47	0.74	0.74	0.78	0.756	0.025	0.031	0.034	0.033	0.033	0.001	8.580	8.600	8.588	8.600	0.008
71	0.36	0.32	0.27	0.317	0.045	0.033	0.041	0.035	0.036	0.003	8.630	8.700	8.659	8.730	0.029

*SD: Standard derivation

Table G-14 NH₃⁺-N production, system pHs and growth, monitored by the turbidimetric method at 660 nm, of PDMZn2008 in N-free malate medium in the presence of Zn plus Cd (20/20 mg/l)

Time (hour)	NH ₃ ⁺ -N (mg/l)			Mean	SD	Optical density (660 nm)			Mean	SD	pH			Mean	SD
	I	II	III			I	II	III			I	II	III		
0	0.00	0.00	0.00	0.00	0.00	0.012	0.011	0.011	0.011	0.000	7.040	7.020	7.030	7.000	0.008
1	3.10	3.10	3.16	3.12	0.04	0.013	0.021	0.012	0.015	0.004	7.320	7.300	7.280	7.080	0.016
3	6.70	6.70	6.65	6.68	0.03	0.020	0.020	0.021	0.020	0.000	7.350	7.310	7.400	7.250	0.037
5	7.08	7.08	7.15	7.10	0.04	0.021	0.021	0.021	0.021	0.000	7.540	7.480	7.480	7.540	0.028
9	11.24	10.90	11.04	11.06	0.17	0.027	0.027	0.023	0.026	0.002	8.080	8.130	8.070	8.080	0.026
13	4.04	4.13	4.10	4.09	0.04	0.036	0.036	0.037	0.036	0.000	8.150	8.120	8.130	8.150	0.012
17	1.88	1.84	2.08	1.93	0.13	0.036	0.036	0.037	0.036	0.000	8.280	8.219	8.330	8.280	0.045
23	1.47	1.51	1.57	1.52	0.05	0.044	0.053	0.047	0.048	0.004	8.300	8.330	8.330	8.300	0.014
35	1.30	1.17	1.28	1.25	0.07	0.068	0.080	0.073	0.074	0.005	8.370	8.350	8.480	8.370	0.057
47	2.11	2.05	2.16	2.11	0.05	0.046	0.046	0.047	0.046	0.000	8.390	8.420	8.488	8.390	0.041
71	1.46	1.54	1.32	1.44	0.11	0.033	0.053	0.037	0.041	0.009	8.430	8.400	8.459	8.400	0.024

*SD: Standard derivation

Table G-15 NH₃⁺-N production, system pHs and growth, monitored by the turbidimetric method at 660 nm, of PDMCd0501 in N-free malate medium

Time (hour)	NH ₃ ⁺ -N (mg/l)			Mean	SD	Optical density (660 nm)			Mean	SD	pH			Mean	SD
	I	II	III			I	II	III			I	II	III		
0	0.00	0.00	0.00	0.00	0.00	0.026	0.018	0.023	0.022	0.003	7.010	7.010	7.020	7.010	0.005
1	0.36	0.36	-0.12	0.20	0.28	0.030	0.025	0.024	0.026	0.003	7.400	7.400	7.370	7.370	0.014
3	0.40	0.40	0.63	0.48	0.14	0.025	0.030	0.029	0.028	0.002	7.350	7.390	7.390	7.390	0.019
5	0.31	0.31	1.35	0.66	0.60	0.031	0.034	0.033	0.033	0.001	7.440	7.480	7.410	7.410	0.029
9	1.51	1.51	1.35	1.46	0.09	0.045	0.044	0.043	0.044	0.001	7.890	7.870	7.830	7.830	0.025
13	3.61	3.61	1.35	2.86	1.30	0.040	0.039	0.041	0.040	0.001	8.220	8.210	8.200	8.210	0.008
17	3.72	3.72	3.33	3.59	0.23	0.032	0.035	0.031	0.033	0.002	8.750	8.690	8.750	8.710	0.028
23	3.70	4.52	4.09	4.11	0.41	0.033	0.032	0.030	0.032	0.001	8.890	8.900	8.980	8.980	0.040
35	9.52	12.10	9.49	10.37	1.50	0.040	0.043	0.040	0.041	0.001	9.010	8.510	8.549	9.010	0.227
47	10.98	10.98	9.92	10.63	0.61	0.036	0.040	0.036	0.037	0.002	9.260	8.620	8.588	9.260	0.310
71	8.84	8.54	8.64	8.67	0.15	0.040	0.041	0.030	0.037	0.005	9.330	9.285	9.290	9.330	0.020

*SD: Standard derivation

Table G-16 NH₃⁺-N production, system pHs and growth, monitored by the turbidimetric method at 660 nm, of PDMCd0501 in N-free malate medium in the presence of Zn plus Cd (20/20 mg/l)

Time (hour)	NH ₃ ⁺ -N (mg/l)			Mean	SD	Optical density (660 nm)			Mean	SD	pH			Mean	SD
	I	II	III			I	II	III			I	II	III		
0	0.00	0.00	0.00	0.00	0.00	0.016	0.016	0.013	0.015	0.001	7.030	7.020	7.030	7.000	0.005
1	4.13	4.55	4.45	4.38	0.22	0.019	0.019	0.018	0.019	0.000	7.100	7.003	7.090	7.100	0.044
3	5.37	5.41	5.49	5.43	0.06	0.020	0.020	0.023	0.021	0.001	7.350	7.390	7.400	7.300	0.022
5	5.69	5.63	5.86	5.73	0.12	0.023	0.023	0.024	0.023	0.000	7.540	7.480	7.450	7.720	0.037
9	4.55	7.30	4.18	5.34	1.70	0.043	0.030	0.030	0.034	0.006	8.550	8.510	8.500	8.500	0.022
13	5.43	4.60	5.81	5.28	0.62	0.040	0.040	0.040	0.040	0.000	8.630	8.710	8.670	8.670	0.033
17	1.64	1.73	1.21	1.53	0.28	0.073	0.078	0.075	0.075	0.002	8.780	8.800	8.780	8.780	0.009
23	1.42	1.26	1.14	1.27	0.14	0.058	0.053	0.060	0.057	0.003	8.890	8.840	8.840	8.840	0.024
35	1.98	1.68	1.77	1.81	0.15	0.034	0.034	0.030	0.033	0.002	9.000	9.010	9.010	9.010	0.005
47	2.97	2.03	2.16	2.38	0.51	0.045	0.045	0.040	0.043	0.002	8.580	8.620	8.970	8.970	0.175
71	2.04	1.86	2.16	2.02	0.15	0.039	0.040	0.040	0.040	0.000	8.600	8.600	9.000	9.000	0.189

*SD: Standard derivation

Table G-17 NH₃⁺-N production, system pHs and growth, monitored by the turbidimetric method at 660 nm, of PDMCd2007 in N-free malate medium

Time (hour)	NH ₃ ⁺ -N (mg/l)			Mean	SD	Optical density (660 nm)			Mean	SD	pH			Mean	SD
	I	II	III			I	II	III			I	II	III		
0	0.23	0.18	0.20	0.21	0.02	0.012	0.010	0.012	0.011	0.001	7.010	7.020	7.000	7.010	0.008
1	0.32	0.21	0.30	0.28	0.06	0.011	0.012	0.011	0.011	0.000	7.490	7.530	7.450	7.480	0.033
3	0.49	0.23	0.63	0.45	0.21	0.015	0.014	0.011	0.013	0.002	7.510	7.500	7.510	7.510	0.005
5	4.95	4.60	4.78	4.78	0.18	0.021	0.020	0.024	0.022	0.002	7.420	7.419	7.420	7.570	0.000
9	6.28	5.63	6.15	6.02	0.35	0.033	0.031	0.032	0.032	0.001	8.000	8.000	8.080	8.000	0.038
13	7.77	7.55	8.31	7.88	0.39	0.034	0.035	0.039	0.036	0.002	8.300	8.270	8.340	8.300	0.029
17	1.53	1.53	1.64	1.57	0.06	0.059	0.057	0.060	0.059	0.001	8.385	8.390	8.396	8.400	0.004
23	1.99	2.07	1.96	2.01	0.06	0.044	0.038	0.042	0.041	0.002	8.390	8.440	8.460	8.450	0.029
35	1.34	1.31	1.38	1.34	0.04	0.033	0.032	0.032	0.032	0.000	8.500	8.500	8.490	8.500	0.005
47	0.14	0.14	0.06	0.11	0.05	0.047	0.043	0.047	0.046	0.002	8.480	8.520	8.488	8.500	0.017
71	0.24	0.27	0.39	0.30	0.08	0.044	0.041	0.040	0.042	0.002	8.560	8.490	8.490	8.540	0.033

*SD: Standard derivation

Table G-18 NH₃⁺-N production, system pHs and growth, monitored by the turbidimetric method at 660 nm, of PDMCd2007 in N-free malate medium in the presence of Zn plus Cd (20/20 mg/l)

Time (hour)	NH ₃ ⁺ -N (mg/l)			Mean	SD	Optical density (660 nm)			Mean	SD	pH			Mean	SD
	I	II	III			I	II	III			I	II	III		
0	0.00	0.20	0.00	0.07	0.12	0.019	0.019	0.014	0.017	0.002	7.000	7.000	7.000	7.000	0.005
1	0.83	0.57	1.02	0.81	0.23	0.018	0.018	0.017	0.018	0.000	7.000	7.003	7.000	7.050	0.001
3	0.83	1.06	1.45	1.11	0.31	0.018	0.016	0.019	0.018	0.001	7.310	7.300	7.300	7.320	0.005
5	4.52	3.93	3.72	4.06	0.42	0.030	0.030	0.031	0.030	0.000	7.780	7.780	7.920	7.870	0.066
9	5.23	5.29	5.58	5.37	0.19	0.033	0.033	0.029	0.032	0.002	8.000	7.840	7.980	8.000	0.071
13	6.67	6.60	6.78	6.68	0.09	0.045	0.045	0.045	0.045	0.000	8.300	8.360	8.300	8.300	0.028
17	1.96	1.64	2.06	1.89	0.22	0.048	0.048	0.047	0.048	0.000	8.370	8.450	8.350	8.370	0.043
23	2.46	2.04	1.69	2.06	0.38	0.037	0.040	0.037	0.038	0.001	8.370	8.360	8.450	8.370	0.040
35	3.44	2.67	2.43	2.85	0.53	0.041	0.041	0.040	0.041	0.000	8.410	8.510	8.490	8.410	0.043
47	1.08	0.91	1.42	1.14	0.26	0.058	0.058	0.060	0.059	0.001	8.490	8.610	8.490	8.510	0.057
71	1.56	1.24	1.43	1.41	0.16	0.043	0.049	0.050	0.047	0.003	8.360	8.290	8.290	8.650	0.033

*SD: Standard derivation

Table G-19 NH₃⁺-N production, system pHs and growth, monitored by the turbidimetric method at 660 nm, of PDMCd2008 in N-free malate medium

Time (hour)	NH ₃ ⁺ -N (mg/l)			Mean	SD	Optical density (660 nm)			Mean	SD	pH			Mean	SD
	I	II	III			I	II	III			I	II	III		
0	1.01	1.21	-0.06	0.72	0.68	0.011	0.011	0.012	0.011	0.000	7.000	7.020	7.000	7.010	0.009
1	1.84	1.95	1.86	1.88	0.06	0.016	0.017	0.015	0.016	0.001	7.000	7.005	7.000	7.041	0.002
3	7.12	7.04	6.63	6.93	0.26	0.020	0.022	0.021	0.021	0.001	7.410	7.430	7.430	7.430	0.009
5	7.13	7.13	7.35	7.20	0.13	0.026	0.026	0.025	0.026	0.000	7.420	7.490	7.462	7.470	0.029
9	12.27	12.27	12.24	12.26	0.02	0.028	0.028	0.029	0.028	0.000	7.780	8.000	8.080	7.930	0.127
13	3.74	3.60	3.64	3.66	0.07	0.031	0.030	0.034	0.032	0.002	8.020	8.080	8.000	8.000	0.034
17	2.15	2.15	2.21	2.17	0.03	0.037	0.038	0.035	0.037	0.001	8.450	8.400	8.426	8.420	0.020
23	1.47	1.48	1.45	1.47	0.01	0.031	0.030	0.032	0.031	0.001	8.439	8.440	8.490	8.470	0.024
35	1.44	1.20	1.09	1.24	0.18	0.030	0.030	0.031	0.030	0.000	8.500	8.540	8.490	8.500	0.022
47	0.61	0.61	0.60	0.61	0.01	0.025	0.028	0.026	0.026	0.001	8.500	8.580	8.520	8.520	0.034
71	0.78	0.70	0.67	0.72	0.06	0.022	0.030	0.029	0.027	0.004	8.580	8.590	8.550	8.560	0.017

*SD: Standard derivation

Table G-20 NH₃⁺-N production, system pHs and growth, monitored by the turbidimetric method at 660 nm, of PDMCd2008 in N-free malate medium in the presence of Zn plus Cd (20/20 mg/l)

Time (hour)	NH ₃ ⁺ -N (mg/l)			Mean	SD	Optical density (660 nm)			Mean	SD	pH			Mean	SD
	I	II	III			I	II	III			I	II	III		
0	0.36	0.40	0.33	0.36	0.04	0.019	0.019	0.020	0.019	0.000	7.030	7.029	7.030	7.000	0.000
1	4.51	6.18	4.45	5.05	0.98	0.021	0.021	0.023	0.022	0.001	7.000	7.003	7.000	7.070	0.001
3	7.38	7.68	7.73	7.60	0.19	0.025	0.025	0.026	0.025	0.000	7.310	7.300	7.300	7.120	0.005
5	7.47	8.15	7.73	7.78	0.35	0.024	0.024	0.026	0.025	0.001	7.420	7.419	7.420	7.340	0.000
9	8.45	7.91	7.99	8.12	0.29	0.028	0.028	0.026	0.027	0.001	7.290	7.190	7.200	7.700	0.045
13	1.53	2.55	2.03	2.04	0.51	0.053	0.053	0.051	0.052	0.001	7.290	7.190	7.200	7.900	0.045
17	0.36	0.70	0.68	0.58	0.19	0.047	0.047	0.046	0.047	0.000	8.160	8.120	8.090	8.120	0.029
23	0.70	0.48	0.74	0.64	0.14	0.043	0.045	0.046	0.045	0.001	8.440	8.240	8.290	8.240	0.085
35	0.10	0.36	0.44	0.30	0.18	0.040	0.040	0.060	0.047	0.009	8.760	8.360	8.290	8.360	0.207
47	1.77	1.94	1.71	1.81	0.12	0.048	0.048	0.041	0.046	0.003	8.700	8.480	8.720	8.480	0.109
71	2.46	1.66	1.73	1.95	0.44	0.033	0.049	0.036	0.039	0.007	8.510	8.500	8.480	8.500	0.012

*SD: Standard derivation

Table G-21 NH_3^+ -N production, system pHs and growth, monitored by the turbidimetric method at 660 nm, of PDMZnCd1502 in N-free malate medium

Time (hour)	NH_3^+ -N (mg/l)			Mean	SD	Optical density (660 nm)			Mean	SD	pH			Mean	SD
	I	II	III			I	II	III			I	II	III		
0	0.57	0.57	0.40	0.51	0.10	0.008	0.010	0.009	0.009	0.001	7.030	7.029	7.030	7.010	0.000
1	0.79	0.70	0.73	0.74	0.05	0.015	0.013	0.017	0.015	0.002	7.000	7.003	7.000	7.410	0.001
3	1.81	1.80	1.92	1.85	0.06	0.034	0.037	0.036	0.036	0.001	7.431	7.450	7.420	7.450	0.012
5	7.25	7.55	6.78	7.20	0.39	0.038	0.037	0.039	0.038	0.001	7.500	7.520	7.520	7.510	0.009
9	9.14	8.84	7.86	8.61	0.67	0.041	0.040	0.042	0.041	0.001	8.050	8.000	8.080	8.000	0.033
13	2.80	2.97	2.88	2.88	0.09	0.045	0.047	0.047	0.046	0.001	8.290	8.270	8.240	8.260	0.021
17	1.38	1.42	1.60	1.46	0.12	0.048	0.048	0.045	0.047	0.001	8.310	8.290	8.300	8.300	0.008
23	1.69	1.26	3.31	2.09	1.08	0.034	0.032	0.036	0.034	0.002	8.490	8.480	8.490	8.490	0.005
35	2.20	2.03	2.03	2.08	0.10	0.023	0.023	0.024	0.023	0.000	8.450	8.540	8.490	8.500	0.037
47	1.13	1.13	1.17	1.14	0.02	0.035	0.035	0.022	0.031	0.006	8.570	8.548	8.545	8.550	0.011
71	1.81	1.26	1.56	1.54	0.28	0.029	0.031	0.028	0.029	0.001	8.580	8.590	8.589	8.590	0.004

*SD: Standard derivation

Table G-22 NH₃⁺-N production, system pHs and growth, monitored by the turbidimetric method at 660 nm, of PDMZnCd1502 in N-free malate medium in the presence of Zn plus Cd (20/20 mg/l)

Time (hour)	NH ₃ ⁺ -N (mg/l)			Mean	SD	Optical density (660 nm)			Mean	SD	pH			Mean	SD
	I	II	III			I	II	III			I	II	III		
0	0.70	0.69	0.57	0.65	0.07	0.018	0.017	0.018	0.018	0.000	7.030	7.029	7.030	7.000	0.000
1	1.17	0.96	0.70	0.94	0.24	0.021	0.021	0.029	0.024	0.004	7.000	7.003	7.000	7.180	0.001
3	1.43	2.03	1.80	1.75	0.30	0.024	0.024	0.025	0.024	0.000	7.310	7.300	7.300	7.500	0.005
5	5.33	5.45	5.41	5.40	0.07	0.028	0.028	0.029	0.028	0.000	7.320	7.710	7.320	7.710	0.184
9	5.80	5.71	5.41	5.64	0.20	0.070	0.070	0.050	0.063	0.009	8.000	8.000	8.300	8.000	0.141
13	6.30	6.87	5.97	6.38	0.46	0.050	0.050	0.045	0.048	0.002	8.320	8.260	8.200	8.260	0.049
17	5.28	5.33	5.27	5.29	0.03	0.059	0.059	0.060	0.059	0.000	8.410	8.290	8.100	8.290	0.128
23	1.26	1.52	1.26	1.35	0.15	0.044	0.050	0.043	0.046	0.003	8.600	8.310	8.460	8.310	0.118
35	2.03	2.04	2.03	2.03	0.00	0.038	0.038	0.039	0.038	0.000	8.670	8.430	8.567	8.430	0.098
47	0.83	1.04	1.13	1.00	0.15	0.057	0.057	0.050	0.055	0.003	8.670	8.520	8.672	8.520	0.071
71	1.13	1.10	1.26	1.16	0.08	0.051	0.048	0.050	0.050	0.001	8.580	8.550	8.880	8.550	0.149

*SD: Standard derivation

Table G-23 NH₃⁺-N production, system pHs and growth, monitored by the turbidimetric method at 660 nm, of PDMZnCd2003 in N-free malate medium

Time (hour)	NH ₃ ⁺ -N (mg/l)			Mean	SD	Optical density (660 nm)			Mean	SD	pH			Mean	SD
	I	II	III			I	II	III			I	II	III		
0	1.60	1.56	1.26	1.47	0.19	0.011	0.010	0.013	0.011	0.001	7.030	7.029	7.030	7.010	0.000
1	2.16	2.28	2.07	2.17	0.11	0.017	0.015	0.020	0.017	0.002	7.000	7.003	7.000	7.310	0.001
3	2.41	2.41	2.35	2.39	0.04	0.027	0.025	0.026	0.026	0.001	7.310	7.300	7.300	7.400	0.005
5	3.27	3.27	3.07	3.20	0.12	0.029	0.029	0.030	0.029	0.000	7.420	7.419	7.420	7.430	0.000
9	6.74	6.74	7.60	7.03	0.49	0.030	0.030	0.029	0.030	0.000	8.050	8.000	8.080	8.000	0.033
13	1.73	1.90	1.86	1.83	0.09	0.032	0.032	0.033	0.032	0.000	8.390	8.410	8.380	8.310	0.012
17	2.04	2.08	2.07	2.06	0.02	0.025	0.025	0.027	0.026	0.001	8.450	8.439	8.460	8.470	0.009
23	2.14	2.20	2.11	2.15	0.04	0.030	0.024	0.030	0.028	0.003	8.590	8.580	8.590	8.570	0.005
35	2.20	2.20	2.33	2.24	0.07	0.037	0.037	0.031	0.035	0.003	8.750	8.740	8.790	8.760	0.022
47	2.11	2.11	1.34	1.86	0.45	0.041	0.040	0.037	0.039	0.002	8.900	8.890	8.972	8.930	0.037
71	1.47	1.51	1.77	1.58	0.16	0.042	0.035	0.040	0.039	0.003	9.090	9.070	9.070	9.000	0.009

*SD: Standard derivation

Table G-24 NH₃⁺-N production, system pHs and growth, monitored by the turbidimetric method at 660 nm, of PDMZnCd2003 in N-free malate medium in the presence of Zn plus Cd (20/20 mg/l)

Time (hour)	NH ₃ ⁺ -N (mg/l)			Mean	SD	Optical density (660 nm)			Mean	SD	pH			Mean	SD
	I	II	III			I	II	III			I	II	III		
0	0.39	0.40	-0.15	0.21	0.31	0.019	0.019	0.017	0.018	0.001	7.030	7.029	7.030	7.00	0.000
1	0.91	0.84	1.02	0.92	0.09	0.020	0.021	0.020	0.020	0.000	7.000	7.003	7.000	7.17	0.001
3	1.28	1.50	1.41	1.40	0.11	0.021	0.021	0.023	0.022	0.001	7.310	7.300	7.300	7.31	0.005
5	2.37	2.41	2.43	2.40	0.03	0.028	0.028	0.023	0.026	0.002	7.420	7.419	7.420	7.710	0.000
9	5.63	5.71	5.73	5.69	0.05	0.026	0.026	0.025	0.026	0.000	7.420	7.419	7.420	7.700	0.000
13	6.55	6.05	6.25	6.28	0.25	0.028	0.028	0.027	0.028	0.000	8.020	8.000	8.020	8.020	0.009
17	0.84	1.57	1.73	1.38	0.47	0.026	0.026	0.025	0.026	0.000	8.400	8.340	8.400	8.400	0.028
23	2.00	1.68	1.86	1.85	0.16	0.030	0.025	0.027	0.027	0.002	8.430	8.300	8.430	8.430	0.061
35	3.06	2.54	2.76	2.78	0.26	0.022	0.022	0.023	0.022	0.000	8.500	8.450	8.500	8.500	0.024
47	3.01	2.89	2.98	2.96	0.06	0.025	0.025	0.023	0.024	0.001	9.010	9.010	9.010	9.010	0.000
71	2.54	1.90	2.30	2.25	0.32	0.023	0.021	0.023	0.022	0.001	8.990	9.190	9.100	9.100	0.082

*SD: Standard derivation

Plant growth promoting properties of phosphates solubilization

Table G-25 Phosphates solubilization, system pHs and growth, monitored by the turbidimetric method at 660 nm, of PDMZn2008 in NBRIP medium containing 0.5% (w/v) tricalcium phosphate

Time (hour)	PO ₄ ³⁻ -P (mg/l)			Mean	SD	Optical density (660 nm)			Mean	SD	pH			Mean	SD
	I	II	III			I	II	III			I	II	III		
0	2.64	2.30	1.96	2.30	0.34	0.013	0.015	0.013	0.014	0.001	7.000	7.000	7.000	7.000	0.000
1	112.77	113.45	99.29	108.50	7.98	0.025	0.023	0.025	0.024	0.001	6.920	6.910	6.900	6.910	0.008
3	140.91	141.49	140.81	141.07	0.36	0.128	0.122	0.185	0.145	0.028	6.780	6.790	6.800	6.780	0.008
5	167.16	170.20	167.50	168.29	1.67	0.160	0.125	0.150	0.145	0.013	6.350	6.320	6.310	6.330	0.017
9	178.31	178.99	178.31	178.54	0.39	0.229	0.237	0.223	0.230	0.006	5.710	5.720	5.720	5.710	0.005
13	267.84	274.26	273.24	271.78	3.45	0.300	0.259	0.240	0.266	0.025	6.390	6.410	5.400	5.400	0.471
17	284.73	288.78	290.14	287.88	2.81	0.291	0.291	0.231	0.271	0.028	5.300	5.300	5.270	5.270	0.014
23	199.26	204.66	206.01	203.31	3.58	0.300	0.300	0.330	0.310	0.014	5.260	5.230	5.240	5.240	0.012
35	177.64	182.36	183.04	181.01	2.95	0.385	0.342	0.346	0.358	0.019	5.120	5.140	5.110	5.120	0.012
47	214.80	215.14	217.50	215.81	1.47	0.128	0.201	0.215	0.181	0.038	5.020	5.010	5.011	5.010	0.004
71	209.05	208.04	208.04	208.38	0.59	0.231	0.246	0.245	0.241	0.007	5.010	5.000	5.010	5.010	0.005

*SD: Standard derivation

Table G-26 Phosphates solubilization, system pHs and growth, monitored by the turbidimetric method at 660 nm, of PDMZn2008 in NBRIP medium containing 0.5% (w/v) tricalcium phosphate in the presence of Zn plus Cd (20/20 mg/l)

Time (hour)	PO ₄ ³⁻ -P (mg/l)			Mean	SD	Optical density (660 nm)			Mean	SD	pH			Mean	SD
	I	II	III			I	II	III			I	II	III		
0	27.97	24.59	27.97	26.85	1.95	0.014	0.020	0.023	0.019	0.004	7.000	7.000	7.000	7.000	0.000
1	44.19	44.19	44.19	44.19	0.00	0.012	0.019	0.015	0.015	0.003	6.960	7.000	7.000	7.000	0.019
3	39.12	39.12	39.12	39.12	0.00	0.047	0.042	0.039	0.042	0.004	6.980	6.970	6.991	6.990	0.009
5	42.84	42.84	42.84	42.84	0.00	0.048	0.049	0.045	0.047	0.002	5.980	5.950	5.900	6.950	0.033
9	45.88	45.88	45.88	45.88	0.00	0.028	0.036	0.033	0.032	0.003	6.820	6.810	6.830	6.990	0.008
13	80.34	77.97	80.34	79.55	1.37	0.024	0.021	0.023	0.023	0.001	6.520	6.490	6.520	6.990	0.014
17	205.34	205.34	205.34	205.34	0.00	0.028	0.023	0.023	0.025	0.002	6.310	6.320	6.310	6.870	0.005
23	262.09	262.09	262.09	262.09	0.00	0.020	0.022	0.023	0.022	0.001	6.800	6.720	6.700	6.700	0.043
35	49.93	49.93	49.93	49.93	0.00	0.021	0.021	0.023	0.022	0.001	5.460	6.450	6.460	6.460	0.469
47	45.54	45.54	45.54	45.54	0.00	0.014	0.020	0.023	0.019	0.004	6.130	6.150	6.120	6.150	0.012
71	49.26	41.15	49.26	46.55	4.68	0.017	0.020	0.023	0.020	0.002	6.000	6.020	6.000	6.020	0.009

*SD: Standard derivation

Table G-27 Phosphates solubilization, system pHs and growth, monitored by the turbidimetric method at 660 nm, of PDMCd0501 in NBRIP medium containing 0.5% (w/v) tricalcium phosphate

Time (hour)	PO ₄ ³⁻ -P (mg/l)			Mean	SD	Optical density (660 nm)			Mean	SD	pH			Mean	SD
	I	II	III			I	II	III			I	II	III		
0	90.14	91.15	89.12	90.14	1.01	0.025	0.026	0.030	0.027	0.002	7.000	7.000	7.000	7.000	0.000
1	89.80	89.80	90.14	89.91	0.20	0.028	0.029	0.025	0.027	0.002	6.620	6.610	6.620	6.620	0.005
3	101.96	103.31	101.32	102.20	1.02	0.017	0.016	0.014	0.016	0.001	6.250	6.230	6.240	6.240	0.008
5	139.12	133.38	140.81	137.77	3.90	0.018	0.020	0.020	0.019	0.001	6.390	6.410	5.400	5.410	0.471
9	190.14	185.74	184.73	186.87	2.87	0.010	0.016	0.014	0.013	0.003	4.910	4.890	4.880	4.880	0.012
13	295.20	295.88	301.62	297.57	3.53	0.030	0.025	0.024	0.026	0.003	4.490	4.510	4.500	4.500	0.008
17	297.57	298.24	295.88	297.23	1.22	0.046	0.046	0.044	0.045	0.001	4.500	4.500	4.470	4.480	0.014
23	245.88	248.58	245.20	246.55	1.79	0.050	0.042	0.044	0.045	0.003	4.300	4.310	4.330	4.310	0.012
35	201.28	202.40	208.04	203.91	3.62	0.079	0.063	0.064	0.069	0.007	4.220	4.240	4.210	4.230	0.012
47	243.18	245.24	238.45	242.29	3.48	0.043	0.045	0.045	0.044	0.001	4.520	4.510	4.511	4.510	0.004
71	235.91	245.20	238.45	239.85	4.80	0.048	0.043	0.044	0.045	0.002	4.010	4.000	4.010	4.510	0.005

*SD: Standard derivation

Table G-28 Phosphates solubilization, system pHs and growth, monitored by the turbidimetric method at 660 nm, of PDMCd0501 in NBRIP medium containing 0.5% (w/v) tricalcium phosphate in the presence of Zn plus Cd (20/20 mg/l)

Time (hour)	PO ₄ ³⁻ -P (mg/l)			Mean	SD	Optical density (660 nm)			Mean	SD	pH			Mean	SD
	I	II	III			I	II	III			I	II	III		
0	25.61	25.61	25.61	25.61	0.00	0.006	0.004	0.003	0.004	0.001	7.000	7.000	7.000	7.000	0.000
1	52.64	52.64	52.64	52.64	0.00	0.016	0.014	0.015	0.015	0.001	7.000	6.970	7.000	7.000	0.014
3	56.01	56.01	56.01	56.01	0.00	0.011	0.013	0.014	0.012	0.001	6.990	6.990	7.030	6.990	0.019
5	65.14	65.14	66.15	65.47	0.59	0.013	0.019	0.018	0.017	0.003	6.950	6.850	6.980	6.950	0.056
9	210.41	210.41	211.42	210.74	0.59	0.036	0.034	0.030	0.033	0.002	6.982	6.981	6.983	6.980	0.001
13	210.41	181.69	179.66	190.59	17.19	0.064	0.063	0.065	0.064	0.001	6.790	6.790	6.820	6.790	0.014
17	249.26	265.47	266.99	260.57	9.83	0.084	0.079	0.081	0.081	0.002	6.610	6.620	6.631	6.600	0.009
23	160.07	159.73	158.72	159.50	0.70	0.074	0.073	0.075	0.074	0.001	5.980	5.890	5.96	5.960	0.045
35	133.38	133.38	133.38	133.38	0.00	0.013	0.016	0.020	0.016	0.003	5.500	5.510	5.470	5.490	0.017
47	176.96	176.96	176.96	176.96	0.00	0.024	0.023	0.021	0.023	0.001	5.330	5.300	5.280	5.310	0.021
71	160.74	160.74	160.74	160.74	0.00	0.030	0.027	0.029	0.029	0.001	5.260	5.250	5.270	5.260	0.008

*SD: Standard derivation

Table G-29 Phosphates solubilization, system pHs and growth, monitored by the turbidimetric method at 660 nm, of PDMCd2007 in NBRIP medium containing 0.5% (w/v) tricalcium phosphate

Time (hour)	PO ₄ ³⁻ -P (mg/l)			Mean	SD	Optical density (660 nm)			Mean	SD	pH			Mean	SD
	I	II	III			I	II	III			I	II	III		
0	92.16	88.48	90.47	90.37	1.84	0.000	0.000	0.000	0.000	0.000	7.000	7.000	7.000	7.000	0.000
1	91.82	89.80	90.14	90.59	1.09	0.007	0.006	0.005	0.006	0.001	6.820	6.810	6.830	6.830	0.008
3	90.14	88.78	90.14	89.68	0.78	0.090	0.072	0.071	0.078	0.009	6.520	6.490	6.520	6.520	0.014
5	107.03	104.83	91.49	101.11	8.41	0.130	0.177	0.199	0.169	0.029	6.310	6.320	6.310	6.310	0.005
9	194.86	190.47	188.78	191.37	3.14	0.183	0.175	0.185	0.181	0.004	6.000	6.020	6.000	6.000	0.009
13	285.74	282.36	282.36	283.49	1.95	0.354	0.380	0.310	0.348	0.029	5.500	5.520	5.527	5.520	0.011
17	255.34	245.54	243.51	248.13	6.32	0.195	0.180	0.140	0.172	0.023	5.430	5.453	5.470	5.460	0.016
23	211.08	211.76	214.80	212.55	1.98	0.053	0.052	0.057	0.054	0.002	5.360	5.350	5.370	5.371	0.008
35	223.58	223.92	225.95	224.48	1.28	0.078	0.094	0.093	0.088	0.007	5.300	5.340	5.310	5.300	0.017
47	211.42	213.45	209.39	211.42	2.03	0.122	0.113	0.160	0.132	0.020	5.020	5.000	5.001	5.010	0.009
71	197.91	193.85	177.64	189.80	10.73	0.200	0.180	0.140	0.173	0.025	5.010	5.000	5.010	5.010	0.005

*SD: Standard derivation

Table G-30 Phosphates solubilization, system pHs and growth, monitored by the turbidimetric method at 660 nm, of PDMCd2007 in NBRIP medium containing 0.5% (w/v) tricalcium phosphate in the presence of Zn plus Cd (20/20 mg/l)

Time (hour)	PO ₄ ³⁻ -P (mg/l)			Mean	SD	Optical density (660 nm)			Mean	SD	pH			Mean	SD
	I	II	III			I	II	III			I	II	III		
0	20.20	0.78	20.20	13.73	11.22	0.007	0.009	0.004	0.007	0.002	7.000	7.000	7.000	7.000	0.000
1	19.53	19.19	19.53	19.41	0.20	0.005	0.004	0.005	0.005	0.000	7.000	6.970	7.000	7.000	0.014
3	32.70	32.03	32.70	32.48	0.39	0.009	0.010	0.010	0.010	0.001	7.000	6.966	7.030	7.030	0.026
5	26.28	27.64	26.28	26.73	0.78	0.017	0.017	0.019	0.018	0.001	7.090	7.000	7.100	7.100	0.045
9	42.16	37.09	42.16	40.47	2.93	0.013	0.014	0.018	0.015	0.002	7.030	7.000	7.090	7.090	0.037
13	207.70	208.04	207.70	207.82	0.20	0.021	0.017	0.019	0.019	0.002	7.000	7.000	7.000	7.000	0.000
17	206.69	206.35	206.69	206.58	0.20	0.093	0.070	0.030	0.064	0.026	6.990	6.990	7.000	6.990	0.005
23	134.05	134.39	134.05	134.17	0.20	0.170	0.170	0.183	0.174	0.006	6.960	6.950	6.980	6.960	0.012
35	57.03	61.08	57.03	58.38	2.34	0.300	0.270	0.293	0.288	0.013	6.862	6.851	6.883	6.860	0.013
47	37.43	39.12	37.43	38.00	0.98	0.280	0.270	0.293	0.281	0.009	6.179	6.190	6.120	6.140	0.031
71	67.53	76.32	67.53	70.46	5.07	0.168	0.167	0.159	0.165	0.004	6.610	6.620	6.631	6.090	0.009

*SD: Standard derivation

Table G-31 Phosphates solubilization, system pHs and growth, monitored by the turbidimetric method at 660 nm, of PDMCd2008 in NBRIP medium containing 0.5% (w/v) tricalcium phosphate

Time (hour)	PO ₄ ³⁻ -P (mg/l)			Mean	SD	Optical density (660 nm)			Mean	SD	pH			Mean	SD
	I	II	III			I	II	III			I	II	III		
0	5.68	5.68	5.68	5.68	0.00	0.019	0.016	0.017	0.017	0.001	7.000	7.000	7.000	7.000	0.000
1	93.18	92.50	93.18	92.95	0.39	0.010	0.012	0.010	0.011	0.001	6.910	6.910	6.900	6.910	0.005
3	119.19	118.51	119.19	118.96	0.39	0.010	0.014	0.010	0.011	0.002	6.480	6.490	6.480	6.480	0.005
5	124.26	124.93	124.26	124.48	0.39	0.017	0.018	0.017	0.017	0.000	5.835	5.832	5.831	5.830	0.002
9	200.95	200.95	197.57	199.82	1.95	0.017	0.016	0.017	0.017	0.000	5.310	5.320	5.320	5.310	0.005
13	262.77	263.11	262.77	262.88	0.20	0.038	0.034	0.038	0.037	0.002	6.130	6.110	5.100	5.100	0.481
17	309.05	308.04	309.05	308.72	0.59	0.062	0.057	0.062	0.060	0.002	5.300	5.300	5.270	5.070	0.014
23	301.28	293.85	301.28	298.81	4.29	0.073	0.074	0.078	0.075	0.002	5.000	5.030	5.000	5.000	0.014
35	243.18	245.54	243.18	243.96	1.37	0.109	0.094	0.109	0.104	0.007	5.000	5.060	5.010	5.000	0.026
47	277.64	277.30	277.30	277.41	0.20	0.098	0.097	0.098	0.098	0.000	4.980	4.980	4.971	4.970	0.004
71	268.51	261.76	268.51	266.26	3.90	0.080	0.064	0.078	0.074	0.007	4.980	4.970	4.970	4.970	0.005

*SD: Standard derivation

Table G-32 Phosphates solubilization, system pHs and growth, monitored by the turbidimetric method at 660 nm, of PDMCd2008 in NBRIP medium containing 0.5% (w/v) tricalcium phosphate in the presence of Zn plus Cd (20/20 mg/l)

Time (hour)	PO ₄ ³⁻ -P (mg/l)			Mean	SD	Optical density (660 nm)			Mean	SD	pH			Mean	SD
	I	II	III			I	II	III			I	II	III		
0	28.65	27.97	-0.27	18.78	16.50	0.020	0.024	0.021	0.022	0.002	7.000	7.000	7.000	7.000	0.000
1	25.61	27.30	30.51	27.80	2.49	0.020	0.018	0.025	0.021	0.003	7.000	6.970	7.000	7.000	0.014
3	46.89	62.43	44.83	51.39	9.62	0.034	0.044	0.041	0.040	0.004	6.990	6.900	7.030	6.990	0.054
5	61.76	38.45	32.13	44.11	15.61	0.044	0.046	0.042	0.044	0.002	6.950	6.950	7.000	6.950	0.024
9	94.86	114.46	96.22	101.85	10.94	0.043	0.046	0.045	0.045	0.001	6.930	6.950	6.930	6.930	0.009
13	205.00	202.40	205.00	204.13	1.50	0.046	0.045	0.044	0.045	0.001	6.762	6.751	6.783	6.739	0.013
17	209.39	211.76	209.39	210.18	1.37	0.045	0.042	0.042	0.043	0.001	6.279	6.290	6.320	6.300	0.017
23	194.19	194.53	194.19	194.30	0.20	0.029	0.028	0.022	0.026	0.003	6.610	6.620	6.631	5.860	0.009
35	169.86	170.20	169.86	169.98	0.20	0.019	0.020	0.020	0.020	0.000	5.300	5.300	5.36	5.320	0.000
47	194.19	187.77	194.19	192.05	3.71	0.015	0.017	0.020	0.017	0.002	5.000	5.010	5.070	5.010	0.031
71	201.28	193.51	182.03	192.27	9.69	0.020	0.023	0.021	0.021	0.001	4.980	4.990	4.980	4.984	0.005

*SD: Standard derivation

Table G-33 Phosphates solubilization, system pHs and growth, monitored by the turbidimetric method at 660 nm, of PDMZnCd1502 in NBRIP medium containing 0.5% (w/v) tricalcium phosphate

Time (hour)	PO ₄ ³⁻ -P (mg/l)			Mean	SD	Optical density (660 nm)			Mean	SD	pH			Mean	SD
	I	II	III			I	II	III			I	II	III		
0	73.58	76.62	66.15	72.12	5.39	0.012	0.013	0.012	0.012	0.000	7.000	7.000	7.000	7.000	0.000
1	81.35	100.27	81.35	87.66	10.92	0.012	0.017	0.018	0.016	0.003	6.760	6.730	6.750	6.750	0.012
3	221.22	224.93	224.59	223.58	2.05	0.016	0.016	0.017	0.016	0.000	6.440	6.400	6.410	6.400	0.017
5	215.47	216.82	215.47	215.92	0.78	0.042	0.044	0.043	0.043	0.001	5.810	5.800	5.810	5.800	0.005
9	219.19	225.95	219.19	221.44	3.90	0.143	0.149	0.143	0.145	0.003	5.100	5.060	5.000	5.060	0.041
13	201.28	208.38	235.07	214.91	17.81	0.145	0.153	0.145	0.148	0.004	5.000	5.010	5.000	5.000	0.005
17	216.49	216.49	222.57	218.51	3.51	0.165	0.163	0.165	0.164	0.001	5.100	5.100	5.060	5.100	0.019
23	215.47	215.47	212.43	214.46	1.76	0.200	0.196	0.200	0.199	0.002	5.200	5.230	5.200	5.200	0.014
35	268.51	268.51	265.14	267.39	1.95	0.199	0.197	0.199	0.198	0.001	5.160	5.190	5.170	5.170	0.012
47	287.77	287.77	288.11	287.88	0.20	0.156	0.170	0.156	0.161	0.007	5.130	5.150	5.120	5.140	0.012
71	262.09	262.09	251.96	258.72	5.85	0.160	0.158	0.166	0.161	0.003	5.130	5.130	5.140	5.140	0.005

*SD: Standard derivation

Table G-34 Phosphates solubilization, system pHs and growth, monitored by the turbidimetric method at 660 nm, of PDMZnCd1502 in NBRIP medium containing 0.5% (w/v) tricalcium phosphate in the presence of Zn plus Cd (20/20 mg/l)

Time (hour)	PO ₄ ³⁻ -P (mg/l)			Mean	SD	Optical density (660 nm)			Mean	SD	pH			Mean	SD
	I	II	III			I	II	III			I	II	III		
0	-0.27	0.95	-0.27	0.14	0.70	0.023	0.029	0.023	0.025	0.003	7.000	7.000	7.000	7.000	0.000
1	3.48	5.00	3.48	3.99	0.88	0.033	0.031	0.029	0.031	0.002	6.930	6.910	6.920	6.910	0.008
3	146.18	150.27	146.18	147.55	2.36	0.027	0.065	0.066	0.052	0.018	6.900	6.900	7.900	6.900	0.471
5	126.72	143.85	126.72	132.43	9.89	0.112	0.087	0.093	0.097	0.011	6.870	6.895	6.890	6.880	0.011
9	164.80	164.80	163.78	164.46	0.59	0.183	0.163	0.180	0.175	0.009	6.730	6.705	6.730	6.700	0.012
13	206.69	206.69	207.87	207.08	0.68	0.144	0.143	0.145	0.144	0.001	6.230	6.310	6.300	6.310	0.036
17	205.00	205.00	194.53	201.51	6.05	0.148	0.145	0.149	0.147	0.002	6.000	6.000	6.020	6.000	0.009
23	205.34	205.34	207.57	206.08	1.29	0.170	0.158	0.108	0.145	0.027	5.760	5.720	5.760	5.720	0.019
35	210.07	210.07	208.04	209.39	1.17	0.171	0.152	0.188	0.170	0.015	5.220	5.240	5.210	5.240	0.012
47	255.34	255.34	267.16	259.28	6.83	0.105	0.108	0.105	0.106	0.001	4.670	4.670	4.530	4.670	0.066
71	245.20	245.20	249.59	246.67	2.54	0.120	0.098	0.105	0.108	0.009	4.540	4.620	4.540	4.620	0.038

*SD: Standard derivation

Table G-35 Phosphates solubilization, system pHs and growth, monitored by the turbidimetric method at 660 nm, of PDMZnCd2003 in NBRIP medium containing 0.5% (w/v) tricalcium phosphate

Time (hour)	PO ₄ ³⁻ -P (mg/l)			Mean	SD	Optical density (660 nm)			Mean	SD	pH			Mean	SD
	I	II	III			I	II	III			I	II	III		
0	116.15	116.82	116.15	116.37	0.39	0.019	0.020	0.012	0.017	0.003	7.000	7.000	7.000	7.000	0.000
1	137.43	140.47	137.43	138.45	1.76	0.018	0.022	0.018	0.019	0.002	6.620	6.610	6.620	6.730	0.005
3	104.66	103.31	104.66	104.21	0.78	0.027	0.018	0.017	0.021	0.005	6.250	6.230	6.240	6.420	0.008
5	230.34	224.93	230.34	228.54	3.12	0.049	0.041	0.043	0.044	0.003	6.390	6.410	5.400	5.710	0.471
9	248.24	235.07	248.24	243.85	7.61	0.063	0.071	0.064	0.066	0.004	4.910	4.890	4.880	4.880	0.012
13	347.91	343.31	347.91	346.37	2.65	0.085	0.091	0.085	0.087	0.003	4.490	4.510	4.500	4.540	0.008
17	376.62	374.93	376.62	376.06	0.98	0.106	0.099	0.095	0.100	0.005	4.500	4.500	4.470	4.550	0.014
23	303.31	316.49	303.31	307.70	7.61	0.121	0.130	0.120	0.124	0.004	4.500	4.510	4.530	4.510	0.012
35	270.20	280.00	270.20	273.47	5.66	0.187	0.197	0.199	0.194	0.005	4.320	4.340	4.321	4.320	0.009
47	309.05	316.82	309.05	311.64	4.49	0.122	0.152	0.156	0.143	0.015	4.352	4.410	4.536	4.370	0.077
71	285.07	285.74	285.07	285.29	0.39	0.132	0.128	0.266	0.175	0.064	4.710	4.380	4.370	4.370	0.158

*SD: Standard derivation

Table G-36 Phosphates solubilization, system pHs and growth, monitored by the turbidimetric method at 660 nm, of PDMZnCd2003 in NBRIP medium containing 0.5% (w/v) tricalcium phosphate in the presence of Zn plus Cd (20/20 mg/l)

Time (hour)	PO ₄ ³⁻ -P (mg/l)			Mean	SD	Optical density (660 nm)			Mean	SD	pH			Mean	SD
	I	II	III			I	II	III			I	II	III		
0	6.01	6.01	10.07	7.36	2.34	0.003	0.002	0.003	0.003	0.001	7.000	7.000	7.000	7.000	0.000
1	27.97	27.97	27.13	27.69	0.49	0.016	0.012	0.016	0.015	0.002	7.000	7.000	7.000	7.000	0.000
3	31.01	31.01	31.32	31.11	0.18	0.033	0.032	0.032	0.032	0.000	7.050	7.000	7.030	7.030	0.021
5	21.55	21.55	21.99	21.70	0.25	0.041	0.043	0.043	0.042	0.001	7.090	7.000	7.100	7.100	0.045
9	44.86	44.86	32.03	40.59	7.41	0.032	0.051	0.051	0.045	0.009	7.130	7.100	7.190	7.190	0.037
13	217.50	217.50	199.59	211.53	10.34	0.076	0.080	0.080	0.079	0.002	7.000	7.000	7.000	7.000	0.000
17	261.08	261.08	261.42	261.19	0.20	0.085	0.082	0.081	0.083	0.002	6.590	6.590	6.610	6.600	0.009
23	261.35	261.35	264.12	262.27	1.60	0.130	0.153	0.162	0.148	0.013	5.860	5.850	5.880	5.860	0.012
35	261.42	261.42	268.85	263.90	4.29	0.220	0.220	0.220	0.220	0.000	5.220	5.210	5.230	5.210	0.008
47	302.30	302.30	300.95	301.85	0.78	0.137	0.137	0.137	0.137	0.000	4.670	4.670	4.530	4.530	0.066
71	302.64	310.07	283.38	298.69	13.77	0.142	0.153	0.144	0.146	0.005	4.540	4.620	4.540	4.540	0.038

*SD: Standard derivation

BIOGRAPHY



Biography

Name	Payungsak Taboonma
Date of birth	1 December 1988
Place of birth	Roi Et Province Thailand
Institution attended	
	2000 Primary education: BanLaoyung School, Roi-Et, Thailand
	2006 High School: Khoklarpittayakhom School, Roi-Et, Thailand
	2010 Bachelor of Science (Biology): Maharakham University, Maharakham, Thailand
	2014 Master of Science (Biology): Maharakham University, Maharakham, Thailand

Contact address

103/1, Mu 13, Laoyung villages, Khok Lam Subdistrict,
Chaturaphak Phiman District, Roi-Et, 45180 Thailand

Scholarship

2010-2011	Scholarship research to generate new knowledge (Grant year 2011) of Maharakham University
2011-2013	Science Achievement Scholarship of Thailand (SAST)

Research output

Taboonma, P., Nakbanpote, W. and Sangdee, A. (2014) "Resistance and plant growth-promoting properties under Zn/Cd stress of *Pseudomonas* sp. ZnCd2003", Proceeding of the International Conference on Future Trends In Bio-Informatics and Environmental Science-FTBES 2014, ISBN: 978-1-63248-016-3 doi: 10.15224/978-1-63248-016-3-04. p.15-20.

